THE ROLE OF MICROVASCULAR TUMOUR ENDOTHELIUM IN THE RECRUITMENT OF CD8+ T LYMPHOCYTES IN COLORECTAL CANCER

By

Dr Elizabeth Amanda Hepburn

MBChB, MRCS

A thesis submitted to the University of Birmingham for the degree of DOCTOR OF PHILOSOPHY

School of Immunity & Infection
College of Medical & Dental Sciences
University of Birmingham
July 2016

ABSTRACT

Tumour vasculature is structurally different to that of surrounding tissue, and tumour endothelial cells (TEC) display an angiogenic phenotype. Targeting tumour endothelium provides a means to deliver chemotherapeutic drugs. Tumour microvascular endothelium also regulates CD8+ T-lymphocyte trafficking into the tumour stroma and is important because increased CD8+ infiltration is associated with improved patient survival. Thus, understanding the unique phenotype of tumour endothelium and how CD8+ T-cell recruitment is regulated may identify targets for anti-cancer therapeutics.

Despite multiple possible treatment strategies, colorectal cancer remains the 3rd most common cause of cancer related deaths in the world. Therefore, the aims of this thesis were to develop a method to isolate and culture human colorectal tumour endothelium, to characterize the TEC phenotype, and investigate how microenvironmental signals within the tumour may influence this phenotype, and to investigate the molecular regulation of CD8+ T-cell recruitment by TEC.

In this thesis, I have used tissue from patients with colorectal cancer and paired non-involved control tissue to isolate primary endothelial cells. Endothelial cell phenotype was explored in CRC and normal colon (NC) using immunohistochemistry and TEC phenotype was validated using flow cytometry, ELISA and QPCR. I also used both flow-based and static adhesion assays to quantify CD8+ lymphocyte adhesion in the presence or absence of blocking reagents.

I have successfully devised a method to isolate TEC, which expressed characteristic endothelial markers (CD31, VWF, CD105, VEGFR's, and VE-Cadherin), as

well as tumour specific markers TEM8, and CD13. Interestingly CD13 expression was not specific to TEC. Increased CD8+ T-cell adhesion was observed in TEC compared to benign controls (NEC) in which adhesion was augmented after conditioning with CRC derived tumour associated fibroblast (TAFB) supernatant. Increased concentrations of IL-6 and CCL2/MCP-1 were produced by TEC and TAFB and inhibition of IL-6 and CCL2 reduced CD8+ T-cells adhesion to TEC. Endothelin-1 (ET1) was produced by TAFB supernatant. And increased levels of the corresponding Endothelin Receptor B (ET_B) were found on CRC endothelium, inhibition of which resulted in a significant increase in ICAM-1 expression and CD8+ T-cell adhesion to TEC.

Thus, the data from my validated *in vitro* TEC model for CRC has confirmed that tumour specific endothelium has a unique phenotype as a result of microenvironmental signals from within the tumour. My functional studies using these cells suggest that ET_B inhibition could augment ICAM-1 expression and facilitate increased recruitment of CD8+ T-lymphocytes into the tumour stroma. This commands further investigation with the aim of developing an anti-cancer therapy in CRC.

DEDICATIONS

My thesis is dedicated to my wonderful husband Pete, our daughter Isla and to my mum, Pat. They have always believed in me and without their love and support, I would not be where I am today.

ACKNOWLEDGMENTS

I would like to thank my lead supervisor Dr Trish Lalor for all her excellent help, advice, patience, support and direction. I would also like to thank Mr Tariq Ismail Professor David Adams and Dr Bertus Eksteen for encouragement, guidance and the opportunity to study at the University of Birmingham. Thanks and acknowledgements are also extended to Dr Steve Ward, Dr Evagelia Liaskou, Dr Shankar Suresh and Dr Gary Reynolds for sharing their expertise and many others in the liver laboratories who have offered assistance.

I would like to thanks Cancer Research UK for funding this work.

Special thanks to Dr Phillipe Tanniere, Dr Rahul Hejmadi, the Cellular pathology department, all colorectal surgeons and surgical registrars and colorectal theatre staff from the Queen Elizabeth Hospital Birmingham who assisted in sample collection.

Thank you to Dr Naschberger from Universitätsklinikum Erlangen for welcoming me to visit and sharing your technique.

It is important to thank all the patients with colorectal cancer who gladly donated their tissue for medical research, without whom this work would not have been possible

PUBLICATIONS AND PRESENTATIONS DURING THIS THESIS

Publications

- **Easing the learning curve from surgeon to scientist.** Hepburn E, Ward ST, Bulletin of RCSEng. Volume: 97 Issue: 7, July 2015, pp. 309-311

- **Evaluation of serum lysyl oxidase as a blood test for colorectal cancer.** Ward ST, Weston CJ, Hepburn E, Damery S, Hejmadi R, Morton D, Middleton G, Ismail T, Adams D.H. Eur J Surg Oncol. 2014 Jun;40(6):731-8.

- **The effects of CCR5 inhibition on regulatory T-cell recruitment to colorectal cancer.** Ward ST, Li KK, **Hepburn E**, Weston CJ, Curbishley SM, Reynolds GM, Hejmadi RK, Bicknell R, Eksteen B, Ismail T, Rot A, Adams DH. Br J Cancer. 2015 Jan 20;112(2):319-28.

Abstracts

- **Characterization of adhesion molecule and chemokine expression by tumour endothelium isolated from colorectal cancer,** E.Hepburn, S. T. Ward, S. Suresh, R. K. Hejmadi, T. Ismail, P. F. Lalor, Immunology, Volume 140, S. 1, December 2013

- **Selective recruitment and retainment of regulatory T cells in human colorectal cancer**, Ward ST, Hepburn E, Li K, Curbishley SM, Hejmadi R, Ismail T, Bicknell R, Rot A, Adams DH, The Lancet 2013, 381, S113: 27

Submitted manuscripts/ In draft

- **Tumour endothelial cell from CRC express TEM8 in culture and produce enhanced levels of CCL2.** Hepburn E, Ward ST, Ali S, Suresh S, Hejmadi RK, Ismail T, Adams DH Lalor PF. (Submitted).

- **Inhibition of Endothelin-1 and Endothelin receptor can promote CD8+ T lymphocyte and tumour endothelial adhesion in CRC.** Hepburn E, Ward ST, Suresh S, Hejmadi RK, Ismail T, Lalor PF. (In draft).

Presentations

- **Tumour associated fibroblast production of IL-6 regulates cytotoxic T-cell adhesion to human colonic endothelium**, Hepburn E, Ward ST, Suresh S, Liaskou E, Hejmadi R, Ismail T, Lalor PF, National cell adhesion meeting, Birmingham, 2013 (Poster)

- **Characterization of tumour endothelial cell expression of adhesion marker expression in CRC,** Hepburn E, Ward ST, Suresh S, Hejmadi R, Ismail T, Lalor PF, NCRI, Liverpool 2013, BSI, Liverpool 2013 (Poster)

- **Selective recruitment and retainment of regulatory T cells in human colorectal cancer**, ST Ward, E Hepburn, K Li, SM Curbishley, R Hejmadi, T Ismail, R Bicknell, A Rot, DH Adams, Keystone symposium, February 2013 (Poster)

CONTENTS

LIST OF FIGURES

LIST OF TABLES

ABBREVIATIONS

3,3'-diaminobenzidine	DAB
Adeno polyposis coli	APC
American joint committee on cancer	AJCC
Analysis of Variation	ANOVA
Anthrax toxin receptor-1	ANTXR1
B-Raf proto-oncogene, serine/threonine kinase	BRAF
C-lectin type	CLEC-14a
Cancer associated fibroblast	CAF
Cluster differentiation	CD
Colorectal cancer	CRC
colorectal liver metastatic endothelial cell	CRLMEC
colorectal liver metastasis	CRLM
CpG island methylator phenotype (CIMP	CIMP
Cytotoxic lymphocyte	CTL
Cytotoxic T cells	CTL
Cytotoxic T-Lymphocyte Associated protein-4	CTLA-4
Delta like 4	DLL4
Deoxyribonuceic acid	DNA
Endothelial cells	EC
Endothelin receptor B	ET_B
Endothelin receptor B (gene)	EDNRB
Endothin 1	ET1
Enzyme-linked immunosorbent assay	ELISA
Epidermal growth factor	EGF
Ethylenediaminetetra acetic acid	EDTA
Fibroblast growth factor	FGF
Flow assisted cell sorting	FACS
Flow cytometry	FC
Haemachromatosis	HFE
Hepatic sinusoidal endothelial cells	HSEC
Hepatocyte growth factor	HGF

Human umbilical vascular endothelial cell	HUVEC
Hypoxia inducible factor	HIF
Immunocytochemistry	ICC
Immunohistochemistry	IHC
Inferior mesenteric artery	IMA
Intercellular adhesion molecule 1	ICAM-1
Interferon	IFN
interleukin	IL
Irinotecan plus Fluorouracil and Leucovorin	IFL
Kirsten rat sarcoma viral oncogene homolog	KRAS
Macrophage inducible factor	MIF
major histocompatibility complex-1	MHC-1
MAPK	MAPK
Matrtix metalloproteinases	MMP
Median channel volume	MCV
Microsatellite instability	MSI
Mis-match repair	MMR
Monoclonal antibody	Mab
Monocyte chemotactic protein -1	MCP-1
Mucosal addressin cellular adhesion molecule	MAdCAM-1
Myeloid derived suppressor cell	MDSC
Nitric Oxide Synthase	eNOS
Normal colon	NC
P-selectin glycoprotein ligand 1	PSGL1
Plasminogen activator	PA
Platelet derived growth factor	PDGF
Platelet endothelial cell adhesion molecule-1	PECAM-1
Polymerase chain reaction	PCR
Positron emission tomography	PET
Programmed Death-1	PD-1
Quantitative polymerase chain reaction	QPCR
Real time polymerase chain reaction	RTPCR
Regulated on activation, normal T cell expressed and secreted	RANTES

Regulatory T cells	T-Reg
Roundabout homolog 4	ROBO4
smooth muscle actin	α-SMA
Superior mesenteric artery	SMA
T helper	Th
TNF Related Apoptosis Inducing Ligand	TRAIL
Transforming Growth factor	TGF
Tumour associated fibroblasts	TAFB
Tumour associated macrophage	TAM
Tumour endothelial cells	TEC
Tumour endothelial markers	TEM
Tumour infiltrating lymphocytes	TIL
Tumour necrosis factor	TNF
tumour, node, metastasis	TNM
Ulcerative Colitis	UC
Union for International Cancer Control	UICC
Vascular cell adhesion molecule 1	VCAM-1
Vascular endothelial growth factor	VEGFR
Vascular endothelial growth factor A	VEGF-A
Very late antigen 4	VLA-4
Von Willebrand factor	VWF

CHAPTER 1

General introduction

Colorectal cancer is newly diagnosed in approximately 40,000 people in the UK each year (1). Despite multiple possible treatment strategies, colorectal cancer remains the 3rd most common cause of cancer related deaths in the world. Interesting data regarding the number of tumour infiltrating lymphocytes (TIL), in particular, CD8+ T lymphocytes, within the tumour stroma of CRC can provide more accurate prognostic information than current, standard histopathological staging. Improved patient survival was seen in patients who had tumours containing high numbers of TILs (2). One way in which lymphocytes ultimately end up in the tumour stroma is to be actively recruited by the tumour microvascular endothelium. To this end, much evidence confirms that tumour endothelium is different phenotypically and functionally from non-involved endothelium (3, 4). This means that tumour endothelium is already the target of anti-tumour treatments via inhibition of angiogenesis (5, 6). In this thesis, I hypothesize that the tumour endothelium may regulate the quantity of CD8+ T-lymphocytes that are recruited into the tumour. I also propose that other tumour stromal cells such as tumour associated fibroblasts (TAFB) influence endothelial lymphocyte recruitment. In this thesis, I aimed to characterize tumour endothelial cells (TEC) from human CRC, produce an in vitro model to investigate the adhesive properties of TEC and explore how the stromal TAFB regulate the adhesion of CD8+ T-lymphocytes to TEC. Therefore, my introduction begins with

an overview of the anatomy and blood supply of the human colon and the blood supply of before moving on to discuss the changes which occur during carcinogenesis. I will then turn to the significance of tumour endothelium and how these cells, and their interplay with the host immune system present a good target for therapeutic intervention. Finally, I will highlight the experimental aims that were addressed in my investigations. This general introduction serves to set the context for the thesis work and more detailed information pertinent to the specific chapters follows in each subsequent result section.

1.1 The colon and rectum

Gross anatomy of the colon and the rectum

The caecum, colon and the rectum are the latter parts of the digestive tract and form the large intestine. This luminal tract receives partially digested contents from the small intestine. The main roles of the colorectum are digestion, absorption, and transport of water and electrolytes. Digestion and absorption of remaining complex carbohydrates are facilitated by fermentation by obligate anaerobes that reside in the gut microflora.

The colon begins with the caecum at the terminal ileum within the left iliac fossa, and proceeds as the ascending colon in the right paracolic gutter towards the liver inferior. Here it bends sharply, as the hepatic flexure, and traverses left, as the transverse colon, towards the spleen, inferior to which it bends sharply again, as the splenic flexure, and descends the left paracolic gutter as the descending colon (Figure 1.1). The colon continues towards the rectum as the sigmoid colon finally joining the rectum at the rectosigmoid junction. The rectum terminates at the anorectal junction denoted by the dentate line. The rectum is approximately 12cm in length and has an

approximate capacity of 500mls. It is divided into 3 parts depending upon its relationship with the peritoneal reflection.

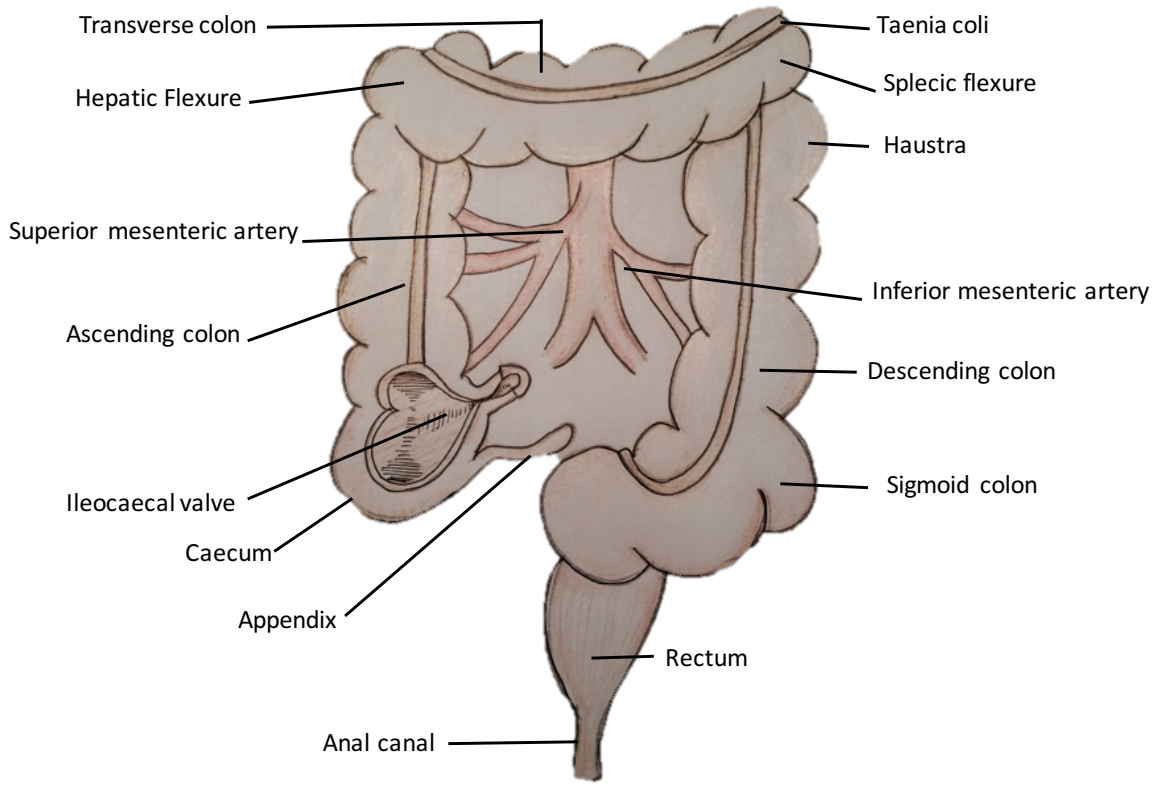

Figure 1.1. The gross anatomy of the colon, and rectum with main arterial supply and venous drainage. Illustration is authors own.

The arterial supply to the colon comes from the superior mesenteric artery (SMA) and inferior mesenteric artery (IMA) which travel through, and branch into the ileo, right and middle colic arteries, and the left and sigmoid arteries respectively, through the mesentery. The SMA supplies the caecum up to the proximal two thirds of transverse colon and the IMA supplies the distal third of transverse colon to the

rectum. The IMA and SMA communicate via the marginal artery, which ensures blood supply at the SMA/IMA division. The superior rectal artery and middle and inferior rectal arteries supply the rectum. Arterial supply is mirrored by venous drainage resulting in inferior mesenteric vein draining into the splenic vein and the superior mesenteric vein joining the splenic vein to for the hepatic portal vein. Lymphatic drainage also mirrors the arterial supply.

Histology of the normal colon

The colon is divided into four layers; mucosal, sub-mucosal, muscularis propria and a serosal layer (Figure 1.2). The mucosal layer is the most luminal layer and usually smooth. The mucosal layer, surfaced by low columnar to cuboidal epithelial cells interspersed by Goblet cells that secrete a lubricating mucous and endocrine cells of Paneth in right side of the colon, form deep, straight folds called the Crypts of Leiberkün. Deep within the epithelial layer is the lamina propria, which contains microvasculature and lymphatics in addition to infiltrating immune cells. The muscularis mucosa is a thin, uniform muscle layer separating the mucosal and submucosal layer. Histologically, the muscularis mucosa represents an important structure, as it is a landmark used to identify stage of colorectal cancer.

The submucosal layer, below the muscularis mucosa contains loose connective tissue, microvasculature, lymphatics, inflammatory cells and the submucosal plexus of Meissner, containing only parasympathetic nerve fibers supplying secretormotor innervation to the glandular cells of the mucosal layer. The muscularis propria consists of an inner circular and outer longitudinal muscle layer and also contains the plexus of Auerbach, which consists of para-sympathetic and sympathetic nerve fibers.

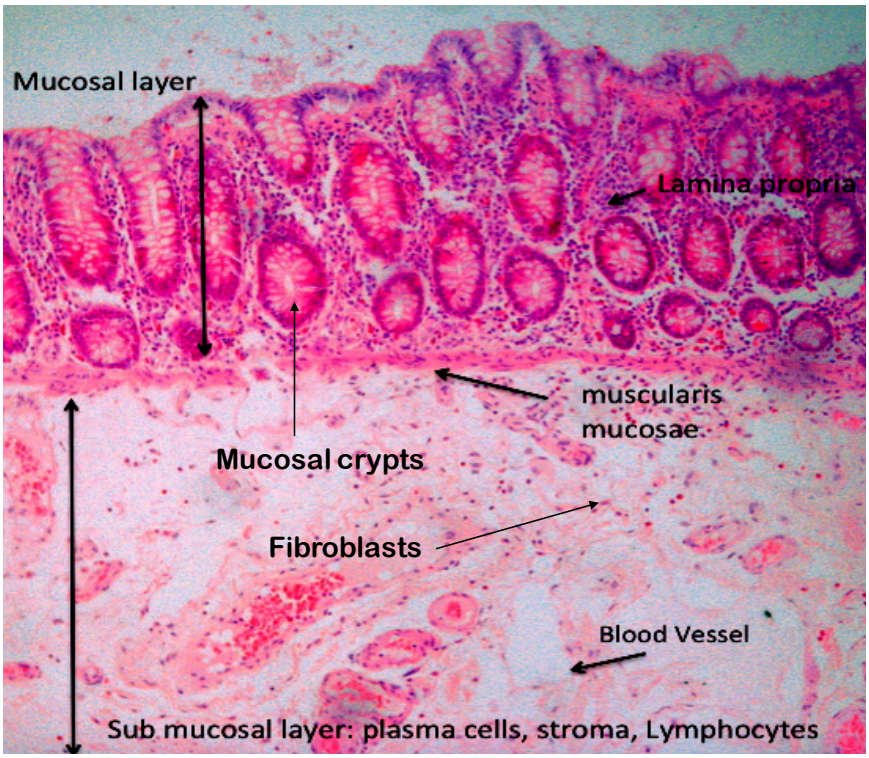

Figure 1.2. The structure of normal colon mucosa. Representative image showing a section of normal colon stained with Haematoxylin & Eosin. Original magnification x10. Labels indicate characteristic anatomical features and histological constituents. The mucosa and submucosa are separated by muscularis mucosae. Within the mucosa resides the surface epithelium arranged into crypts. Surrounding each epithelial crypt is lamina propria comprising of stroma, fibroblasts blood vessels, plasma cells and lymphocytes. These stromal constituents are also seen in the stromal compartment of the submucosa. Deep to the submucosa are the muscularis propria and serosal layers (not shown). Image is authors own.

1.2 Colorectal cancer

Histopathology of colorectal cancer

Colorectal adenocarcinoma occurs within the epithelial cells of the colorectal mucosa as a result of inherited or acquired genetic and epigenetic mutations. One of the most

common sequences has been termed the adeno-carcinoma sequence and is outlined in Figure 1.3. This process is initiated by adeno polyposis coli (APC) gene abnormalities and subsequent disruption to the Wnt signaling pathway, which results in epithelial hyperplasia and early adenoma formation (7).

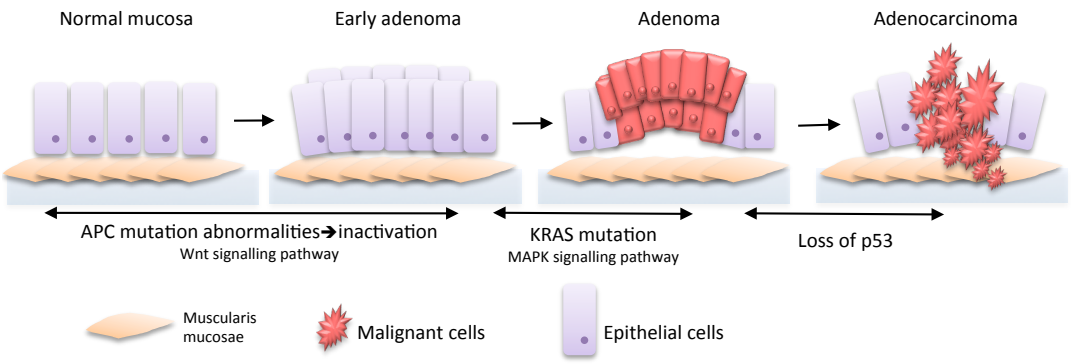

Figure 1.3. The adenocarcinoma sequence. The schematic illustrates the series of mutations occurring during the adeno-carcinoma sequence. Initially, mutation in the APC gene causes uncontrolled proliferation via Wnt signalling pathway and early adenoma formation. Further mutations lead to alterations in MAPK signalling and downstream dysplasia. Further mutation and loss of tumour suppressor gene, P53, results in carcinoma formation. Image is authors own amended from (8).

Further to APC gene inactivation, pro-oncogene Kirsten Rat Sarcoma viral oncogene homolog (KRAS) mutations (9) and hyper/hypomethylation further develop adenomatous polyp formation. In particular, mutations in KRAS, which are part of the MAPK signalling pathway, responsible for regulating cell proliferation, differentiation, migration and apotosis (10), lead to uncontrolled changes in regulation of these key cellular processes and ultimately result in malignancy.

Approximately 10-20% of CRC undergo an alternative pathway, known as the serrated pathway, which arises in serrated adenomas and leads to microsatellite

instability(11). In these, there is a distinctively different genetic profile; methylation of CpG rich areas or islands occurs often resulting in tumour suppressor gene silencing, an occurrence termed CpG island methylator phenotype (CIMP). Tumours with CIMP are associated in mutations of the pro-oncogene B-Raf proto-oncogene, serine/threonine kinase (BRAF) which, like KRAS, is a component of the MAPK signalling pathway (12). This pathway does not start with mutation of the APC gene. Beyond the pathogenesis of CRC, proliferation and invasion of malignant epithelial cells are supported by stromal cells (plasma cells, fibroblasts, infiltrating leukocytes and cells from the vasculature) and invade the mucosal layer as the cancer becomes more invasive (13) penetrating the muscularis mucosae followed by the sub-mucosal layer (Figure 1.4).

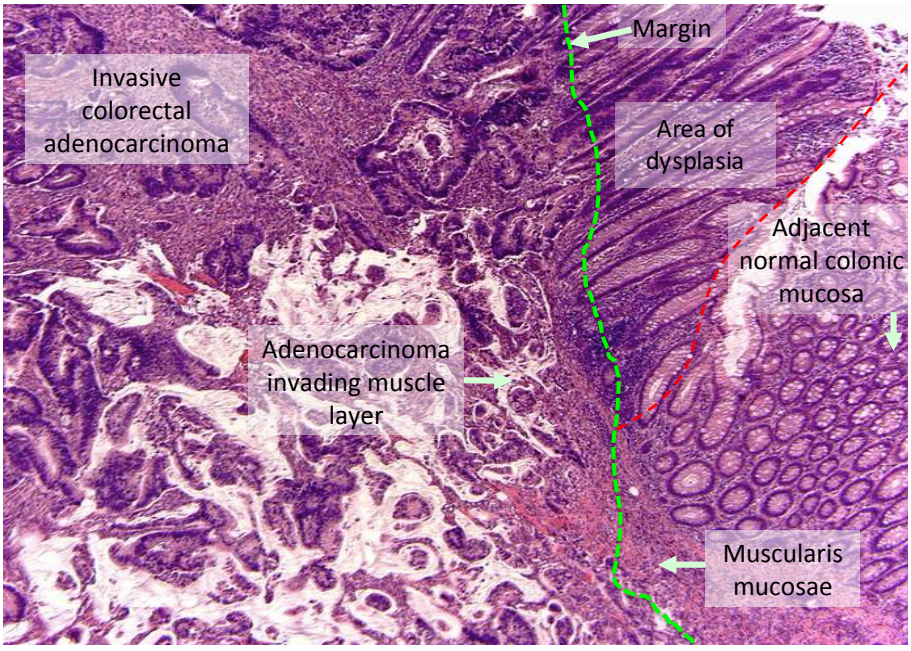

Figure 1.4: Histology of colorectal adenocarcinoma.
The tissue section shows the invasive margin of colorectal adenocarcinoma and adjacent dysplastic tissue and normal colon. Section is stained with Haematoxylin & Eosin. Original magnification x 10. Labels indicate characteristic features and anatomical landmarks. Image is authors own.

Presentation and diagnosis

Common symptoms in patients with colorectal cancers may include constitutional malaise, weight loss, fatigue and loss of appetite. Left sided cancers often cause patients to present with fresh rectal bleeding, change in bowel habit, and abdominal pain or palpable mass. In large obstructing cancers, complete constipation and signs of bowel obstruction may also occur. Right-sided bowel cancers may present with subtler features such as iron deficient anaemia, abdominal mass or pain, and general malaise. Advanced colorectal cancer and metastatic cancer may present with extra-colonic manifestations, such as capsular pain in liver colorectal metastasis.

In the U.K., there are broadly two pathways that patients follow to be investigated for colorectal cancer. Patients who have attended clinic with symptoms of colorectal cancer and those who have been identified in the national screening program as having occult blood in their faecal sample. Both groups will undergo endoscopic and/or radiological investigation. Where a lesion is identified, biopsy samples are taken for histological diagnosis. In the case of a malignant biopsy result, the patient undergoes further radiological imaging to identify if there are metastatic lesions and, in the case of some large invasive rectal cancer, to identify if the patient requires pre-operative radiotherapy to enable curative clearance with surgical excision. In this project I have utilized samples from patients who have all had surgical excisions of colon and rectal tumours prior to pre-operative neo adjuvant therapy.

Staging

Colorectal cancer was first classified based upon invasiveness using the Dukes staging system, which was devised by the English pathologist Cuthbert Dukes. The system grades tumours depending upon their depth of invasion regarding histological landmarks, and presence of lymph node and metastatic involvement. Dukes stage A corresponds with an invasive tumour that does not extend through the muscularis propria. Dukes B describes a tumour that invades through the bowel wall but does not involve lymph nodes. A Dukes C tumour extends through bowel wall and involves lymph nodes and Dukes D describes a tumour with metastatic spread of disease. Although the Dukes staging system is often still documented, for diagnostic purposes in the U.K. colorectal cancer is staged by the tumour, node, metastasis (TNM) staging system. This is recognised by the Union for International Cancer Control (UICC) and American Joint Committee on Cancer (AJCC) and provides more information about the extent of tumour invasion. This system characterizes the depth of invasion according to histological landmarks, apical lymph node involvement and classifies the tumour accordingly. Figure 1.5 is an outline of the TNM classification in colorectal cancer. TNM subdivides the level of invasion through the wall of the bowel more comprehensively than Dukes staging and facilitates more accurate prognostic information. For example, Dukes B can involve T3 and T4 tumours. Another method of staging, often used in America is where T1/T2, tumours are described as stage 1. T3/T4 tumours are stage 2. N1 tumours are stage 3 and any tumour with metastatic spread is described as stage 4. In this thesis, because tumours that had received previous pre-operative radiotherapy were not used, TX and To tumours are not represented. Most often tumours were T1-3 and nodal involvement varied.

Primary tumour	
TX	Unable to assess the tumour
T0	No evidence of tumour
Tumour insitu (Tis)	Tumour limited to the epithelium or lamina propria
T1	Tumour involves the submucosal layer
T2	Tumour involves the muscularis propria
T3	Tumour invades through muscularis propria into sub-serosa or into non-peritonealised pericolic or perirectal tissues
T4a	Tumour penetrates to the surface of the visceral peritoneum
T4b	Tumour directly invades or is adherent to other structures or organs
Lymph node involvement	
NX	Nodal involvement cannot be assessed
N0	No lymph node metastasis
N1	1-3 regional lymph node involvement
N1a	Nodal involvement in 1 regional lymph nodes
N1b	Nodal involvement in 2-3 regional lymph nodes
N1c	Tumour deposit in the subserosa, mesentery or non-peritoneal perirectal tissues without regional node metastasis.
N2	Metastasis in 4 or more lymph nodes
N2a	Metastasis in 4-6 regional lymph nodes
N2b	Metastasis in 7 or more regional lymph nodes
Distant metastasis	
M0	No distant metastasis
M1	Distant metastasis
M1a	Metastasis confined to 1 organ or site
M1b	Metastasis to more than one organ

Figure 1.5. An overview of the tumour, node, metastasis (TNM) classification of colorectal cancer. Provided in the dataset for colorectal cancer histopathology reports (3rd edition) by the Royal college of pathologists (14).

Treatment of colorectal cancer

The mainstay of colorectal cancer treatment falls into 3 categories and depends upon the location and stage of the cancer. Most colorectal cancers will undergo surgical excision as primary curative treatment. The principals for surgical resection include resection of the tumour, along with the supplying vessels, mesentery, and accompanying lymph nodes.

For right-sided cancers this usually requires a right hemi-colectomy procedure, whilst left sided cancers require either a left hemi-colectomy or an anterior resection. Rectal cancers can often be excised using an anterior resection however, if they are close to the anal verge, an abdominal perineal resection should be performed where the anus is excised and an end colostomy is created. Cancers deemed not amenable to resection will be considered for pre-operative radiotherapy, palliative stent insertion or other palliative procedures. Patients with colorectal cancers that are high risk stage (T2 or cT3b or greater), have lymph node involvement, show signs of extramural vascular invasion or metastatic invasion will be offered adjuvant chemotherapy consisting of capecitabine or oxaliplatin in combination with 5-fluorouracil and folinic acid (15).

Despite the current treatment options, median overall survival is about 22-24 months (16) and therefore investigation into further treatment options for all stages of CRC is warranted. Several preparations have been investigated *in vitro* and in animal models, and human phase III trials in advanced and metastatic colorectal cancer (mCRC) that target the vascular endothelium of tumour blood vessels. Blood vessels of solid tumours and their endothelium are reported to be structurally, functionally and phenotypically different from non–involved blood vessels (3, 18). Before discussing these agents and how the tumour endothelium can be modulated and exploited by

therapeutic targets, we must first understand how the tumour endothelium differs from nearby non-involved endothelium.

1.3 Vascular endothelium in colorectal cancer

Vascular endothelium

Generally, the endothelium consists of a single layer of endothelial cells (ECs) on the luminal surface of blood vessels that exists upon a supportive basement membrane. The ECs throughout the body are heterogeneous in structure allowing for differences in organ-specific function (17). For example, EC may be continuous or discontinuous and may be fenestrated or non-fenestrated. Structural, functional and phenotypic heterogeneity of endothelium is dependent upon the cellular role. In health and disease, generally ECs serve the following functions: haemostatic balance, permeability, regulation of vasomotor tone, proliferation, blood cell trafficking, survival and innate and adaptive immunity (2).

Macrovascular endothelial cells from arteries and veins are continuous and bound by tight junctions, which are required to maintain a patent lumen, and withstand the high intra-luminal pressures inside larger vessel blood flow. Macrovascular endothelial cells grow as a single layer of impermeable endothelium, tightly adhered to the basement membrane providing a non-thrombogenic surface, which prevents adhesion of platelets and other cells. Examples include cerebrovascular endothelium where ECs are continuous and non-fenestrated allowing tight control of transportation across the blood brain barrier (19). In contrast, hepatic sinusoidal endothelium is dis-continuous and fenestrated allowing cellular trafficking and

movement of nutrients to and from blood vessels to hepatocytes (20). The environmental conditions that develop within tumours stimulate a different endothelial cell phenotype in vessels that supply benign tissue to that of malignant tissue.

The microvasulature of colorectal cancer

In the healthy colon and rectum, the arteries meet the mesenteric border and are distributed round towards the anti-mesenteric border and transversely along the luminal layers. Corrosion casts have illustrated that these arteries divide in the sub-mucosa into arterioles and then sub-epithelial capillaries forming a regular hexagonal plexus around mucosal glands. This produces a regular honeycomb appearance (21)(see Figure 1.6). In human colorectal adenocarcinoma, the regular, honeycomb structure, described in normal colon, is lost (See Figure 1.6) (21). These studies show that tumour vessels have lost normal hierarchy, heterogeneous density within the tumour, and blind-ending vessels. Other features of tumour microvasculature include anastomosing capillaries and frequently extravasation of resin suggestive of leaky vessels. Skinner *et al.* have illustrated that capillaries within human colon tumour microvasculature exhibit increased density of microvasculature between tumour cells, a larger mean diameter and increased vascular volume compared to normal colon capillaries (22).

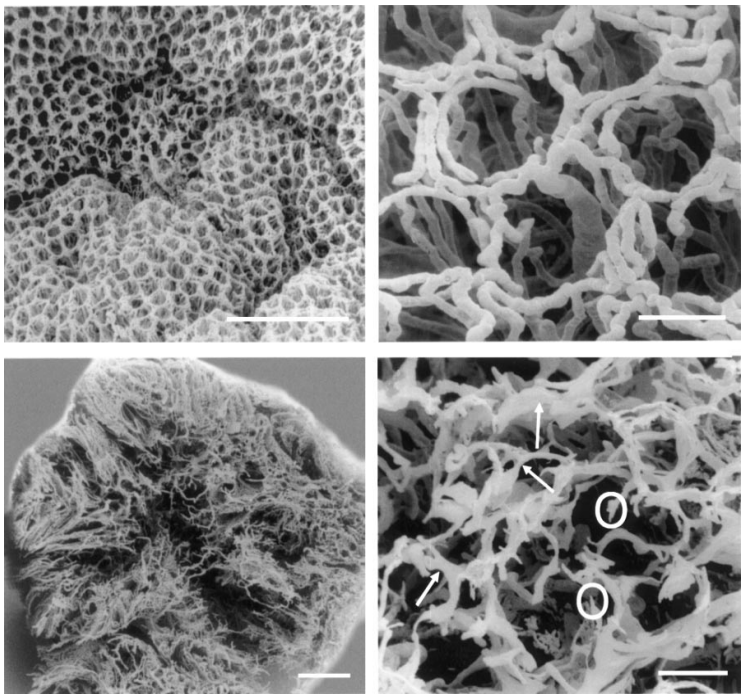

Figure 1.6: The normal microvascular structure is lost in colorectal tumours.
Micrographs of casts from normal colon (top two images) and colorectal cancer (bottom two images) show a distinct loss of organization in the tumour. The figure is adapted from Konerding et al (21).

Furthermore, differential changes in microvasculature structure occur with the spectrum of disease. Konerding *et al.,* found that in casts produced from larger, more invasive disease, the core of the tumour suggested external compression on the microvasculature resulting in a reduced number of vessels and a necrotic center (21). At the other end of the spectrum of disease, casts from adenomas exhibit a variety of structural characteristics ranging from minimal changes with elongation and an increased vein, venule and capillary diameter (22) up to an appearance indistinguishable from cancer microvasculature by blinded observers (21). Alterations

in tumour vessel architecture are also reproduced in animal models of disease. For example data from a murine tumour implantation model (23) shows an overall increase in tumour microvascular density and volume compared to uninvolved tissue. However, other structural characteristics diminish the flow of blood within these vessels. In this instance tumour microvasculature flow has been found to be chaotic, unpredictable, absent, and even bi-directional via vascular shunts (24). As a consequence, in terms of supplying tissue with oxygenated blood and removing products of tissue metabolism, tumour microvasculature is inefficient. Thus tumours in rodents (25) and humans (26) contain blood which is measurably hypoxic.

Endothelium in colorectal cancer

It is understood that for tumours to progress, grow and become more invasive, formation of new blood vessels is required (27). New vessel formation can either occur via vasculogenesis during embryological vessel formation or angiogenesis, which is the formation of new blood vessels from pre-existing vessels. This requires the "angiogenic switch" which was first described by Folkman (27). This refers to a point in the tumour development where for the tumour to grow beyond 0.4mm, the tumour must develop its own blood supply and it does this by producing angiogenic factors. There are two established methods of vessel formation; sprouting and intersusseptive or splitting angiogenesis (28). Intersusseptive angiogenesis occurs in vasculogenesis of embryological development and is therefore not described in this report. Sprouting angiogenesis, however, occurs in healing tissue and tumourigenesis and involves shoots growing from endothelial stalk cells towards a stimulatory signal such as VEGF-A (Vascular endothelial growth factor A). This is accompanied by degradation of

basement membrane by proteolytic enzymes, endothelial cell proliferation, and direct migration of endothelial cells, tubulogenesis, vessel fusion, and pericyte stabilization to yield a mature and appropriately supported branching vessel.

Conditions where angiogenesis is required in adults include wound healing, ischaemia and tumour progression and in all cases ECs are required to proliferate. The ischaemic conditions found in tumours initiate the surrounding parenchyma to express Hypoxia inducible factor 1 (HIF-1), which stimulates transcription of VEGF-A, FGF and TGF genes. Similarly, infiltrating macrophages that are recruited to wound healing or inflamed tissue can also produce these factors. VEGF-A is recognised by respective receptors (VEGFR-1&2) which are located on the filopodia or 'tip' endothelial cells (28, 29). Binding initiates a number of events including secretion of proteolytic enzymes from filopodia on tip cells which break down the extra cellular matrix, resulting in filopodia migration towards the VEGF-A. This leads to contraction of actin filaments, which pulls the tip cells behind. In addition, VEGF-A activates production of a cell surface ligand, Delta like 4 (DLL4), which binds to its Notch receptors, and initiates stalk cells to proliferate (29).

The mechanisms which promote tumour angiogenesis are not fully understood, however the tumour endothelial cells (TEC), which develop as a result of tumour related angiogenesis are structurally, functionally and phenotypically different than those found in the surrounding uninvolved tissue (30, 31). This is very significant as it provides a means to selectively target tumour resident cells, whilst avoiding non-malignant cells, as a means to treat cancer. As mentioned earlier, the angiogenic process of tumour endothelial cells in CRC has been targeted as a mechanism for anticancer therapeutics. Hence, growth factors such as VEGF, EGF, PDGF and EGF

have all been targeted to inhibit tumour angiogenesis. Furthermore, anti-angiogenic agents are often used in combination therapy where their "normalization" of tumour blood vessels allows concomitant delivery of other chemotherapeutic agents (32, 33).

Bevucizumab is a humanized monoclonal antibody that binds to VEGF and prevents receptor binding and subsequent down-stream angiogenesis. Bevucizumab has been approved by the FDA and is recognised as a treatment for mCRC based on some improvement in progression free survival and overall survival. When trialed as part of a combination therapy (irinotecan plus fluorouracil and leucovorin (IFL) plus Bevacizumab at 5 mg per kilogram of body weight every two weeks) against a placebo in combination with IFL, Bevacizumab improved median and progression free survival, and rates of response were significantly improved (5). However, a higher incidence of side effects in the Bevacizumab arm, including diarrhea, leukopenia, bleeding, hypertension, and colonic perforation was reported. In particular, a significantly increased incidence of all grade 3 and grade 4 (described by Common Toxicity Criteria of the National Cancer Institute where grade 3 is "serious" and grade 4 is "life threatening") side effects and grade 3 hypertension was observed in patients from the Bevacizumab arm (5).

In vitro studies have suggested that VEGF inhibition delays wound healing (34). Receptor tyrosine kinase inhibitors have also shown improved patient survival in renal cell carcinoma in phase III clinical human trials, however Sorafenib has been associated with a significant increase in serious adverse events leading to hospitalization or death compared to a placebo arm and bleeding was more frequent. A suggested mechanism for haemorrhagic adverse events is inhibition of post-traumatic endothelial cell proliferation, exposing and depleting the sub-endothelial

basement membrane. This results in both thrombotic events and reducing vessel integrity (35).

Seemingly, adverse side effects of anti-angiogenic medications are mechanistically a direct consequence of the anti-angiogenic mode of action and, as such are intricately linked with dosing. Thus, side effects are unavoidable to be therapeutically optimal. Furthermore, inhibiting VEGF and VEGFR binding doesn't only affect endothelial cells of tumour blood vessels but also to vessels that supply normal healing tissue found at the site of surgical wounds (36). These effects of anti-angiogenic treatments have manifested in wound infection and complications (37) and bowel anastomotic leaks (38, 39, 40). These complications reveal that although anti-angiogenic therapies have anti-tumour potential, they are not tumour specific and are associated with serious side effects. This highlights that therapeutics have not targeted genuinely tumour-specific phenotypic characteristics and cellular pathways; if the tumour vasculature is to be exploited, it is essential that the tumour specificity of endothelium is targeted.

Identification of tumour-specific endothelial cell markers

One of the challenges that has stalled development of genuinely tumour-specific vascular targeting, relates to the difficulty in isolating and culturing human colorectal TEC for use in *in-vitro* investigations. The methods of isolating pure populations of endothelial cells commonly depend upon molecules that are expressed by endothelial cells such as CD31 (41) and CD146 (42), which allows methods such as immunomagnetic selection and flow assisted cell sorting. Limitations of using surface expressed molecules are due to cross expression of endothelial cell surface molecules

by other cells for example, macrophages and pericytes. St Croix *et al.,* (42) used laser capture methods for TEC isolation. This method does not permit *in vitro* expansion of cells and may suffer from inclusion of contaminating pericytes, but has been useful in analysis of TEC gene expression. Nevertheless, this work has produced important insights into the field of tumour specific endothelial markers. Some of these key markers are discussed in the sections below.

Tumour endothelial markers (TEM) 1-8

In addition to utilizing laser capture microdissection St Croix *et al.,* performed serial analysis of gene expression of isolated tumour endothelial cells to identify tumour-specific endothelial markers (42). This led to the identification of 8 new potential markers (TEM 1-8). One of these, Tumour endothelial marker 8 (TEM-8) was shown to be absent in uninvolved but present in angiogenic tissue from tumour. Furthermore, in murine studies, TEM-8-/- mice showed normal development and growth but tumour growth was arrested when compared to TEM-8 +/+ mice (43). TEM-8 has not only been identified as tumour specific but reports suggest that in colorectal cancer, mRNA expression increased with stage of disease (44). Furthermore, studies have revealed that DNA-vaccination with a vector targeting TEM-8 can reduce angiogenesis in tumours and generate potential T-cell mediated anti-tumour responses using murine models (45). Other TEMs of interest included TEM1 and 5, both of which were found on angiogenic tissue

CD13

Other studies have also identified molecules enriched in tumour endothelium such as CD13. CD13 (Aminopeptidase N) is a cell surface proteolytic enzyme, which is expressed on cells including endothelium, some leukocyte populations and mesenchymal cells. Diverse functions have been described including metabolism of regulatory peptides (46), cholesterol trafficking (47), modulation of cell motility and migration (48) and immunoregulation (49). The cellular pathways activated, however depend upon cellular context. The importance of CD13 function in cancer has been highlighted by studies documenting differential isoform expression within angiogenic tumour vasculature(50, 51) and correlations between intensity of expression and disease staging (52). Studies examining the potential of CD13 for tumour vasculature targeting by coupling chemotherapeutics such as doxorubicin to NGR peptide (53) a ligand for CD13, and an oral inhibitor, Bestatin, show improved survival after resection in patients with lung tumours in human trials (54). The diverse functions of CD13 have limited its inhibition clinically, as subsequent unwanted side effects manifest from the range of downstream affects.

ROBO4 and other newly identified markers

Increased tumour endothelial expression of the gene for Roundabout homolog 4 (ROBO4), a member of the receptors for slit proteins, was discovered by data mining techniques performed on many tumour types (breast, brain and colon) (55). ROBO4 showed promise as a tumour endothelial target after data suggested expression was absent in non-angiogenic tissue (56) although expression is also found in placenta (57) and non-malignant angiogenic tissue (55). Other proteins described as tumour endothelial markers include C-lectin type CLEC-14a (58). A functional study suggests that mechanistically CLEC-14a regulates tube formation in angiogenesis and so expression may not be limited to tumour vessel formation and thus inhibition may be susceptible to the same complications as other anti-angiogenic therapies (59).

The mechanisms underlying regulation of TEC-specific marker expression by tumour ECs and the function of these receptors remain unclear. Schellerer *et al.*, have described the isolation and culture of cells from colon and their pilot data highlight phenotypic differences that suggest normal and colorectal primary tumour endothelial cells maintain phenotypic stability in culture (60). However, comprehensive tumour-specific phenotyping data is lacking as colonic cells have not been reliably maintained in long-term culture. In addition, the potential uses of these cells as an *in vitro* model for investigating cancer biology have not been explored. An *in vitro* model of TEC would also permit study of the role of tumour endothelial cells in the tumour microenvironment and interplay with other cells within the stroma, such as immune populations and tumour associated fibroblasts. These areas will be explored in my investigations.

1.4 The microenvironment in CRC

Endothelial cells within the tumour are influenced by the microenvironment in which they reside and this, in turn, will alter their ability to recruit key anti-tumour and regulatory populations of immune cells. Lymphocytes that are actively recruited across the endothelium also contribute to the intra-tumoural immune context.

The Adhesion cascade

In health and disease, lymphocytes are recruited from the blood into the tissue through the endothelium lining vessels. This occurs, classically in 4 steps: capture, rolling, firm adhesion and transmigration (61) although recent insights provide a better understanding of the dynamics involved at each step. For the adhesion cascade to be successful, EC must express selectins for rolling and integrin adhesion molecules for firm adhesion. Furthermore, integrins that bind specifically with adhesion molecules must be expressed of receptive T-cells to allow adhesion.

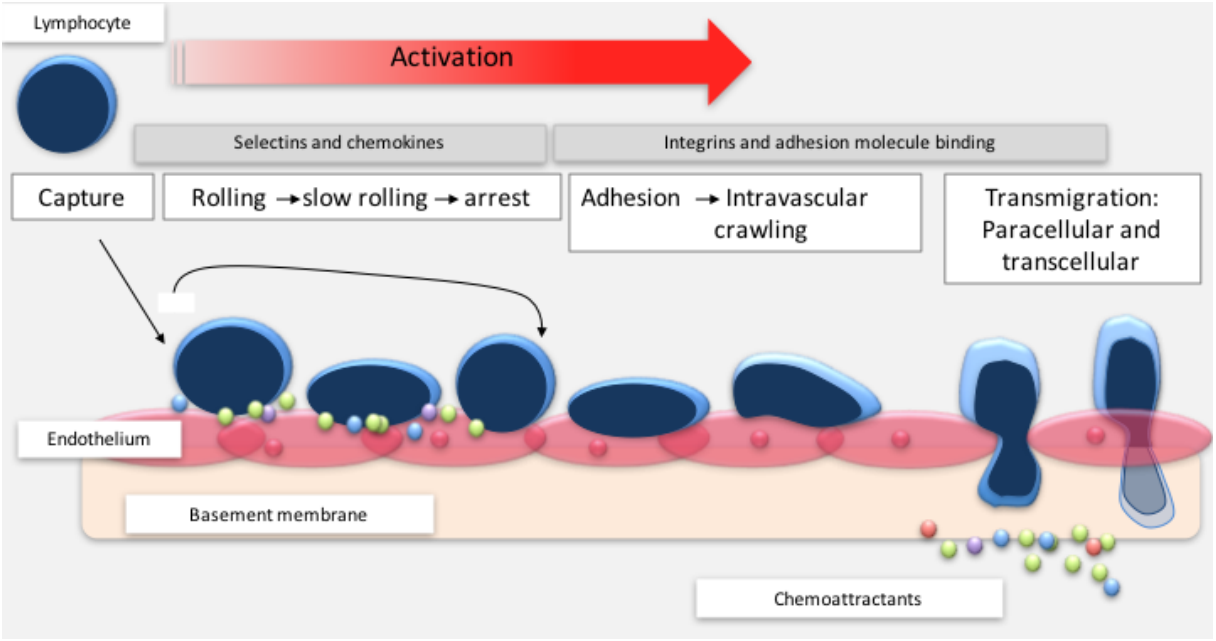

Figure 1.7: The adhesion cascade.
This schematic outlines the key events that occur one after another as a cascade and result in recruitment of leukocytes across the endothelial layer and basement membrane. The initial step of capture occurs as a result of reduced vessel diameter and unavoidable leukocyte-endothelial contact. It is at this point of contact where the leukocyte is able to detect the chemokine profile of the endothelial cell layer. Chemokine-chemokine receptor binding leads to integrin activation and rolling. Once leukocyte integrins are activated, they are able to bind to endothelial expressed adhesion molecules with valence and avidity and results in leukocyte arrest. The leukocyte is able to engage it's cyto-skeleton and reach an endothelial cell-endothelial cell junction via locomotion to migrate along the paracellular route or they migrate directly across an endothelial cell. Image is authors own adapted from (62).

Capture

Capture is a term used to describe the active attraction of immune cells from the circulation towards the endothelial surface of the blood vessel. This is achieved principally by changes in haemodynamics. As vessels reduce in luminal diameter and form networks of post capillary venules, the velocity of flow slows and leukocytes are in much closer contact with the endothelial surface.

As leucocytes flow through vessels they bind to E-selectin, expressed on EC luminal membrane by glycosylated ligands such as P-selectin glycoprotein ligand 1 (PSGL1) (63). This initiates slow rolling where lymphocytes travel at a slower velocity; approximately 5-10μm/s. Selectins are type 1 cell surface glycoproteins that bind to

complex carbohydrate molecules. There are 3 selectins; L, P and E-selectin. L and P-selectin are expressed by leukocytes and platelets respectively, whereas E-selectin is expressed by endothelial cells (64). The structure of E-selectin consists of one N-terminal, one C-type lectin, one EGF-like, six sushi repeat unit, one transmembrane, and one intracellular domain. During rolling, Selectins and ligands that have sialyl Lewis^X complex carbohydrate bind with limited affinity and "bind and release", which with shear forces from blood flow allows continued, low velocity movement (65). The purpose of rolling is to facilitate the activation of integrins by chemokines allowing integrin-adhesion molecule binding (66). This results in firm adhesion and arrest. There is evidence to support binding of vascular cell adhesion molecule 1 (VCAM-1), which is expressed on the endothelial surface, to its integrin ligand $\alpha4\beta1$, also known as very late antigen 4 (VLA-4), which is expressed on lymphocyte populations, contributes to slow rolling and tethering (67) (Figure 1.7).

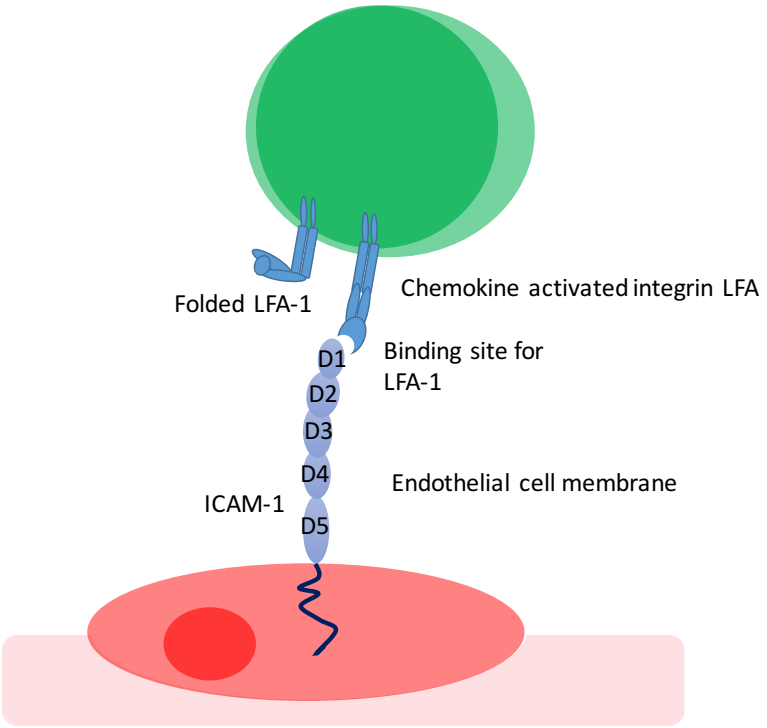

Figure 1.8: ICAM-1 and LFA-1 binding.
The image represents ICAM-1 with 5 domains present on the endothelial cell surface. The β2 integrin LFA-1, is reported to bind to domain 1 of ICAM-1 by the I domain (68). Initially, LFA-1 is inactive and folded. To achieve binding, the integrin must first be activated by chemokines on the endothelial surface. Image in authors own, adapted from (69).

Arrest

Firm arrest arises because of lymphocyte integrin activation achieved by chemokines on the endothelial surface. Chemokines are cytokines with chemotactic properties. They are approximately 10 kilodaltons in size and are secreted by several cell types. In the adhesion cascade they are secreted by various cells at the site of inflammation.

They bind to specific chemokine receptors found on target cells and activate cytoplasmic G-proteins producing downstream intracellular signaling pathways. Chemokines are classified into CXC, CC, CX3C and XC groups according to minor

differences in structure (70). Chemokines that lead to integrin β1 and 2 activation include CCL3, CCL4, CCL19, CCL20, Regulated on Activation, Normal T Expressed and Secreted (RANTES)/CCL5, CXCL9, CXCL10, CXCL12, CCL17 (68, 69, 70, 71, 72, 73). Chemokine-dependent activation, termed inside-out signaling, results in unfolding of integrins and increases the affinity of binding with the receptor. Furthermore, chemokine activation allows integrin clustering, which promotes multivalent binding and thus increased valency (74). Integrin ligands expressed on endothelial cells within a vessel lumen are Intercellular adhesion molecule 1 (ICAM-1) which binds with αLβ2 (CD11a/CD18) and αMβ2 (CD11b/CD18), VCAM-1, which binds with α4β1/VLA-4 and Mucosal addressin cellular adhesion molecule (MAdCAM-1), which binds with α4β7 (78). Downstream signaling as a result of integrin binding, termed outside-in signaling, is thought to result in adhesion(62).

Adhesion strengthening and spreading

Integrin binding results in anchoring the leukocyte cytoskeleton via proteins Talin and Vinculin (79, 80) and can lead to increased integrin clustering and activation (81, 82). The resultant integrin binding leads to arrested movement of the lymphocyte on the endothelial cell surface.

Intra-vascular crawling and trans-endothelial migration

Inflammatory cells use their integrins to crawl along the endothelial layer, termed locomotion, until they reach a point which is suitable to migrate across the endothelial layer (83). Migration of leukocytes across the endothelial layer has been described to occur by both paracellular and transcellular routes (84). Paracellular migration occurs at endothelial cell-cell junctions. CD31, Junctional adhesion molecules (JAMs),

Endothelin selective adhesion molecule (ESAM), ICAM-1 and VCAM-1 are preferentially expressed at these sites and actively facilitate transmigration(85, 86, 87). In addition, cell-cell junctions consist of adherens junctions comprised of VE-Cadherin complexes necessary for endothelial cell-cell adhesion (88). Increased endothelial cytoplasmic calcium, caused by ICAM-1 cross linking, allows cell-cell junctions to disassemble and thus provides a passage for leukocytes to migrate across (89).

Ultimately, dynamics and velocity of blood flow, expression of adhesion molecules on endothelial cells (ECs) and lymphocytes, and products of EC and leukocyte activation such as chemokines are key regulatory factors in lymphocyte adhesion (90). Expression of key regulators of this process is site and context specific and thus adhesion molecules and chemokines present opportunities for therapeutic intervention. In particular, Mucosal Addressin Cellular Adhesion Molecule (MAdCAM-1) has been found to be specifically expressed by venules within the lamina propria of human gut mucosa (91) and relies upon CCL25 present on the endothelial surface which binds to immune populations that express CCR9 (92). This activates integrin $\alpha 4\beta 7$ and facilitates adhesion to MAdCAM-1 expressed on the endothelial surface (93). Interestingly MAdCAM-1 expression is tissue specific and has increased expression in venular endothelium within foci of inflammatory tissue found in Ulcerative Colitis (UC) and Crohns' disease (94). This highlights possibilities to target the chemokine and receptor interactions to modify trafficking of immune populations across the endothelium.

Similarly, expression of endothelial adhesion molecules may also be a source to regulate immune cell trafficking. Reports exist suggesting reduced expression of ICAM-1 in renal tumour vasculature (95) and VCAM-1 in tumour-infiltrating vessels in human lung (96) which result in reduced TIL numbers. Similarly work in ovarian tumours has

implicated Endothelin B receptor in inhibiting recruitment of tumour infiltrating lymphocytes (TIL) (97), and up regulation of the chemokine CXCL16 by tumours following therapeutic interventions has been shown to be important for the recruitment of tumour-specific CD8+ lymphocytes (98).

Key Immune cell and stromal sub-populations within colonic tumours

In colorectal cancer the type, location and environment of tumour-resident immune cells alters the effects these cells have upon tumour and disease progression (2). The protective role that immune surveillance provides against tumour formation, and how this can be used therapeutically, has been explored recently.

CD8+ T lymphocytes

Cytotoxic T cells (CTL) that arise when CD8+ T cells are activated are known to destroy tumour cells (99) through lysis. Tumours have cell surface antigens that are tumour-specific making the process of tumour cell recognition by CTLs possible. The processes of CD8+ T cell activation and tumour cell recognition requires an antigen-presenting cell, usually a dendritic cell (100), that presents major histocompatibility complex-1 (MHC-1) molecules to CD8+ cells (101).

Intratumoural CD8+ and activated memory T cells have prognostic relevance. The characteristics and location of immune populations in tumours have been shown to impact disease progress and patient survival (2). Galon *et al*., characterized the immune cells found in colorectal cancer samples by microarray and immunohistochemical techniques. They found a significant correlation between

density of overall CD3+, CD8+ T cells and activated T memory cells within the tumour and disease-free and overall patient survival. Furthermore, these densities were more accurate predictors of disease-free and overall patient survival than the conventional TNM histological classification. A strong positive correlation with T memory and CTL markers and reduced tumour recurrence was observed (102). Higher intratumoural CD8+levels, relative to CD4+, have also been shown to correlate significantly with an improved 5 year survival (103). These findings suggest prognosis is dependent upon the adaptive immune response and, as such, augment the potential to manipulate the immune response for a therapeutic gain. Mechanisms that prevent intratumoural immune down-regulation by inhibiting Cytotoxic T-Lymphocyte Associated protein-4 (CTLA-4) or Programmed Death-1 (PD-1) molecules have been explored. Human trials using Ipilimumab have shown that CTLA-4 checkpoint blockade can improve survival in patients with metastatic melanoma (104). Other studies show some tumour objective response in melanoma, non-small cell lung, and renal cancers using PD-1 antibodies (105), however no response was found in colorectal cancer.

Th17 lymphocytes

Not all immune populations provide an anti-tumour response. While naïve CD4+ T cells can be differentiated into T helper 1 (Th1) when stimulated by interleukin 12 (IL-12) (106), T helper 17 (Th17) form when CD4+ T cells are stimulated by IL-6 and TGF-β (107). The presence of Th17 cells correlates with a poor prognosis (102). This may be through IL-17 production which has been reported to promote tumour growth and angiogenesis (108).

Regulatory T lymphocytes

Foxp3+CD25+CD4+ Regulatory T- cells (T-regs) are produced *de-novo* by the thymus as a mature subset of T cells and they can also be derived from naïve T-cells in response to TGF-β (109). Their immuno-suppressive characteristics are well understood with regards to preventing autoimmune disorders (110). In the context of tumours, T-regs are described to maintain their immunosuppressive qualities by eliminating T-cell responses to self tumour antigen (111). T-regs occupy approximately 10% of the CD4+ intra-tumoural population (112) which is driven by CCL22 (112). T-reg accumulation is associated with a worsened prognosis in ovarian cancer models (113) and low densities within the stroma of colorectal cancer is associated with a response to neoadjuvant therapy (114).

Tumour associated macrophages

Macrophages originate from bone marrow in the form of monocytic precursors (115). Monocytes are recruited by tumour cells secreting VEGF, PDGF-1 and chemokines CCL2, CCL3, CCL4 and CCL5 from the circulation into tumour tissue (116)(117). They differentiate into M1 or M2 Tumour Associated Macrophages (TAMs) according to environmental stimuli (118). Differentiation towards an M1 profile occurs as a result of IFN-γ, LPS and toll-like receptor agonists (TLR)(119). M1 TAMs express pro-inflammatory cytokines, TNFα, IL-12, IL-23 (119). The M2 polarized macrophages are further subdivided into a, b, c, and d. The Th2 cytokines IL-4 and IL-13 facilitate M2a differentiation. LPS, TLRs, and interleukin 1 receptor agonist (IL-1ra) facilitate M2b differentiation. IL-10 and TGFβ are able to induce M2c type macrophages (120). In tumours, macrophages follow a M2 differentiation which is driven by tumour derived

factors (121) and they produce factors which support the growth of the tumour by promoting tumour angiogenesis, immunosuppression and metastases.

Tumour associated fibroblasts

With regards to T-lymphocyte sub populations, it is unclear whether the dominant immune populations within tumours are entirely due to regulation of intra-tumoural proliferation, differentiation or endothelial recruitment. This is likely to be governed by tumour cells directly or by tumour associated fibroblasts. The chemokines and growth factors that define the differentiation pathway in tumours are produced and secreted by stromal cells such as tumour cells and tumour associated fibroblasts. Fibroblasts are predominantly responsible for producing the collagen matrix supporting the structure of tissues. In colorectal cancer, the number of fibroblast-like cells is greater than found in the adjacent normal colorectal tissue (122). Furthermore, tumour associated fibroblasts exhibit different phenotypes than those from the surrounding host tissue. Often fibroblasts in tumours display an "activated" phenotype typical of myofibroblasts by expressing smooth muscle actin (α-SMA), in addition to standard fibroblast markers. This may be initiated by growth factors such as TGF-β and PDGF released by cancer cells (123). It is likely that, once activated, they may not only contribute to cancer progression directly, through formation of the extracellular matrix, but also through releasing cytokines, such as IL-6, that can influence the pathway of TIL differentiation as shown in murine models (124). It is unclear whether the expression of phenotypic markers and adhesion molecules displayed by tumour endothelial cells (TEC) is entirely self-determined or requires stimulation by factors

either presented or secreted by tumour cells (125) or tumour-associated fibroblasts within the stroma.

Summary

This chapter provides an introduction into how tumour endothelium provides an attractive target for anti tumour therapies. Furthermore, it highlights how the endothelium may be exploited and regulated to increase CD8+ T-cell adhesion in tumours and overcome evasion of the host immunological anti-tumour response. Investigation of these theories depends upon developing *in vitro* models of human primary colorectal tumour endothelial cells. Thus, the hypotheses underlying my research project are as follows and the specific experimental aims are detailed below.

1.5 Hypotheses

- Tumour endothelial cells (TEC) in human colorectal cancer express a different phenotype than non-malignant endothelium in normal colorectal tissue
- By exploiting the tumour specific phenotype, primary human colorectal cancer tumour endothelial cells can be cultured *in vitro*
- The cell surface adhesion molecule profile of colorectal tumour endothelial cell differs to normal endothelial cells (NEC) and moreover, the levels of adhesion molecule expression will vary across CRC samples reflecting the variance in density of tumour infiltrating lymphocytes. Some tumours will strongly express adhesion molecules and some will not express high levels of adhesion molecules.
- The stromal, tumour associated fibroblasts in CRC regulate the adhesion profile and function of primary human colorectal tumour endothelial cells.

1.6 Aims and objectives

1. To develop a method to effectively isolate pure populations of tumour endothelial cells. These will be used to characterize cell phenotype and to develop and validate a method for long-term culture of primary human colorectal tumour endothelial cells.
2. To use primary human colorectal NEC and TEC in *in vitro* models to quantify and investigate adhesion of CD8+ T-lymphocytes under static and flow conditions.

3. To evaluate the effect of tumour associated fibroblasts on the adhesion molecule profile and function of NEC and TEC, and to characterize the soluble factors produced by TAFB.

4. To investigate the effect of inhibiting individual soluble factors produced by TAFB on the adhesion molecule profile and function of NEC and TEC.

CHAPTER 2

Methods and materials

2.1 Human tissue and blood collection and storage

All human colorectal tissue was obtained from the Queen Elizabeth Hospital (QEH Birmingham, UK) from patients who were undergoing resection of colon or rectal tumours of all stages, not requiring preoperative neo adjuvant chemo-radiotherapy. Liver tissue was also collected from patients undergoing liver resection or explanted livers collected during liver transplantation at the QEH. Matched specimens were sent for routine histopathology. Those with malignancy were staged using the TNM classification and for colorectal cancer, Dukes staging was also performed. Colorectal tissue was transported from surgical theatre to the Department of Pathology where consultant histopathologists provided a sample for processing *in vitro*. These were transported to the Liver Laboratories in Dubecco's modified eagle's medium (DMEM, Gibco, CA, USA), supplemented with 4% foetal bovine serum, 1%L-Glutamine and 50 units/mL penicillin/streptomycin (Gibco, CA, USA). Samples were either stored or used immediately. Liver tissue samples were also collected from surgical specimens and stored in DMEM at 4^{o}C for up to 36 hours before use for cell isolation. Samples for histological analysis were snap frozen or formalin-fixed immediately upon receipt in the lab.

Fresh tissue samples were either in the form of approximately 1-2cm^3 chunks used for cell culture and/or isolation, or biopsies of colorectal tumour and neighboring

normal tissue, that were approximately 5mm^3 in size. In general, biopsies were placed in bijou containers, labeled and frozen at -80ºC for later use. For cryopreservation, cell pellets were resuspended in 1ml of FCS with 5% Dimethyl sulphoxide (DMSO), purchased from Sigma, UK, and then immediately transferred to a pre-labeled sterile cryovial, placed in a freezing container (Mr Frosty™) and frozen at -80°C for 24 hours, after which, for long-term storage, they were then transferred to liquid nitrogen.

Blood was collected into Ethylenediaminetetraacetic acid solution (EDTA, molar concentration, Sigma, UK) from either healthy volunteers, patients with haemachromatosis (being therapeutically venesected: HFE blood) or patients undergoing resection of primary or metastatic colorectal tumours (CRC blood). All tissue samples and blood were collected and used with local research ethics approval and informed written patient consent.

2.2 Tissue culture reagents and supplies

Cell culture was performed under sterile conditions using class II laminar hoods, cleaned with industrial methylated spirits (IMS; Adams Healthcare, Leeds, UK) and plastic gloves (Premier Nitric). Sterile pastettes, pipettes (5,10 and 20ml), plastic tubes (15 and 50mls), culture flasks (25 and 75 cm^2) and cryovials were purchased from Corning Costar Incorporated, Bucks, UK. 1.5% Gelatin, or 1% rat-tail collagen (RTC, both purchased from Sigma, UK) were used for flask coating. Phosphate buffered saline (PBS) was prepared by dissolving PBS tablets purchased from Oxoid, UK with de-ionized water according to manufacturer's guidelines. Dubeccos Modified Eagles Media (DMEM), 1%L-Glutamine and 50 units/mL penicillin/streptomycin (PSG), heat inactivated foetal calf serum and human serum were purchased from Gibco, Invitrogen, UK. Roswell Park Memorial Institute 1640 media (RPMI 1640) was

purchased from Sigma-Aldrich, UK. Complete Endothelial Basal growth Media (EBM) was purchased from Gibco, Invitrogen, UK. Hepatic sinusoidal endothelial cell (HSEC) media was made up with EBM supplemented with 1% PSG and 10% human serum, 10ng/ml of vascular endothelial growth factor (VEGF) and 10ng/ml of hepatocyte growth factor (HGF, both available from Peprotech, UK).

Cell separation buffer (CSB) was prepared using PBS with 1% PSG 4% and 0.5mmol of EDTA. Fibroblast media was made with DMEM supplemented with 1% PSG and 4% FCS. Media used for Peripheral Blood Monocyte Cell (PBMC) isolation was made with RPMI 1640 supplemented with 10% FCS. Specific microvascular media "endothelial growth media -2- bullet kit" (EGM-2 bulletkit) purchased from Lonza, UK (cat. No. CC3202,), comprising basal endothelial media (cat. no. CC3156) which was supplemented by a pre-packaged chemokine/growth factor kit (cat no. CC4147) including human Epidermal Growth Factor (hEGF), hydrocortisone, gentamicin with Amphotericin-B (GA-1000), 25mls of foetal bovine serum (FBS), vascular endothelial growth factor (VEGF), human fibroblast growth factor B (hFGF-B), R3 insulin like growth facor-1 (R3 -IGF-1) and ascorbic acid. Accutase, purchased from PAA Laboratories Ltd., and Tryp-LE, purchased from Gibco Invitrogen, UK, were used for detachment of cells in culture.

Size of flask	Number of cells (per well)	Volume of media	Volume of PBS per well or flask	Volume of Accutase/Trypsin per well or flask
96 well	3×10^4	100-200µls	100-200µls	100-200µls
24 well	0.2×10^6	500µls	500µls	500µls
12 well	0.4×10^6	1ml	500µls	500µls
6well	1.2×10^6	2.5mls	1ml	500µls
$25cm^3$	2.8×10^6	5mls	5mls	3mls
$75cm^3$	8.4×10^6	10mls	10mls	6mls

Table 2.1. Volumes of solutions used for cell culture in different flask and plate sizes.

2.3 *General cell culture and passage*

Details of individual cell culture requirements are outlined below (Section 2.4). Cells were maintained at 37°C in a humidified 5% CO2 incubator and checked for growth, contamination and viability with an inverted phase contrast microscope (Olympus IX50). Media was changed according to adherent cell proliferation assessed subjectively. Where necessary, cell viability was quantified using trypan-blue and a Haemocytometer (CAM LAB, Cambridge, UK) according to standard protocols.

Solutions appropriate for cell type were used to detach adherent cells for passage. Accutase was used for colorectal endothelial cells, and Tryp-LE for all other cells types. Initially, media was removed and cells were washed with PBS and then a sufficient volume of proteolytic enzymes using Accutase or Tryp-LE (see Table 2.1) was added to cover the monolayer and left for approximately 5 minutes with intermittent agitation or until cells were detached at which point cells were collected with 1ml of FCS and up to 5mls of PBS and centrifuged at 550g for 5 minutes at room temperature. The supernatant was discarded and the cell pellet was used as required. Cells in suspension (non-adherent) were collected and centrifuged at 550g for 5 minutes at room temperature. The cell pellet was re-suspended in CSB buffer and used accordingly.

2.4 Final protocols for culture of specific cell populations

The protocols described below detail the optimized protocols used for specific human cell isolation and culture. Whilst the HSEC protocol reflects that used currently in the Centre for Liver Research, all tumour and colon protocols were developed by me and optimized during the current investigation.

2.4.1 Human Hepatic sinusoid endothelial cells (HSEC)

Liver specimens (approximately 50g of tissue) were diced in a sterile beaker with 20mL of sterile PBS and 5mls of type-1A collagenase (0.4µg/mL, Sigma-Aldrich, UK) followed by an incubation period of 30-40 minutes at 37°C. The tissue was then strained through fine mesh. Once strained and washed several times in PBS with centrifugation at 550g for 5 mins, the cells were suspended over a 33/77% (wt/vol) Percoll gradient (Amersham Biosciences, UK) and subsequently centrifuged at 550g for 25 mins with no brake. The cells collecting at the interface of the Percoll gradient were collected and washed several times to remove debris and mucous. Immunomagnetic depletion of epithelial cells was performed with mouse anti-HEA-125 (Progen Biotechnic, Germany; 50µg/ml) and then EC were positively selected using mouse anti-human CD31 dynalbeads (Dynal A.S.,Norway). Cell counts and viability assessment were then performed using Trypan blue and cells were then placed into rat tail-collagen coated culture flasks.

2.4.2 *Total cell isolation from human tumour and non-involved colorectal tissue*

All tumour samples were processed before any associated normal tissue. 6 X 15ml falcon tubes were prepared with 3mls of warmed endothelial basal medium (EBM, Lonza, Cat. no. CC3201) and then weighed. Meanwhile, the tissue biopsies were washed vigorously in 4x 40ml of cold PBS supplemented with antibiotics outlined above. Biopsies were transferred to a sterile petri dish and cut into $1mm^3$ pieces with a scalpel using a rocking motion. The diced samples were then distributed between the 3x 15ml tubes, which were then re-weighed, and the difference was calculated resulting in the weight of the tissue. Collagenase II (Biochrom AG, Cat. no. C2-22) was added (50µl of collagenase per 0.1g of tissue) and the total volume was made up to 2ml with EBM. The samples were then placed in a rotating shaker at 37°C for one hour. This was performed for both normal and tumour tissue. After one hour, the tissue was filtered through a cell-strainer (100µm nylon, BD, cat.no. 352360). The single cell suspension was centrifuged at 500xg for 5 mins at 20°C, the supernatant was discarded and the pellet was re-suspended in EBM-2-MV and transferred to a T-25 flask pre-coated gelatin (1.5%, Sigma, U.K.) and incubated over-night. After 24 hours the, supernatant was removed, the flask was washed gently sterile PBS and 5mls of fresh (pre-warmed) EBM-2-MV was replaced. Cell attachment to the flask was observed and media was changed daily until total cells reached 50-70% confluence at which point they underwent immunomagnetic bead-based selection to purify endothelial cell populations.

Total colonic cell populations in culture, were detached from flasks to produce a single cell suspension that was suitable for subsequent endothelial cell isolation.

2.5 Endothelial cell purification from tumour and normal colorectal cell cultures.

Several immunomagnetic bead techniques were trialed to isolate endothelial cells from the colorectal cultures described above. The protocols for the use of anti-human CD31 Dynabeads, MACs microbeads and MACs anti-flurochrome microbeads are outlined below. However, for some QPCR methods, endothelial cells were isolated using flow assisted cell sorting.

2.5.1 *Use of Dynabeads*

After digestion of tissue as described above, the single cell suspension, in a 15ml falcon tube, was centrifuged at 500g for 5 mins, after which the supernatant was removed and discarded. The remaining pellet was resuspended in 500µl of CSB to which 7 µl of anti-human CD31 dynabeads (11155D, Lifesciences, Invitrogen, U.K) were added and mixed well by pipetting. This solution was then incubated for 20mins at 4ºC with agitation. After incubation, 5mls of CSB was added to this suspension and the tube was inserted into a magnet (Invitrogen, cat. no. 12301D). Once the magnetic beads were identified to have separated from the solution, all the supernatant was aspirated from the tube and kept for fibroblast isolation. The tube with the positively selected cells was removed from the magnet. A further 5mls of CBS was used to gently wash the bead-bound cells and the magnetic process was repeated, however at subsequent washes the supernatant was discarded. The washed cells were resuspended in 5mls of pre-warmed EBM-2-MV (Lonza, UK) media and placed into a T-25 flask which had been pre-coated with 1% RTC. Cells were observed for growth and morphology, and the media was changed on every 24 hours until 50-60% confluence, at which point the cells either

underwent passage to a T-75 flask for expansion, or underwent a further anti-CD31 bead selection process and were replaced into a T-25 flask.

2.5.2. *MACS micro bead method to isolate human TEC and NEC*

Cells isolated as described above were pelleted by centrifugation at 300g for 3 mins. The supernatant was removed completely by aspiration. The cells were re-suspended in CSB buffer to a maximum concentration of $1x10^7$ per 60µl. To this, 20µl of FCR blocking agent was added, and cells were mixed briefly before 20µl of anti-human CD31 microbeads (both 130-091-935, CD31 microbead kit, Miltenyi Biotec) were added. The mixture was incubated for 15mins at 4°C, after which 1ml of CSB buffer was added before centrifugation at 300xg for 3mins. The supernatant was removed and the cells were re-suspended in 1ml CSB buffer ready to undergo magnetic separation. LS columns (130-041-306, Miltenyi biotec) were placed in the magnetic field of a midiMACS separator (Miltenyi biotec). The columns were prepared by rinsing through with 3mls of CSB buffer. The cell suspension was then applied to the column. Here, unlabeled cells within the solution flowed through the column and the magnetically labeled cells were retained within the column reservoir. Subsequent washing steps with 3x3mls of CSB buffer ensured that minimal contaminating cells were collected. Once the column reservoir was empty, the labeled cells were collected by removing the column from the magnet onto a collecting tube (15mls falcon), pipetting in 5mls of pre-warmed EBM-2-MV media and then pushing the plunger through the column. The eluted cells were then placed into a T-25 flask, pre-coated with rat-tailed collagen (RTC, 1%, Sigma, UK). Of note, for initial plating gelatin was used as a flask coating (as mentioned above) and for subsequent passages when endothelial cells were pure, RTC was used.

2.5.3. *Flow assisted cell sorting*

This process utilized a single cell suspension from freshly processed CRC and normal colorectal tissue. The pellet was re-suspended in 100μL CSB and 20% of the cells were taken as a "cells only" control sample. The remaining 80% of the cells were incubated with FITC-conjugated to anti human CD31 primary antibodies (Appendix 2) at 4°C in the dark on a rocking chamber. After incubation, the cells were washed in CSB with a live/dead cell marker at a concentration of 1μl/ml (eFlour780, ebioscience, U.K.) as per manufacturers guidelines and transferred to the cell sorter. Cell sorting was performed by Mr S. Suresh using the Mo-Flo High performance cell sorter (Beckman & Coulter, UK) and Summit 5.2 software. The cells only tube was used to correct for FITC auto-florescence. Gating strategies entailed gating upon 100% of the live CD31 + populations within the FITC channel. The remaining cells were discarded. All CD31 positive cells were collected in CSB and re-washed. The cell pellet was resuspended in 600μl of RLT buffer containing 6μl of β-Mecaptoethanol and stored at -80°C for later use.

2.6 Use of normal and tumour-associated colorectal fibroblasts (NFB &TAFB)

2.6.1 Purification of Fibroblasts from cell populations in culture

Fibroblasts were isolated from primary colorectal tumour and matched normal colorectal tissue as a byproduct from the endothelial cell isolation protocol. As such, the initial steps of tissue digestion, filtration and culture of total cell population were as described in 2.4.2. After isolation of the endothelial cells with positive selection using CD31 immunomagnetic beads at passage 1, the cell suspension containing the remaining CD31- cell populations were centrifuged at 550g for 5 minutes and the pellet was resuspended in 10mls of fibroblast media and placed in a T-75 flask to culture at 37°C.

2.6.2 Conditioning of NEC with supernatant from tumour fibroblasts

Supernatant from cultured primary colorectal TAFB and NFB was collected and fibroblasts were detached and counted. Supernatants were diluted based on the number of cells from which it derived. The standardised supernatant concentration was 2.5mls from $1x10^6$ fibroblasts. Any necessary dilutions were by using standard EBM-2-MV media. Confluent monolayers of NEC received 5mls in total of either NFB or TAFB supernatant solution or received standard EBM-2-MV media as a control. After 24 hours endothelial cells were detached and the resultant cell pellets were used as required.

2.7 *Purification of CD8+ T lymphocytes* from peripheral blood mononuclear cells

20mls of HFE blood or whole blood obtained from CRC patients (details outlined in 2.1.1) was diluted with 20mls of MACS buffer (PBS, 2mmol EDTA, 2% FCS). 15mls of Lympholyte (Cedarlane Technologies, US) was placed in 2x 50mls Falcon tubes, 20mls of diluted blood was layered on top and samples were centrifuged for 25mins at 500g with no brake. Cells were collected from the interface, washed further with CSB buffer and centrifuged at 550g for 5 mins. The supernatant was discarded and the pellet of cells was resuspended in RPMI supplemented with 10% FCS. This cell suspension was plated in an uncoated T-25 flask and incubated at 37°C for 24 hours. After 24 hours, monocytes were observed to have attached to the flask, and remaining non-adherent lymphocytes in suspension were collected and counted. At 24 hours, the total live count of cells (using Trypan blue) was typically $23x10^6$. These cells were washed with

CSB buffer and centrifuged at 550g for 5 mins. The supernatant was discarded and the pellet was then resuspended in 200µl of CSB buffer. To this a further 40µl of heat inactivated FCS was added and 40µl of antibody mix from the 'Dynabeads Untouched Human CD8+ T cells kit' (Invitrogen, cat. no. 11348D) was added. The mixture was incubated for 20 mins at 2-8°C. After this, the cells were washed in 1ml of CSB buffer and centrifuged at 350xg for 8 mins at 2-8°C. The supernatant was discarded and the pellet was resuspended in CSB buffer. 200µl of pre-washed Dynabeads was added to the cell suspension which was then incubated for 15mins at 18-25°C with gentle rotation. After incubation, 1ml of CSB buffer was added and the cells were pipetted thoroughly without foaming. The tubes were placed on a magnet (Invitrogen, cat. no. 12301D) for 2 mins. The supernatant (containing all untouched CD8+ T cells) was transferred to a new tube. 1ml of CSB buffer was added to the tube containing Dynabeads to resuspend the beaded cells (unwanted cells) and magnetic selection was repeated to permit elution of any remaining unbound CD8+ cells

2.8. Flow cytometry

Antibodies used for flow cytometrical analysis are listed in Appendix 2.

2.8.1. *Single and multi-colour flow cytometry*

Endothelial cells isolated using CD31 selection, either from fresh tissue or from cultured populations, were investigated using cytometry to characterize their cell surface expression profiles. Cell pellets were re-suspended in 100μL MACS buffer (PBS, 2mmol EDTA, 4%FCS) and transferred to the appropriate number of FACS tubes allowing for Isotype matching controls (IMCs) for each antibody. The ECs were then incubated with optimal concentrations of primary antibody (Appendix 2) at 4°C in the dark on a rocking chamber. Cells were analysed using the Becton Dickenson FACS caliber flow cytometer which has 488nm, 405nm and 642nm lasers. This allowed the measurement of FITC, PE, PE-Cy5, PE-Cy7, V460 Pacific orange, APC and APC-Cy7 florochromes. A "cells only" control tube was always analysed first. Cell debris and detached beads were excluded by gating on populations within an endothelial gate based on size and side scatter. Voltages were adjusted so that isotype control peaks were positioned between $0\text{-}10^1$ on the intensity axis (See Figure 2.1). Experiment tubes were subsequently analysed against their respective IMCs (Appendix 3).

Where multi-colour flow cytometry was performed, single colour tubes of normal colorectal endothelial cells stained with a single fluorochrome- conjugated antibody per tube were used for compensation. To compensate for fluorochrome spillover, median fluorescence intensity (MFI) of the positive and negative populations were aligned against the relevant channels and then cells were analysed. Both percentage positivity and median channel value (MCV) were collected.

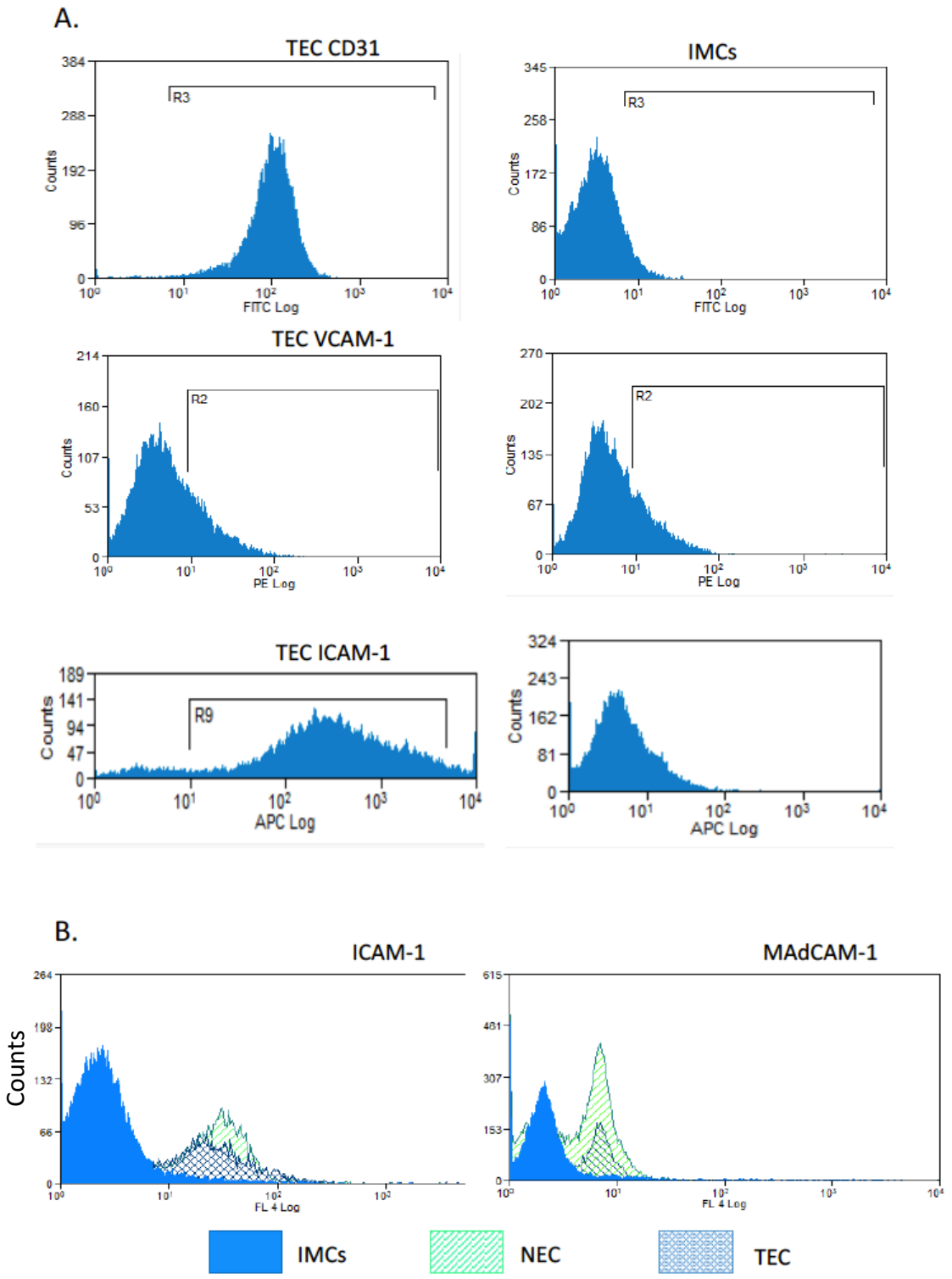

Figure 2.1: Representative Flow cytometry univariate histograms.
Flow cytometry was performed to assess the percentage and MCV expression for cell surface markers on both NEC and TEC using Summit v4.3 software. These plots are representative of data obtained. Event counts are plotted on the x axis and is set between 10^0 and 10^1. A. contains data for TEC only with matching IMCs in the adjacent histogram. B. contains data for matching NEC and TEC with matching IMCs superimposed in one histogram.

2.9. Polymerase Chain Reaction (PCR)

2.9.1. mRNA extraction from whole tissue and human cells

Whole tissue, stored either at -80°C or in RNA later (Sigma, UK), or cultured cells were used for mRNA extraction. For extraction of total RNA, the RNeasy kit (QIAGEN, UK) was used according to manufacturer's instructions. Where whole tissue was used, no more than 30mg was homogenised in 600µl of RLT buffer containing 6µl of β-Mecaptoethanol. The resultant solution was then passed through a blunt 20-gauge needle fitted to an RNAse free syringe, 5 times. When tissues were homogenised, it was centrifuged at full speed for 3 mins. The lysate was carefully transferred to a new 1.5 ml collection tube. To homogenise cells after culture, immediately after detachment they were placed into a 1.5ml collection tube in 600µl of RLT buffer containing 6µl of β-Mecaptoethanol and cells were lysed using a blunt 20-gauge needle fitted to an RNAse free syringe, 5 times. Homogenised tissue or cells were either used immediately or stored at -80°C for future use. For mRNA extraction, all preparations were treated using the manufacturers standard protocol (Qiagen, UK) and the resultant mRNA was eluted using RNase free water. Purity and yield of mRNA were calculated using a nanodrop spectrophotometer (Implen, UK).

2.9.2. cDNA synthesis from mRNA extracts

cDNA was made from mRNA extracted as described above using an iScript ™ Select cDNA synthesis kit (BioRad laboratories, U.K.) according to the manufacturers guidelines. The components were added (4µl of 5X iSript select reaction mix, 2µl of random primers, 1µl reverse transcriptase, 1µl mRNA sample, Nuclease free H_2O to make up to 20µl) to a 0.2ml PCR tube and samples were incubated through 25°C for 5mins, then 42°C for 30mins, then at 85°C for 5 mins using the G-Storm Thermocycler

(Labcare, UK), then stored at -20°C. Of note, the same amount of mRNA was used in samples being compared. The volume used was calculated from the concentration of mRNA provided by the nanodrop measurement.

2.9.3. Standard PCR and semi-quantitative analysis

PCR was performed using BioMix Red (Bioline,UK) with self-designed primers of approximately 200 base pairs (Sigma, UK, see Appendix 4). The components were added (1µl Primer mix, 1µl cDNA, 3µl ddH_2O, 5µl BioMix Red) to a 0.2ml PCR tube and then incubated using G-Storm Thermocycler (Labcare, UK). The thermal profiling details are outlined in Appendix 5. Proteins were separated through a 2% agarose gel incorporating 1.5µl ethidium bromide in 1L of 1%TBE for 90 minutes at 133volts. Semi-quantitive information of gene expression was visualized using GeneGenius Bio Imaging System (Syngene, UK) and Genesnap software (Syngene, UK).

2.9.4. Quantitative PCR and analysis

All mRNA isolation and cDNA synthesis was performed as outlined in sections 2.9.1 and 2.9.2. Where ECs were isolated from fresh tissue, flow assisted cell sorting with collection of ECs directly into 600µl RLT buffer (QIAGEN minikit) with 6µl β-MTE was performed. Due to low concentrations of mRNA extracted from some samples, 45ng of mRNA was used to synthesize cDNA for subsequent RT-QPCR.

A) QPCR using TaqMan® (Lifetime technologies) primer and probes (Appendix 6). Using 96 well, skirted plates (Applied Biosystems, UK), primers for our genes of interest or housekeeping genes (β-actin and GAPDH) were placed into triplicate wells ensuring that wells on the edge of the plate were avoided. GAPDH and β-actin were

chosen as best housekeeping genes for comparing colorectal cancer tissue and matched normal colon tissue based on current literature (126). To each well, the following was added; 1 µl cDNA, 5µl of 2xTaqMan MasterMix (Applied Biosystems, UK), 0.25µl of primer of interest (above), 3.75µl of RNAse free water (QIAGEN, UK). This made up 10µl of solution in which we were careful not to create air bubbles. An optical adhesive cover (Applied Biosystems, UK) was applied and a seal was achieved. The plate was then centrifuged for 3 mins at 550g.

B) RT²- profiler PCR array (QIAGEN, 96-well format, human endothelial cell biology kit, cat no 330231 PAHS-015ZA). Before starting, the 2xRT² SYBR green mastermix (QIAGEN, U.K.) was centrifuged for 10-15 seconds to bring the contents to the bottom of the tube. For each 96well plate, 1350µl of mastermix, 102 µl of cDNA (at 45ng of mRNA/µl), 1248 µl of DNAse free water (QIAGEN, U.K.) was mixed in a 5ml bijoux before being transferred to a RNAse free loading reservoir. Each RT² profiler PCR array plate was removed from its foil wrapping. Using an 8-channel pipette and DNAse free filtered tips, 25µl of the mix was added to each of the 96 wells. The tips were replaced for each well to reduce the risk of primer contamination between wells. 12 thin wall 8-cap plastic strips, provided with the 96 well plates, were used to tightly seal the plate, which was then centrifuged at 1000g for 1 minute at room temperature to remove all air bubbles.

2.9.5. QPCR Analysis

For both methods detailed above, a Stratagene® (model Mx3000P) QPCR machine was used to run a standard QPCR protocol for 2hours 31 mins. During set up of the cycler, the 96-well plate was kept on ice and when inserted into the machine, a compression pad was applied as recommended by the cycler manufacturer. This protocol involves 1 cycle at 95°C for 10 minutes to activate the DNA Taq polymerase and is then followed by 40 cycles at 95°C each lasting 15 seconds followed by a single 1 minute cycle at 60°C to collect fluorescence data. Data was then collected in the form of CT values and amplification curves. To work out the differential expression of the gene of interest the ΔΔCT formula was used (Figure 2.2).

$$\Delta CT_{TEC} = (CT_{TEC} \text{ gene of interest}) - (CT_{TEC} \text{ housekeeping gene})$$

$$\Delta\Delta CT = \Delta CT_{TEC} - \Delta CT_{NEC}$$

$$\text{Fold change} = 2^{-\Delta\Delta CT}$$

Fig 2.2. Calculation used for relative quantification of gene expression. Adapted from Pfaffl et al (127).

2.10. Immunohistochemistry

Immunohistochemistry was performed using 5-7μm tissue sections from human colorectal tumour, uninvolved colorectal tissue, colorectal liver metastasis and uninvolved liver tissue. Frozen sections were cut at 7μm and mounted onto coated slides (Leica Biosystems, UK) before being acetone-fixed, and stored in foil at -20°C. Frozen tissue sections were removed from storage but kept in foil and warmed to room temperature for 30 minutes prior to staining. Endogenous peroxidases were blocked using 0.3% hydrogen peroxide solution in methanol (both Sigma UK) for up to 40 minutes. Slides were then washed. 10% Casein was used for 30 minutes to block non-specific staining. The slides were then incubated at room temperature on a rocking moisture chamber with optimal concentration of primary antibody or IMC control for 1 hour (see Appendix 7). After further washing, the slides were then incubated with vector Immpress Anti mouse MP7402 secondary reagent (Vector labs, UK) for 30 minutes. Impact DAB (Vector labs, UK) was then used as a substrate and left for 2 minutes, and filtered Mayers haematoxylin was used as a counterstain. The slides were dehydrated using ascending sequence of alcohol and clearene and then mounted with cover slips using DPX mountant. Slides were viewed with bright field microscopy using a Zeiss Aviovert microscope and images were collected using Axiovision software. Images were captured at 10x magnification unless otherwise stated on the results. Semi quantification of the images was performed by 2 or more observers and both proportion of cells/vessels stained and intensity of staining were observed. Positive staining was marked as following; 0 = absent or no positive staining, 1 = partial or weak staining, 2 = most or strong staining and 3 = all or intense staining observed. Quantification of IHC staining was performed using Image J software which is described in section 2.13.

2.11. Enzyme Linked Immunosorbant assay (ELISA)

2.11.1. Indirect ELISA technique for cultured cells

Endothelial cells were grown to confluence on RTC-coated 96 well plates (Microtest tissue culture plate, BD sciences, U.K.) and underwent stimulation with recombinant human Interleukin-1β (IL-1β, Peprotech, U.K) or recombinant Tissue Necrosis Factor (TNFα, Peprotech,U.K.). Concentrations of 10ng/ml of IL-1β and TNFα and 100μg/ml of Bestatin hydrochloride (Sigma, U.K.) were made up using 50% EBM-2-MV media and 50% of un-supplemented EBM. Where endothelial cells were treated with fibroblast supernatant, the solution contained 50% harvested supernatant and 50% EBM-2-MV media. After treatment, each well was washed twice with 100μl of PBS and then fixed with 100μl 100% methanol. After incubation, the methanol was removed and then 100μl of PBS was added and cells were either used immediately or stored at 4°C for future use.

To develop the ELISA, PBS was aspirated and the cells were washed once with PBS, and then incubated with 1% goat serum and 1% horse serum (Sigma,UK) for 20 minutes to block non-specific binding. This was then removed and cells were washed twice in PBS, before 50μl of primary antibody or isotype control antibody, was added (Appendix 8) and incubated for 3 hours. After incubation with the primary antibody, the cells were washed 3 times in 100μl PBS with 0.1% tween (Sigma, UK). 50μl of secondary antibody (goat anti-mouse horseradish peroxidase-conjugated antibody 1:1000, Sigma, UK) was then added and wells were incubated at 4°C, in the dark, for 60 minutes. Following incubation, the secondary antibody was aspirated and the cells washed 5 times with 1% PBS with 0.1% tween. 50μl of TMB buffer substrate (Sigma, U.K.) was added and left for 5 mins, immediately after which, 50μl of stop reagent (1M Sulphuric acid, Sigma, U.K.) was added. Absorbance of each well was determined at

450nm. All antibodies and treatments were tested in triplicate and absorbance values were calculated as a mean triplicate absorbance, which was either pooled or tabulated as a ratio with non-treated values, once the isotype matched control value had been deducted.

2.11.2. Sandwich ELISA to quantify soluble mediators

To quantify soluble IL-6 produced by TAFB and NFB, a commercially available human IL-6 sandwich ELISA duo kit (R&D, U.K. cat DY206) was used according to manufacturer's guidelines. Similarly, CCL2 in supernatants of NEC and TEC, was quantified using a commercially available human CCL2 (MCP-1) sandwich ELISA (ready-set-go88-7399 eBioscience, Affymetrix, U.K). Briefly, the capture antibody was used to coat the 96-well plate, which was then incubated with a blocking agent followed by either a recombinant protein to create a standard curve or cell supernatants in triplicate. Streptavidin HRP conjugated secondary antibodies were used followed by a stop solution and plates were read immediately at 450nm. Each kit contained a positive control recombinant cytokine which was used to generate a calibration curve for protein concentration.

2.11.3. Proteome profiling arrays

Supernatants taken from several endothelial and fibroblast cell cultures were centrifuged at 500g for 5 mins to remove any solid debris, and samples were stored at -20°C until use. These were assayed using the human chemokine array kit or angiogenesis kit (Proteome Profiler Array, cat numbers ARY005 and ARY007 respectively, R&D, UK). The chemokine array was used to identify differences present in supernatants produced by primary human colorectal tumour and normal colonic

endothelial cells in culture. In addition, the array was used to investigate the differences between supernatants produced by primary human colorectal tumour associated fibroblasts and normal fibroblasts in culture. The angiogenesis array was used for TAFB and NFB supernatants only. The arrays were performed following the manufacturers guidelines. The array kit contained an antibody cocktail and a nitrocellulose membrane with capture proteins bound to the membrane at defined "spot" locations in duplicate. The supernatants were mixed with the biotinylated antibody cocktail whilst the membrane was incubated with a blocking agent. The membrane and the supernatant-antibody mix were then incubated together overnight. Proteins present in the supernatant, having formed antibody complexes could be captured on the membrane. A Streptavidin-Horseradish Peroxidase reagent and chemiluminescent detection reagents are added to allow imaging of the duplicate protein "spots". The intensity and size of the signal produced at the "spot" locations is proportionate to the amount of chemokine bound to the membrane. Signals were imaged by developing chemiluminescence detection film (Amersham, Biosciences) for 10mins with a Kodac X-omat 1000 processor (Birmingham, U.K.). The signal intensity was quantified using an Image-J macro courtesy of Dr S.T.Ward (see Appendix 9). To allow comparisons between samples, quantification was normalized against the median of the positive reference spots.

2.12. Functional adhesion assays

2.12.1. Stamper Woodruff (static adhesion assay)

Frozen tissue sections of CRC and matched NC cut at a thickness of 10 microns, either fixed with acetone or not fixed, were collected for use. The sections were prepared on the same day as CD8 + T cell isolation (see Section 2.7.4). The sections were defrosted at room temperature for 30 mins, then underwent rehydration with PBS for a further 30 mins. For specific blocking of adhesion molecules of interest, a reservoir was drawn around the section with a wax pen and then function-blocking monoclonal antibodies were applied at optimal concentrations (based on immunohistochemical staining see Appendix 10) for 1 hour at room temperature in a moisture chamber on a rocker. The antibody was then gently washed off with PBS and tween (0.1%) before applying 100µl total untreated CD8+T-cells at a concentration of 5×10^5 cells per ml. The slides were left static at room temperature for 30 minutes. After this the slides were washed gently with PBS 3 times, before being fixed for 2 mins in acetone and then undergoing haematoxylin and eosin staining. The slides were mounted with coverslips using Immunomount. Once dry, 3 representative fields illustrating cell adhesion were captured with a bright field microscope (Zeiss axioscope, Axiovision software) and the numbers of cells in the superior plane to the tissue were counted by two blinded reviewers, to account for inter-observer variability, using Image J software (cell counter tool).

2.12.2. Static adhesion assay using endothelial cell monolayers

Endothelial cells from tumour and normal colorectal tissue were grown to confluence in RTC-coated 24-well plates. Once confluent, cells were treated with agents of interest or left untreated. Agents used for treatment are outlined in Appendix 9. Whilst the

endothelium was stimulated on day 1, PBMCs were simultaneously prepared for CD8+ T cells isolation (see Section 2.7.4). CD8+T-cells were either left untreated or underwent prior incubation with blocking antibodies (see Appendix 11). Where receptor-blocking antibodies were used, incubation periods and washes were followed in according to manufacturer's guidelines. CD8+T-cells were then labeled with CSFE cell tracker according to manufacturer's guidelines (C34554 Invitrogen, UK) and then resuspended in EBM-2 (LONZA, UK) with 1% BSA at a concentration of $25x10^4$ CD8+T-cells/ml. NEC and TEC were incubated in the dark at 37°C for 30 minutes with 500µl of labeled CD8+T-cells. Adherent CD8+T-cells and TEC were fixed with methanol as previously described, and triplicate images captured at x20 magnification using Ultra violet microscopy (Nikon eclipse TE2000-5). Labeled cells bound to the endothelial monolayer, were counted using Image J software (cell counting tool). To compare data, the mean and SEM of the three images taken for triplicate wells was obtained.

2.12.3. *Chemotaxis assays*

To assess how CCL2 in colorectal TEC supernatant may affect the homing of CD8+ T cells TEC chemotaxis assays were performed across inserts with 5µm pores. (See Figure 2.3.) Anti-human CCL2 blocking antibody (R&D systems, U.K.) was used to treat triplicate wells of confluent primary human colorectal TEC (passage 4) in a 24 well plate. The wells were incubated with the blocking antibody for 1 hour. Simultaneously, CD8+ T-cells were isolated using CD8+T-cell untouched isolation bead kit (Invitrogen, UK) from HFE PBMCs. Lymphocytes were labeled with CSFE cell tracker and CD8+ T-cells were resuspended in EBM-2 (LONZA, UK) with 1% BSA at a concentration of $25x10^4$ CD8+T-cells/ml. Both antibody-treated and control TEC were incubated in the dark at 37°C for 12 hours with 500µl of labeled CD8+T-cells separated by Transwell

inserts (5µm sized pores, Corning Inc. USA, purchased from VWR U.K. cat no. 29442-118) after which inserts were removed, cell supernatant was aspirated and CD8+T-cells were counted using trypan blue and a haemocytometer. Adherent CD8+T-cells and TEC were fixed with methanol as previously described, and triplicate images captured at x20 magnification (Nikon eclipse TE2000-5). Data for captured cells were presented as absolute figures. Labeled cells adhered to the endothelial monolayer, were counted using Image J software (cell counting tool). To compare data, the mean and SEM of the three images taken for triplicate wells was obtained.

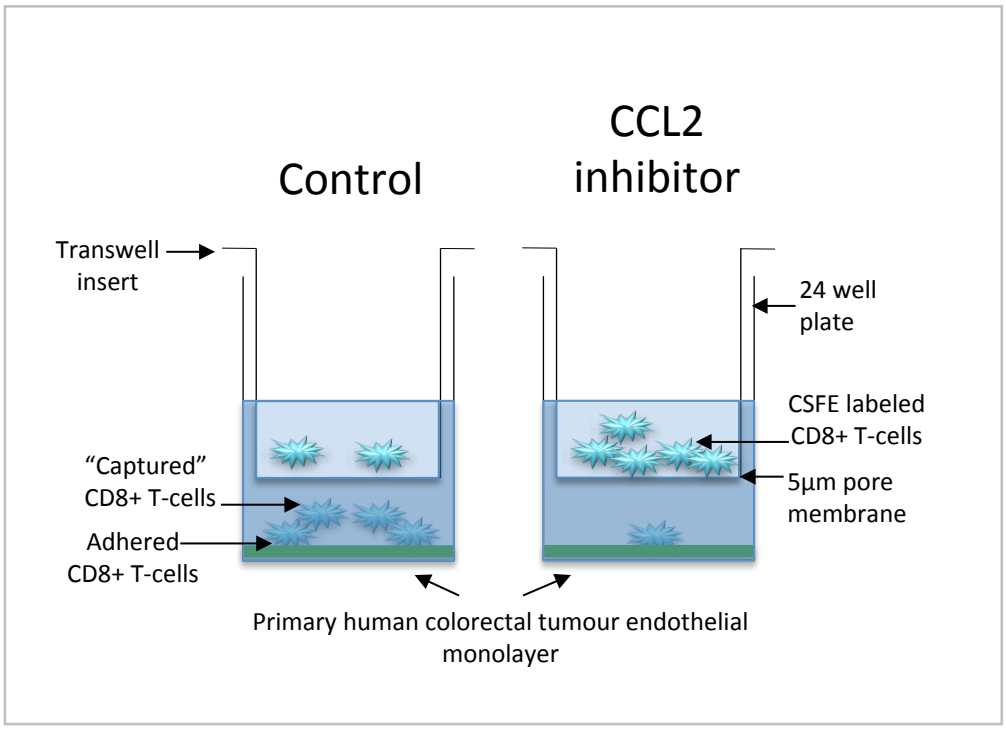

Figure 2.3. A diagrammatic representation of chemotaxis assay set up.
To understand if CCL2 produced by tumour endothelial cells may contribute to chemotaxis of CD8+ lymphocytes, Transwell inserts that would cause a partial barrier were employed. Quantification of cells attracted towards the TEC monolayer was performed microscopically in the presence and absence of CCL2 inhibitor.

2.12.4 Flow-based adhesion assays

Endothelial cells from tumour and normal colorectal tissue were grown to confluence in Ibidi μ-slide $sVI^{0.4}$ (IB-80606, Thistle Scientific, U.K.) according to manufacturer's guidelines (see Figure 2.4). This facilitates the study of lymphocyte rolling and adhesion in conditions similar to those *in vivo* (see photo insert of Ibidi slide in Figure 2.4). Once confluent, the cells in each lane either underwent specific treatments as required or were left untreated. Agents used for treatment are listed in Appendix 9. Simultaneously CD8+T-cells were isolated from HFE PBMCs. For flow assays CD8+ T-cells were used untreated. The flow-based assay was set up so that cultured Ibidi slides were adhered to the stage micrometer with masking tape and flushed with wash buffer (EBM-2 with 1% BSA) to ensure air bubbles are avoided. The equipment was set up as shown in the representative diagram (Figure 2.4); the syringe pump was set to a flow rate of 0.28ml/minute; the field area was 10x magnification; one syringe contained cells at a concentration of $1x10^6$/ml; the TV and recorder were set up ready for use. After 1 minute of washout the washout, a 5 minute cell perfusion period occurred during which rolling was recorded for the middle 3 minutes. The endothelial layer was then washed again with buffer for 4 minutes and the latter 3 minutes were recorded for adhesion. Recording, for both rolling and adhesion, was performed in 12 fields lasting at least 5 second, from the "out end" to avoid recording duplicate cells. This was repeated from each lane of the Ibidi slide. Rolling and adherent cells were then analyzed and counted off line. Rolling cells were described as those moving slower (typically 10-20um/sec) than the non-adherent cells in free flow of liquid (typically 100's of um/sec) but not static. Adherent cells were all those considered static, transmigrated, or adherent and shape changed/activated. Rolling was presented as a

percentage of adherent cells. Adherent cells were calculated using the equation in Figure 2.5.

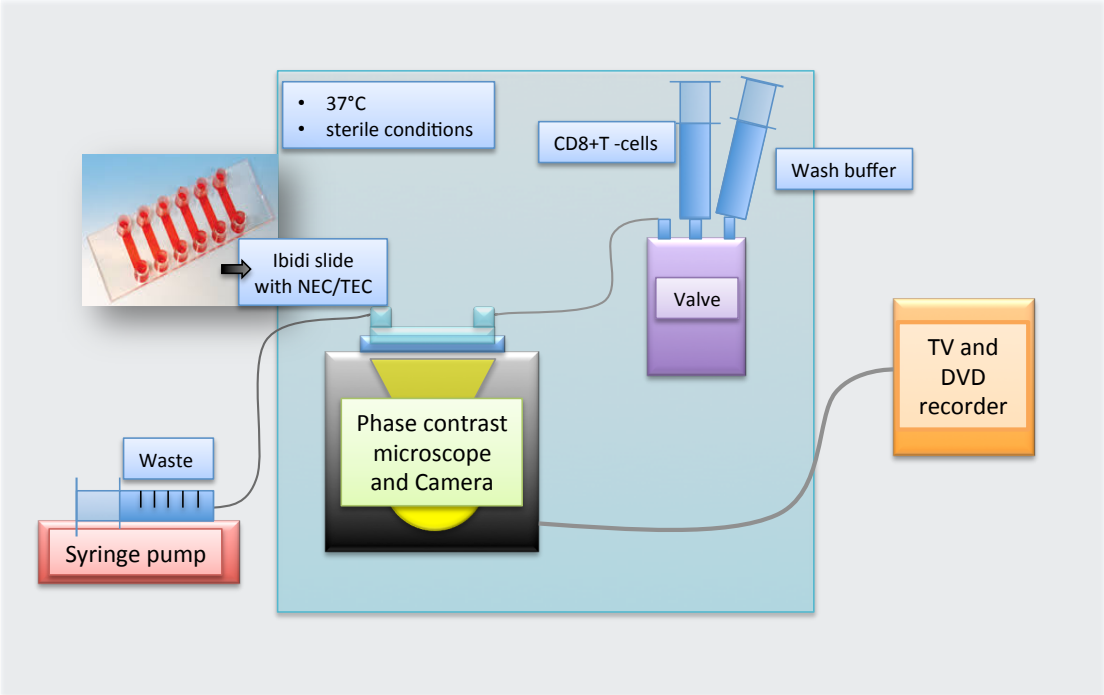

Figure. 2.4. A diagramatic representation of the flow assay set up.
Here, the ibidi slide, with a confluent endothelial cell monolayer, is placed on a stage of a microscope which is attached to a TV and DVD recorder. Lymphocytes and wash buffer are perfused over the endothelial monolayer and into the waste syringe. Real time video recordings are analysed off line to permit quantification of CD8+ T cell interactions with the monolayer.

$$\frac{\text{Number of cells counted}}{\text{Flow-rate x time x Area}} = \text{Adhered cells /mm}^2\text{/10}^6$$

$$\frac{\text{Number of cells counted}}{0.28 \times 3 \times 3.8} = \text{Adhered cells /mm}^2\text{/10}^6$$

Figure. 2.5. The equation used to calculate CD8+T-cell adhesion to the primary human colorectal tumour and normal endothelial monolayer after flow-based assay. Courtesy of Dr P. F.Lalor.

2.13. Image J analyses and Statistical Analysis

Image J is a Java image and processing and analysis program. The cell counter tool was used by downloading and opening available plug ins for "cell counter". Simultaneously, the image captured required for counting is opened. After initializing the image, counting can begin by selecting each identifiable cell with a coloured number corresponding to the cell type. After each click the counter is updated. Other Image J tools used included quantification of immunohistochemical staining. This was performed by converting the required image to greyscale, isolating positive DAB staining setting the threshold at 33% and then measuring the threshold areas as percentages of the image area.

Where data were continuous, results were presented in graphs as a mean and standard error. Within the results data was also presented as mean and standard deviation and this is annotated. Between multiple comparisons, statistical significance was calculated using ANOVA and significance between single comparisons were calculated using two-tailed Student's t-test. Both using SPSS software (IL,USA). Spearman's rank correlation coefficient by PRISM software (Graphpad, USA) was used to analyse the significance of correlation on two occasions; between CD31 expression of vessels in tumour and the corresponding number CD8+ tumour infiltrating lymphocytes and between αSMA expression in tumours and corresponding number CD8+ tumour infiltrating lymphocytes. Data was considered significance where $P < 0.05$. Data annotated with the following asterisks refers to significance accordingly; * denotes $P<0.05$ but >0.005, ** denotes $P<0.005$ but > 0.0005 and *** denotes $P<0.0005$.

CHAPTER 3

Long term culture and phenotype of endothelial cells derived from human primary colorectal tissue and colorectal cancer.

3.1 Introduction

Pre-clinical studies aimed at targeting TEC-specific markers have often used cell lines to explore the regulatory mechanisms of "molecules of interest" (128). Murine models are then used to test synthetic analogues or antibodies that inhibit the "molecule of interest", where tumours are implanted subcutaneously into nude mice, before being trialed in cancer patients (129, 130). Whilst these approaches generate valuable information, cell lines and murine models are not truly representative of what occurs *in vivo*. Differences between microvascular and HUVEC or large vessel endothelium are well documented and include variation in E-selectin, ICAM-1 and VCAM-1 expression in response to cytokine stimulus between small bowel (131) and dermal microvascular EC (132). For example, Haraldeson et al report increased expression of total cellular E-selectin in response to Il-1β stimulation in human intestinal microvascular endothelial cells (HIMEC) up to 72 hours, in contrast to a rapid biphasic response in HUVEC and a dose dependent up-regulation of VCAM-1 by IL-4 treated HUVEC, peaking after 8 hours compared to minimal effect on HIMEC. Similarly, dermal microvascular endothelial cells (HDMEC) show no significant VCAM-1

expression in response to IL-1β whereas this cytokine causes significant VCAM-1 up-regulation by HUVEC.

These findings provide our rationale for using tissue- and disease- specific endothelial cell culture models for functional studies and so, to understand the functional role or potential for targeting of TEC in CRC we must investigate the phenotype and conduct functional assays using primary endothelial cells derived specifically from human colorectal tumours. To date, only 2 laboratories have successfully isolated and cultured primary human TEC and matched host NEC. This is largely due to the convenience of cell lines and the perceived difficulties of culturing primary cells. Phenotyping data from these 2 studies collectively reveal *in vitro* colorectal NEC and TEC isolated by positive CD31 selection, express endothelial markers CD105 and VE-Cadherin. *In vitro* stimulated NEC and TEC are reported as expressing adhesion molecules E-selectin, ICAM-1 and VCAM-1 (133, 134). TEC are also documented to express higher levels of VEGFR-2 (134) than their matched host NEC. Despite these findings, to date, there is no available data to confirm whether TEC maintain tumour specific phenotype *in vitro.* Further to this there are no data describing use of cultured human colorectal NEC and or TEC in *in vitro* functional assays.

Therefore, this chapter outlines our data reporting the *in vivo* and *ex vivo* phenotype of NEC and TEC. I also describe how the optimal culture conditions were ascertained for NEC and TEC.

The key aims of this chapter are listed below.

1. To investigate the *in vivo* phenotype of microvascular endothelium derived from colorectal tumour and matched normal colon.
2. To explore whether the *in vitro* and *in vivo* phenotypes of NEC and TEC correlate.
3. To identify the optimal culture conditions for long term culture of these cell types.
4. To explore if there is a tumour specific phenotype of endothelial cells derived from CRC.

3.2. Results

3.2.1. CD31 is expressed by human colonic tumour microvascular endothelium

To assess the potential for isolation of endothelial cells from human colonic tumours, we sought to identify the most consistently expressed vascular-endothelium specific surface marker. We began by using immunohistochemical staining to assess the density of vessels in colorectal cancer and normal colon tissue sections. Examination of tissue sections stained with CD31 (see representative images in Fig 3.1) revealed positive cytoplasmic and membrane staining of the vascular endothelium through all tissue layers from mucosa to the deeper muscle layers in normal colon and through invasive mucosal and tumour stromal layers in colorectal cancer sections.

The intensity, consistency and microvascular-endothelial specific localisation of positive staining was reviewed and graded with a consultant histopathologist. Normal colon and colorectal cancer sections both displayed membrane and cytoplasmic CD31 staining on microvascular endothelial cells throughout the mucosal, submucosal and deeper muscle layers of NC and invasive and stromal tumour tissue from CRC. In addition, CD31 positive staining was also present in lymphocyte populations within both normal colon and colorectal cancer tissue.

Normal colon and colorectal cancer both displayed CD146 staining of the vascular endothelial cells. Importantly, CD146 expression was not present on the microvasculature of the lamina propria of the normal colon mucosal layer but predominantly on larger vessels. CD146 was also expressed by the smooth muscle and pericytes surrounding the larger vessels (Figure 3.1). Semi-quantitative analysis was performed to compare the intensity and proportion of positive staining by all cell types within both NC and CRC (Table E, Figure 3.1). Positive CD31 and CD146 staining was scored from 0-3 (where 0 is no positive staining and 3 is intense staining and staining of all cell types) for 9 pairs of matched NC and CRC. The mean proportion of microvascular endothelial cells stained positive with CD31, 2.6± 0.58, was significantly more than CD146, 1.3±0.58 ($p=0.047$). However, there was no statistical difference between the intensity of staining. There were significantly more immune cells stained by CD31, (mean 1.3±0.58 compared to 0, $p=0.016$), and more smooth muscle pericytes stained by CD146 (mean 0 compared to 1.6±0.58, $p=0.007$). There were no differences between NC and CRC in staining of CD31 or CD146 by cell type.

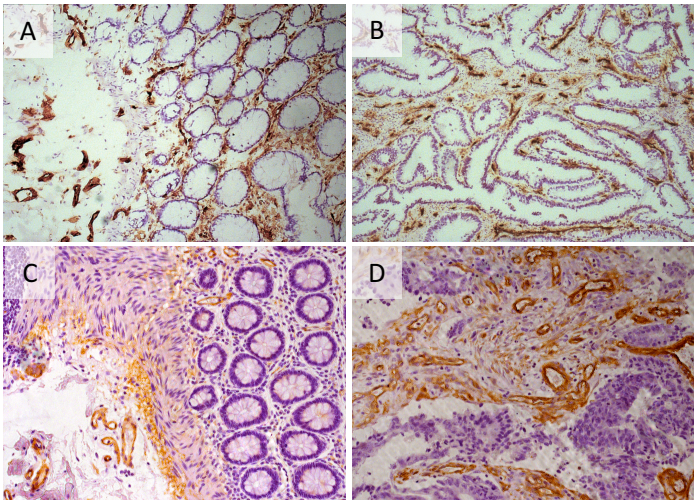

E

Antibody	Cell type	Endothelial cells		Immune cell infiltrates		Epithelial cells		Fibroblasts		Smooth muscle	
		NC	CRC	NC	CRC	NC	CRC	NC	CRC	NC	CRC
CD31	Proportion of staining	2.6 (2-3)	2.6 (2-3)	1.3 (1-2)	1.6 (1-2)	0	0	0	0	0	0
	Intensity of staining	3	2.6 (2.3)	1.3 (1-2)	1.3 (1.2)	0	0	0	0	0	0
CD146	Proportion of staining	1.3 (1-2)	1.3 (1-2)	0	0	0	0	0	0	1.6 (1-2)	1.6 (1-2)
	Intensity of staining	2.6 (2-3)	2.6 (2-3)	0	0	0	0	0	0	1.6 (1-2)	1.6 (1-2)

F

Tissue type / **Antigen**	**Normal colon** % Area of most intense positive staining (number of samples)	**Colorectal cancer** % Area of most intense positive staining (number of samples)
CD31	16.16±4.17 (5)	9.34±5.84 (6)
CD146	0.67±0.67 (3)***	0.56± 0.89 (3)*

Figure 3.1 CD31 expression in whole tissue NC and CRC. All images represent immunohistochemical staining with microwave antigen retrieval technique of either anti-CD31 (A&B) or anti-CD146 (C&D) antibody with indirect DAB staining and haematoxylin counterstaining in paraffin wax embedded sections of normal colon (NC, images A and C) and Dukes C primary colorectal cancer (CRC, images B and D). Sections were imaged with Zeiss Axiovert microscope and images were captured with Axiovision software. Images were then assessed for positive endothelial cell membrane and cytoplasm staining within the microvasculature of both NC and CRC at x20 magnification by CD31 and CD146. A semi-quantitative and descriptive analysis of immunohistochemical staining using anti-CD31 and anti-CD146 antibodies to stain normal and tumour colorectal tissue is presented in table E**.** This was performed for 3 matched samples NC and CRC. Both the intensity of staining and the proportion of vessels stained by each protein was scored by one reviewer, and given a value between 0-3 where 0 is no positive staining/ none cells of interest present stained and 3 is very intense positive endothelial staining/ all cells of interest present in the field view positively stained. Data is presented as mean and standard deviation and, where appropriate (range). A quantitative analysis of positive CD31 and CD146 staining throughout normal and tumour colorectal tissue is presented in table F**.** The percentage area of most intense positive staining was obtained on 3 matched samples of NC and CRC that had undergone immunohistochemistry for anti-CD31 and anti-CD146 antibody. Stained section images were captured by Axiovision software which were then analysed with image J software (see section 2.13). Data shown is as a mean % of positive staining per field view area. Significance of data for CD31 compared to CD146 were assessed using paired Student's t- test.

Next a quantitative analysis was performed of the percentage positive staining across a section using Image J software. Using field areas that were comparable in terms of amount of stroma and numbers of vessels, CD31 expression, mean 16.2±4.17%, was found to be higher than CD146, mean 0.67±0.67% in NC (p=0.008). CD31 expression was also higher in CRC samples (Table F, Figure 3.1) where the mean CD31 expression was 9.34±5.84% compared to 0.56±0.89% found in CD146 staining (p=0.04). As a result of these findings, CD31 was subsequently used as the membrane bound endothelial marker of choice for endothelial isolation procedures.

3.2.2. Development of a protocol for isolation and culture of primary endothelial cells from colorectal tumour and matched normal colon tissue

The final protocol I used for isolation of colonic endothelium is detailed in the main Material and Methods chapter (sections 2.4.2 and 2.5). However, this chapter details the development of this final protocol and so additional methodological detail is supplied here. The following sections outline the changes made to existing protocols, and their success. The success of either a protocol or the changes made was judged on the following criteria in order.

1. The yield of total cell population before culture
2. The absence of infection
3. The typical endothelial cell morphology and lack of contaminating cells
4. The viability of endothelial cells in long-term culture
5. The yield of endothelial cells at each passage

Below are the evolutionary steps and progress made from September 2011 to May 2012 and refers only to work done during that time frame followed by the learning points and subsequent changes made as a result my visit to Dr Naschberger at the Division of Molecular and Experimental Surgery, at the University Medical Center Erlangen.

The Birmingham Experience

In total from 15th October 2011 to 1st May 2012, 32-paired fresh tissue specimens were used for pilot isolation and culture of endothelial cells from colorectal tumour and matched normal colon (TEC and NEC) in order to develop an optimized protocol. To achieve this, systematic adaptations were made to published protocols for isolation (20) and culture of endothelial cells from non-malignant samples and tissue other than colon or rectum (20, 135, 136).

Methods of digestion were based on in-house human primary hepatic endothelial isolation protocols (HSEC isolation) and used a slicing technique with 2 sterile scalpels followed by a 30-minute incubation period with collagenase 1b (SIGMA, C9891 >125units/mg). In addition, a mechanical method of digestion was adopted by using the Miltenyi Biotech GentleMACS™ digestor, and human tumour dissociation program 1. This increased the total cell population yield from normal colon (NC). A mean of 5.5 x 10^6 cells were extracted using GentleMACS™ compared to a yield of 0.41 x 10^6 cells per gram of tissue from 5 independent experiments for each method of digestion. However, despite an improved yield in single-cell suspension with the Gentlemacs, only 1 out of 5 preparations expanded in culture after use with the mechanical digestion compared to 4 out of 5 from the enzymatic digestion alone. I also noted excess mucous in the preparation of normal colon and mucinous tumour types, which was most noticeable at filtration immediately after digestion and interfered with cell

isolation. To address this, an increased volume of PBS was used to dilute the cell suspension and this lead to an increased mean yield of total cells from NC to 6.89 x 10^6 cells per gram of tissue. After this initial digestion, I used a cell selection step with CD31 or Ulex lectin immunomagnetic beads according to the HSEC protocol or the Bicknell tumour endothelium isolation protocol (Appendix 1) respectively. Irrespective of the target protein used to isolate the ECs, excess mucous inhibited the yield from the bead separation step. The bead-bound cells would persistently be trapped within the mucous and thus did not attach to the magnet effectively. Increased dilution steps at this point also increased total cell yields from approximately 6 x 10^4 to 2 x 10^6 cells per gram of tissue.

Use of biotinylated immunomagnetic beads attached to Ulex lectin has been reported to isolate microvascular endothelium (137). In our experience, where Ulex Lectin was used to isolate endothelium (Appendix 1), the resultant cultures did not exhibit typical endothelial morphology but instead, appeared spikey and characteristic of overgrowing fibroblasts (not shown). In contrast when CD31 Dynabeads (section 2.5.1) were used, most cultures exhibited typical cobblestone endothelial morphology (see representative images in Figure 3.2). On occasion we still saw contaminating non-endothelial populations using this strategy (Figure 3.2) but results were preferable to using Ulex Lectin, and therefore, CD31 Dynabeads was used to isolate the endothelium for the remainder of isolation protocols.

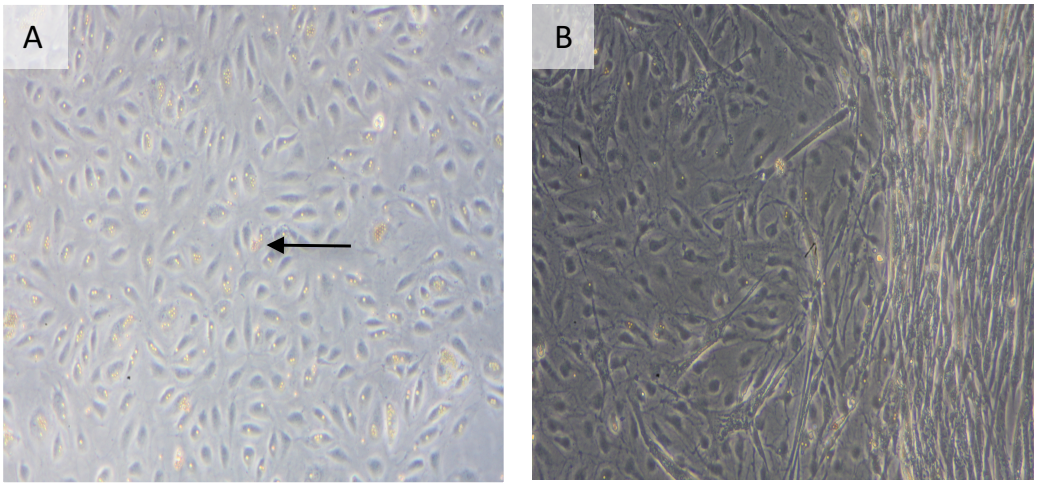

Figure 3.2: Primary colorectal tumour endothelial cells isolated with CD31 dynal beads display a cobblestone appearance in culture. Image represents two photos taken of the resultant cells from 2 different isolation techniques (2011-May 2012). Image A. represents the resultant cells at passage 2 after using CD31 coated immunomagnetic beads to isolate the endothelial cells. The black arrow represents the anti-CD31 immunomagnetic Dynabeads used in the isolation process. Image B. shows isolated endothelial cells on the left abutting contaminating fibroblasts on the right. Images taken at original x10 magnification with a phase contrast microscope.

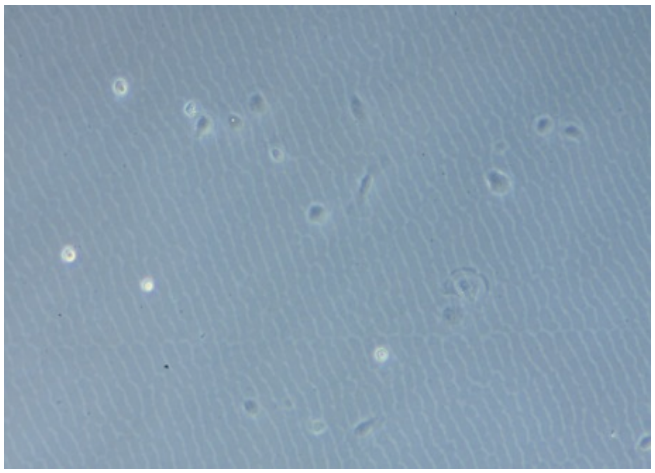

Figure 3.3: Primary Human TEC derived from colorectal cancer 2 hours post Flow assisted cell sorting. Image represents TEC *in vitro* adherent to culture plate of a t-25 flask with 10 minutes of isolation by Flow assisted cell sorting using anti-CD31 antibody conjugated to FITC. Image is captured at x20 magnification with a light phase contrast microscope.

Of note, although this selection strategy was generally reliable, problems were identified with some loss of endothelial morphology after first passage and occasional bacterial or yeast infections during culture. During the pilot phase, 8 infections occurred. On 3 occasions, both NC and CRC were affected (2 x bacterial, 1x yeast) and the remaining 5 related to either NC or CRC (3 and 2 infections respectively) with either yeast or bacterial contamination. All infections occurred from October 2011 to May 2012. The problems and our successful refinements to avoid them are summarized in Table 3.2. At this point email contact was made with Dr Naschberger at the division of molecular and experimental surgery, Erlangen to obtain some advice about their published protocol (60) and how they maintained endothelial cell morphology and eliminated infections.

In addition, I tested the potential of cell isolation by flow assisted cell sorting using fluorescence conjugated anti-human CD31 antibodies. The method is outlined in Chapter 2. On 2 occasions the resultant cells were plated in culture under our standard growth conditions. Both NEC and TEC were observed to adhere to the culture plate after FACS (Figure 3.3) however over the course of the subsequent 48 hours cell detachment was noted and expansion was not possible.

Stage and initial method	Problem with protocols, October 2011 -May 2012	Protocol amendment
Bicknell tumour endothelial isolation protocol	Fibroblastic contamination	Switch to CD31 as a selection strategy
Tissue dissociation with both Bicknell tumour Ulex Lectin isolation and HSEC CD31 methods	Excess mucous leading to lower yields and reduced isolate specificity	Mechanical digestion in larger samples
	Excess mucous reducing isolate specificity	Multiple washes at post collagenase stage and magnet stage
Bicknell tumour Ulex Lectin isolation and HSEC CD31 methods	Persistent loss of endothelial cell morphology after cell detachment at passage	Contact made with Erlangen -Use Accutase instead of Trypsin based cell detachment
Bicknell tumour Ulex Lectin isolation and HSEC CD31 methods	Either bacterial or yeast infections in culture of about 40% of both normal colon and CRC isolates	Contact made with Erlangen -Increase washes and use antibiotic supplemented PBS

Table 3.1. A summary table of the main problems encountered when using both the HSEC CD31 endothelial culture and isolation protocol, and the Bicknell tumour isolation Ulex Lectin protocol to isolate and culture tumour and normal endothelial cells from colorectal tissue. This table charts the problems from October 2011-May2012 and the steps taken to address the problems.

Objectives of trip	Protocol changes resulting from trip
Reduce risk of infection	Wash both normal colon and CRC tissue vigorously at least 3 times in a minimum of 40mls buffer solution (supplemented with antibiotics) prior to digestion step.
Improve yield of cell count in single cell population	Use collagenase II from Biochrom, which has a high unit of activity
	Avoid shearing forces when cutting the tissue with scalpels
Reduce contamination cells and improve Endothelial cell purity	Place ECs in culture before bead isolation step

Table 3.2. Table outlining the remaining problems with the endothelial cell isolation protocol changes adopted based on discussion with Erlangen. Protocol changes that resulted from the trip to Erlangen, to resolve outstanding protocol issues are outlined

The Erlangen Experience

Our early data demonstrated that cultures of cells, which displayed endothelial cell morphology, lost this after passage. Flow cytometry also showed passaged cells to be CD31 negative and CD90 positive (not shown). Thus our method for passage and cell detachment was re-assessed. Schellerer and Naschberger et al (60) are the only group who have published data from cultured NEC and TEC from colorectal tissue. Their methods state that 1 x 0.5 g/l trypsin and 0.2 g/l ethylenediaminetetraacetic acid (EDTA) was used to dissociate their cells, which is similar to the HSEC protocol. However, on contact with Dr Naschberger, from the group, she noted, there had been issues with the trypsin cleaving cell surface CD31 and that subsequently, further CD31 isolation at passage 1 was ineffective. Interestingly, using Trysin and Tryp-LE on HSEC does not have the same effect on the CD31 epitope. However, Accutase, a gentler form of enzymatic cell detachment was recommended to preserve expression. This had a dramatic effect and at one-week post detachment further purification steps with CD31 beads were possible for both NEC and TEC. CD31 positivity maintained by NEC and TEC, was confirmed by our flow cytometrical, indirect ELISA and immunocytochemical analysis (Figure 3.4, detailed later). This would not have been possible without this change in protocol and has meant that phenotyping of NEC and TEC post culture and future functional studies can be performed. Other learning points from the trip included increased number of preparation washings with buffer and increased use in Gentamycin and amphoteracin and Penicillin, streptomycin and glutamine. In addition, the use of collagenase differed to collagenase II from Biochrom. This produced yields between 5-6x10^6 cells/gram of tissue for both NC and CRC without mechanical digestion; which was preferable. Furthermore, as a result of the visit, culture of total cell populations was performed and isolation with anti-human

CD31 immunomagnetic beads occurred after expansion in culture, which allowed expansion to passage 4 more frequently that isolates prior to initial culture expansion (data not shown).

3.2.3 Validation of in vitro model of colorectal tumour Endothelium

To confirm that both NEC and TEC maintain typical vascular endothelial cell characteristics *in vitro,* immunocytochemistry (ICC), flow cytometry and in-direct enzyme-linked immunosorbent assay (ELISA) were performed. CD31 was expressed by both NEC and TEC at the plasma membrane throughout most the monolayer and occasionally cytoplasmic CD31 expression was within the cytoplasm by ICC. Cytoplasmic VWF was identified in NEC but was reduced in TEC. Flow cytometry of TEC confirmed at least 93% CD31 positivity (Figure 3.4). CD31, VWF and ICAM-1 expression was found on un-stimulated and stimulated NEC. ELISA confirmed that CD31 was expressed more than VWF or ICAM-1 by un-stimulated NEC, and was slightly up regulated by IL-1β stimulation but not TNFα. In contrast ICAM-1 expression was most increased after stimulation with TNFα. The effects of TNF stimulation were more marked for TEC with the percentage of cells that expressed VCAM-1 increasing over 4 fold (un-stimulated 2.5% to TNFα 12.6%) and the median channel value increasing (un-stimulated 19.4 to TNFα 26.8) after 8 hours of TNFα treatment (Figure 3.4).

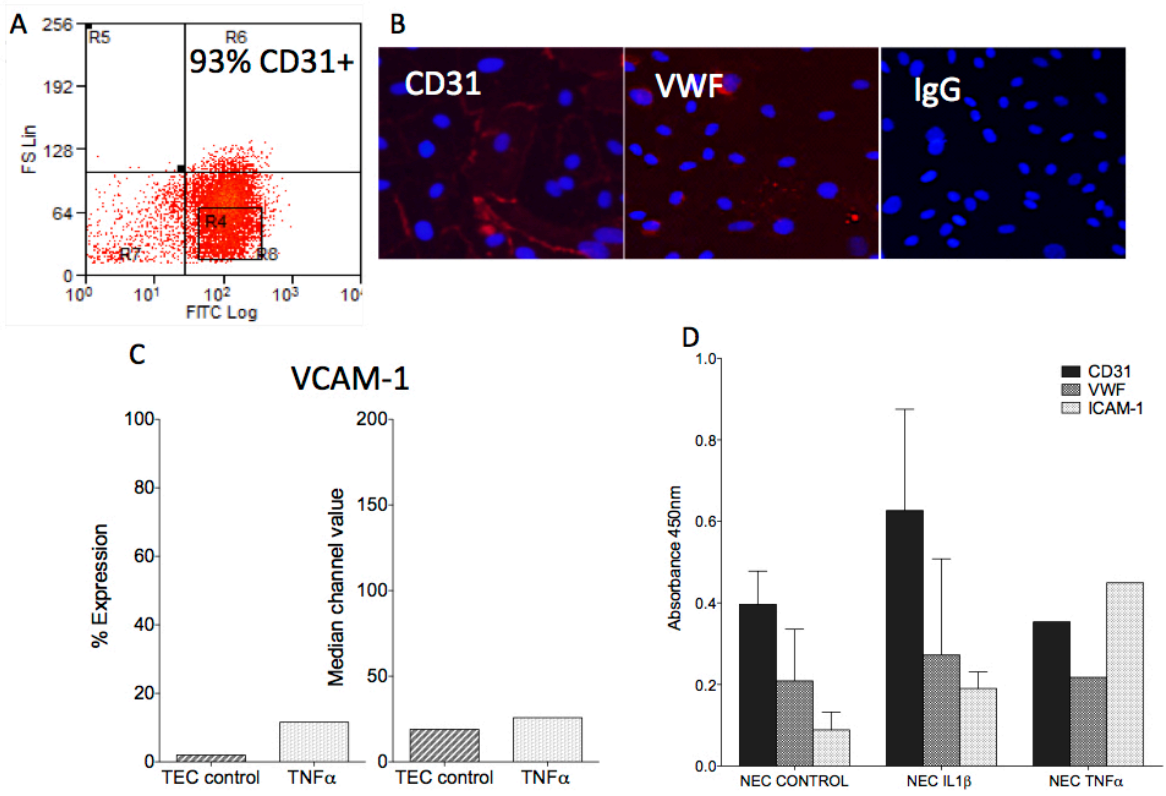

Figure 3.4: In vitro expression of vascular endothelial markers by NEC and TEC.
Primary human endothelial cells that had undergone positive CD31 selection from human normal and malignant colorectal tissue samples were cultured and subsequently purified up to passage 4. CD31 and TNFα induced VCAM-1 expression by TEC was assessed using Flow cytometry. For CD31 expression, cells were detached from culture, stained and washed for 30 mins with mouse anti-human antibodies with isotype matched controls for all antibodies (Appendix 2&3). To assess VCAM-1 expression in response to TNF-α , TEC were starved from usual (MV-2, LONZA,UK) media growth factors for 12 hours and then stimulated with 10ng/ml of human recombinant TNF-α for 8 hours and then detached. Cells then underwent flow cytometric analysis on a standardized protocol using Becton Dickenson Cyan flow cytometer and was analyzed using Summit v4.3 software. Immunocytochemistry was used to assess CD31 and VWF expression on TEC. Texas red was used as a secondary antibody with a DAPI nuclear counterstain. Images were taken at x10 magnification and staining with isotype control antibodies was negative. ELISA was performed on confluent monolayers of *in vitro* NEC (passage 4) in flat bottom 96 well plates. Triplicate wells were either untreated (from 3 patient samples) or treated with10ng/ml human recombinant IL-1β (3 patient samples) or TNF-α (1 patient sample). Cells were then stained with CD31, VWF or ICAM-1 and expression was determined using indirect HRP and TMB indirect ELISA. Absorbance was read at 450nm using an absorbance plate reader and calculated against isotype matched controls. Image A is a representative flow cytometry plot illustrating 93% CD31+ TEC. Image B shows representative images of positive CD31 and vWF staining by TEC. Image C graphically represents the % inducible expression (left) and MCV (right) of VCAM-1 expression by TEC in response to TNF-α. Image D shows relative inducible expression of CD31, VWF and ICAM-1 of NEC after IL-1βand TNF-α by ELISA.

Expression of endothelial phenotypic markers in normal human colonic endothelium and tumour microvascular endothelium.

In addition to identifying reliable endothelial markers for subsequent isolation methods, we sought to characterize expression of von Willebrand Factor (VWF), VE-Cadherin, Vascular endothelial growth factor receptor 2 (VEGFR-2) and CD105 in both colorectal tumour endothelium (TEC) and non-diseased colorectal endothelium (NEC) to understand the differences between un-involved and malignant tissue. Immunohistochemical techniques were used to identify the localisation and quantity of positive staining of the molecules of interest through NC and CRC tissue sections (see representative images in Figure 3.5).

Positive cytoplasmic VWF staining of the endothelium was seen throughout both NC and CRC tissue and within the microvasculature of mucosal, submucosal and deeper muscle layers of NC and invasive mucosa and stroma of CRC, with expression more abundant in NC. However, a semi-quantitative analysis performed on 3 paired NC and CRC sections, revealed the same mean score reflecting intense positive endothelial staining of 3 for both NC and CRC (Figure 3.5). However, the proportion of vessels stained was higher in NC than CRC (3 v's 2.6 respectively).

There was very little positive endothelial staining for VE-Cadherin in either NC or CRC compared to the isotype-matched control. In NC sections and to a lesser extent in CRC, cytoplasmic staining was found in a few microvasculature endothelial cells of the submucosal layer and stromal layer, but not all endothelial cells of the same vessel showed positive expression. Where staining occurred, the intensity appeared less in CRC sections. Semi-quantitative analysis of VE-Cadherin expression produced a mean

score of 0.3 (2 sections scored 0, and one scored 1) for proportion of vessels stained and for intensity; NC scored 1, whereas CRC scored a mean of 0.6.

Membrane and cytoplasmic VEGFR-2 expression by the microvascular endothelium in the lamina propria of NC and through the stroma of CRC was observed (Fig 3.5 panels E and F). Small amounts of artifact staining were seen at the mucosal edge of NC but no non-specific staining was seen in NC or CRC compared to isotype-matched control. Where endothelial positive staining was seen, not all endothelial cells from a vessel expressed VEGFR-2 in both NC and CRC. Semi-quantitative analysis suggested a similar proportion of vessels were stained in NC section compared to CRC (mean score of 1.3 v's 1.3) whereas the intensity score suggested CRC displayed slightly more intense positive staining (mean score of 1 v's 1.3).

Cytoplasmic and membranous CD105 expression (Fig 3.5 panels G and H) was noted on all endothelial cells of micro vessels of the submucosal layer of NC, particularly near areas of high lymphocytic infiltration and extensively throughout the stroma of CRC sections. Findings from the subjective analysis were supported by semi-quantitative assessment, which suggested CD105 expression was relatively high in both NC and CRC compared to other proteins. CD105 was found on a higher proportion of vessels and was more intense in CRC compared to NC (mean scores of 2.3 v's 2.6 and 1.6 v's 2.3 respectively).

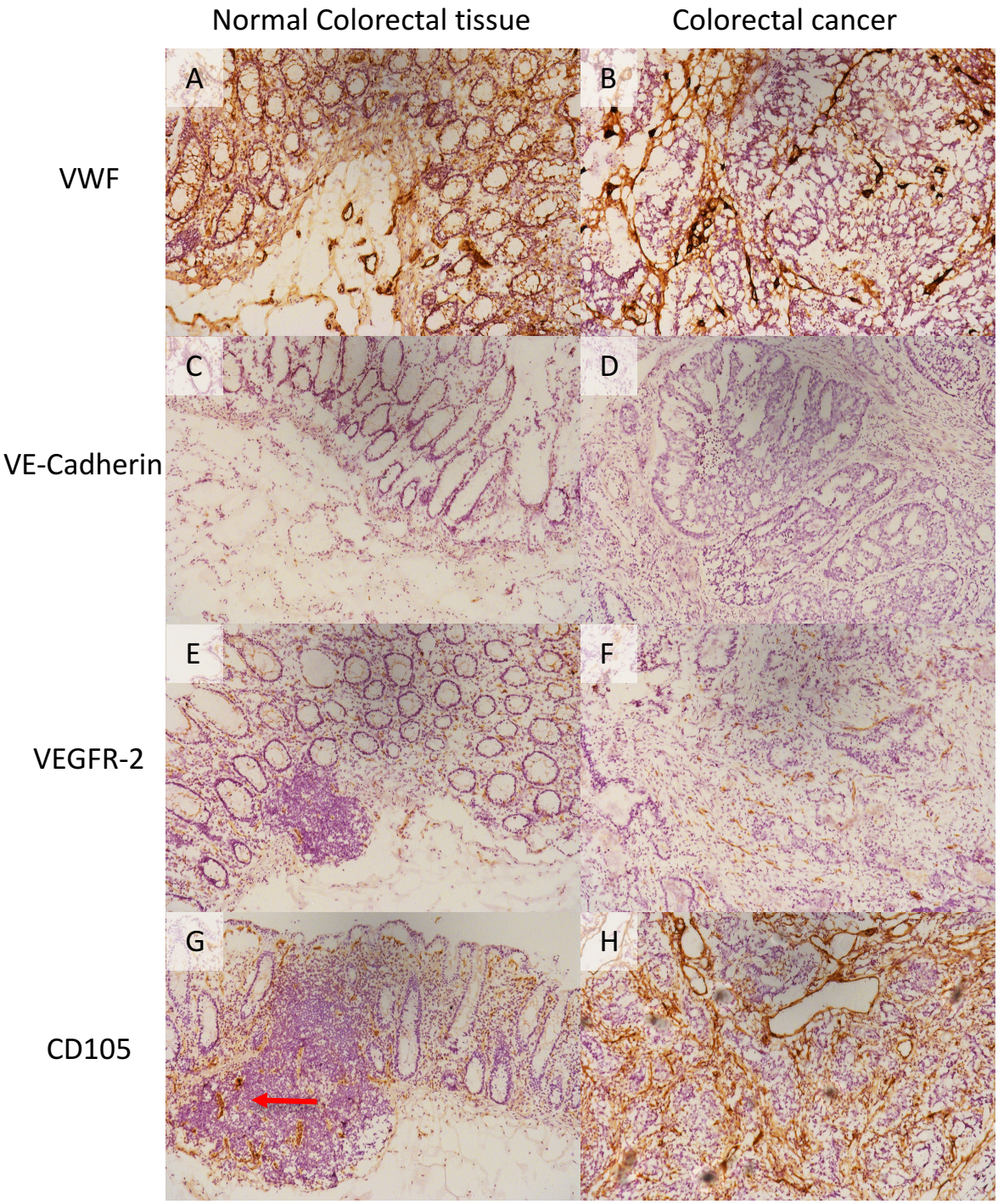
Normal Colorectal tissue
Colorectal cancer
VWF
VE-Cadherin
VEGFR-2
CD105
A
B
C
D
E
F
G
H

I

		Mean semi-quantification score (n=3)	
		NC	CRC
VWF	Proportion of endothelial staining	3	2.6±0.58 (2-3)
	Intensity of staining	3	3
VE-Cadherin	Proportion of endothelial staining	0.3±0.58 (0-1)	0.3±0.58 (0-1)
	Intensity of staining	1	0.6±0.58 (0-1)
VEGFR-2	Proportion of endothelial staining	1.3±0.58 (1-2)	1.3±0.58 (1-2)
	Intensity of staining	1	1.3±0.58 (1-2)
CD105	Proportion of endothelial staining	2.3±0.58 (2-3)	2.6±0.58 (2-3)
	Intensity of staining	1.6±0.58 (1-2)	2.3±0.58 (2-3)

Figure 3.5: Expression of endothelial markers by normal colorectal tissue and colorectal cancer. Immunohistochemistry was performed using unfixed frozen whole tissue sections of NC and CRC (7µm thickness) by an indirect DAB staining method. Mouse anti-human antibodies against Von Willebrand factor (VWF), VE-Cadherin, Vascular Endothelial growth factor 2 (VEGFR-2) and CD105 were used in addition to isotype matched controls. Representative images were taken at 20x magnification and retrieved using Axiovision software. Images A,C,E,G represent NC and B,D,F,H represent CRC. A&B show VWF, C&D show VE-Cadherin, E&F show VEGFR-2, G&H show CD105 staining. A semi-quantitative score was performed for 3 matched samples for both the intensity of staining and the proportion of vessels stained by each protein between 0-3 where 0 is no positive staining/ none of the endothelial cells present stained and 3 is very intense positive endothelial staining/ all endothelia present in the field view positively stained. The mean (range) is shown as a table in image I. Significance was tested using student T test. Data between NC and CRC were not significant.

Quantitative flow cytometry (Figure 3.6) was used to explore the expression of VE-Cadherin, CD105, and VEGFR-2 by isolated endothelial cells derived from CRC and NC (TEC and NEC). There were no significant differences between the mean percentage membranous expression of VE-cadherin in NEC, over 6 paired and non-paired samples, compared to CRC (28.66% vs 17.75%, Figure 3.6). The data describing percentage expression suggests VE-cadherin is expressed by fewer cells compared to CD105 but not VEGFR-2 for both TEC and NEC although using ANOVA, there is no statistical difference. Furthermore, the data indicates that a higher percentage of NEC express CD105 and VEGFR-2 compared to TEC. However, analysis of the median channel value expression for these molecules suggests that VE-Cadherin is expressed significantly less intensely compared to VEGFR-2 and CD105 in NEC ($p=0.023$ and $p=0.01$). VE-cadherin expression is also significantly less intense compared to VEGFR-2 in TEC ($p=0.027$, Figure 3.6).

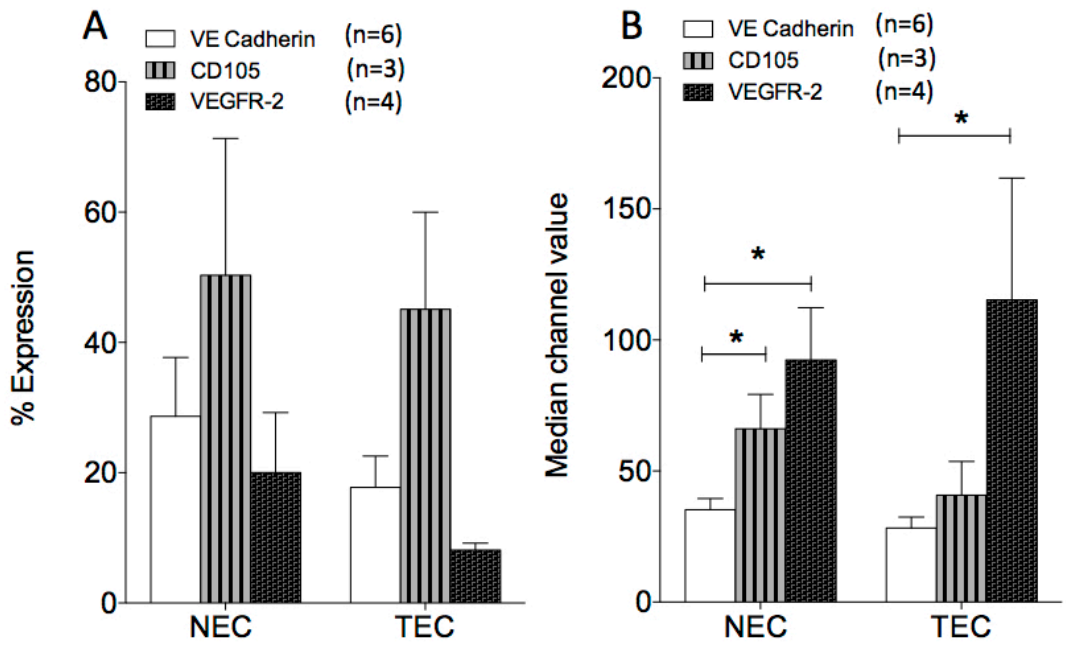

Figure 3.6: Cell surface expression of VE-Cadherin, CD105 and VEGFR-2 by isolated primary human colorectal endothelial cells. Primary human endothelial cells were isolated from human normal colorectal and paired colorectal cancer tissue samples by positive selection using anti-human CD31 immunomagnetic beads. Cells were then stained and washed for 30 mins with mouse anti-human VE-Cadherin, CD105 and VEGFR-2 antibodies with isotype matched controls (tables 2.2, 2.3). The isolated normal and tumour endothelial cells then underwent flow cytometrical analysis on a standardised protocol using Becton Dickenson Cyan flow cytometer and Summit v4.3 software. Images A illustrate data obtained describing VE-Cadherin, CD105, VEGFR-2 expression by both NEC and TEC. Both graphs show data for unpaired samples in both percentage expression (left panel) and median channel value (right panel) expressed as mean and SEM.. Statistical analysis was performed using two way ANOVA, significant differences were found between VE-Cadherin and CD105 expression in NEC, and VE-Cadherin and VEGFR-2 in TEC.

3.2.4 Analysis of key functional genes expressed by normal human colonic and tumour microvascular endothelium.

Gene expression data were obtained by performing a commercially available profiling array containing 85 genes of interest and additional controls (Figure 3.7). The genes are divided into functional groups such as those contributing to angiogenesis, inflammatory response and cellular adhesion. Data retrieved from 3 Flow assisted cell sorted (FACS) TEC with matched NEC, were organized into those genes down and up-regulated in TEC using NEC as a comparative baseline after comparison to GAPDH and β-Actin as housekeeping genes. This revealed little consistency in gene expression across the samples. Very few genes were consistently either up or down regulated by all 3 samples. Within the angiogenesis gene grouping, the gene that transcribes VEGF-A, a ligand for VEGF-2 was upregulated by all TEC samples relative to matching NEC and resulted in a mean up-regulation in TEC of 7.2. Although the mean gene expression for EDN1, EDNRA and eNOS were also increased (mean fold increase in TEC relative to NEC of 7.04, 23.5 and 4.06 respectively), there was significant heterogeneity between expression of these genes between individual samples to provide significant data (Figure 3.7).

Within the functional group for inflammatory response, the mean expression of genes transcribed for inflammatory chemokines IL-6, CCL2 and CCL5 were up-regulated (mean fold increase of 4.65, 1.42 and 1.83 in TEC relative to NEC respectively) however, this was not statistically significant. In addition, the mean expression of genes transcribing for proteins E-selectin and Vascular Cellular Adhesion Molecule -1 (VCAM-1) were marginally upregulated at mean 6.08 and 8.42 fold increase in TEC relative to matched NEC, but significant heterogeneity of gene expression between individual samples mean data is not generalizable.

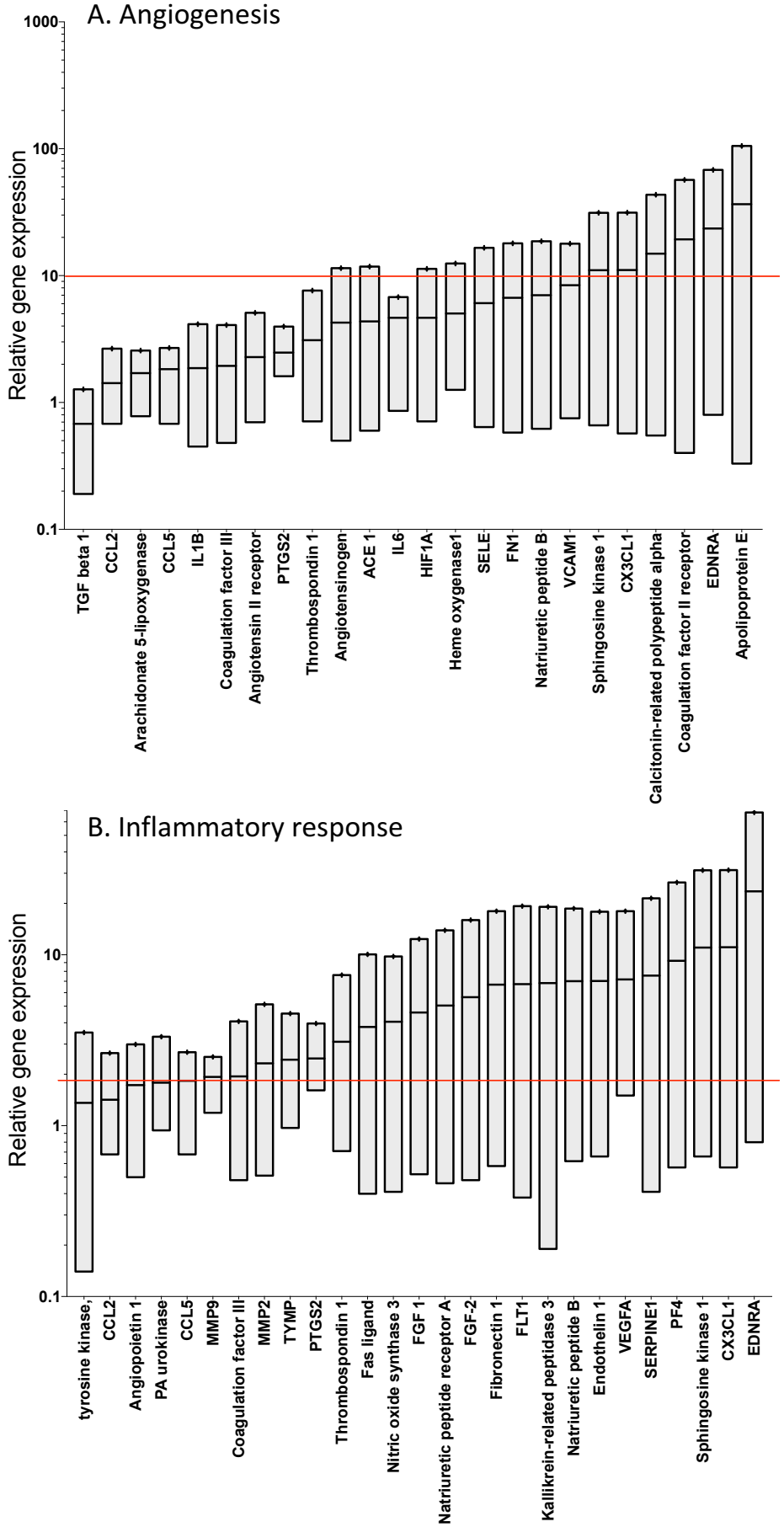
A. Angiogenesis
Relative gene expression
1000
100
10
1
0.1
TGF beta 1
CCL2
Arachidonate 5-lipoxygenase
CCL5
IL1B
Coagulation factor III
Angiotensin II receptor
PTGS2
Thrombospondin 1
Angiotensinogen
ACE 1
IL6
HIF1A
Heme oxygenase1
SELE
FN1
Natriuretic peptide B
VCAM1
Sphingosine kinase 1
CX3CL1
Calcitonin-related polypeptide alpha
Coagulation factor II receptor
EDNRA
Apolipoprotein E
B. Inflammatory response
Relative gene expression
10
1
0.1
tyrosine kinase,
CCL2
Angiopoietin 1
PA urokinase
CCL5
MMP9
Coagulation factor III
MMP2
TYMP
PTGS2
Thrombospondin 1
Fas ligand
Nitric oxide synthase 3
FGF 1
Natriuretic peptide receptor A
FGF-2
Fibronectin 1
FLT1
Kallikrein-related peptidase 3
Natriuretic peptide B
Endothelin 1
VEGFA
SERPINE1
PF4
Sphingosine kinase 1
CX3CL1
EDNRA

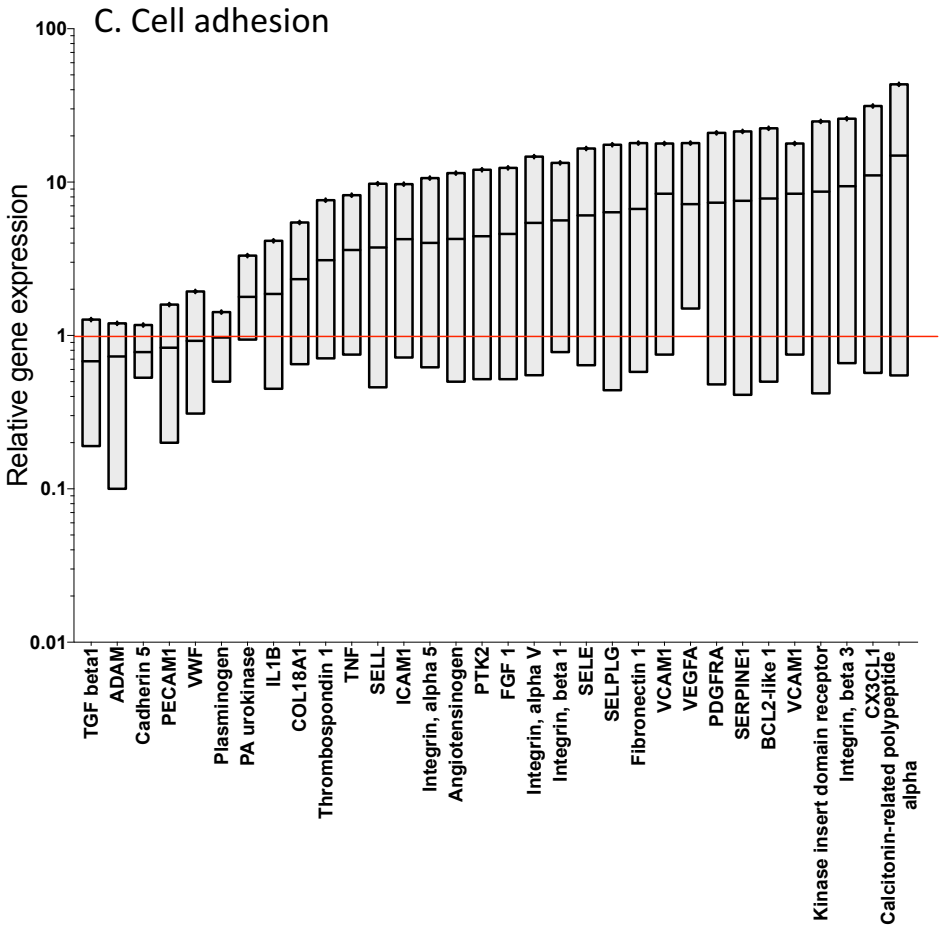

Figure 3.7: Profiling of change in gene expression between normal and tumour endothelial cells.

Primary human colorectal endothelial cells were isolated with Flourescence assisted cell sorting (FACS) from single cell suspensions of 3 matched NC and CRC samples using CD31 FITC and a live/dead cell marker (Section 2.5.3). Isolated cells were collected in RLT buffer (Qiagen, UK), homogenized and underwent mRNA extraction (Qiagen Rneasy minikit, UK) and cDNA extraction (Iscrip, Biorad, uk). RT-QPCR was undertaken using an original concentration of 45ng /µl of mRNA for all samples using the commercially available RT^2 profiling PCR array Endothelial cell biology (SABiosciences, QIAGEN, UK). Analysis was performed using ΔΔCT method (Section 2.9.5) using GAPDH and Beta Actin as housekeeping genes and obtaining the TEC value as sample of interest against matched NEC. Data in each graph is presented as floating bars showing the max, minimum and mean (shown by mid bar line) values of the 3 relative gene expression values. Data is presented in each graph according to grouping of cell function. The red line on each graph is drawn at 1 to represent NEC value. Data did not reach significance.

Expression of genes transcribing other proteins of interest, were grouped under the cell adhesion function. These included PECAM-1 (CD31), Cadherin-5 (VE-cadherin), VWF, ICAM-1. Our data shows the mean gene PECAM-1, Cadherin-5 and VWF gene expression was lower in TEC samples compared to relative expression in NEC (mean fold change of 0.83, 0.78, 0.92 in TEC relative to NEC respectively). The mean ICAM-1 gene expression was 4.3 fold higher in TEC samples relative to matched NEC however, this data did not reach statistical significance (Figure 3.7).

3.2.5 Key differences between TEC and NEC are maintained in culture

To investigate if TEC maintain a tumour-specific phenotype in culture, protein and gene expression of TEC and NEC were quantified using immunocytochemistry and qPCR. Tumour marker endothelium 8 (TEM-8) was tested as a marker of tumour endothelium, by performing immunohistochemistry with anti-human anti-TEM-8 on CRC tissue sections (see Figure 3.8). Cytoplasmic and membranous TEM-8 staining was seen within the microvascular endothelial cells of CRC and not in nearby NC (see Figure 3.8, image B). Comparison of TEM-8 expression in NEC and TEC by flow cytometry revealed both MCV and percentage of cells expressing TEM-8 were higher in freshly isolated TEC than NEC (see Figure 3.8). Expression of TEM-8 was also analysed on cultured cells using flow cytometry, suggesting that both percentage expression and median channel value of TEM-8 expression remains higher in TEC compared to NEC (Figure 3.9). This was confirmed using ELISA on 3 *in vitro* NEC samples compared to one TEC sample where the absorbance values suggested TEM-8 was elevated in TEC (Fig 3.9).

Fig 3.9 illustrates with standard PCR, a visible band representing TEM-8 gene expression in freshly isolated NEC, however the signal is less intense than that representing CD31 or that produced by matched freshly isolated TEC. In contrast, cultured NEC did not produce a visible band for TEM-8 gene expression whilst expression is similar in cultured TEC. Expression was quantitatively assessed using qPCR (Figure 3.9) which confirmed increased expression in TEC with a mean of over 15-fold increase in expression in TEC relative to NEC.

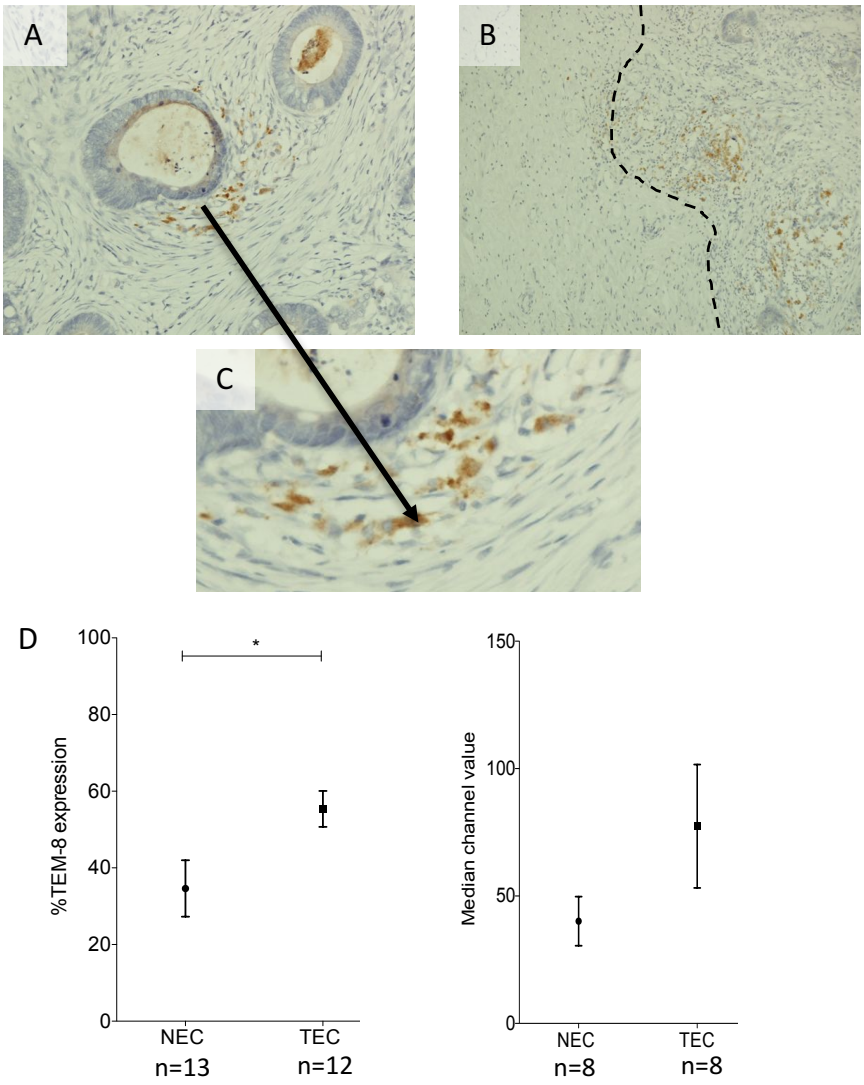

Figure 3.8: Tumour endothelial marker 8 (TEM-8) is expressed by Colorectal tumour endothelium in whole tissue and isolated primary TEC from human CRC. Immunohistochemistry was performed using unfixed frozen whole tissue sections of Dukes D CRC (7µm thickness) by an indirect DAB staining method. Mouse anti-human antibody against TEM-8 were used in addition to isotype matched controls. Images A-C show representative sections of CRC with positive endothelial cell anti-human TEM-8 antibody staining taken using Axiovision microscope at 20, 10 and 40x magnification respectively. Images were retrieved using Axiovision software. The dashed black line in image B illustrates the margin between invasive CRC (right) and nearby NC (left). Image C is a closer look at the staining in image A and the black arrow linking image A to C highlights positive endothelial staining. Primary human endothelial cells were isolated from human normal colorectal and colorectal cancer tissue samples. Cells were then stained and washed for 30 mins with mouse anti-human TEM-8 antibody with isotype matched control (Appendix 3). The isolated normal and tumour endothelial cells then underwent flow cytometrical analysis on a standardised protocol using Becton Dickenson Cyan flow cytometer and Summit v4.3 software. Images D illustrates flow cytometric data describing TEM-8 expression by both NEC and TEC. Both graphs show data for unpaired samples in both percentage expression (left panel) and median channel value (right panel) expressed as mean and SEM. Statistical analysis was performed using un-paired, two tailed T-test. % TEM-8 expression was significantly higher in TEC.

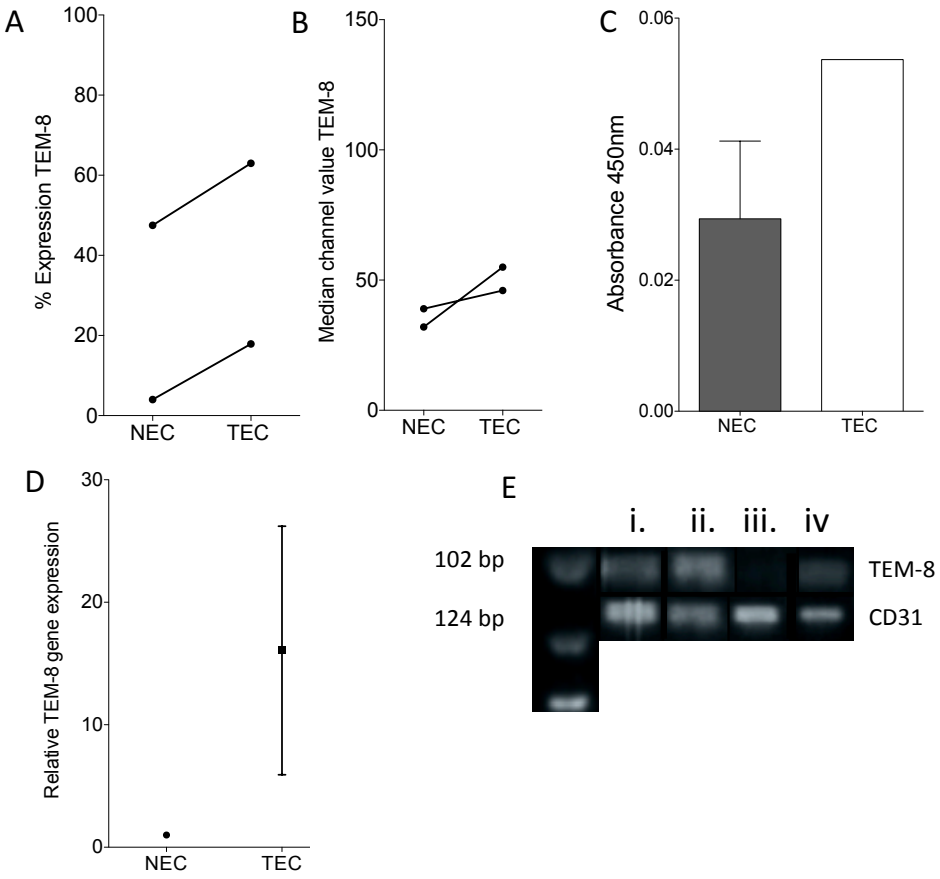

Figure 3.9: Tumour endothelial marker 8 (TEM-8) expression by in vitro primary isolated TEC from human CRC.
Primary human endothelial cells that had undergone positive CD31 selection from human normal colorectal and malignant tissue samples were cultured to confluence (passage 4). Cells were stained and washed for 30 mins with mouse anti-human TEM-8 antibody with isotype matched control (see appendix 3). NEC and TEC then underwent flow cytometrical analysis on a standardised protocol using Becton Dickenson Cyan flow cytometer and Summit v4.3 software. Images A illustrates TEM-8 expression by both NEC and TEC. Both graphs show data for paired samples in percentage expression (left) and MCV (right) expressed as mean and SEM. *In vitro* NEC and TEC in flat bottom 96 well were then stained with TEM-8 and expression was determined using indirect HRP and TMB indirect ELISA. Absorbance was read at 450nm using an absorbance plate reader and calculated against isotype matched controls. Image C illustrates the mean comparative absorbance of TEM-8 by 3 *in vitro* NEC samples and 1 *in vitro* TEC sample. *In vitro* cells underwent mRNA extraction (Qiagen Rneasy minikit, UK) and cDNA synthesis (Iscrip, Biorad, uk). Real time qPCR and standard PCR was undertaken using an original concentration of 45ng /µl of mRNA for all samples using Taqman gene probes and primer (Invitrogen) or Sigma self designed primers (see appendix). For qPCR, CT values were calculated using Stratagene Mx3000P and analysis was performed using ΔΔCT method (Section 2.9.5) using GAPDH and Beta Actin as housekeeping genes and obtaining the TEC value relative to NEC. Images of gene expression by standard PCR was visualized using GeneGenius Bio Imaging System (Syngene, UK) and Genesnap software (Syngene, UK). Image D illustrates resultant qPCR data. Image E illustrates standard PCR data for TEM-8 expression against CD31 gene expression as a positive control. The bars represent; i. freshly isolated NEC, ii. freshly isolated TEC, iii. NEC in culture at passage 4, iv. TEC in culture at passage 4. Where applicable, statistical analysis was performed using un-paired, two tailed Student's t-test.

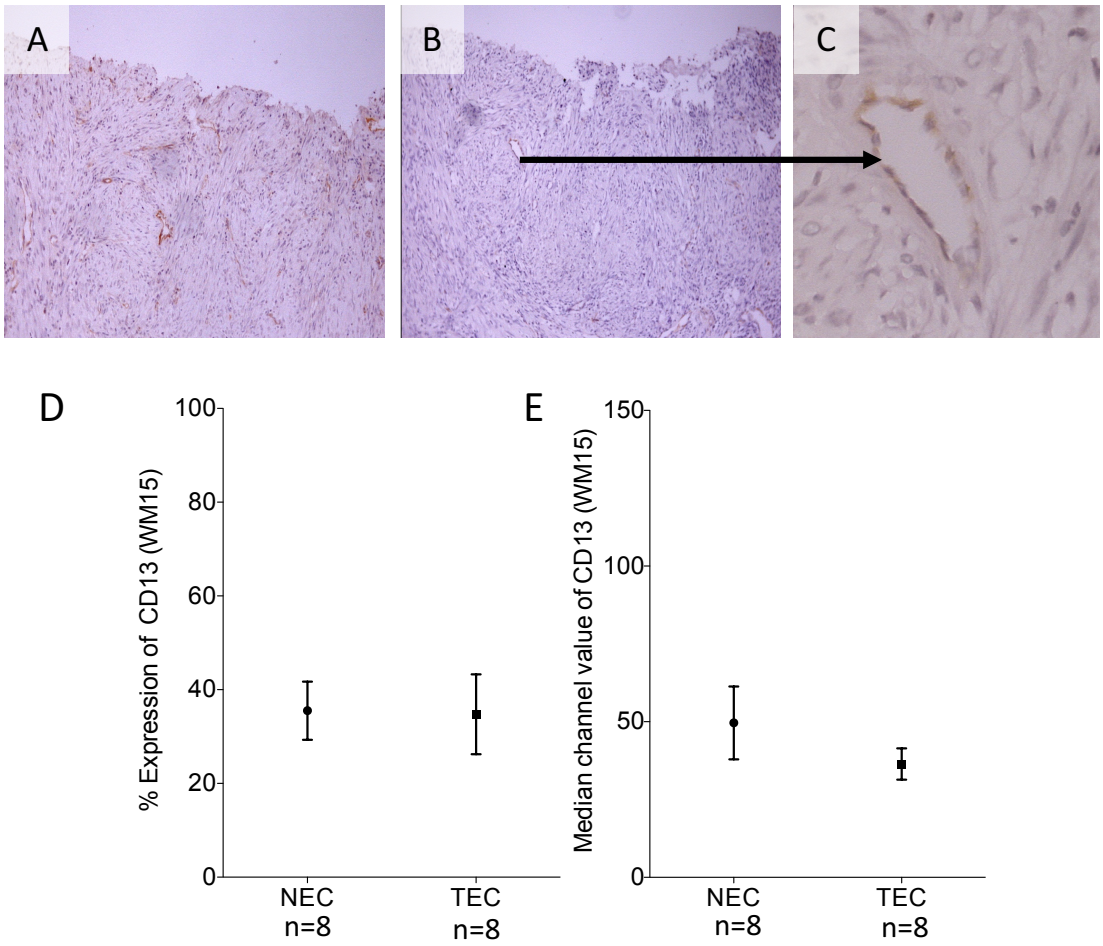

Figure 3.10: CD13 (WM15) expression by NC and CRC whole tissue and primary NEC and TEC isolated from human NC and CRC. . Immunohistochemistry was performed using unfixed frozen whole tissue sections of Dukes C CRC (7µm thickness) by an indirect DAB staining method. Mouse anti-human antibodies against CD31 or CD13 (WM15) were used in addition to isotype matched controls. Images A, representing CD31 staining, and image B, representing CD13 (WM15) staining were taken using Axiovision microscope at 10x magnification and image C, which also represents CD13 (WM15) staining and is a closer look at image B, was taken at 40x magnification. Images were retrieved using Axiovision software. The black narrow connecting images B&C illustrates positive endothelial staining. Primary human endothelial cells that had undergone positive CD31 selection from human normal colorectal and colorectal cancer tissue samples were cultured and subsequently purified up to passage 4. Cells were stained and washed for 30 mins with mouse anti-human CD13(WM15) antibody with isotype matched control (see appendix). The isolated normal and tumour endothelial cells then underwent flow cytometrical analysis on a standardised protocol using Becton Dickenson Cyan flow cytometer and Summit v4.3 software. Images D illustrate data obtained describing CD13(WM15) expression by both NEC and TEC. Both graphs show data for paired and unpaired samples in both percentage expression (Image D) and median channel value (Image E) expressed as mean and SEM. Data in table (F) is presented as mean, standard deviation and (number of samples). Statistical analysis was performed using paired, two tailed T-test, and did not reach significance.

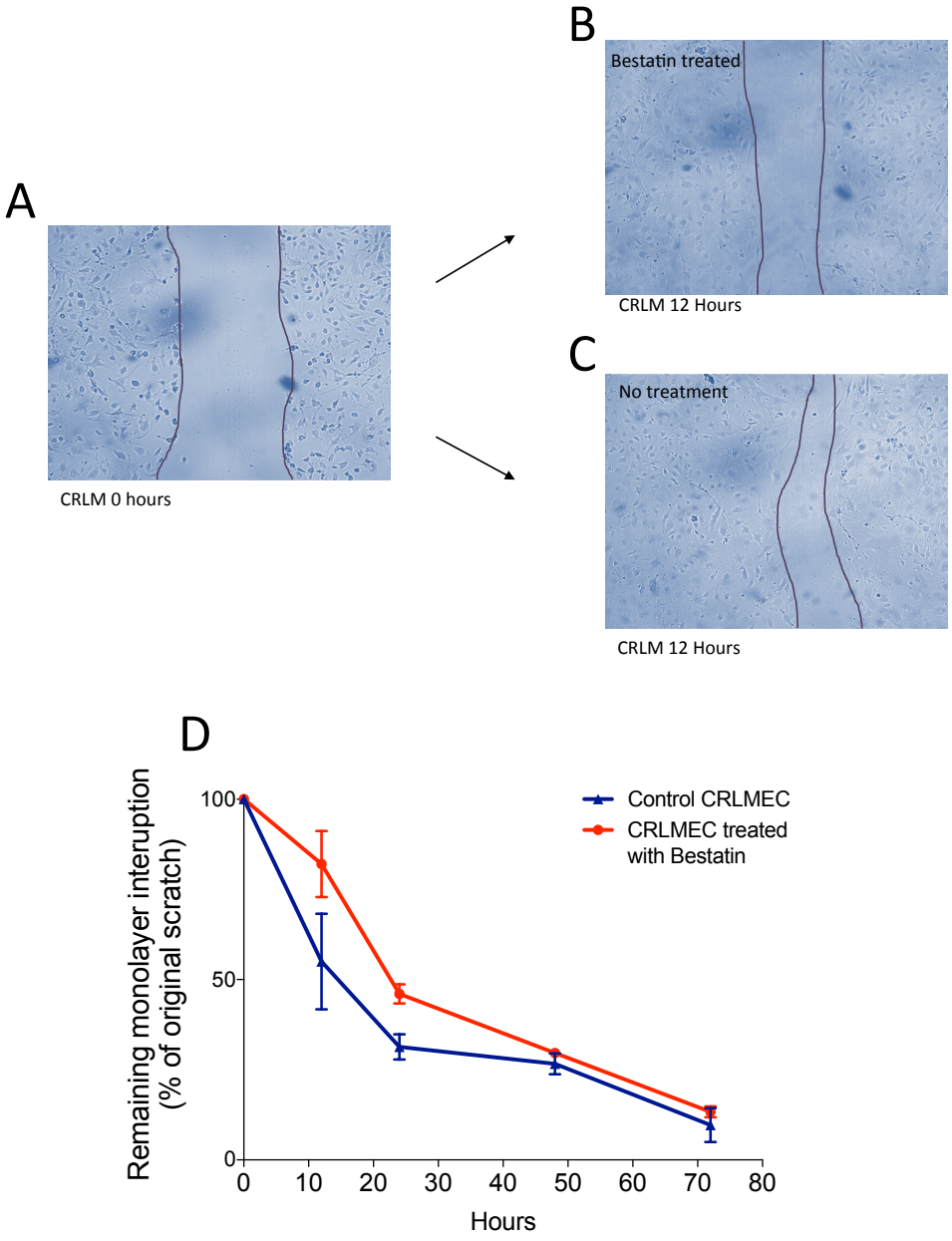

Figure 3.11: Bestatin hydrochloride prolongs interruption in CRLMEC monolayer up to 12 hours.
Human primary endothelial cells derived from liver metastasis from colorectal primary disease were isolated by positive selecting using antI-CD31 immunomagnetic Dynabeads and cultured up to passage 4 in 6 well plates. Monolayers were treated with bestatin hydrochloride for 12 hours or left untreated as a control and then the monolayer was interrupted as outlined in chapter 2. Images were obtained using phase contrast microscope at 20x magnification and approximate measurements were made based on the images taken. Semi-quantitative analyses were made by calculating the % remaining distance between endothelial monolayer as a result of the scratch in comparison to the distance at time 0 hours. Image A represents CRLM immediately after a scratch. Image B illustrates the area of the remaining scratch in CRLM endothelial cells. Image C illustrates the area of the remaining scratch in CRLM endothelial cells that were a control and left untreated. Graph D outlines the data collected by measuring the distance between the scratch test edges in both Bestatin treated CRLM endothelium and the control from 0 to 72hours at 5 time points. Data represents the mean of 3 test repeats for 1 biological repeat. Significance was not tested.

A similar approach was applied to the quantification of CD13 expression by NEC and TEC. Expression of the isoform WM15 was initially explored by immunohistochemistry of CRC tissue sections. Expression through tumour stroma was expressed by membrane and cytoplasm of some endothelial cells of microvasculature but not all vessels revealed positive staining (see examples in Figure 3.10). Cytometric analysis suggested values for NEC and TEC from both paired samples and un-paired samples were not significantly different. We also tested for function of CD13 between colorectal liver metastatic EC (CRLMEC) by using Bestatin, an inhibitor of the aminopeptidase activity of CD13. Bestatin-treated and untreated monolayers of CRLMEC were scratched and imaged at 12, 24, 48 and 72 hours to assess the distance between the two edges of the monolayer (Figure 3.11). The distance was measured semi-quantitatively and reported as a percentage of the initial scratch distance. The distance between edges in the scratch test assay in the Bestatin treated CRLMEC remained wider for longer compared to the non-treated group.

Results summary:

- We achieved successful development of long term in vitro model of NEC and TEC from CRC.
- Expression of basal CD31 was similar between NEC and TEC.
- There were no significant differences between expression of CD105, VEGFR-2 and VE-Cadherin between endothelial cells from CRC or NC.
- TEM-8 is significantly upregulated by TEC but not NEC.
- TEM-8 expression is maintained in TEC but not NEC through long term culture
- CD13 WM15 expression was not tumour specific

3.3 Discussion

3.3.1 Generation of my protocol for isolation of colonic endothelial cells

I began by seeking a suitable endothelial marker to use for cell isolation. Staining experiments suggested that CD31 is a more specific endothelial cell marker than CD146. This was found for both NC and CRC where predominantly endothelial cells lining blood vessels throughout the whole tissue, and only few immune cells expressed CD31. A Nature protocol (136) published similar data from pre-isolation immunohistochemistry where human normal colon, colorectal cancer and placenta tissue sections were stained with anti-CD31, CD34, CD105 and anti-CD146 antibodies to identify which of these four endothelial markers would be the most endothelial-specific to use in isolation methods. They found that CD31 would be the optimal marker given that CD105 positive staining was found within the stromal cells of both NC and CRC and that CD146 was not endothelial specific. CD31, also known as PECAM-1 is a cellular adhesion molecule of 130kDa. It has an extracellular domain with 6 immunoglobulin folds (138) which can bind homo-typically to CD31 as a ligand, and also hetero-typically to integrins αvβ3 (139). The CD31 expression on vascular endothelial cells in most tissues (140) and its homophilic binding property allows endothelial cell-cell adhesion. Some leukocyte populations (141) also express CD31 which can facilitate monocyte, T-cell and neutrophil transmigration (30, 31) across the endothelium. Interferon gamma (IFN-ϒ) and Tissue necrosis factor α (TNFα) may down regulate (143) or redistribute (144) the expression of CD31 as shown in HUVEC. Any variance in CD31 expression between ECs in different tissue samples may compromise standardization of its use as a tool for EC isolation methods. However, my semi-quantitative analysis of "proportion of vessels stained" and "intensity of staining" across immunohistochemistry of 9 matched samples of NC and CRC reveals that the

proportion of vessels stained and intensity of CD31 expression is similar between NC and CRC. Thus, I was confident in my decision to proceed using this receptor for isolation

There are few published protocols for NEC and TEC isolation specifically from colon, and therefore protocol optimization was a major aim of this chapter. Existing protocols from the literature include; Isolation and culture of EC derived from small bowel (135); Isolation and culture of human EC derived from CRC and matched NC (60) (134); Isolation only, using anti-ulex lectin (137), anti-CD146, anti-VE-cadherin, or anti-CD105 immunomagnetic beads; Isolation of EC derived from human CRC using anti-CD31 and flow assisted cell sorting (FACS) (136) and FACS isolation and culture expansion of murine EC (136). The key aspects of the protocols highlighted by these papers collectively are outlined below.

Isolating endothelium from larger vessels such as the umbilical vein for HUVEC involves direct cannulation of the vessel. This is not possible with colorectal microvasculature and tissue must be homogenised whole and the endothelial cells must be isolated from this cell mixture. For each method, a single cell suspension is obtained. This is achieved by enzymatic digestion. The use of collagenase (60) and dipase is common and is used together (134) with DNAse in some protocols (135, 136). Time of incubation with enzymes ranges from 30 mins to 18 hours, and alterations in cell phenotype after incubation with enzymes for just 1 hour has been reported for some cells (145). This has been explored most thoroughly in immune cells (146, 147) for which loss of cell surface proteins occur readily with collagenase and protease but not with mechanical digestion. Data is scarce regarding potential consequences for EC, however variations in the enzymes and incubation times used makes it difficult to determine the consequences of differing protocols. Homogenization by hand also

poses the problem of standardization between preparations, risk through exposure to aerosolized material and shear-induced tissue damage.

New commercially available mechanical dissociation kits and systems such as the Gentlemacs allow performance of standardized and optimized protocols for specific tissues. In addition such mechanical methods are reported to preserve the phenotypic profile of immune cells (147). However, I found that EC that had undergone mechanical separation did not expand in culture and so for functional *in vitro* assays, this method was not preferable. Mechanical separation methods may also be beneficial by potentially optimizing cell yields, which is useful where tissue samples are small, as is the case in tumour samples where care is taken not to compromise the material required for patient staging. Van Beijnum et al (136) recommend using >1 gram tissue as a minimum, however Schellerer et al (60) report success with as little as 0.5 grams. I have refined my protocol over the course of this year to develop a means to isolating CD31+ cells from approximately 0.5-1 grams of normal or tumour tissue.

Once a single cell suspension is obtained the mixture is filtered allowing passage of particles up to 100µm to remove mostly debris and mucous. Some report that the use of a density gradient centrifugation at this point can eliminate erythrocytes, granulocytes and cell debris (135, 136). This step has the advantage of purifying the cell mixture before endothelial isolation however it is entirely operator dependent and therefore more difficult to standardize.

Endothelial isolation can occur prior to expansion or after one passage. My experiences are similar to those from Erlangen with improved subsequent expansion and growth of both NEC and TEC after allowing initial culture, with cells such as smooth muscle cells, fibroblasts, and monocytes and in TEC, tumour cells. All culture conditions are 'artificial' and so allowing EC to initially expand in "co-culture"

potentially mimics the tissue environment *in vitro,* by permitting production of regulatory factors found in tissue or tumour milieu. Historically, various manual methods such as cell scraping, diathermy and even laser have been used to remove contaminating colonies (148) *in vitro*, however, these methods are time consuming, tedious and ineffective. Immunomagnetic selection is a better option, and Schellerer et al (60) have described successful culture at 93% purity in both NEC and TEC using this technique. They detach the cells once ECs have colonized and use CD31 magnetic beads to isolate the ECs, which are then re-plated. We had similar success with CD31 beads in this study, and therefore have used CD31 over any other antibody in our final protocol.

Rather than using beads to select cells from a heterogeneous population, fluorescence activated cell sorting has been described for isolation of microvascular murine EC using anti-CD31 (136) and bovine adrenal microvascular EC based upon the uptake of acetylated low density lipoprotein (149). FACS and subsequent expansion in culture of NEC and TEC from human CRC has not been described in the literature to date. Difficulties with FACS include the direct effect on cell viability due to the shearing forces applied during the sorting and the cost. However, the benefits of a pure sample for subsequent assays such as next generation sequencing and functional assays are obvious. I have been able to successfully isolate human colonic EC using this approach. Our data suggesting that the procedure does not cause undue harm to cells and our photographs of EC reattaching in culture after this isolation route are therefore promising.

3.3.2 TEC in culture maintain a distinct and appropriate phenotype

The phenotype of isolated microvascular EC is often characterized by confirming expression of CD31, VWF, ICAM-1 and inducible VCAM-1 in response to inflammatory cytokines. Other molecules such as VEGFR-2, CD105, VE-Cadherin, TEM-8 and CD13 are often reported as expressed in angiogenic tumour endothelium. Further to developing a reproducible protocol at my institution, I analysed CD31 expression of NEC and TEC by flow cytometry revealing that more than 93% of isolated NEC and TEC at passage 4 express cell surface CD31. This was a reassuring finding that was supported by immunochemical staining. Interestingly, the cytometric cell surface CD31 expression was similar between both NEC and TEC in percentage and median channel value, although PCR data suggested that PECAM-1, the gene coding for CD31 is down regulated in TEC. The differences between *in vitro* ICC and FC data and the PCR data may relate to the time point of these experiments. The PCR results came from freshly isolated cells immediately upon removal from tissue in contrast to cultured cells used for antibody-based detection. Thus TEC may have responded to regulatory factors, such as IFN-ϒ and TNFα within the tumour microenvironment. This is supported by our ELISA data, where although experimental repeats are low, the expression of CD31 moderately decreased in NEC when stimulated with TNFα. Interestingly, CD31 production appeared to be up-regulated by IL-1β. Certainly, when TEC were stimulated by TNFα and analysed by FC, the percentage and MCV VCAM-1 expression increased, which is typical of NEC and TEC (60). Basal expression of VCAM-1, ICAM-1 and other adhesion molecules is discussed in later chapters however here, they have been used to characterize vascular endothelial phenotype.

VWF was expressed at a protein and transcription level in CRC and NC based on IHC and gene expression data. However, only modest differences were found between NC and CRC shown by semi-quantitative IHC analysis and QPCR supporting current data (150). VWF is a glycoprotein produced by vascular endothelial cells in most tissues and is stored in the Weibel-Palade bodies. It's main purpose is to bind to other proteins such as factor VIII via its D'/D3 domain and collagen which is important to coagulation (151), hence expression in megakaryocytes is also seen. *In vitro* studies with HUVEC suggest that VWF is up regulated by angiogenic factors such as VEGF and FGF-2 and hypoxia at a transcriptional level (152). Interestingly, the same study performed preliminary data using tissue from CRC and matched NC for semi-quantitative rt-PCR. This revealed heterogeneity, described previously (153), in VWF gene expression with a similar or even lower level of gene expression in CRC tissue in 3 of 9 patients (152). Furthermore, expression of VWF in CRC tissue by IHC, was reportedly not related to stage of disease (150). I found that TEC express less intracellular VWF than matched NEC, shown by qualitative analysis of ICC which supports similar findings *ex vivo* and *in vitro* (60). Interestingly Schellerer et al (150) found that when stimulated with cytokines, NEC down-regulate VWF expression similar to matched TEC. Thus, expression of VWF by my cells confirms their vascular endothelial nature and in addition suggests that cytokines within the tumour environment may modestly downregulate expression on TEC compared to NEC.

CD105 overexpression is reported in human tumour types and has been suggested to contribute to tumour angiogenesis. Levels are increased on neovessels, and studies have explored the use of CD105 as a prognostic marker in colorectal cancer (154). CD105 is a homodimeric transmembrane that binds with *TGF*-β (155) and is expressed by microvasculature of many tumour types including colorectal cancer (156).

My FACS data suggested that TEC have moderate expression, along with strong positive vascular endothelial CD105 staining by IHC on both NEC and TEC. Regulatory factors for CD105 include TGF-β 1 (157) and gene expression can be induced by hypoxia (158). Although our IHC findings did not reach statistical significance the semi-quantitative score revealed a marginal increase in *ex vivo* expression in CRC compared to NC, which could be supported by QPCR data where Endoglin gene expression, which codes for CD105 protein, was up regulated in TEC. Thus, my data support the concept that expression of CD105 is enhanced on TEC compared to NEC. However, the endothelial specificity of CD105 has been questioned as expression has been identified in macrophages, fibroblasts and smooth muscle cells, although (159) lymphatic endothelial cells do not express CD105. Thus, CD105 would not be valuable as a confirmatory marker to positively identify endothelial cells in the absence of negative staining for key immune cell and pericyte markers.

Semi-quantitative analysis showed that microvascular endothelial expression of VE-cadherin expression is present in both CRC and matched NC tissue, although this was at low levels and intermittently throughout the tissue. VE-cadherin, a member of the cadherin superfamily is key to endothelial cell-cell adhesion (160)(161). The transmembrane glycoprotein has an extracellular compartment that engages in homophilic binding where VE-cadherin acts as both ligand and receptor (162). The intracellular compartment then attaches the plasma membrane to the cytoskeleton via catenins (163). Interestingly, our FC findings based on 6 matched samples, suggests that VE-cadherin is expressed on approximately 25% of NEC and almost 20% of TEC. The overall percentage expression of VE-Cadherin by both NEC and TEC is lower than expected and may be a result of the isolation process. This may cause lysis of the adherin junction by enzymatic activity as encountered previously (164). Although not

reaching statistical significance, lower levels of expression on TEC was expected. The tumour vessel "leakiness" may result from down-regulation, or internalisation of endothelial VE-cadherin or tyrosine-phosphorylation of VE-cadherin junctions. This may derive from VEGFR-2 signaling since soluble VEGF may cause "loosening" of the EC-EC junction thus increasing HUVEC permeability (165). Down-regulation of Cadherin-5, the gene that codes for VE-adherin in tumour endothelium is supported by our QPCR data. This shows down-regulation at a transcription level of Cadherin-5 in TEC relative to matched NEC however the regulatory mechanisms have not been explored.

So, in total my data support the identification of cells isolated using my protocol as endothelial and that TEC maintain some 'tumour-specific' markers in vitro. However, some data sets had large error bars suggestive of heterogeneity within the sample group, which is relatively small consisting of just 6 patients. Thus, use of larger numbers of patients from well-characterized disease stages may be warranted.

Despite interesting differences of pan-endothelial marker expression, the main objective of this data was to compare the phenotype of isolated EC with that available in the literature and provide a baseline phenotype to compare to that of *in vitro* cultured NEC and TEC. To that end, we investigated the expression of TEM-8 to confirm 'tumour' phenotype and, importantly, we showed that tumour endothelial cells demonstrate tumour phenotype through multiple passages. This finding is crucial as successful isolation and culture of tumour endothelium, which require immunomagnetic bead isolation processes through passage to achieve the high purity essential for subsequent functional assays.

Tumour endothelial marker 8 was identified as a result of serial analysis of gene expression (SAGE) of tumour endothelium isolated by laser capture by St Croix et al

(2000) (42). TEM-8 is a cell surface glycoprotein and an Anthrax toxin receptor (ANTXR1) up-regulated by many human and mice tumour types (18), (166). Functionally, TEM-8 has been shown to bind to basement membrane collagens and promote EC migration. Although our data has not investigated the functionality of TEM-8, expression suggests that tumour specific functions are preserved. Although the gene expression for TEM-8 is down regulated in NEC, it is still present at low levels per our rtPCR data. It is interesting that through culture passages, gene expression is lost in NEC but not in TEC. This suggests that there are regulatory factors in tissue that regulate TEM-8 expression. It is unlikely that such regulatory factors derive from angiogenic pathways, as unlike other angiogenic markers in tumours, TEM-8 is absent from benign, physiological angiogenic tissues such as corpus luteum and ovaries (42), and TEM-8 -/- knockout mice have been reported to be near normal (43) albeit with reduced growth (167). Furthermore, TEM-8 gene expression reportedly increases with stage in CRC (4). This 'tumour', and not 'angiogenic' expression pattern provides an attractive case for use of TEM-8 both as a tumour marker, and as a vehicle to deliver anti-cancer therapies. Thus, studies have targeted TEM-8, also known as anthrax toxin receptor-1, by utilizing internalisation lethal toxin upon binding of PA (one of three proteins comprising the anthrax toxin) to the TEM-8 cell surface receptor (168)(169).

CD13/Aminopeptidase-N expression, has been identified by the vascular endothelium of several types of inflamed tissue and tumour tissue, including colorectal (170). Expression is isoform specific with the WM15 isoform being more specific to tumour vessels than other isoforms. Our data reveal similar CD13 expression levels in tumour and normal endothelium, with staining of whole CRC tissue suggesting there was endothelial specific staining evident. A commercially available agent Bestatin, that binds cell surface CD13 Wm15 has been explored for its value as an anti-tumour

therapy. Bestatin competitively inhibits the protease effects of CD13 WM15 and its efficacy in prolonging survival as a post-operative adjuvant therapy after curative resection of stage 1 squamous cell lung cancer has been highlighted by clinical trials (54). Reduced angiogenesis (171) and capillary tube formation has been reported in HUVEC by using Bestatin to block CD13, but not in primary endothelial cells from colorectal liver metastasis. Our data demonstrating delayed proliferation/migration of EC derived from CRLM with Bestatin may indicate its use in the treatment of Dukes D CRC, which currently has a <5% 5 year survival. Chemokine profiling is underway to identify factors and chemokines that may be predominantly responsible for regulation of CD13. Data from monocyte populations suggests that lipopolysaccharide (LPS) and TGF-β, Il-10 and TNF-α regulate CD13 expression. Areas open to further exploration include the efficacy of modulating CD13 driven monocyte adhesion and diapedesis by chemokines. A CD13 positive immunosuppressive T-cell subpopulation has also been described in lung tumours (172), in addition to myeloid derived suppressor cell (MDSC) population that express CD13 (173). Thus, there is much potential for therapeutic intervention targeting CD13.

In this chapter I have developed a protocol for isolation and longterm culture of primary human tumour endothelial cells derived from colorectal cancer. I have characterised the NEC and TEC as microvascular in origin and explored their phenotype and gene expression relative to their origin. Furthermore, for the first time I have revealed that colonic tumour derived endothelium persistantly express tumour specific markers in culture. In the next chapters, I use NEC and TEC in models to investigate the differences in lymphocyte recruitment between NEC and TEC and explore possible regulatory factors to tumour lymphocyte recruitment for therapeutic exploitation.

CHAPTER 4

Endothelial adhesion molecule expression and cytokine production in colorectal cancer.

4.1 Introduction

In a process called immunosurveillance, first described in the early 20th century by Ehrlich, the immune system can prevent tumour formation by recognizing cells that are undergoing malignant transformation before malignancy is identified clinically (174). This tumour suppressor role of the immune system was further strengthened in studies using athymic nude mice which were found to be only partially immunodeficient having functional natural killer cells and cytotoxic T- lymphocytes that responded to concanavalin -A (175). Further detail on the anti-cancer properties of the immune system was discovered largely by the discovery of tumour specific antigens (176) which are identified by T-cells (177) and initiate an immune reaction, leading to tumour cell death (178, 179). This knowledge of tumour specific antigens arose from increased understanding of host rejection of tissue grafts during and after WW2 (180), and the apparent host protection against subsequent tumours after induction and removal of a primary tumour, illustrating both specificity for and memory of the tumour antigen by the host immune system (176).

Activated CD8+ T-cells, known as cytotoxic lymphocytes (CTLs) induce death of foreign cells, including tumour cells (177, 178). Thus, an increased number of CD8+ T-cells in colorectal cancer (2) and some other solid tumour types (*e.g*. ovarian, (181,

(182) is associated with improved prognosis. CTLs release pro-inflammatory cytokines and cytotoxic granules containing perforin and granzyme-A and B (183). Perforin perforates the tumour cell membrane to allow entry of granzymes A and B into the cell to degrade intracellular proteins. CTLs can also kill tumour cells using TNF-related apoptosis-inducing ligand (TRAIL) and Fas receptor–ligand binding which induce apoptosis or cell death (184, 185). These mechanisms also allow regulation of activated CTLs so that the body can down-regulate an immune response as desired.

Despite the efficacy of the cell-based anti tumour responses described above, tumours have been found to escape the body's immune system *via* immune-escape or editing (186, 187). These mechanisms have clear clinical relevance, with future therapeutics possibly exploiting and manipulating the mechanisms of immune escape to reinstate effective immune control. For example, methods have been identified to promote the lifespan of CTLs in the tumour stroma, and focus on checkpoint blockade and the efficacy of CTLA-4 inhibitors often in combination with programmed –death-1 (PD-1) inhibitors to increase the effector T-cell function and promote an anti-tumour response (188, 189).

There are broadly two subsets of colorectal cancer; Antigenic and Non-antigenic (190). Unfortunately, clinical treatment does not account for these differences to date. Antigenic tumours stimulate the recruitment of CD8+ T-cells but employ immune-escape pathways (187). In contrast, Non-antigenic tumours, which in CRC have a worse prognosis, lack cytokine expression but exhibit very little immune effector cell inhibition. Thus, it is interesting to speculate whether modulation of CD8+ T cell recruitment into non-angiogenic tumour stroma by up-regulating EC adhesion molecule expression would be prognostically beneficial? To answer this question, the

role of adhesion molecules in tumour EC and the proinflammatory factors produced by fibroblasts, epithelial, endothelial and immune cells must be explored.

C-C chemokine ligand (CCL2) is a chemotactic cytokine, also known as monocyte chemotactic protein 1 (MCP-1), with a monomeric polypeptide structure weighing 13kDa. As the name MCP-1 suggests, it has a well-described role in recruiting monocytes and clinically is implicated in diseases characterized by monocytic infiltrates. Although CCL2 is predominantly released by monocytes, macrophages and DC, evidence suggests CCL2 is expressed by human microvascular endothelial cells (191) and can be induced by low-density lipoprotein (LDL). CCL2 has been implicated in T cell recruitment (192) and therefore has been investigated in this chapter.

Elevated levels of adhesion molecule expression by colorectal cancer cells and tumour fibroblasts have been described (193, 194, 195) and in murine models this has been associated with tumour pathogenesis or worsened tumour outcomes (196). Presence of intercellular adhesion molecule-1 (ICAM-1), Vascular cell adhesion molecule-1 (VCAM-1), and E-selectin has been quantified in CRC patient serum, and are elevated compared to healthy controls (197). However, reporting of expression of adhesion molecules specific to EC is often inconsistent and predominantly based on semi-quantified immunohistological data (193, 198, 199, 200).

Therefore, this chapter aims to shed light upon the mechanisms, which may govern CD8+ T lymphocyte recruitment into colorectal tumours by;

- Characterizing colorectal cancer and matched normal colorectal endothelial cell expression of the adhesion molecules, ICAM-1, VCAM-1, MAdCAM-1 and E-selectin.
- Comparing chemokine and chemotactic soluble factor profiles produced by tumour endothelial cells and normal endothelial cells
- Identifying the *in vitro* function of adhesion molecules and chemokines by their selective and strategic inhibition through a series of static adhesion assays.

4.2 Results

4.2.1 Colorectal tumours are infiltrated by lymphocytes and numbers correlate with vessel density

In this chapter my aim was to understand the differences in the expression of adhesion molecules by NEC and TEC and how this affects CD8+ T-cell recruitment. I began by staining tissue sections from CRC to assess the amount of infiltration by CD8+ T cells within the tissue stroma (Figure 4.1). This enabled quantification of CD8+ lymphocytes in all the samples within our cohort and correlation with disease stage. Figure 4.1 shows representative images for CD8 positive cells in two Dukes stage C cancers, but with the left image representing tissue that is highly infiltrated by CD8+ lymphocytes (panel A) and the image on the right representing tissue with few infiltrating lymphocytes (panel B). When we considered our cohort we found that mean number of CD8+ cells ranged from 93 to 328 CD8+T-cells per field view. When the numbers of CD8+ T-cells were plotted against the anatomy of the primary tumour, there was a trend towards higher tumour infiltrating lymphocyte number in those tumours originating in the right hand side, which includes the caecum ascending colon, hepatic flexure and right of the midpoint transverse colon (Figure 4.1E). When plotted against Dukes stage of disease there was no significant correlation. Finally, to identify if there was any relationship between the number of TILs and the abundance of vessels within the sample, tissue sections from the same specimen underwent CD31 immunohistochemistry. Representative images of tissues found to have low and high CD31+ vessel density are shown in panels 4.1 C and D respectively. The percentage of CD31 staining found within each tissue section was significantly and directly proportional to the number of TILs (Spearmans rank correlation coefficient, $p=0.05$).

4.2.2. Expression of MAdCAM-1, ICAM-1, VCAM-1 and E-Selectin in CRC and NC.

To understand the mechanisms that might contribute to trafficking towards, and retention of CD8+ cytotoxic T-cells within CRC and NC, IHC was performed on whole tissue to identify the locality of adhesion molecules. Both NC and CRC microvasculature expressed positive cytoplasmic and membranous MAdCAM-1 staining within the mucosal lamina propria and submucosal layers of NC (Figure 4.2). In CRC, positive MAdCAM-1 staining of the stromal vessels was also noted, however this was less consistent than NC and generally staining was less intense (see Figure 4.2), confirmed by semi-quantitative analysis of 6 paired samples. This revealed a significantly higher proportion of positively stained vessels, but not intensity, in NC compared to matched CRC (Figure 4.3, 2.3 v's 1.5, p=0.0041).

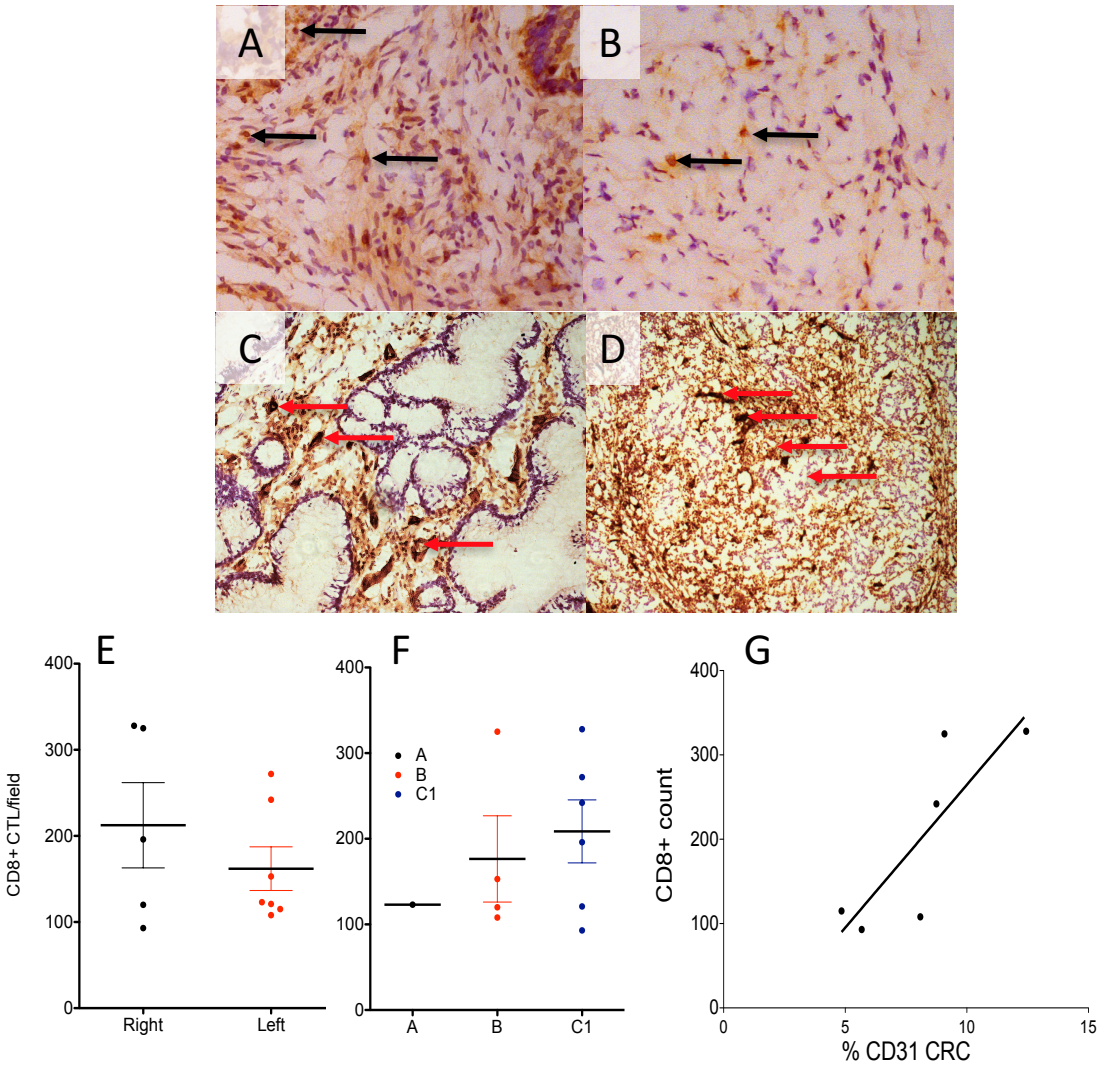

Figure 4.1. Variation in the density of tumour infiltrating CD8+ lymphocytes amongst Colorectal tumours. CD8 count was performed using immunohistochemistry of frozen tissue sections with rabbit anti-human CD8+ antibody and DAB substrate with haematoxylin counterstain. 3 different fields were captured from 3 different sections of each CRC samples at 20x magnification and retrieved using Axiovision software. This resulted in 9 different field views per sample, each of which was used to count the CD8+ cells within the tissue stroma, using cell-counter from Image J software. From this the mean was calculated. Images A and B represent tissue where CD8+ T-cells were more and less abundant respectively. Images C and D are from representative CRC sections stained with CD31 to reveal the extent of the vasculature in the tissue stroma. Image C illustrates a tissue section with few vessels whereas D illustrates tissue with more abundant vasculature.

Tumour infiltrating lymphocyte abundance was assessed for correlation with the anatomy of the primary tumour (E, left panel) and Dukes stage of the disease (E center panel). 1 specimen only was found to be Dukes A, 4 specimens were Dukes B, and the remaining were Dukes C. The final chart (E right panel) presents the correlation between %CD31 staining, and CD8+ count. Data presented in E are mean and SEM. Differences between data in E (left and center panels) were analysed for statistical significance using two tailed student T test and significance was accepted where $p<0.05$. A significant correlation between variables in E, right panel was found (Spearmans rank correlation coefficient, $p=0.049$).

ICAM-1 was constitutively expressed by vessels and occasionally fibroblasts within the and submucosa of NC and through CRC stroma (see representative images in Figure 4.2). In addition, ICAM-1 was expressed at the membrane of several lymphocyte subsets throughout both NC and CRC. Positive staining of larger blood vessels found nearer the deeper muscle layers was also noted. The staining in both tissue types was noted predominantly at the cell membrane although some cytoplasmic staining was seen. Semi quantitative scoring of 4 paired sections revealed a significantly higher proportion of positively stained vessels in CRC compared to NC (Figure 4.3, 3 v's 2.25, p=0.05), but no difference in the intensity of staining.

Similar analyses were performed for VCAM-1, and we saw positive vascular endothelial staining in both NC and CRC (Figure 4.2). Positive cytoplasmic and membranous endothelial staining in NC was predominantly within the submucosal layer, and VCAM-1 was also expressed by vascular smooth muscle cells and within the muscularis mucosa (see representative image in Figure 4.2). In CRC the positive staining was more specific to the cytoplasm and membrane of vascular endothelium (Figure 4.2). Whilst the intensity of staining for VCAM-1 tended to be higher in NC samples and the proportion of vessels stained tended to be higher in CRC in 4 matched samples (Figure 4.3), these changes were not significant.

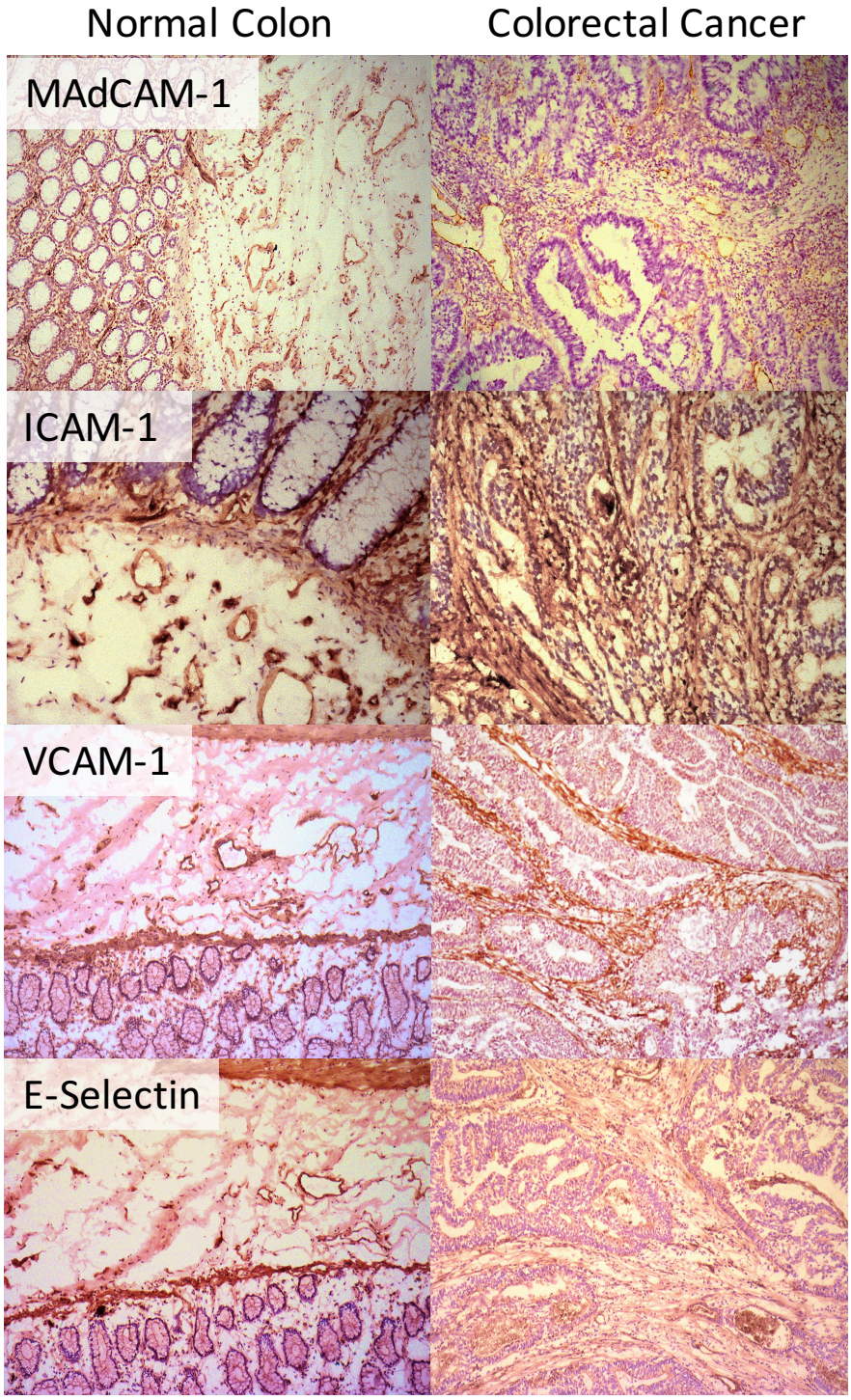

Figure 4.2: **Expression of vascular endothelial adhesion molecules by NC and CRC.**
Immunohistochemistry was performed using unfixed frozen whole tissue sections of NC and CRC (7µm thickness) by an indirect DAB staining method. Mouse anti-human antibodies against indicated molecules were used in addition to isotype- matched controls. Representative images shown were taken at 20x magnification and retrieved using Axiovision software.

		Mean score (range)		
		NC	CRC	P value
MAdCAM-1 (n=6)	Proportion of vessels stained	2.3 (2-3)	1.5 (1-2)	0.004**
	Intensity of staining	1.3 (1-2)	1.3 (1-2)	1.0
ICAM-1 (n=4)	Proportion of vessels stained	2.5 (2-3)	3 (3)	0.18
	Intensity of staining	2.25 (2-3)	1.5 (1-2)	0.06
VCAM-1 (n=4)	Proportion of vessels stained	2.5 (2-3)	3 (3)	0.9
	Intensity of staining	2.25 (2-3)	1.5 (1-2)	0.21
E-selectin (n=3)	Proportion of vessels stained	2(2)	2.3 (2-3)	0.42
	Intensity of staining	2.3 (2-3)	1.7 (1-2)	0.18

Figure 4.3: **Semi-quantitative assessment of expression of vascular endothelial adhesion molecules by NC and CRC.**
Immunohistochemistry was performed using unfixed frozen whole tissue sections of NC and CRC using an indirect DAB staining method. A semi-quantitative score was performed for 3 matched samples for both the intensity of staining and the proportion of vessels stained by each protein between 0-3 where 0 is no positive staining/ none of the vessels present stained and 3 is very intense positive endothelial staining/ all vessel endothelia present in the field view positively stained. Staining was compared to isotype-matched control samples in all cases. Statistical analysis was performed using paired student T-test. Significance was considered where $p>0.05$ * (**$p>0.005$, ***$p>0.0005$)

IHC also confirmed E-selectin expression by CRC and NC. In NC, vascular endothelial expression was cytoplasmic and membrane bound and mostly sub-mucosal although specific staining was found in smooth muscle cells and infiltrating lymphocyte populations (Figure 4.2). In CRC, specific staining was limited to the vascular endothelium within the stroma and some smooth muscle although there was some additional artifact staining noted (Figure 4.2). When this was assessed by semi-quantification score, the proportion of vessels stained was higher in CRC compared to NC (mean score 2.3 v's 2, respectively, Figure 4.3) however, NC scored a higher mean score of 2.3 for the intensity of vessels stained compared to 1.7 which was the mean score for the CRC sections.

4.2.3 Expression of MAdCAM-1, ICAM-1, VCAM-1 and E-Selectin in endothelial cells derived from colorectal tumour and normal colorectal tissue.

Primary human colorectal tumour (TEC) and normal colorectal microvascular endothelial cells (NEC) were analysed by flow cytometry (FC). Analysis of membranous MAdCAM-1 expression showed a higher percentage MAdCAM-1 expression by NEC compared to matched TEC (mean % NEC 36.6± 35 v's TEC 11.6±16.2, p=0.04, Figure 4.4 A). Whilst this agreed with our findings in tissue sections, the difference was not maintained when data was pooled to including non-paired samples and reflects the variation in the different donors. Of note the amount of MAdCAM-1 expressed per cell (median channel value (MCV)) for paired NEC and TEC was the same (51.9±48.3 and 52.9±75.9) respectively, (Figure 4.4 B).

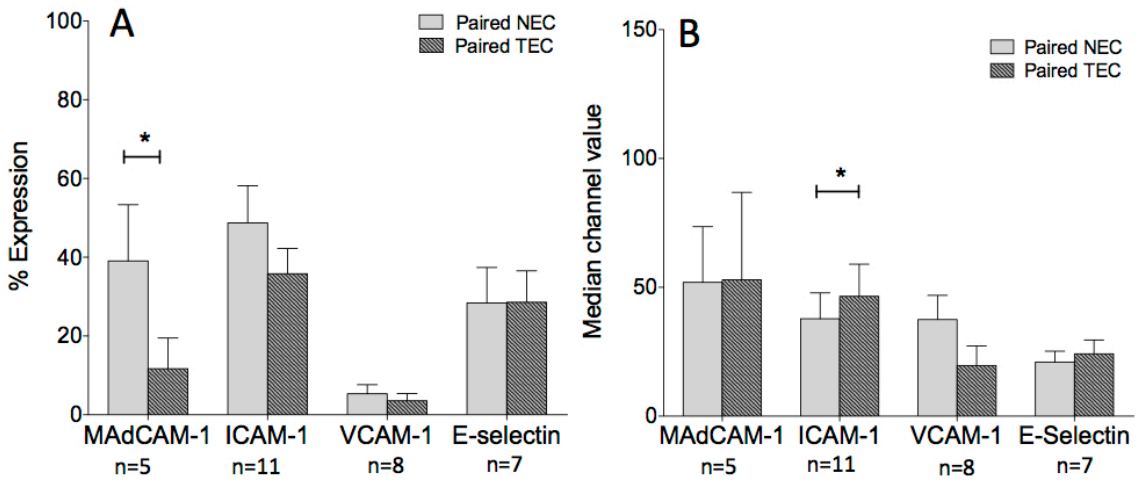

Figure 4.4: Cell surface expression of MAdCAM-1, ICAM-1, VCAM-1 and E-selectin by isolated primary human NEC and TEC.
Primary human endothelial cells were isolated from human normal colorectal and colorectal cancer tissue samples by positive selection using anti-human CD31 immunomagnetic beads. Cells were then stained and washed for 30 mins with mouse anti-human MAdCAM-1, ICAM-1, VCAM-1 and E-selectin antibodies with isotype matched. Cells then underwent flow cytometrical analysis on a standardised protocol using Becton Dickenson Cyan flow cytometer and Summit v4.3 software. Images A and B illustrate data obtained describing MAdCAM-1, ICAM-1, VCAM-1 and E-selectin cell surface expression, respectively, by both NEC and TEC. Graphs show data for paired samples for both percentage expression (left panel) and median channel value (right panel) expressed as mean and SEM. Statistical analysis was performed using two tailed Student's t-test.

Expression of ICAM-1 by isolated primary TEC and NEC indicated a trend towards lower percentage expression of membranous ICAM-1 by TEC than NEC although this was not statistically significant (Figure 4.4 A). However, there was significantly higher MCV expression of membranous ICAM-1 in TEC indicating that where cells did express cell surface ICAM-1, in TEC this was more intense than in NEC (Figure 4.4 B, mean MCV TEC 46.52±39.3 v's NEC 37.79±31.8, p=0.05). Similar to our data for MAdCAM-1, when we compared all samples that were not paired, no significant difference in expression between TEC and NEC was found (Figure 4.4 C, mean MCV TEC 41.9±41.7 v's NEC 64.4±97.4).

Constitutive VCAM-1 expression in paired and unpaired NEC and TEC was much lower than seen for MAdCAM-1 and ICAM-1 although there was little difference between NEC and TEC. The higher MCV for cell surface VCAM-1 found in paired NEC compared to TEC (Figure 4.4 B, 41.3 NEC v's 22.5 TEC,) was not maintained in the larger unpaired cohort. Similarly, there was little difference between percentage expression and MCV for membranous E-selectin expression in NEC and TEC, (Figure 4.4).

Total NEC and TEC expression of ICAM-1, MAdCAM-1 and VCAM-1 protein was investigated by ELISA. Higher levels of ICAM-1 were identified across 3 x NEC samples compared to 1x TEC sample (Figure 4.5 A), and ICAM-1 was the most abundant adhesion molecule found in 3 *in vitro* primary NEC and 1 *in vitro* sample of primary TEC. In NEC, the mean ICAM-1 expression was twice that of VCAM-1 or MAdCAM-1. Overall VCAM-1 and MAdCAM-1 levels were similar in the single TEC sample although slightly lower than the mean value for NEC. After treatment with IL-1β and TNFα for 12 and 8 hours respectively, NEC ICAM-1 expression increased significantly compared to untreated NEC. However, expression of MAdCAM-1 and VCAM-1 did not change following treatment with either IL-1β of TNFα (Figure 4.5 B).

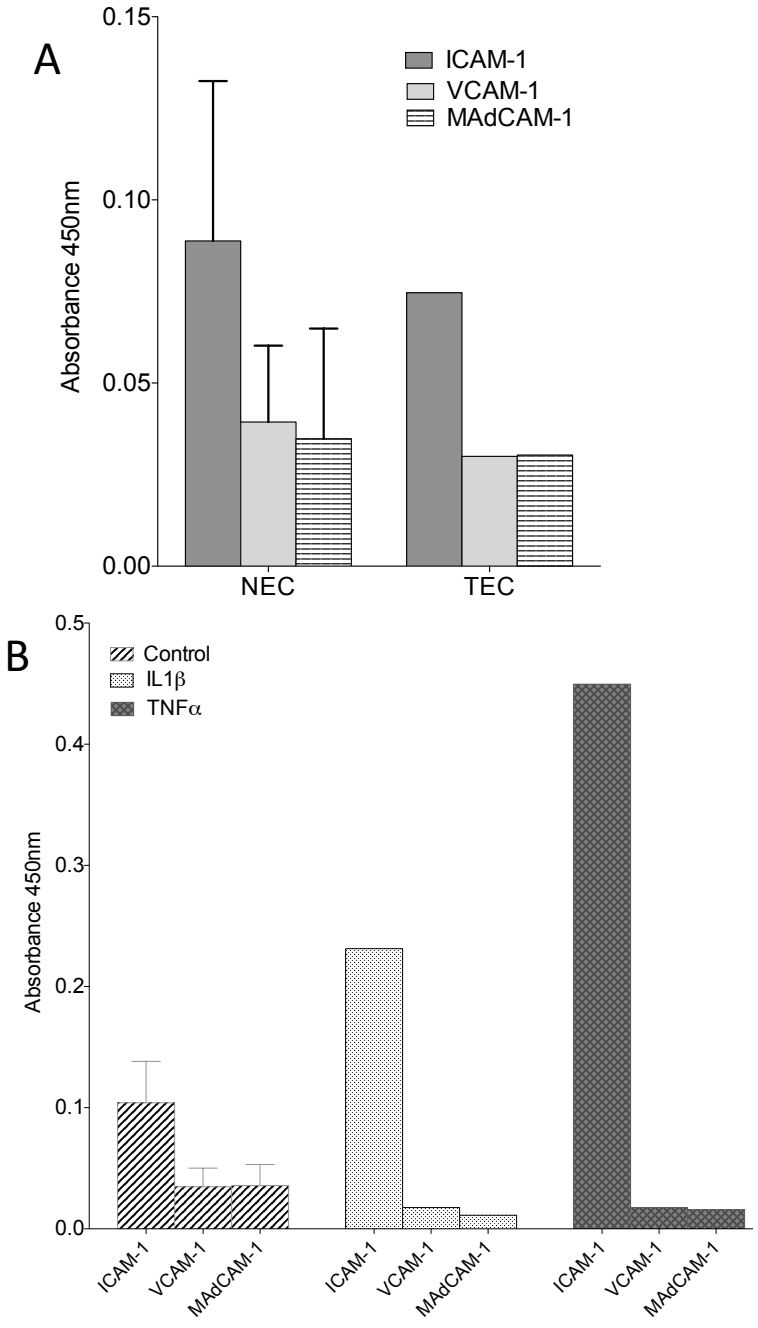

Figure 4.5: ICAM-1, VCAM-1 and MAdCAM-1 expression in human primary *in vitro* NEC and TEC.

In vitro NEC and TEC were cultured at passage 5 in flat bottom 96 well plates until confluent. Where indicated, cells were stimulated with 10ng/ml of IL1β or TNF α for 12 hours. Expression was determined using indicated primary antibodies and HRP-conjugated secondary antibody with TMB substrate. Absorbance was read at 450nm and background values for isotype matched controls were subtracted from test data. Graphical data is presented as mean and SEM. Graph A presents data comparing adhesion molecule expression by untreated in-vitro NEC and TEC. Comparative data using stimulated NEC by IL1β or TNFα after 12 hours incubation is presented in graph B. Statistical analysis was performed using 2 tailed student T-test. Significance was considered where $p<0.05$.

4.2.4. MAdCAM-1, ICAM-1, VCAM-1 and E-Selectin gene expression in colorectal TEC and NEC.

Quantification of MAdCAM-1, ICAM-1, VCAM-1 and E-Selectin gene expression by QPCR revealed that in most cases, expression was higher in TEC than NEC, although there was no significant increase found in TEC compared to NEC. VCAM-1 gene expression was even more variable between donors. In two samples TEC expressed more than 20 times the VCAM-1 mRNA seen in NEC. Similarly, E-Selectin gene was found to at least double in 3 out of 4 cases (Figure 4.6). Thus there was clear variation in individual mRNA expression for key adhesion molecules between donors and no pattern of regulation within the same TEC sample.

A

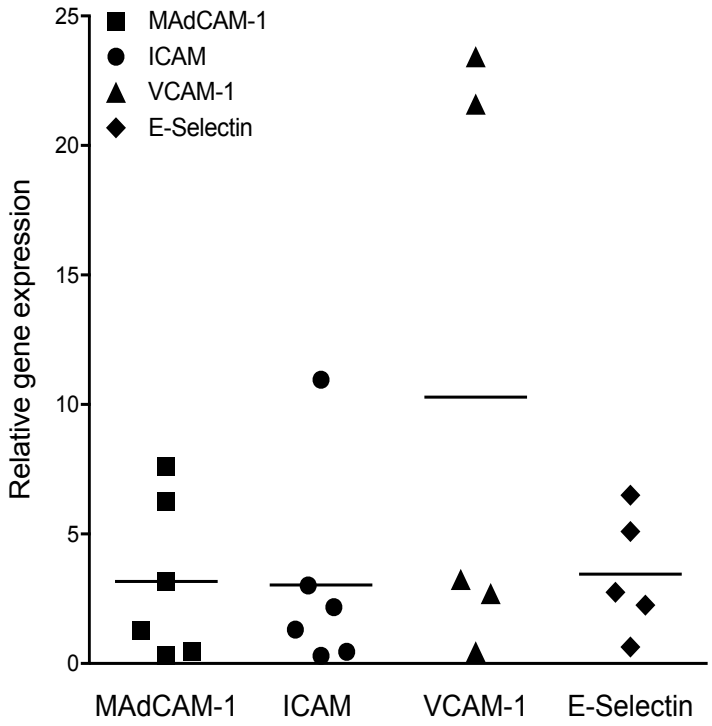

B

Gene of interest	CT values for TEC relative to matched NEC					
MAdCAM-1	3.2	6.3	1.3	0.3	7.6	0.5
ICAM-1	3.0	1.3	11.0	2.2	0.3	0.5
VCAM-1	3.3	23.4	2.7	0.5	21.6	-
E-Selectin	5.1	2.8	2.3	0.6	6.5	-

Figure 4.6: Adhesion molecule mRNA is increased in TEC compared to matched NEC.
Primary human endothelial cells were isolated from human normal colorectal and colorectal cancer tissue samples by positive selection using anti-human CD31 immunomagnetic beads. Isolated NEC and TEC homogenates underwent mRNA extraction (Qiagen Rneasy minikit, UK) and cDNA synthesis (Iscript, Biorad, uk). Real time qPCR was undertaken using an original concentration of 45ng /µl of mRNA for all samples using Taqman gene probes and primer (Invitrogen). CT values were calculated using Stratagene Mx3000P and analysis was performed using ΔΔCT method using GAPDH and Beta Actin as housekeeping genes and obtaining the TEC value as sample of interest against matched NEC.
This method was subsequently used to evaluate MAdCAM-1, ICAM-1, VCAM-1 and E-selectin transcripts by QPCR. Graph presents CT values for relative gene expression of MAdCAM-1, ICAM-1, VCAM-1 and E-selectin of TEC normalised to matched NEC. B presents actual CT values for data in A. Statistical analysis was performed using paired student T-test. Data was not found statistically significant.

4.2.5 CRC tissue displays increased CD8+T-cell adhesion compared to NC

To understand the functional properties of adhesion molecules in CRC we used frozen preserved whole tissue sections to perform static adhesion assays using CD8+T-cells. All 5-matched untreated NC behaved differently to CRC sections where higher numbers of CD8+ T-cells bound compared to NC (mean number of CD8+ T-cells counted in field of view 409 ± 318 v's 233.4 ±148 respectively Figure 4.7). The image in Figure 4.7.B represents a CRC tissue section and the black arrows indicate adhered CD8+T-cells to the surface of tissue identified. After ICAM-1 blockade the number of CD8+ T cells binding to normal tissue did not change significantly (mean control NC, 168.25±35 v's ICAM-1 inhibited NC, 206.5±97.6 Figure 4.7.C). In contrast, there was a significant reduction in CD8+T-cell adhesion to CRC sections when ICAM-1 was inhibited (CRC control 532.14 v's ICAM-1 inhibited CRC 377.43, paired Student's t-test p=0.0069 n=7 samples, Figure 4.7.D). MAdCAM-1 blockade did reduce CD8+ T cell binding to normal colon samples (mean control NC, 173.00±41.6 v's 127.00±36.1 MAdCAM-1 inhibited NC, n=3 samples Figure 4.7.C) but the change was not significant. However as with ICAM-1, for CRC tissue, there was a significant reduction in mean CD8+T-cell adhesion when MAdCAM-1 was blocked (CRC control 587.67 v's 363.83 MAdCAM-1 inhibited CRC 377.43, paired Student's t-test p=0.0069, paired Student's t-test p=0.0169, Figure 4.7.D).

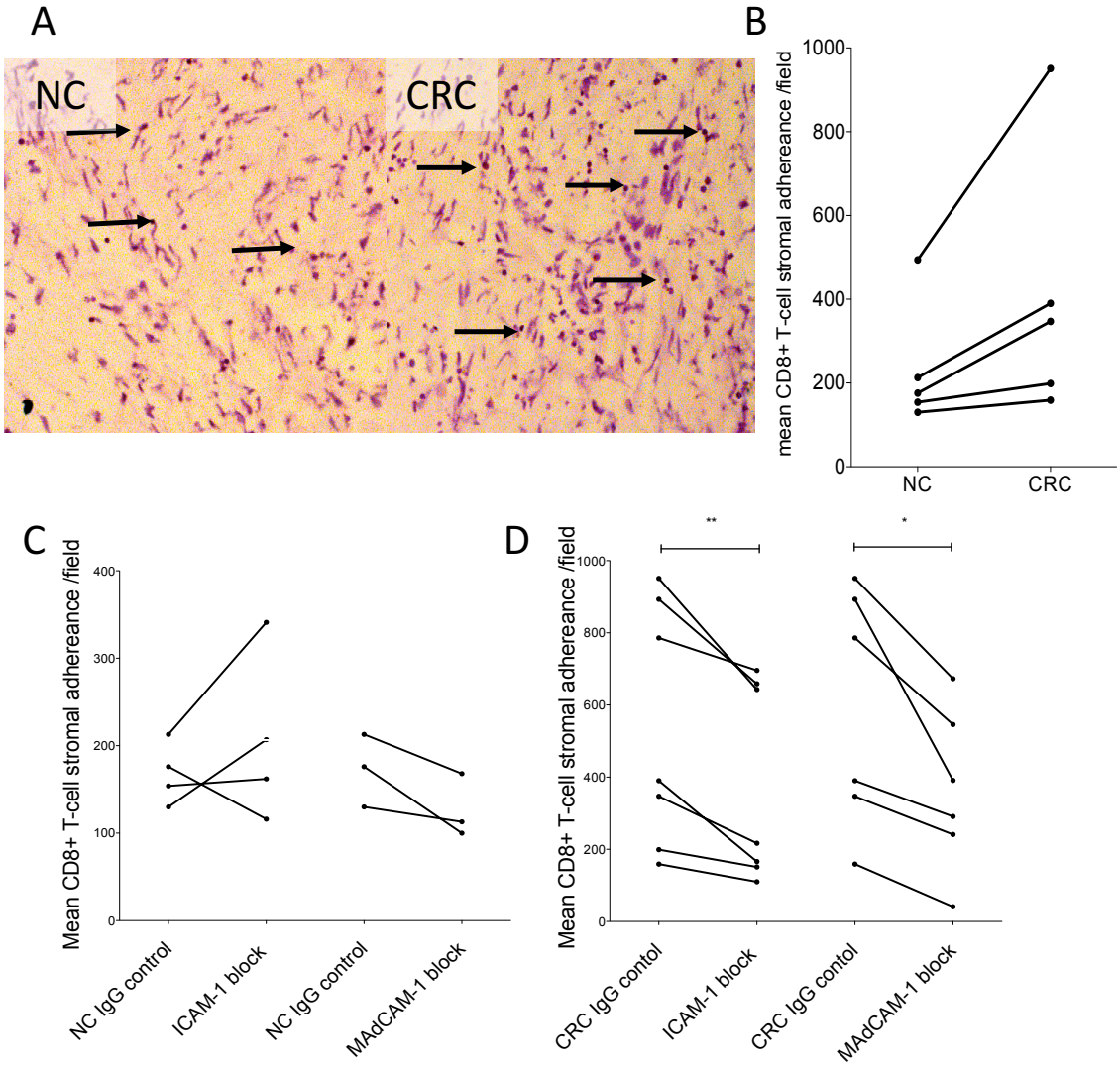

Figure 4.7: CRC tissue supports increased CD8+T-cell adhesion compared to NC.
CD8+ cells, isolated from human PBMCs, were incubated with unfixed frozen tissue sections of NC and CRC treated with either an anti human ICAM-1or MAdCAM-1 antibody or a isotype matched control under static conditions. Sections were stained using haematoxylin and eosin. 3 different fields were captured from 3 different sections of each NC and CRC sample at 20x magnification and retrieved using Axiovision software. This resulted in 9 different field views per sample, each of which was used to count the CD8+ cells, using cell-counter from Image J software. Image A represents NC and matched CRC sections with adhered CD8+ T lymphocytes highlighted by black arrows. Graph B illustrates the control binding of CD8+ T cells to untreated tissue Graphs C and D compares the mean number of CD8+ T lymphocyte count per field view for when ICAM-1 and MAdCAM-1 were blocked compared to their isotype matched control for NC and CRC respectively. Data illustrates the mean number of adhered CD8+ T-lymphocytes of 9 field views. Each dot represents data for one biological repeat. Statistical analysis was performed using paired Student's t-test.

4.2.6. Cytokines produced by colorectal-derived NEC and TEC and the influence of CCL2 on CD8+ lymphocyte chemotaxis and adhesion.

By using proteome profiling arrays and culture supernatants, I compared cytokine production by colorectal derived NEC and TEC (Figure 4.8 A and B). The most abundant analytes in both NEC and TEC were CD40, CXCL1/GRO, IFN-gamma, IL-8, IL-23, MIF, CCL5/RANTES. IL-8 was more than 5 times more abundant, and IL-23 was twice as abundant in NEC supernatant than TEC supernatant (Figure 4.9.C). In contrast, CCL2 was 5 times more abundant in supernatant of TEC compared to NEC (Figure 4.9). Thus, further quantification of CCL2 by ELISA was performed confirming that CCL2 protein was present at higher levels in 3 TEC supernatant samples, where the mean concentration was 1102.3pg/ml, compared to one sample of NEC where the concentration was 862.3pg/ml. Statistical analysis was not conducted as only one NEC sample was used.

TEC was treated with a functional inhibitor of CCL2 and then a CD8+ T-cell transmigration assay was performed. The number of lymphocytes that migrated across the membrane towards the CCL2-inhibited TEC was less than 20% that of the control TEC (Figure 4.10.C). The proportion of these cells that adhered to the TEC in the bottom of the wells was also reduced by CCL2-blockade. The mean adhesion of lymphocytes to CCL2-inhibited TEC was reduced to 36.3±20.0 cells per field view compared to control TEC where a mean of 171.7±60.5 cells per field view was observed.

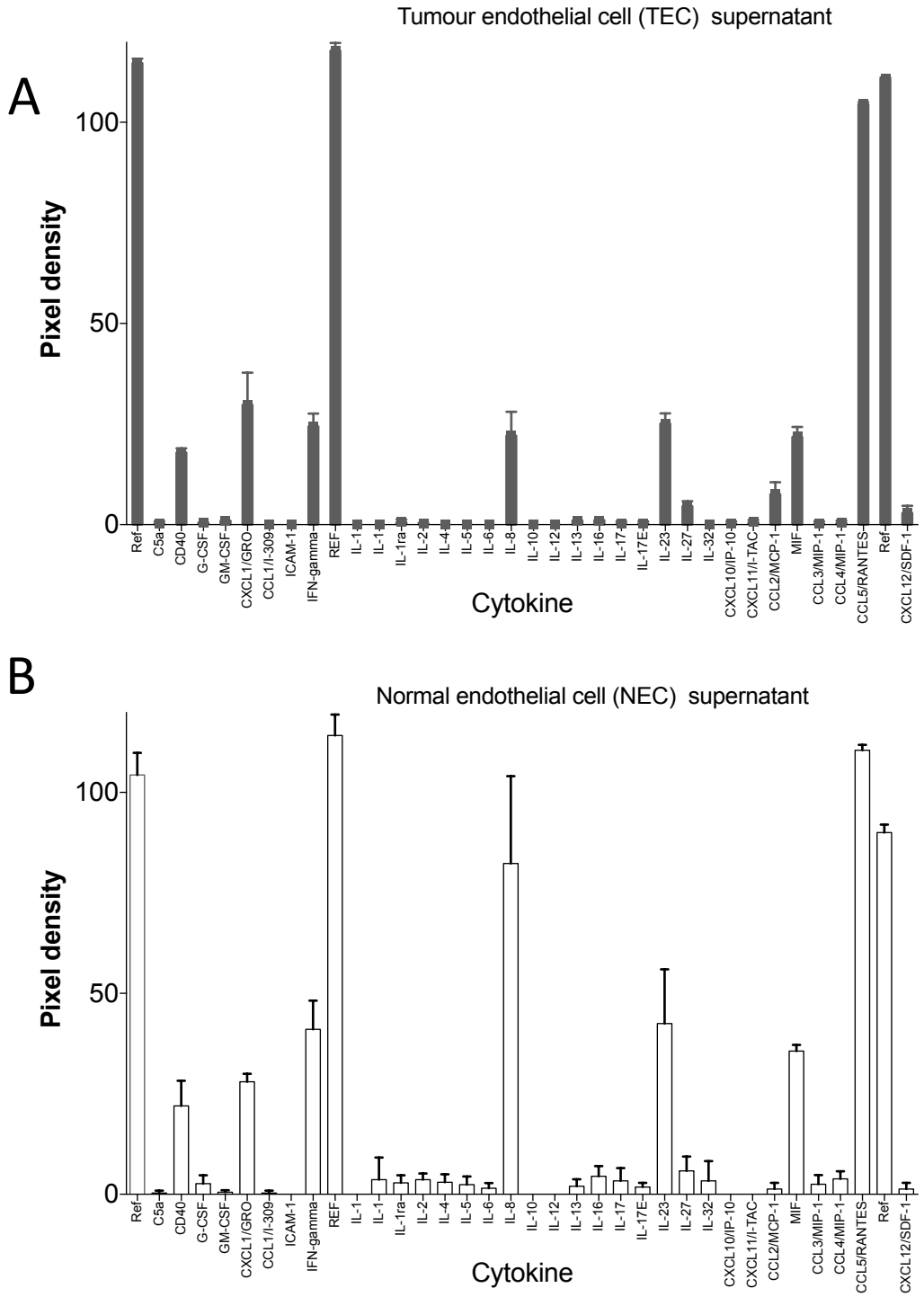

Figure 4.8: Differential expression of key cytokines in supernatants from colorectal derived NEC and TEC.
Graphs represent quantification of soluble cytokines from the culture supernatant produced by primary tumour endothelial cells (TEC, bottom panel) isolated from human colorectal cancer and the supernatant of matched normal endothelial cells (NEC, top panel) from matched uninvolved colorectal tissue. Cytokines were detected using a Proteome Profiler (Human Cytokine Array Panel A, R&D, UK) as per manufacturers guidelines. The supernatants were incubated with a pre-mixed biotinylated detection antibody cocktail mix and a nitrocellulose membrane (pre-spotted with capture antibodies). Streptavidin-HRP and chemiluminescent reagents were used to the detect bound cytokine/detection antibody complexes. The intensity of signal for each spot is relative to the amount of cytokine bound. Quantification of the abundance of cytokine produced was performed by measuring pixel density with Image J software. Data are mean of 2 spots in 3 biological repeats using matched NEC and TEC.

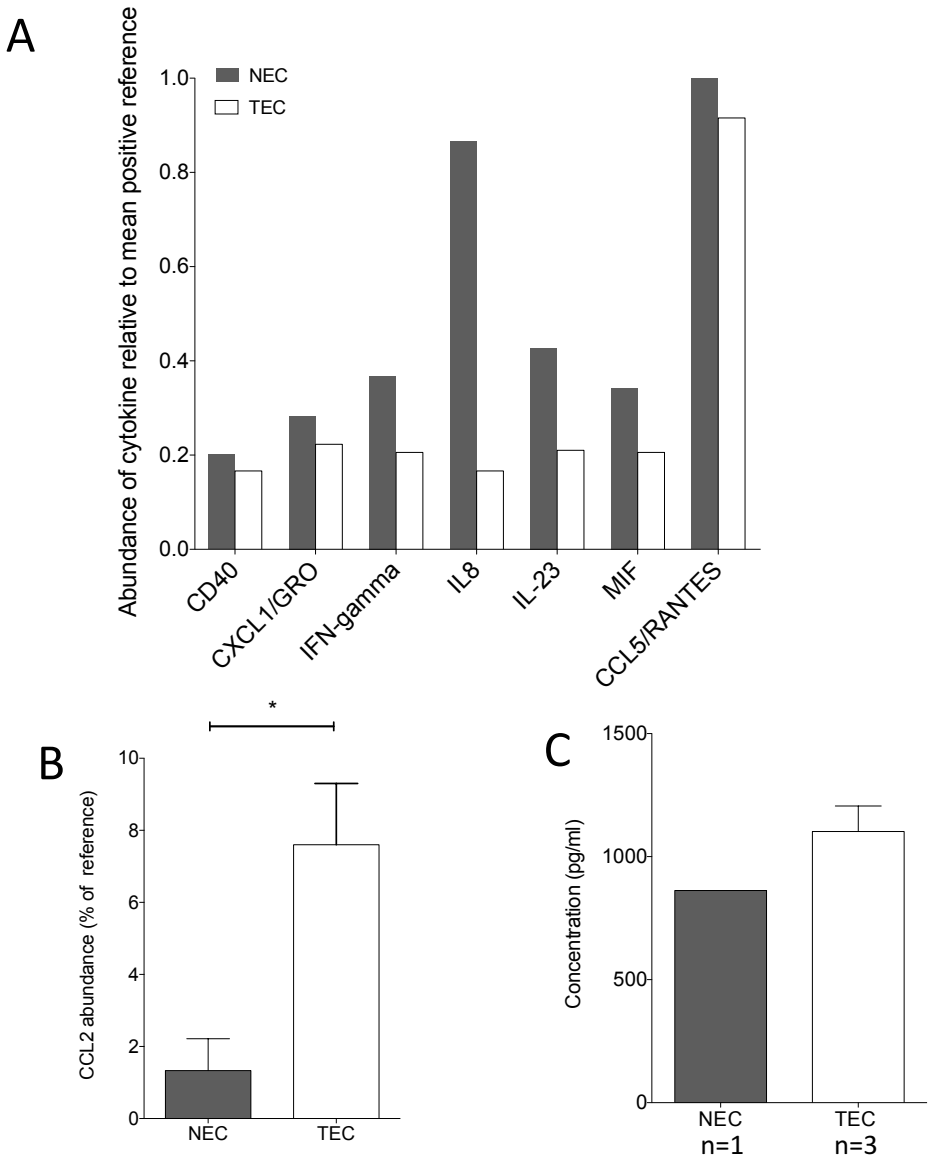

Figure 4.9: Quantification of key cytokines in supernatants from colorectal derived NEC and TEC.

Graphs represent quantification of soluble cytokines from the culture supernatant produced by primary tumour endothelial cells (TEC, white bars) isolated from human colorectal cancer and the supernatant of matched normal endothelial cells (NEC, black bars) from matched uninvolved colorectal tissue. Cytokines were detected using a Proteome Profiler (Human Cytokine Array Panel A, R&D, UK) as per manufacturers guidelines. Graph A illustrates the pixel density of the most abundant cytokine in NEC and TEC supernatants presented as abundance relative to the mean positive control pixel density for the respective samples. B illustrates the pixel density of CCL2 in each of the 3 supernatants illustrated as a percentage of the mean pixel density of the 3 positive reference spots for the respective sample, p=0.03. C represents the concentration of CCL2 found in NEC and TEC supernatants (standardised by dilution to number of cells in culture) by sandwich ELISA (Ready-set-go, Affymetrix, UK). The absorbance values were collated in triplicate for 3 TEC supernatant samples and concentration was interpolated from mean absorbance value (450nm) against the standard curve of known CCL2 concentration.

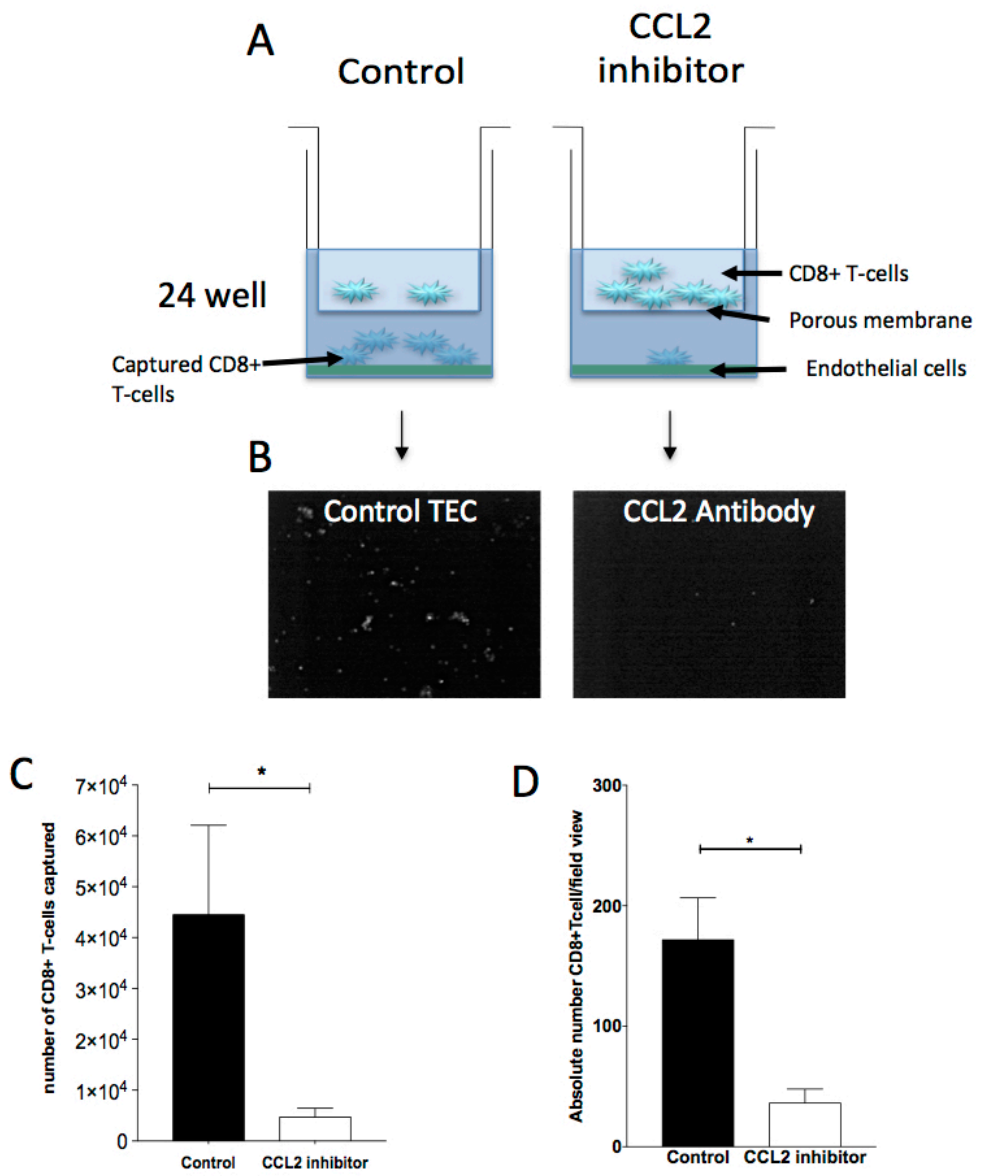

Figure 4.10: CCL2 blockade reduces chemotaxis of CD8+ T-cells towards TEC across a permeable membrane and adhesion of CD8+ T-cells to TEC.

Mouse anti-human CCL2 blocking antibody was used to treat triplicate wells of 1 sample of primary *in vitro* human colorectal TEC, cultured in a 24 well plate, for 1 hour. During which time CD8+ T-cells were isolated using CD8+T-cell untouched isolation bead kit (Invitrogen, UK) from PBMCs from HFE blood. Lymphocytes were labeled with CSFE cell tracker (Lifetechnologies, UK), and resuspended in EBM-2 (LONZA, UK) with 1% BSA at a concentration of $25x10^4$ CD8+T-cells/ml. Both control and antibody-treated inhibited TEC were incubated in the dark at 37°C for 12 hours with 500µl of labeled CD8+T-cells overlaid into the Transwell inserts. Inserts were removed, cell supernatant was aspirated and migrated CD8+T-cells on the base of the inserts were counted. Transmigrated CD8+T-cells and TEC were fixed, triplicate images captured at x20 magnification and cells were counted using Image j software. A is a schematic of the methodological process. B. illustrates representative images of migrated CD8+T-cell adhesion to treated and control TEC. Graph C shows the number of CD8+T-cells that migrated through the permeable membrane towards the control or antibody-treated TEC and were captured. Data is presented as mean and standard deviation of 3 field view counts for 1 biological replicate (P=0.013, 2 tailed unpaired student T-test). Data in graph D presents the mean CD8+T-cell adhesion to TEC in CCL2 inhibitor-treated and control wells of 3 field view counts for 1 biological replicate. (*p=0.039, 2 tailed unpaired student T-test).

4.2.7. T-cell adhesion by primary *in vitro* NEC and TEC

Next we determined whether changes in adhesion molecule and cytokine production by TEC had functional consequences for T cell binding. Figure 4.11.A shows that data from our larger cohort and illustrates that higher numbers of CD8+Tcells bind to cultured TEC than NEC in static assays (mean number of CD8+T-cell per field/view 296.88±44.1 v's 501.6±129.0 respectively, p=0.0004 Figure 4.11.A). To ascertain the importance of key adhesion molecules in CD8+T-cell adhesion, 3 different TEC samples were incubated with functional blocking antibodies raised against ICAM-1 or MAdCAM-1 (Figure 4.9.B). Reduced fluorescently labeled CD8+ T-cell adhesion was noted after ICAM-1 and MAdCAM-1 blockade although the decrease was significant (p=0.03) only after MAdCAM-1 blockade (mean number of CD8+T-cell per field/view, control TEC, 440±50.6 v's ICAM-1 inhibited TEC 296.3±154.9, v's MAdCAM-1 inhibited TEC 267.0±104.4, Figure 4.11.B).

When NEC were incubated with functional blocking antibodies, an approximately 50% reduction in CD8+ T-cell adhesion was noted with both individual ICAM-1 and VCAM-1 blockade compared to the NEC control wells. Combination of both ICAM-1 and VCAM-1 blocking antibodies had no additional effect on binding. A similar pattern occurred in TEC (Figure 4.11.C) although the magnitude of the blocking effect was smaller for TEC than NEC. Here, when ICAM-1 was blocked, there was a significant reduction in CD8+ T-cell adhesion (mean number of CD8+T-cell per field/view, TEC control 164.7 v's TEC after ICAM-1 inhibition 128.0, p=0.034,). A reduction was also seen in TEC treated with VCAM-1 inhibiting antibody, although this was not significant either alone, or in combination with ICAM-1 blockade.

Pertussis toxin treatment of which cells also reduced CD8+ T-cell adhesion to both NEC and TEC. The reduction was over 50% in NEC (control NEC mean 28.3 v's pertussis toxin treated NEC mean 63.3) and approximately 40% in TEC (control TEC mean 164.6 v's pertussis toxin treated TEC mean 102.6, p=0.0054, two tailed, unpaired student T-test). In addition to investigating the importance of endothelial surface adhesion molecules in CD8+ T-cell trafficking, we pre-treated the CD8+ T-cells with inhibitory antibodies against CD11a (integrin alpha L) and CD49 (integrin alpha 2). The results for both NEC and TEC suggest that inhibition of CD11a had no effect, whilst CD49-blockade increased adhesion to TEC (mean number of CD8+T-cell per field/view, control TEC 164.7±18.7 v's CD49 inhibited CD8+ T-cells 301.7±23.4, p=0.004, two tailed unpaired student T-test, Figure 4.11.D).

To investigate CD8+ T-cell adhesion under more physiological conditions we conducted flow assay experiments using NEC and TEC grown to confluence in Ibidi flow chambers. Again, we observed higher adhesion of CD8+ T cells to TEC than NEC. The mean number of adhered cells per $mm^2/10^6$ from 2 samples of TEC was 215.5±20.8 v's 59.6± 6.7 by NEC. After inhibition of ICAM-1, VCAM-1 or MAdCAM-1, adhesion to NEC decreased modestly to 46.9±4.6, 55.8±6.2 and 56.5±3.8 cells per $mm^2/10^6$, respectively (n=2, Figure 4.12.A). In contrast when TEC was treated with the functional blocking antibody against ICAM-1, adhesion reduced by about a third to a mean of 128.9±40.9 adhered cells per $mm^2/10^6$. VCAM-1 or MAdCAM-1 inhibition, caused a far less dramatic reduction in CD8+T-cell adhesion to 176.9±13.1 and 183.1±71.7 cells per $mm^2/10^6$, respectively.

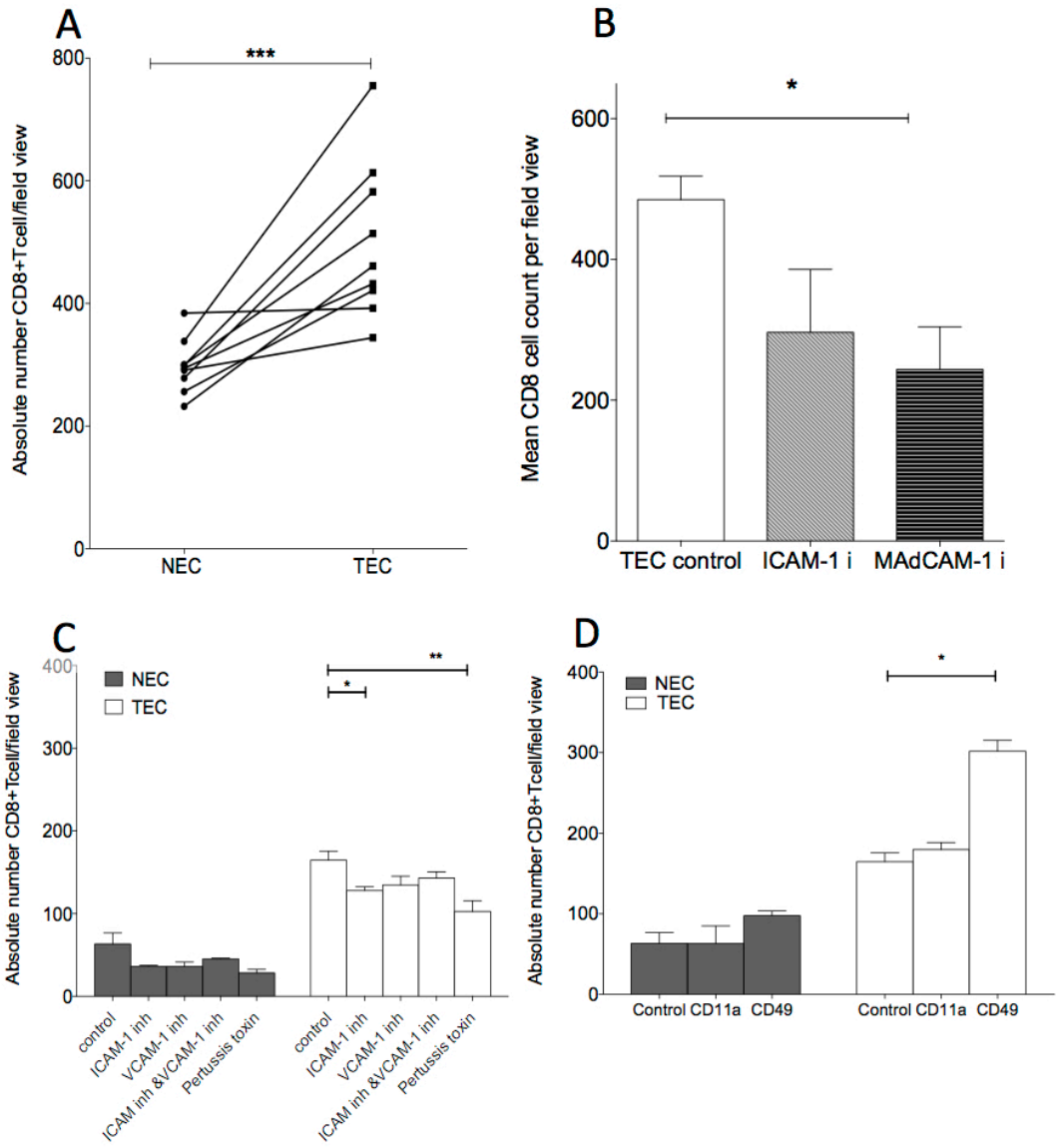

Figure 4.11: Increased numbers of CD8+ T-cells bind to TEC under static conditions and adhesion is reduced by blockade of ICAM-1 and chemokine signaling.

Isolated primary NEC and TEC in 24 well flasks were used either untreated or treated with adhesion molecule inhibitor or pertussis toxin. Endothelial cells were incubated with either untreated or CD11a or CD49 antibody-treated CD8+ T lymphocytes (labeled with CSFE), under static conditions for 30 mins before being washed and fixed. 3 different fields were captured from each well of either NEC or TEC at 20x magnification and retrieved using Axiovision software. This resulted in 9 different field views per experiment, each of which was used to count lymphocytes, using cell-counter from Image J software. A illustrates the difference between absolute CD8+ T lymphocytes adherent to matched NEC and TEC from 9 different patients and 9 different blood donors (not matched). Each data point represents the overall mean from 3 field view counts over a minimum of 3 wells for each of the 9 biological repeats. Graph B illustrates the difference in CD8+ T-cell adhesion to control TEC (untreated) compared TEC incubated with ICAM-1 or MAdCAM-1 antibody. EC were from 3 different patients and blood samples from 3 different donors (not matched). Data represents the mean± SEM adhesion. Graphs C and D illustrate CD8+ T-cell adhesion to control NEC and TEC or cells incubated with indicated blocking antibodies (C) or where T cells were treated with CD11a or CD49 antibodies (D) . Data are from triplicate samples from 1 EC donor and 1 blood donor (not matched). Data are mean± SEM adhesion of 3 field views from 3 different experimental repeats from 1 biological repeat. Statistical analysis was performed using paired Student's t-test.

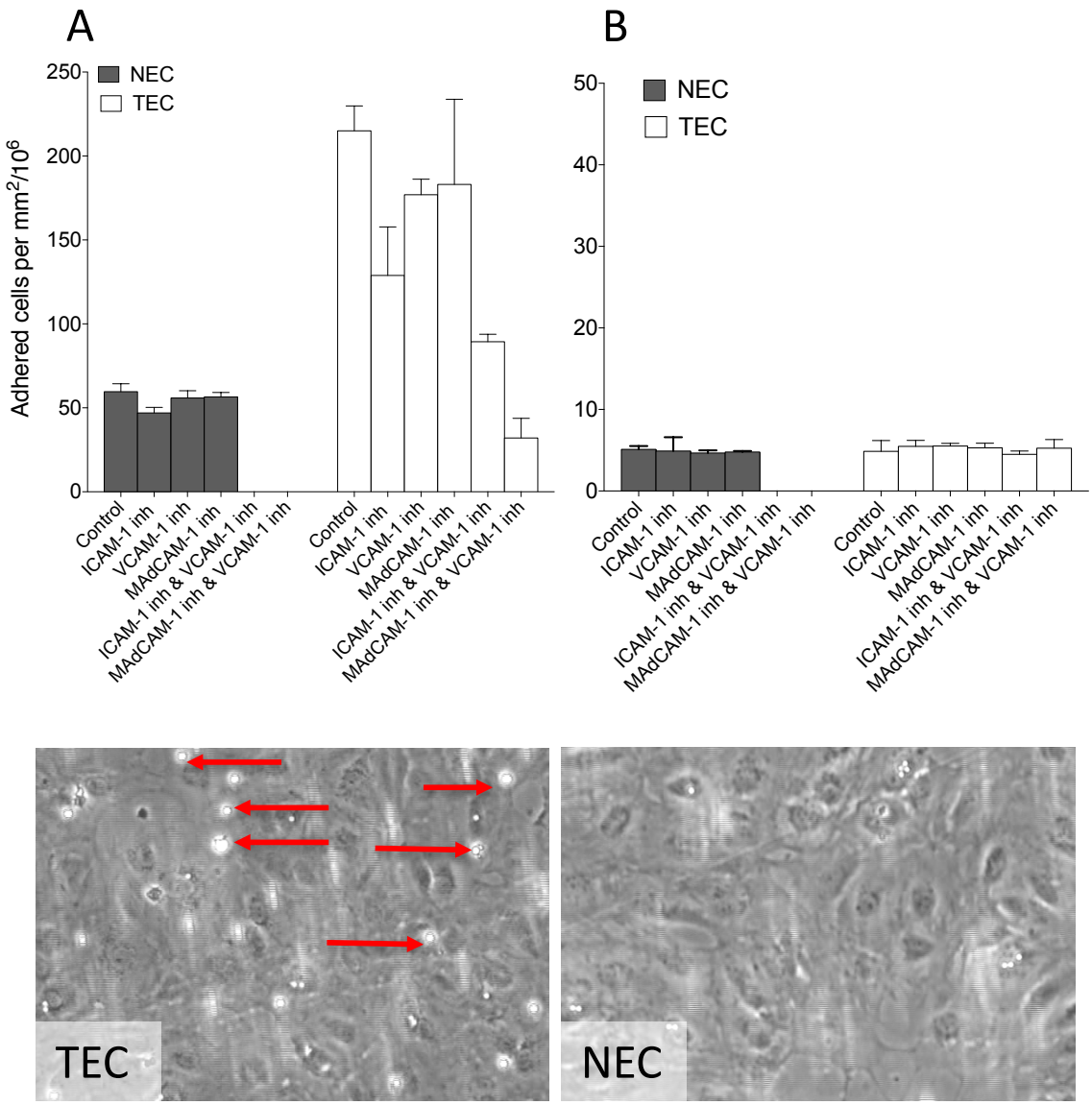

Figure 4.12: CD8+ T-cell adhesion to NEC and TEC under flow conditions.
Primary colorectal derived NEC and TEC were cultured in Ibidi chambers until confluent. EC were incubated with indicated blocking antibodies for 1 hour prior to undergoing flow based adhesion assay with isolated CD8+ T-cells from HFE blood. Images were taken with a phase contrast microscope at x20 magnification. Images were captured using DVD recorder and assessed off-line. Graph A represents mean and SEM adhesion of cells/mm^2/10^6 cells perfused. Graph B represents the % of the adherent CD8+ T-cells that were observed rolling at low velocity over the EC surface. Data are derived from multiple replicate fields of view in 2 independent experiments. Photographic images shown are representative. Arrows indicate adhered lymphocytes.

However, for TEC, combined inhibition was far more effective with combined ICAM-1 and VCAM-1 blockade reducing adhesion by more than 50% (89.4±6.2 cells per $mm^2/10^6$) and combined VCAM-1 and MAdCAM-1 blockade resulting in more than 6 times less adhesion (32.1±16.5 cells per $mm^2/10^6$). Despite differences in numbers of adhered cells, there were no differences in the number of CD8+ T-cells observed rolling across the endothelium. This remained at approximately 5% of cells rolling for both NEC and TEC regardless of inhibitory antibody used (Figure 4.12.B).

Results summary:

- CRC specimens can be categorized into those that contain high numbers of CD8+ Tumour infiltrating T-lymphocytes.
- Tumours with high levels of CD8+ TIL had higher levels of stromal vascular CD31 expression suggesting these specimens have more vessels.
- CRC contain more CD8+ Tumour infiltrating T-lymphocytes than matched normal tissue.
- *In vivo* CRC vessels show less intense ICAM-1 expression and fewer vessels in CRC express MAdCAM-1.
- The *in vitro* adhesion molecule expression is generally similar for endothelial cells in normal colon and in CRC.
- Despite this, CD8+ T cell were more adherent to tumour endothelium in CRC and *in vitro* TEC.
- Inhibition of the key adhesion molecules investigated, resulted in reduced CD8+ T cell adhesion to NC & CRC.
- TEC produced higher levels of CCL2 chemokine than NEC.
- Inhibition of ICAM-1, VCAM-1, MAdCAM-1, CCL2 and pertussis toxin-sensitive receptors resulted in reduced CD8+ T cell adhesion TO NEC and TEC.

4.3 Discussion

4.3.1 Colorectal cancers can be categorized according to number of tumour infiltrating CD8+T-lymphocytes.

Tumour infiltrating lymphocytes are a beneficial prognostic indicator in CRC. There is some evidence to suggest that different pathogenetic mechanisms govern right and left sided colorectal cancers (201, 202, 203) based on differing environmental factors and genetic predispositions. Right-sided colorectal tumours are reported to have microsatellite instability (MSI) and a loss of mismatch repair (MMR) function (204). Colorectal tumours with high levels of activated CTLs are reported as more prevalent in tumours with MSI and loss of MMR (205). To validate the cohort according to the literature, I compared the number of infiltrating CD8+ cells in 12 randomly selected frozen tissue samples from our available bank by IHC analysis. My data confirm that greater numbers of CD8+ cells are found within tumours compared to matched uninvolved tissue and although there was no statistical significance difference, there was a trend supporting a higher number of CD8+ cells in right-sided colorectal tumours in this cohort. Sample heterogeneity is large and therefore a larger group would be required to reach statistical significance but my findings conform to the reported literature.

We compared the CD8+ TIL count to conventional histopathological staging and there was no trend or significant correlation between numbers of CD8+ TIL and Dukes stage of disease. This finding is also not unexpected. Galon *et al* have documented that the immune cell type and their location in a tumour can be a more accurate predictor of overall and disease free survival in colorectal cancer (2). It is conceivable that, the patients with few CD8+ TIL despite being histologically Dukes stage A and B, may have a worse 5-year survival than predicted by Dukes or TNM

staging systems available. I also found there was significant inter-patient heterogeneity within my sample cohort. This wide variation with some colorectal tumours having abundant and some few CD8+ TIL may reflect antigenic and non-antigenic tumour types described in the literature (190). We found that there was a correlation between the number of CD8+ TIL and the expression of CD31 within the same tissue sections. This may simply be an index of tumour inflammation with CD31 positivity being associated with immune populations such as type 2 tumour associated macrophages (TAM2), neutrophils, mast cells and TIE-2 expressing monocytes, all of which can induce VEGF, FGF, TNFα (206, 207, 208, 209). It does, however raise the possibility that more vascular tumour types allow increased opportunity for CD8+ lymphocyte trafficking into tumours and that where tumours had high number of CD8+ TIL, this is due to active recruitment rather than entirely clonal expansion *in situ*. Certainly my staining shown in chapter 3 (Figure 4.3) shows that CD31 expression was predominantly localized to vessel structures. Moreover, endothelial CD31 expression has been shown to be necessary for T-cell recruitment in murine models (210). Thus, an increased density of CD31 –positive vessels drives increase recruitment of immune cells into the tumour environment.

However, the presence of vessels is not a given for active lymphocyte recruitment. When Suzuki *et al* (211) investigated the distribution of lymphocytes in colorectal cancer compared to inflammatory bowel disease they also used CD31 expression in relation to lymphocytic markers (CD3, CD4, CD68) (211). Their findings were similar to Galon *et al* (2) in that the majority of lymphocytes were located at the invasive margin instead of the central core. Although they investigated E-selectin and ICAM-1 expression by endothelium and found a direct correlation with lymphocyte number, they did not investigate mechanisms of recruitment or retention of

lymphocytes within the tumour. They further examined tumour lymphocyte subsets by quantifying granzyme-B and CD45RO expression as markers of CTL and CD8+ memory T-cells respectively. They revealed higher numbers of CTL at the invasive margin but higher numbers of CD45RO cells in the tumour core in all patients (2). Whether the difference in the CD8+ lymphocyte distribution is due to recruitment, retention or apoptosis has not been thoroughly investigated.

4.3.2. Adhesion molecule expression of CRC and TEC reveal little differences between NC and NEC.

Generally, my data suggests that there is little difference between ICAM-1 and MAdCAM-1 and VCAM-1 expression between colorectal tumours and NC and TEC and NEC. However, in tissue, fewer CRC vessels expressed MAdCAM-1 and there was a trend towards less intense ICAM-1 staining in CRC vessels. Significant differences in expression were only noted in paired data suggesting that these comparisons are authentic. Tumour endothelium has been reported to down regulate adhesion molecule expression in other studies (199, 97), more notably in higher stage disease (212), and so my data fits well with this picture. This may also explain why treatment of normal EC with cytokines resulted in a down-regulation of expression of key receptors, perhaps modeling the environment in a less inflamed tumour. However, this experiment was conducted using a single patient sample and data was collected after 12 hours of stimulation. Schellerer *et al* (60) used different timeframes to stimulate their colonic endothelium depending on the cytokine used, and therefore we may be observing a time or cytokine-dependent variation in expression and missing peak expression of MAdCAM-1 and VCAM-1. Further experimental analysis of the temporal effects of different cytokines in increased numbers of patients is therefore required.

Interestingly, higher levels of soluble ICAM-1 have been reported in serum from malignant and metastatic patients, and studies suggest that INF-γ cleaves ICAM-1 from the cell surface of EC (213). Thus, some increased levels of message for adhesion molecules in matched tumour samples and lower protein expression may indicate that these receptors are cleaved within the tumour environment. In studies investigating leukocyte adhesion *in vivo* in murine models of tumour angiogenic tissue, ICAM-1 expression is reported to be down regulated by angiogenic factors such as VEGF and fibroblast growth factor (214, 215). These growth factors were not available on our proteome array so it is not clear if a similar mechanism may be operating in our samples. However, IFN-γ was present in our endothelial supernatants and so this may be one means to explain reduced ICAM-1 expression.

4.3.3 CD8+T Lymphocytes preferentially adhere to TEC and CRC compared to NEC and NC.

It is interesting to consider our observation of enhanced CD8 recruitment in the context of reduced adhesion molecule expression. Stromal cells express ICAM-1 to promote retention of lymphocytes (195). This is supported by IHC data in Figure 4.2 which revealed ICAM-1 expression by fibroblasts and by static adhesion data to whole tissue in Figure 4.7 which shows that inhibition of tissue ICAM-1 reduces CD8+ T cell binding. This may reflect the role of stromal fibroblasts in retention of lymphocytes after initial recruitment. Inhibition of ICAM-1 (β2 dependent) significantly reduced adhesion in static endothelial *in vitro* models in addition to tissue sections, and had a greater impact than VCAM-1 alone (partial β1). The addition of β2 integrin inhibition together with partial β1 integrin adhesion augmented total CD8+ T-cell adhesion, compared to their inhibition in isolation, which is not previously reported. This may

represent a lymphocyte driven up-regulation of β7 integrin, highlighting the importance of MAdCAM-1 in CD8+ T-cell adhesion.

Documented evidence suggests that memory subsets of CD8+ T-cells home specifically to gut mucosa by expressing α4β7 and CCR9, and that intra-tumoural CD8+ T–cells express α4β7 the integrin ligands for MAdCAM-1 (216). Certainly, I found a significant reduction in CD8+T-cell adhesion by MAdCAM-1 inhibitory antibody suggesting a similar mechanism operates within colorectal tumours. All CD8+ expressing T-cells were isolated from blood samples, including potential effector memory T-cells and naïve T-cells. this allowed larger numbers of lymphocytes to be used, but also, the addition of CD45RO memory T-cells is important as their presence within CRC tumour stroma directly correlates with an improved patient survival (2). Furthermore, analysis was not performed to explore if the HFE CD8+T-lymphocytes were activated or naïve. Naïve, in addition to memory and activated CD8+ T-cells are recruited to non-lymphoid tissue specifically via MAdCAM-1 α4β7 binding (217) as in colorectal cancer, it is suggested that some CD8+ cells are activated in situ (218). This may skew data and limit the conclusions drawn from significant data regarding abrogation of adhesion caused by MAdCAM-1 inhibition under static conditions (Figure 4.11).

Static assays using TEC may mimic some conditions in CRC where flow is erratic, slow and static in part and therefore be more physiologically representative of CRC than initially thought. This is unlikely to be the case for NEC static adhesion assays as the blood flow through NC is predictable and uni-directional. In this instance, the static adhesion assays may not support selectin-mediated rolling and then chemokine-activation of lymphocytes. However, significant abrogation of lymphocyte adhesion to TEC but not NEC by pertussis toxin was observed. The

mechanism is via inhibition of chemokine G-protein coupled receptor, and suggests that chemokines are key for lymphocyte binding to tumour endothelial cells in particular, whereas binding of lymphocytes to EC from non-malignant tissue may rely upon rolling mediated lymphocyte activation.

Flow based adhesion assays using primary human tumour endothelial cells are not described in the literature to date. Flow assays in HUVEC cell lines and primary endothelium (219) suggest that we observed relatively low levels of lymphocyte rolling in NEC and TEC. Very little data is available using in vitro primary EC models in their resting state. Our phenotyping and proteome profiling data suggests stimulation with inflammatory cytokines would perhaps not reflect the tumour milieu and would counteract physiological relevance. Further study with different flow rates and systematic inhibition of selectins, is required to rule out significant differences in lymphocyte rolling. Interestingly, for TEC flow based assays data is similar to that of static adhesions assays implying that ICAM-1, VCAM-1 and MAdCAM-1 are key to CD8+ T cell adhesion to TEC, however in isolation ICAM-1 had the greatest impact.

4.3.4. CCL2 is preferentially produced by TEC compared to NEC and may regulate CD8+ T lymphocyte adhesion to EC.

My study represents the first incidence in which validated *in vitro* NEC and TEC have been used to explore T lymphocyte adhesion under static or flow conditions. Chemokines produced by NEC and TEC are of significance in the recruitment of lymphocytes using such models. Therefore, I explored the soluble factors present in supernatants from *in vitro* NEC and TEC. In common with our finding of reduced adhesion molecule expression within the tumour environment, we also saw lower concentrations of key inflammatory cytokines such as IL-8, IL-23, CCL5, IFN-ϒ and

CXCL1/GRO in TEC supernatants from one representative patient. This may suggest that similar mechanisms are responsible for down-regulation of both adhesion receptors and chemotactic factors at this site. However, most literature available describes the usual characteristics of the tumour microenvironment, i.e. hypoxia, increased VEGF levels as up-regulating these chemokine (220, 221, 222). However, since this data was generated from a single individual, and heterogeneity in this patient cohort is evident, it would be important to confirm this result in material from other cases and correlate with clinical details such as stage of disease.

CCL2 was consistently found at higher concentrations in TEC compared to NEC by proteome profiler and ELISA techniques. This is supported by data from studies that have investigated the epithelial, stromal or overall CCL2 levels in tumours including breast, lung and liver cancers (223, 224, 225). Studies investigating the role of CCL2 in tumour progression and metastasis formation found that, in mouse models, circulating inflammatory monocytes are preferentially recruited via CCL2/CCR2 axis to metastases and that inhibition of CCL2 resulted in fewer metastases suggesting that the CCL2/CCR2 axis drives metastatic progression of disease (226).

Our data suggests that CCL2 contributes to CD8+ T-cell adhesion, and where blood flow is static may contribute to CD8+ T-cell migration towards the tumour endothelium, in addition to other lymphocyte subsets and macrophages. Thus enhanced CCL2 expression could account for elevations in CD8 recruitment that we see, and retention in tumour tissue in the absence of differential adhesion molecule expression between matched normal tissue and cancer specimens. It is possible that CCL2 would also have this effect on immunosuppressive regulatory T-cells and monocytes.

Evidence exists that stromal, not epithelial, CCL2 expression correlates with reduced recurrence free survival (223) and that blockade in hepatocellular carcinoma (HCC) inhibits intratumoural TAMs and slows malignant cell growth, inhibits metastases, and improves survival (224). In a study of lung tumours using mice models, blockade of CCL2/CCR2 axis inhibited growth of established tumours. However, surprisingly an increase in the number of lung metastases was observed CCL2-/- and CCR2-/- mice despite a slowing in the growth of the primary tumours. The authors theorize that this indicates a role for CCL2/CCR2 blockade as a therapeutic for established tumours but that this blockade may reduce immunosurveillance and open the door for new tumour formation. A human monoclonal antibody against CCL2 has been trialed in human patients with solid tumours revealing 2 out of 33 patients saw a reduction in serum tumour markers, however non saw an response to treatment (227). By demonstrating CCL2 as a promoter of adhesion of CD8+ T lymphocytes to TEC and showing that pertussis toxin reduced adhesion to TEC, my data suggests a possibility that CCL2 is responsible for triggering firm adhesion to adhesion molecules or chemotaxis. Therefore, blocking CCL2/CCR2 may also impede the hosts anti-tumour immune response.

This chapter has shown that the numbers of tumour infiltrating CD8+ T lymphocytes in different colorectal cancer specimens varies and supports the body of literature that describes CRC divided into those with high numbers of TIL and those that have few TIL, which correlates with patient survival. Generally, there was little difference in the expression of key adhesion molecules between NC and CRC and *in vitro* NEC and TEC. However, the limitations of small sample sizes and heterogeneity of data illustrate the need for larger studies. Despite this, my data confirms that these adhesion molecules are essential for adhesion of CD8+ T-lymphocytes to TEC under

both static and flow conditions by using a novel *in vitro* TEC model. I have also identified CCL2 as a factor preferentially produced by TEC that may promote recruitment of lymphocytes using these receptors thus revealing potential to explore CCL2, and constituents of the stromal tumour microenvironment further, using the colorectal derived TEC model. Interleukins and other molecules within the tumour microenvironment in colorectal cancers and how they may regulate adhesion molecule expression by NEC and TEC derived from colon and CRC is discussed in the next chapter.

CHAPTER 5

How the tumour microenvironment regulates CD8+ T-lymphocyte adhesion to tumour endothelium in CRC.

5.1 Introduction

So far, this thesis has investigated the role of *in vitro* cultured tumour endothelium in recruiting lymphocytes. *In vivo*, endothelial cells are likely to be influenced by neighbouring cells within the tumour stroma. The cellular component of stroma is predominantly formed by fibroblasts, which are spindle shaped cells derived from mesodermal tissue, that produce collagens and glycosaminoglycans to form the extracellular matrix acting as a scaffolding framework supporting other stromal cell types. In benign and non-inflammatory tissue where the stroma is not reactive, phenotyping shows that fibroblasts express vimentin and desmin but do not express the protein alpha smooth muscle actin (αSMA) (228). There is a subset of fibroblasts in the cancer stroma that express αSMA and therefore share a similar phenotype to myofibroblasts, which are considered "activated" fibroblasts. However, it is unclear whether these cells are structurally the same as myofibroblasts found in reactive but benign tissue, and so there is reluctance for these to be termed "myofibroblasts" without evidence from electron microscopy (229). These cells are commonly termed cancer or tumour associated fibroblasts (CAF or TAFB); but in this thesis, the term TAFB will be used.

There is much interest in studying TAFB. They represent a main contributor to the tumour microenvironment and may contribute to tumour genesis and metastasis. Activation of fibroblasts in the context of cancer may occur because of growth factor stimulation. Key factors implicated include TGFβ, EGF, PDGF, FGF-2, adhesion molecules, other molecules produced by tumour cells or in response to injury or trauma (229). The role of fibroblasts in tumour formation is not well understood but the main theory arises from epithelial-mesenchymal transition, where cells undergoing this change, carry a malignant predisposition (230). TAFB are better described to promote epithelial cancer cell proliferation (229, 230) by overproduction of Tenascin-C, MMPs and growth factors (TGFβ and HGF). In addition, TAFB can influence the tumour microenvironment by polarizing stromal immune cells towards a pro-tumour differentiation state (Figure 5.1). For example, TAFB can induce Th17 T-helper differentiation (231) by producing chemokines such as IL-6 (232, 233, 234). IL-6 can interact with a predominantly soluble receptor to activate the glycoprotein, gp130 complex. Both the soluble and the membrane bound IL-6 receptor initiate the Janus activated (JAK) kinase-STAT3 pathway. The down-stream effects of this pathway include cell proliferation, survival migration and chemokine formation (233), thereby enhancing tumour growth.

Furthermore, high levels of IL-6 in the serum of patients with cancer, are associated with a worsening prognosis (231, 232). However, despite evidence that TAFB production of IL-6 may be detrimental, there is also evidence that the reverse may be true. There remains a hypothesis that the stromal TAFB in CRC regulates lymphocyte recruitment and thus can contribute to either a pro or anti-tumour immune-polarity.

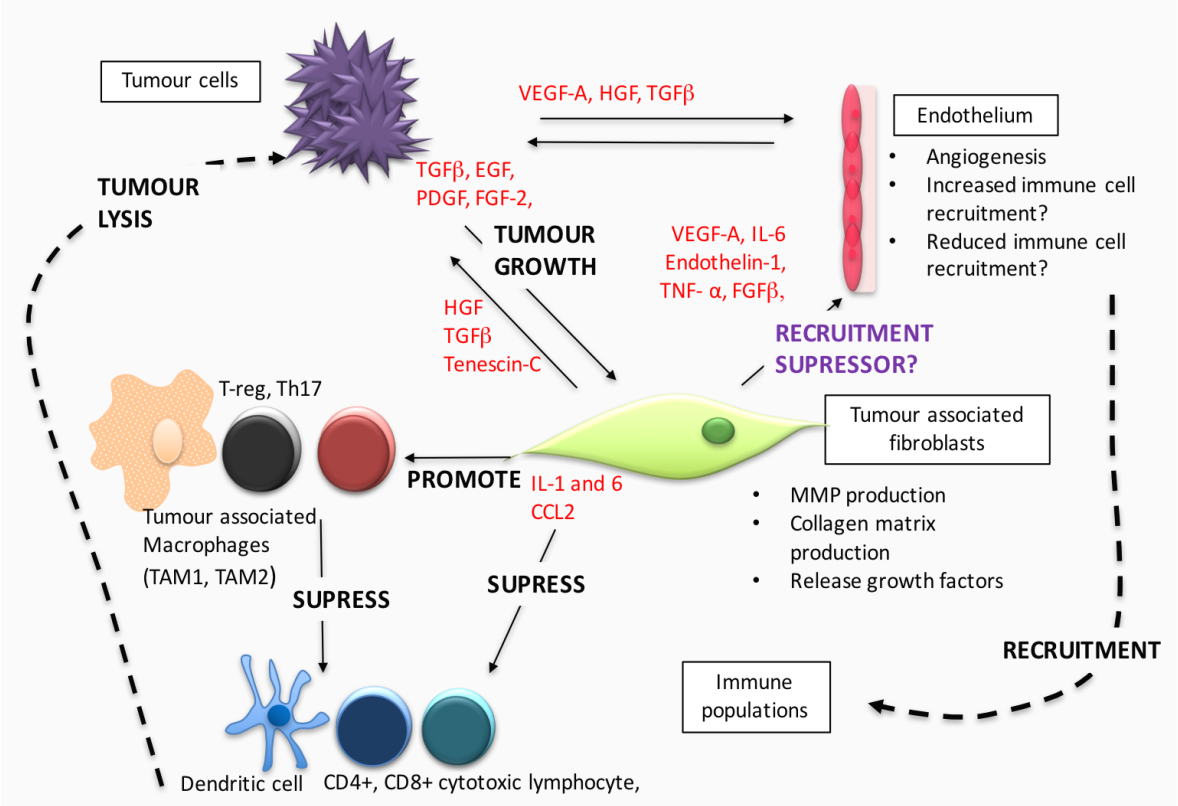

Figure 5.1: The role of TAFB in maintenance of the tumour microenvironment.
This schematic outlines the roles of tumour fibroblasts within the tumour microenvironment. Here, tumour associated fibroblasts, stimulated by tumour cells (EGF, TGFβ, PDGF and FGF-2) suppress anti-tumour immune populations, promote tumour angiogenesis, attract suppressive immune populations and overall, promote tumour growth. Tumour fibroblasts may produce factors that suppress the adhesion of anti-tumour lymphocytes to tumour endothelium thereby suppressing an anti-tumour immune response. Image authors own adapted from (229)

Furthermore, high levels of IL-6 in the serum of patients with cancer are associated with a worsening prognosis (231, 232). However, despite evidence that production of IL-6 by TAFB may be detrimental, there is also evidence that the reverse may be true. There remains a hypothesis that the stromal TAFB in CRC regulate microvascular lymphocyte recruitment and thus can contribute to either a pro or anti-tumour

immune-polarity. Fibroblasts from inflammatory and autoimmune conditions (for example, rheumatoid disease) have previously been shown to regulate lymphocyte trafficking into tissues by vascular endothelium (233, 234, 235). However, the consequences of IL-6, and other molecules produced by TAFB, on CD8+ T-cell adhesion by CRC TEC has not yet been described in the literature.

Therefore, the aims of this chapter were as follows;

- To study ways in which normal and colorectal tumour derived fibroblasts regulate CD8 T-cell adhesion by colorectal NEC and TEC and quantify changes in adhesion molecule expression by conditioned NEC and TEC.
- To investigate the regulation of CD8+ T cell adhesion to NEC and TEC under static and flow conditions because of stimulation by individual proteins found in TAFB supernatants, such as IL-6 and Endothelin-1.

5.2 Results

5.2.1 Colorectal tumour associated and normal fibroblasts (TAFB and NFB) condition colorectal tumour and normal endothelial cells.

Initially, αSMA expression by NC and CRC was examined using immunohistochemical analysis of tissue sections. In NC, strong membrane and cytoplasmic αSMA expression was noted only in the perivascular smooth muscle in all layers from the lamina propria (Figure 5.2 A), across the muscularis mucosa, and into the sub-mucosal layer (Figure 5.2 C). In CRC, moderate membrane and cytoplasmic αSMA staining was noted by stromal fibroblasts with less intense, patchy perivascular staining at the center and invasive margin of the tumour. Fibroblast positive staining was variable between CRC sections independent of stage, illustrated by Figure 5.2 D and E where one Dukes B CRC section revealed extensive fibroblast staining throughout the whole tumour (Figure 5.2 D) and another Dukes B CRC section where very little fibroblast positive αSMA staining is noted. αSMA positive staining was quantified using Image J where the amount of positive αSMA staining was expressed as a percentage of pixels in representative images. The % αSMA staining was then plotted against the number of TIL in the same specimen (based on CD8+ staining as discussed in Chapter 4). Figure 5.2F shows that there was a significant correlation between % αSMA expression and number of CD8+ TIL ($p=0.043$, Figure 5.2 F). Here higher expression of αSMA was associated with lower numbers of CD8+ TIL in tissue. Next, supernatants from *in vitro* NFB and TAFB cultures were used to condition human primary colorectal NEC and TEC to see whether fibroblasts influence immune cell recruitment and expression of adhesion molecules by tumour endothelium.

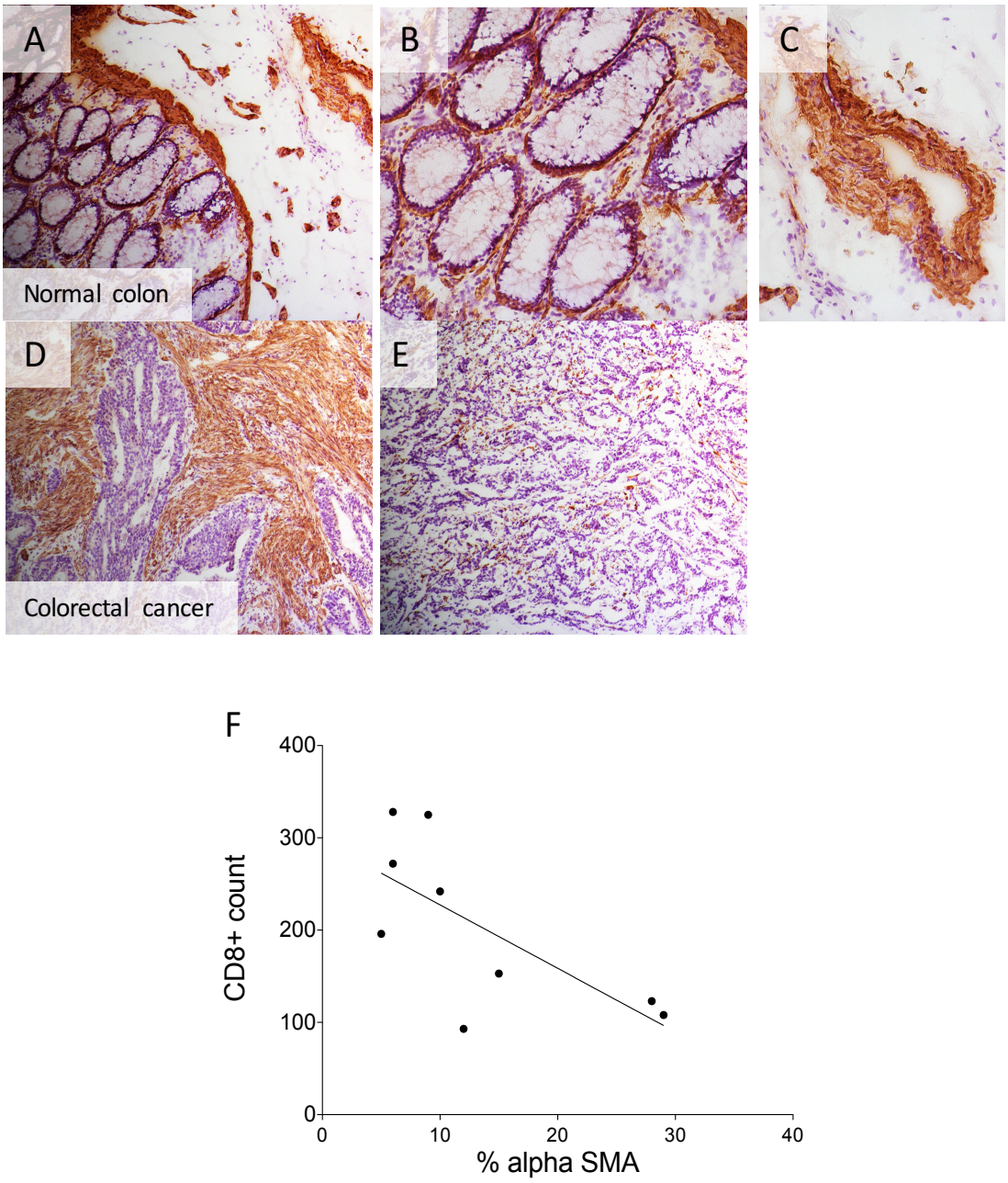

Figure 5.2: αSMA expression in NC and CRC.
To asses the expression of αSMA, immunohistochemical staining was performed on frozen sections of CRC and matched NC. Sections were imaged with Zeiss Axiovert microscope and images were captured with Axiovision software. Image A illustrates positive αSMA expression in a representative section of NC at x10 magnification. Images B&C, illustrate positive αSMA expression in normal colon lamina propria and smooth muscle, respectively, at x20 magnification. Images D and E illustrate αSMA expression in 2 different Dukes B CRC sections at x10 magnification. Panel F shows data from immunochemical staining for αSMA in 9 different CRC sections. % αSMA expression was quantified using Image J software and panel F presents the correlation between %αSMA staining and CD8+ count. Statistical analysis was performed and data were significant using Spearmans rank correlation co-efficient (p=0.04).

Pilot flow cytometry analysis (Figure 5.3) suggests that supernatant from 3 different samples of normal colorectal fibroblasts marginally up-regulated the mean percentage of cell surface MAdCAM-1 to 91.67±2.08% on NEC from the control percentage of 84.88±11.5% (Figure 5.3 A and C), with an increase in median channel value (MCV) from 60±62 to 116±10.5 (Figure 5.3 B and C). In contrast supernatant from tumour derived fibroblasts had no significant effect upon percentage MAdCAM-1 expression compared to control NEC. TAFB supernatant conditioning produced a similar elevation in MAdCAM-1 MCV expression to NFB. Treatment of NEC with supernatant from normal or tumour fibroblasts had no significant effect on the percentage positive or MCV values for ICAM-1 and E-Selectin compared to untreated endothelium as shown in Figure 5.3.

Next we used indirect enzyme linked immunosorbent assays (ELISA) (Figure 5.4A) to quantify membranous and cytoplasmic expression of MAdCAM-1, ICAM-1, and VCAM-1 protein by NEC and TEC monolayers after conditioning with NFB and TAFB supernatants. Expression was quantified for 3 NEC samples, treated with matched NFB and TAFB supernatants. NEC conditioned with NFB supernatant did not significantly alter the expression of MAdCAM-1, ICAM-1 or VCAM-1. TEC displayed different pattern of phenotype to NEC when conditioned with the same matched TAFB supernatants. There was a significant reduction in ICAM-1 expression (0.15±0.1 to 0.1±0.008). MAdCAM-1, and VCAM-1 expression were not significantly altered from TEC control as shown in Figure 5.4B.

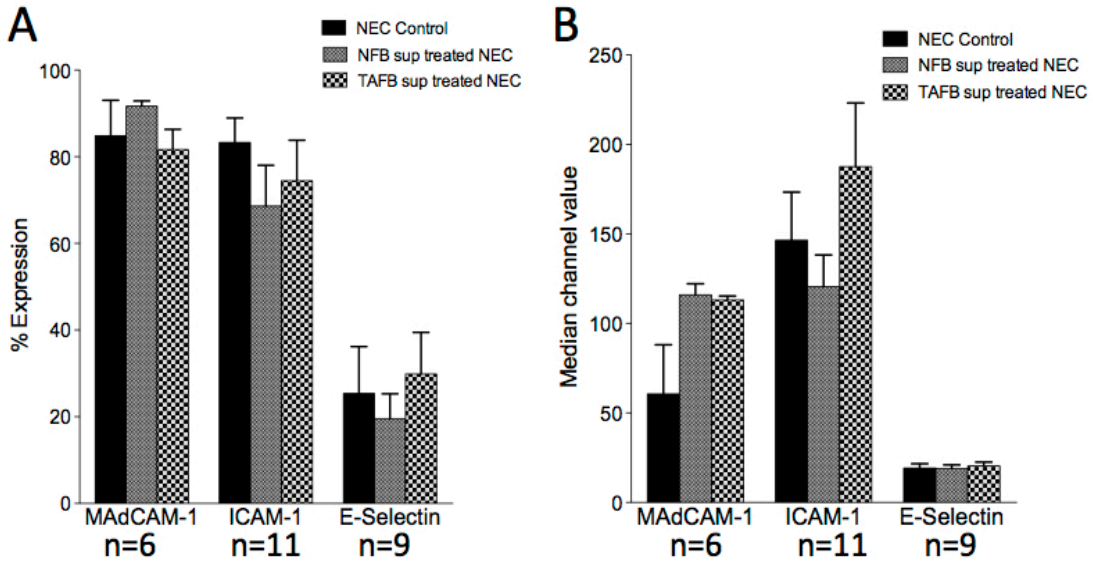

Figure 5.3: Cell surface ICAM-1, MAdCAM-1 and E-selectin expression by primary human colorectal endothelial cells *in vitro* after treatment with supernatant from normal or tumour associated fibroblasts.

NFB and TAFB were isolated and cultured from normal colorectal and tumour tissue. Once confluent, supernatant from standardized numbers of cells was removed. This supernatant was used to condition primary *in vitro* human colorectal NEC for 24 hours after which the cells were stained with mouse anti-human ICAM-1, E-selectin or MAdCAM-1 antibody conjugated to APC, PE-Cy5, or FITC (panels A,B &C) respectively. Positive expression was categorised against isotype-matched control staining (see Chapter 2). Data represent mean± SEM percentage expression (A) or median channel value (B) and mean ± SD are illustrated in the table (C). Statistical analysis was performed using paired T-test or ANOVA where multiple comparisons were made. Significance was considered at $p<0.05$. No data was significant.

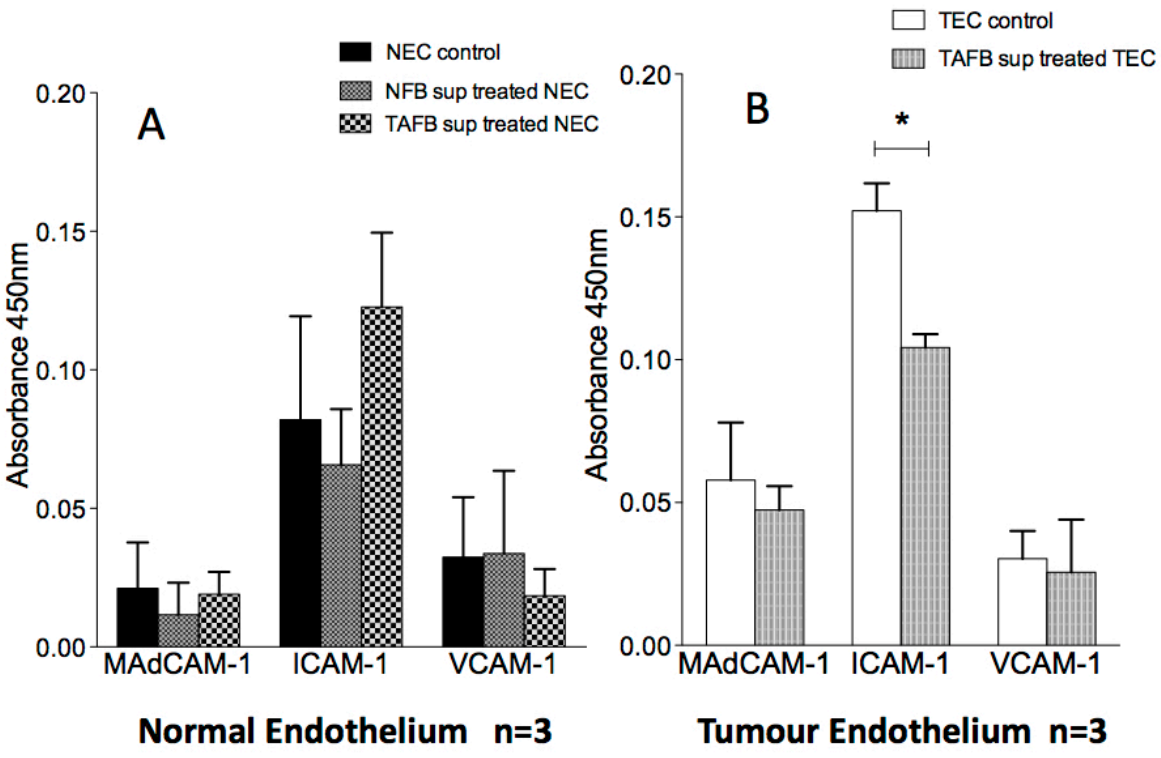

Figure 5.4: Expression of MAdCAM-1, ICAM-1 and VCAM-1 by primary human colorectal normal and tumour endothelial cells (NEC and TEC) after conditioning by tumour and normal associated fibroblast supernatant (TAFB and NFB).

NFB and TAFB were isolated and cultured from 3 samples of CRC and matched normal tissue. Once confluent, supernatant was removed and standardized for cell number. Simultaneously 3 matched *In vitro* NEC and TEC were cultured at passage 4 in flat bottom 96 well plates until confluent. Standardized NFB and TAFB supernatant was used to condition primary *in vitro* human colorectal NEC and TEC for 24 hours. Expression of adhesion molecules was determined using anti-ICAM-1, VCAM-1 and MAdCAM-1 antibodies in an indirect ELISA. Absorbance was read at and expression was documented relative to isotype-matched controls. Graphical data is presented as mean ± SEM. Statistical analysis was performed using 2-tailed paired Student's t-test.

5.2.2 Normal and tumour fibroblast supernatants have differential effects on CD8+ T-cell adhesion to colorectal NEC and TEC under static conditions.

To assess lymphocyte recruitment and adhesion to NEC and TEC *in vitro,* cells were treated with supernatant from patient-matched fibroblasts (i.e. NEC with matched NFB supernatant and TEC with matched TAFB supernatant). Isolated CD8+ T-cells from HFE patients were incubated with 3 samples of control and treated matched NEC or TEC and the number of CD8+ T-cells adhered to the monolayer were counted. Figure 5.5 A illustrates the individual results for 3 samples of matched NEC and TEC conditioned with supernatants from matching fibroblasts. For all three lymphocyte donors, treatment of NEC with NFB supernatant resulted in an increase in CD8+lymphocyte binding (45.5 % mean increase, Figure 5.5A). In contrast, although basal adhesion to TEC was higher than to NEC (mean TEC adhesion 260.1±168 vs NEC adhesion 178.2±110), treatment with supernatant from TFB resulted in a decrease in adhesion in two out of three patients (mean 27% and 38.5% reduction, patient 1&3, Figure 5.5a). For one patient we saw a dramatic increase in binding following treatment of TEC with TFB supernatant (mean 70.6% increase, patient 2, Figure 5.5a). This general adhesion pattern was reflected when we took single paired NEC and TEC isolates after conditioning with 6 different NFB and TAFB supernatants (Fig 5.5B). The collective results show that there is almost a 50% increase in lymphocyte adhesion to NEC when conditioned with NAFB and a significant 250%($p=0.022$) increase when conditioned with TAFB supernatant. However as before for TEC, lymphocyte adhesion falls after conditioning with either NFB or TFB supernatant compared to controls.

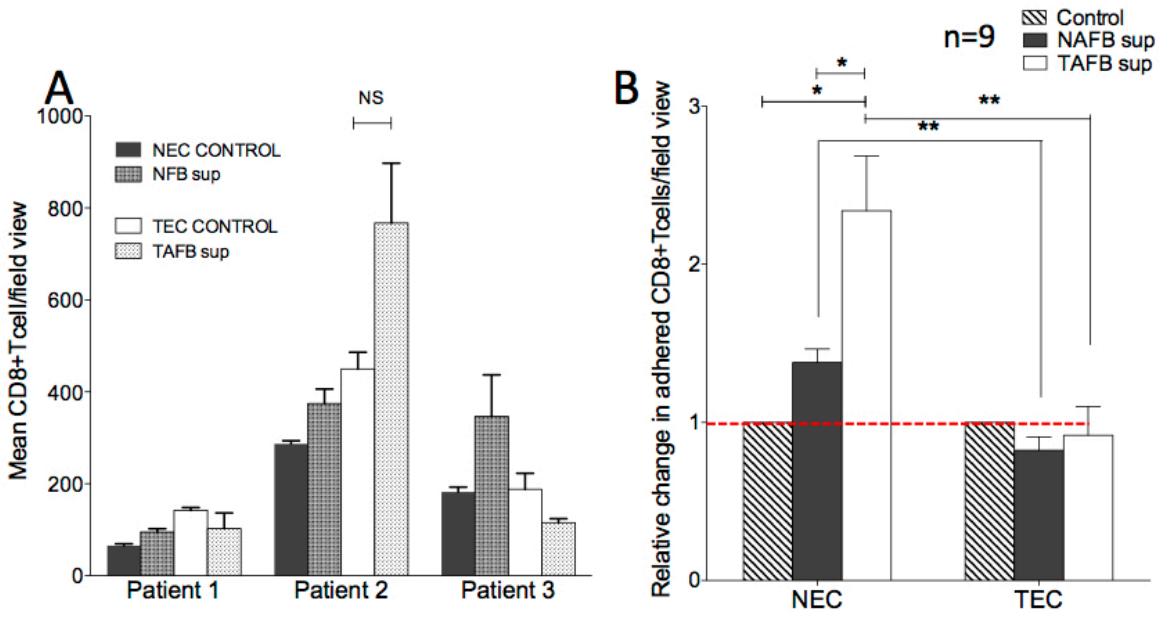

Figure 5.5: CD8+ T-lymphocyte adhesion to primary human colorectal normal and tumour endothelial cells (NEC and TEC) after conditioning by tumour or normal associated fibroblast supernatant (TAFB and NAFB) under static conditions.

NAFB and TAFB were isolated and cultured from normal colorectal and tumour tissue. Once confluent, supernatant was removed and diluted according to cell number to standardize the supernatant concentration. Resultant centrifuged supernatant was used to condition primary *in vitro* human colorectal NEC and TEC for 24 hours. CD8+ T-cell adhesion to endothelium was assessed using HFE patients blood CD8+ T-cells labeled with CSFE. Graph A is mean CD8+ T-cell adhesion per field of view, for 3 different samples of matched NEC and TEC with their matched NFB and TAFB. Graph B displays data describing the mean CD8+T-cell adhesion to 1 sample of NEC and matched TEC independently treated with 6 different NAFB and TAFB supernatants compared to untreated NEC and TEC. CD8+ T-cells were isolated from different donors for each NEC/TEC sample. Data is shown as mean and SEM. Statistical analysis was performed using paired Student's t-test.

5.2.3 Soluble IL-6 is present in CRC and produced by human colorectal derived Tumour Associated Fibroblasts.

Next I wanted to determine the identity of any factors within fibroblast supernatants that could be responsible for changing adhesion to endothelial cells. I used proteome-profiling arrays to assess cytokines production by 3 samples of normal and tumour colorectal derived fibroblasts in culture. The most abundant analytes in NFB supernatant, after comparison to the mean positive reference, were CCL5, IL-6, MIF and components of the IL-1 pathway. Supernatants from TFB also contained abundant IL-6, MIF and CCL5 and additionally CCL2 and CXCL1 (Figure 5.6 A and B) From 3 independent proteome profiling experiments using 3 different samples, the mean IL-6 abundance in NFB supernatants, expressed as a percentage of the reference, was 2.2±2.2% and in TAFB supernatants it was significantly higher, measuring 55.6±11.7% ($p=0.0015$) (Figure 5.6C). This significant increase in IL-6 in TAFB supernatant was confirmed by sandwich ELISA using 3 different-matched NFB and TFB supernatant samples (Figure 5.6 D). These experiments confirmed that more IL-6 is present in supernatants from TFB (114.9±15.4pg.ml) than NFB (82.6±11.7pg/ml, $p=0.0082$).

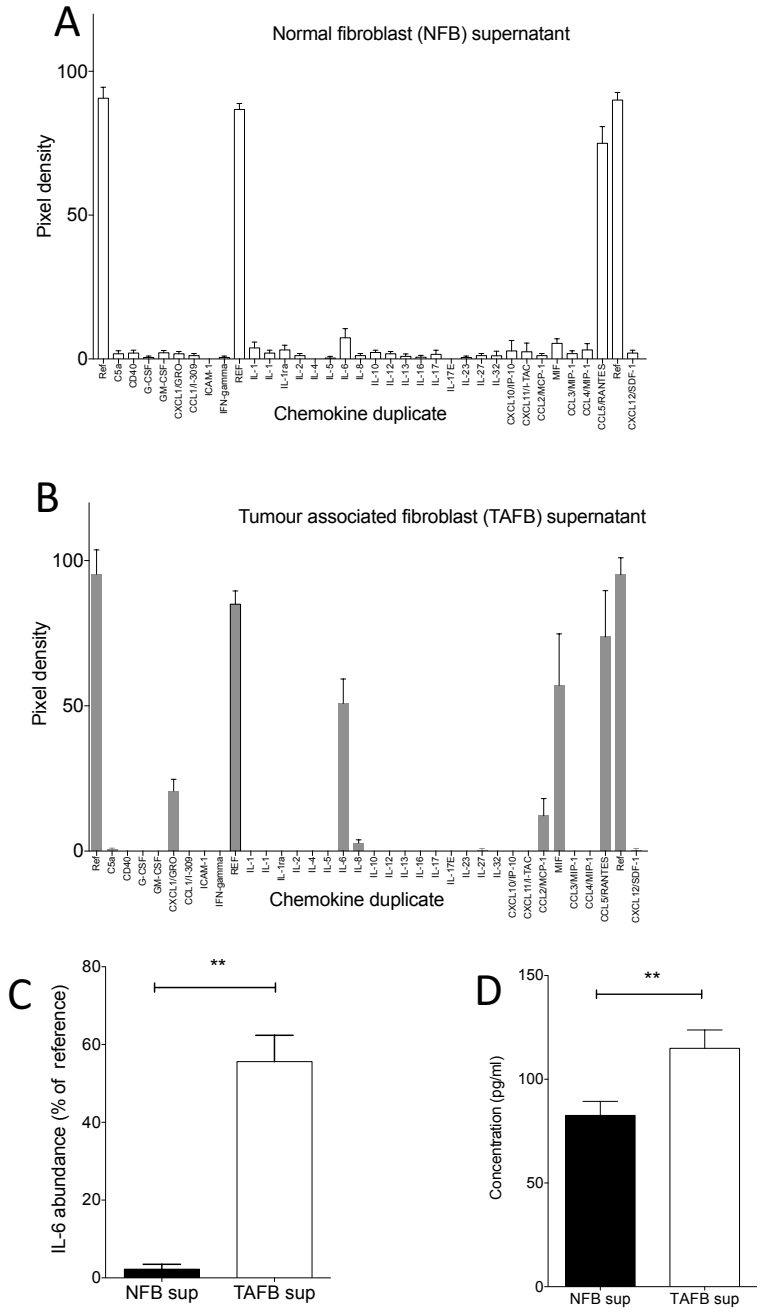

Figure 5.6: Cytokine production by fibroblasts isolated from tumour and normal colorectal tissue.

Cytokines were quantified from the culture supernatant produced by primary fibroblasts isolated from human colorectal cancer and matched uninvolved colorectal tissue by using a Proteome Profiler (Human Cytokine Array Panel A, R&D, UK) as per manufacturers guidelines. Quantification was performed by measuring pixel density with Image J software. Panels A and B illustrate the cytokine profile of supernatant from Normal fibroblasts (NFB) and tumour associated fibroblasts (TAFB) respectively from 3 biological repeats. Graph C illustrates the pixel density of IL-6 in each of the supernatants illustrated as a percentage of the mean pixel density of positive reference spots for the 3 samples. Graph D is the concentration of IL-6 found in NAFB and TAFB supernatants (standardised by dilution to number of cells in culture) determined using sandwich ELISA (Duo kit, R&D according to manufacturers instructions). Statistical analysis was performed using paired Student's t-test.

I performed immunohistochemical analysis to visualize IL-6 in whole NC and CRC tissue. This revealed that in CRC, positive cytoplasmic staining was associated with stromal fibroblasts. This staining pattern was distributed across the tumour and was not seen in corresponding NC (Figure 5.7). The intensity of the staining ranged from weak to strong across 4 of the tumour specimens however the proportion of the fibroblast population that stained positive was less that 20% in all samples. Occasionally positive cytoplasmic staining was also identified in the tumour epithelial cells (not shown).

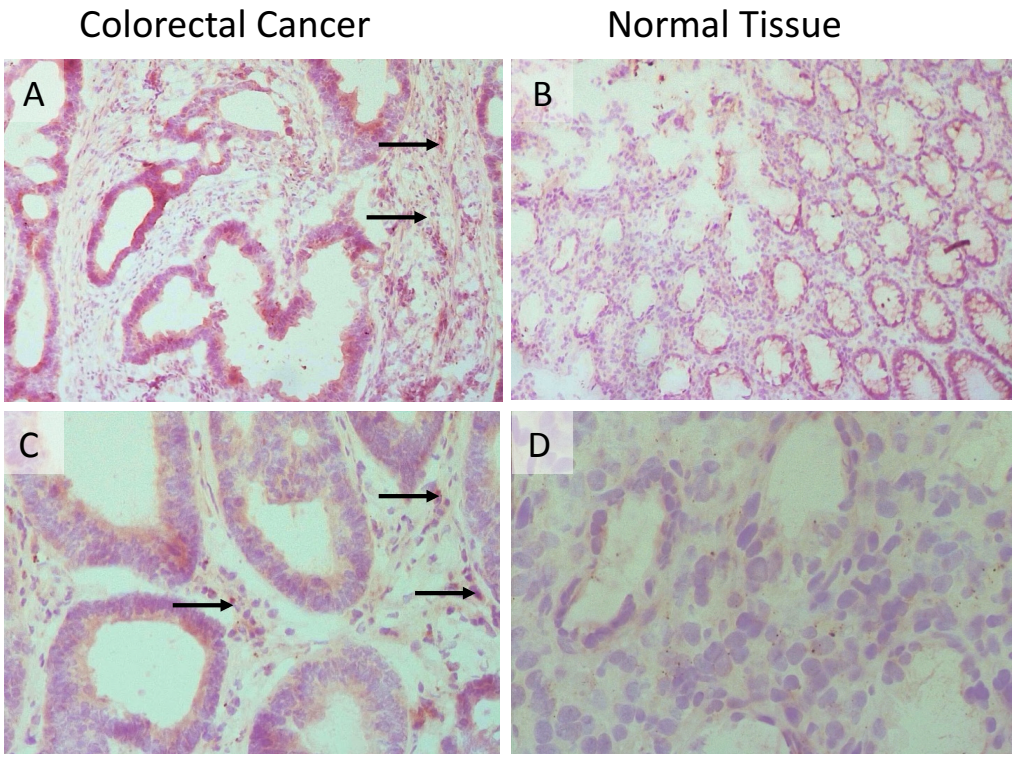

Figure 5.7: Immunochemical detection of IL-6 in colorectal tumour stroma.
To assess the presence and location of IL-6 in colorectal stroma, immunohistochemical analysis of CRC and NC frozen sections was performed. Sections were imaged with a Zeiss Axiovert microscope and images were captured with Axiovision software. Image A illustrates positive stromal fibroblast (arrows) in a representative section of Dukes B CRC at x10 magnification. Image B shows no stromal positivity within the matching NC at x10 magnification. Image C is taken at x20 magnification of Dukes C CRC and illustrates IL-6 positive stromal fibroblasts (arrows). Image D is of NC taken at x40 magnification and reveals no positive stromal staining.

5.2.4 IL-6 alters adhesion molecule expression of human colorectal derived NEC and TEC.

Flow cytometrical analysis was performed to find out if the presence of IL-6 would alter cell surface expression of adhesion molecules by NEC and TEC. FC analyses showed that the mean percentage expression of cell surface of MAdCAM-1 modestly decreased in IL-6 treated NEC from 6.1±4.5 to 5.3±6.4 (Figure 5.8A) as did the mean MCV of MAdCAM-1 (25.6±12.2 to 22.5±2.6, Figure 5.8B). The mean percentage of VCAM-1 expression also reduced from 11.6±10.1 to 3.4±3.2 (Figure 5.8A&E) after stimulation. However, neither the MCV or percentage decrease reached statistical significance. ICAM-1 cell surface expression increased in NEC from 31.2±31.7 to 43.3±36.8 and was supported by an increase in MCV from 19.4±13 to 32.9±14.0 after stimulation with IL-6, although the results did not reach statistical significance. E-Selectin expression also increased (from 43.4±13.3 to 52.3±18.0) after stimulation with recombinant human IL-6. The mean percentage of VCAM-1 expression reduced after treatment with IL-6 from 11.6±10.1 to 3.4±3.2 (Figure 5.8A&E) although the MCV of VCAM-1 in IL-6 treated NEC showed an increased from 26.8±15.5 to 32.0 ±15.1. The mean percentage cell-surface expression of E-selectin by NEC also increased, although not significantly, from 43.4±13.3 to 52.3±18.0 after stimulation with recombinant human IL-6.

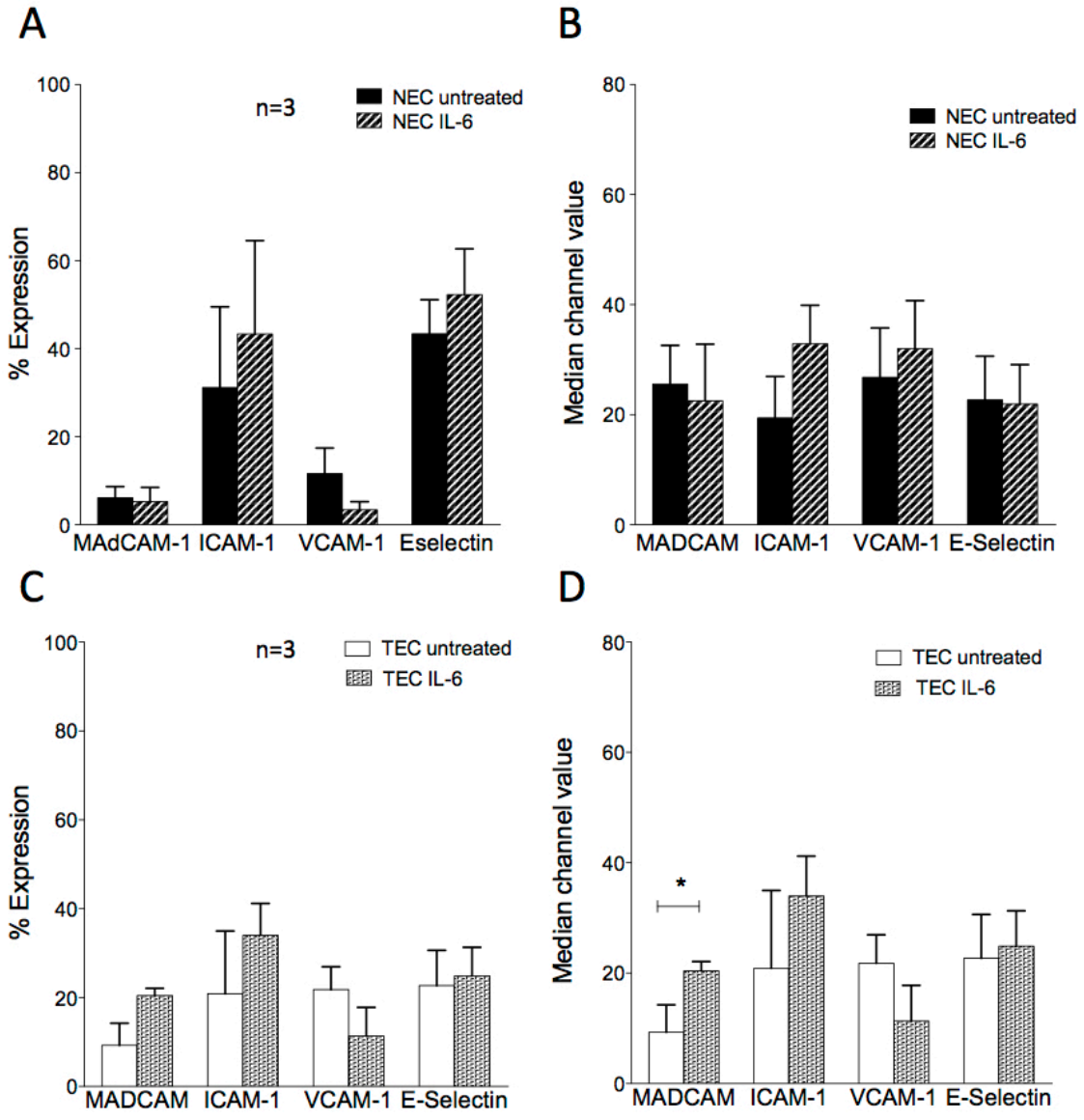

Figure 5.8: MAdCAM-1, ICAM-1, VCAM-1 and E-Selectin expression by NEC and TEC with recombinant IL-6.

Tumour and matched normal human Endothelial cells were isolated from 3 matched CRC and NC samples using immunomagnetic beads described in chapter 2. Immediately after isolation each sample was treated with 100ng/ml of recombinant human IL-6 protein (Peprotech, U.K) in MV-2-EBM (Lonza, U.K) for 24 hours, after which the cells were stained with mouse anti-human MAdCAM-1, ICAM-1, VCAM-1 or E-selectin antibody conjugated to FITC, APC, FITC and PE. Cells underwent single colour flow cytometry analysis of positive expression against isotype matched control (see Chapter 2 for detailed Flow cytometry methods). Data of NEC and TEC (A&B, and C&D respectively) is presented in mean and SEM of the percentage expression and median channel value. Data was analysed for significance using paired (NC) and unpaired (TEC) two-tailed Student's t-test.

The MCV of E-selectin was relatively unchanged from 22.7±13.7 to 22±12.4 after IL-6 treatment. The mean percentage of VCAM-1 expression reduced after treatment with IL-6 from 11.6±10.1 to 3.4±3.2 (Figure 5.8D) although the MCV of VCAM-1 in IL-6 treated NEC showed an increased from 26.8±15.5 to 32.0 ±15.1. However, these changes were small and not statistically significant.

5.2.5 Soluble IL-6 promotes CD8+ T-cell adhesion to human colorectal derived TEC but not NEC.

When primary human colorectal derived NEC were treated with IL-6 and incubated with CD8+ T-cells under static conditions, no difference was observed in the number of adherent lymphocytes. Low numbers of CD8+ T-cells were observed to bind to three independent NEC samples (approximately 50 lymphocytes per field view). In contrast far more (150.4±16.3, Figure 5.9) CD8+T-cells bound to unstimulated TEC, and this increased statistically significantly (209.8±18.1, p=0.014, paired student T-test, figure 5.9A) when TEC were pretreated with IL-6.

We then performed experiments similar to those previously described where 3 different NEC and TEC were conditioned with 3 different NFB and TAFB supernatants. This time we used either supernatant alone or added IL-6 inhibitor to the treatment. Our ELISA data (Figure 5.6D) was used to establish the appropriate concentrations of IL-6 inhibitor to use. As before, approximately 50 CD8+ T-cells adhered to control NEC per field view and this increased significantly to a mean of 136.1±34.5 (p=0.0016) for NEC treated with TAFB. Importantly with TAFB and IL-6 inhibitor, the mean adhesion significantly reduced to 74.9±15.9 cells per field (p=0.002). We saw a similar effect of IL-6 blockade on TEC, except basal adhesion was higher (164.7±18.8), this decreased to 144.7±28.3 after TAFB

conditioning and the magnitude of the inhibitory effect of IL-6 blockade was smaller (116.2±19.3, p=0.024 Figure 5.9B).

To identify whether these effects were replicated under physiological shear forces, flow based adhesion assays were performed with IL-6 stimulated NEC and TEC. Recombinant IL-6 treatment increased CD8+ T cell adhesion to NEC marginally (from 70.3 ±6.9 adherent cells per $mm^2/10^6$ in untreated control NEC to 78.4±9.1 after IL-6 treatment) across 3 independent experiments. However, for TEC the increase was significant. Here mean number of adherent cells per $mm^2/10^6$ in rose from 213.7±15.1 to 280.3±13.1 in IL-6 treated TEC (p=0.004, Figure 5.10 A, B and C). Whilst total numbers of adherent cells increased we saw no difference in the percentage of CD8 T-cells rolling over TEC or NEC following IL-6 treatment (Figure 5.10 D).

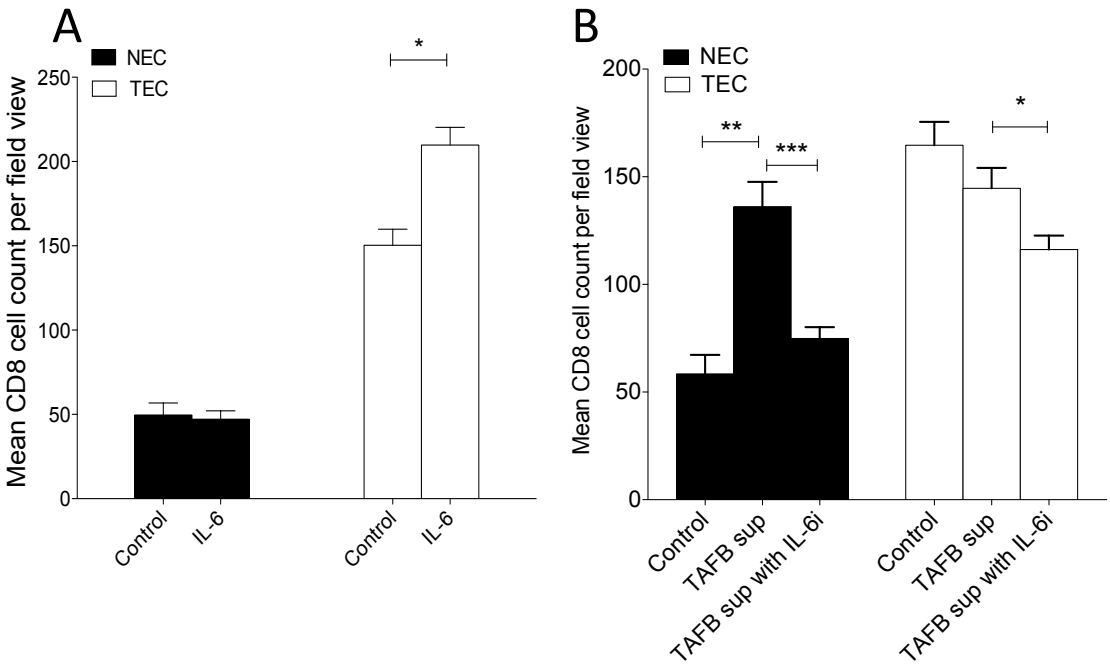

Figure 5.9: IL-6 increases CD8+T-cell adhesion to primary colorectal NEC and TEC under static conditions.

Monolayers of NEC and TEC were treated with either recombinant human IL-6 (120pg/ml) or supernatants from 3 *in vitro* NAFB and TAFB isolates for 24 hours. Where indicated wells included anti-human IL-6 receptor inhibiting antibody for 1 hour (2ng/ml, R&D, UK). CD8+T-cells isolated from HFE blood were resuspended in EBM-2 (LONZA, UK) with 1% BSA at a concentration of $25x10^4$ cell/ml for static adhesion assays. The number of CD8+T-cells adhered to the endothelium were imaged with Zeiss Axioscope and captured with Axiovision software at an original magnification x10. Adherent cells were counted using Image J software. Panels A and B shows CD8+T-cell adhesion to 3 diferent NEC and TEC samples treated (3 biological repeats) with IL-6 compared to control samples, wells treated with 3 different TAFB supernatants alone, and the same supernatants in the presence of IL-6 receptor blocking antibody. Statistical analysis was performed with paired Student's t-test.

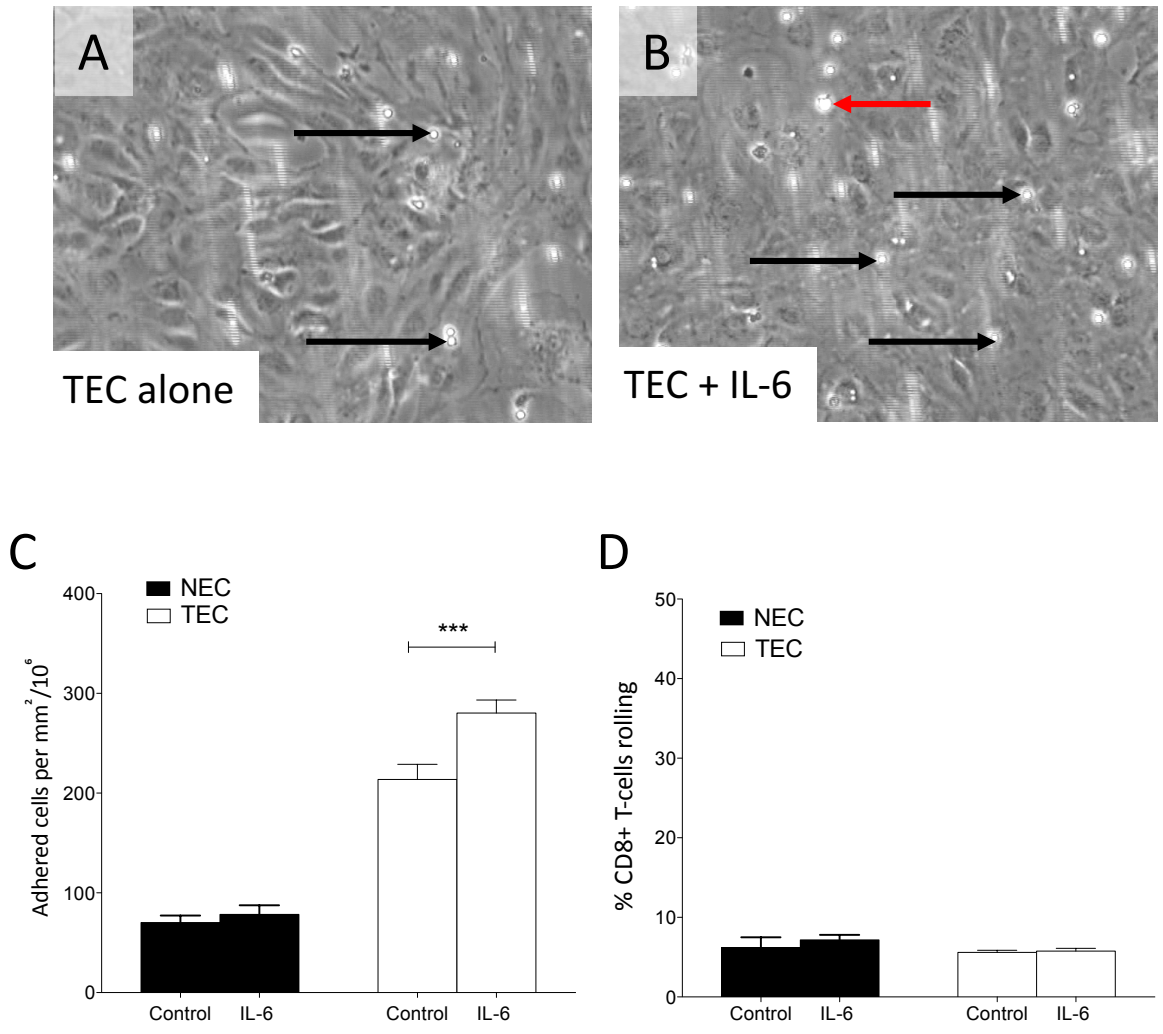

Figure 5.10: IL-6 promotes CD8+T-cell adhesion to primary NEC and TEC under flow conditions.

Primary NEC and TEC were cultured in Ibidi chambers until confluent. EC were incubated with recombinant IL-6 for (120pg/ml, Peprotech, UK) for 12 hours prior to performing flow based adhesion assay with isolated CD8+ T-cells from HFE blood. Representative images (A and B) were taken with a phase contrast microscope at x20 magnification. Black arrows show adherent T cells. The red arrow indicates a T-cell undergoing transmigration through the endothelium. Graph C represents mean ± SEM adherent cells per $mm^2/10^6$ perfused. Graph D represents the % adherent CD8+ T-cells that were observed rolling at low velocity over the EC surface. Statistical analysis was performed with paired Student's t-test.

5.2.6 Endothelin-1 is up regulated in CRC compared to NC

We also assessed the abundance of pro-angiogenic proteins in TAFB and NFB supernatants using a commercially available proteome profiling array (Figure 5.11). Unsurprisingly, 46 of the angiogenesis-related proteins were more abundant in TAFB supernatant (Figure 5.11 A&B). One of these, Endothelin-1 was of particular interest due to reports that the Endothelin-1/Endothelin receptor B axis alters the expression of ICAM-1 in ovarian solid tumour vascular endothelium (97). From 3 independent proteome profiling experiments using 3 different matched supernatants, the mean percentage of Endothelin-1 in NFB supernatants, expressed as a percentage of the reference was 5.8±5.4% and in TAFB supernatants it was significantly higher, measuring 23.7±11.9% ($p=0.04$) (Figure 5.11C). Furthermore, the gene EDN-1 that drives expresses of Endothelin-1 protein was up regulated in whole CRC based on qPCR from 3 different matched CRC and NC samples (Figure 5.11 D). This qPCR analysis confirmed that EDN-1 gene expression was 26.8 times higher in CRC than matched NC ($p=0.03$, Figure 5.11 D).

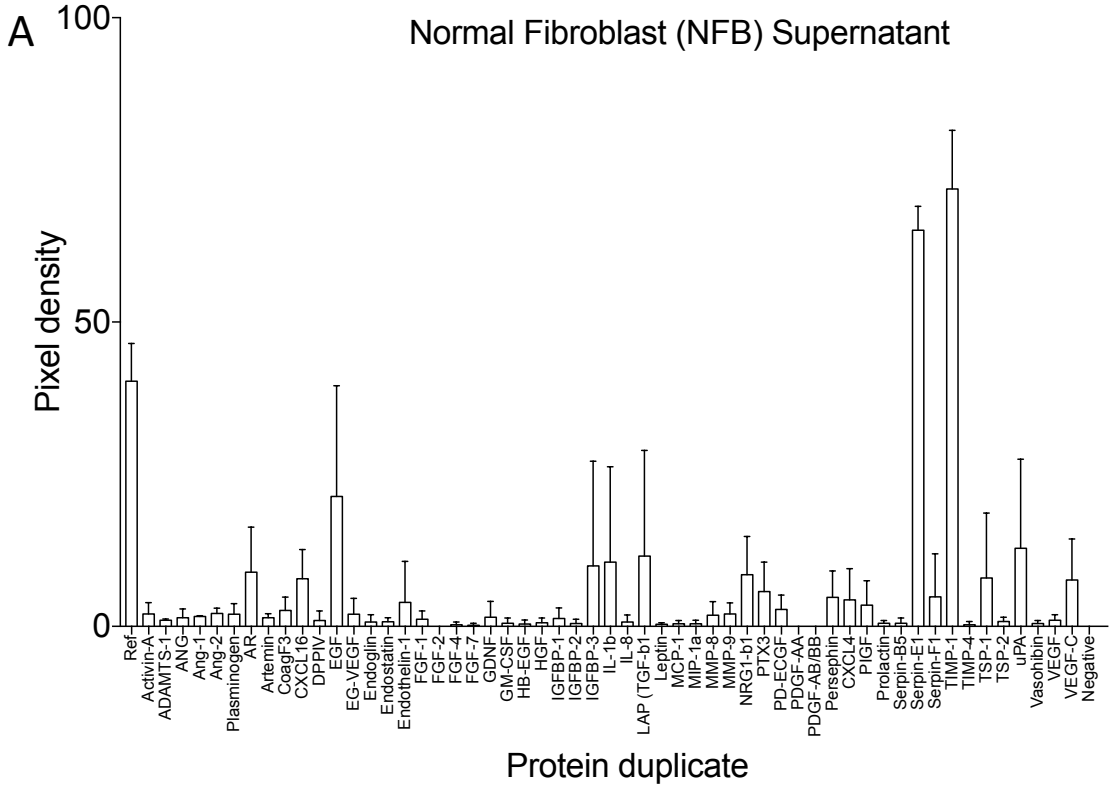
A
Normal Fibroblast (NFB) Supernatant
Pixel density
100
50
0
Ref
Activin-A
ADAMTS-1
ANG
Ang-1
Ang-2
Plasminogen
AR
Artemin
CoagF3
CXCL16
DPPIV
EGF
EG-VEGF
Endoglin
Endostatin
Endothelin-1
FGF-1
FGF-2
FGF-4
FGF-7
GDNF
GM-CSF
HB-EGF
HGF
IGFBP-1
IGFBP-2
IGFBP-3
IL-1b
IL-8
LAP (TGF-b1
Leptin
MCP-1
MIP-1a
MMP-8
MMP-9
NRG1-b1
PTX3
PD-ECGF
PDGF-AA
PDGF-AB/BB
Persephin
CXCL4
PlGF
Prolactin
Serpin-B5
Serpin-E1
Serpin-F1
TIMP-1
TIMP-4
TSP-1
TSP-2
uPA
Vasohibin
VEGF
VEGF-C
Negative
Protein duplicate

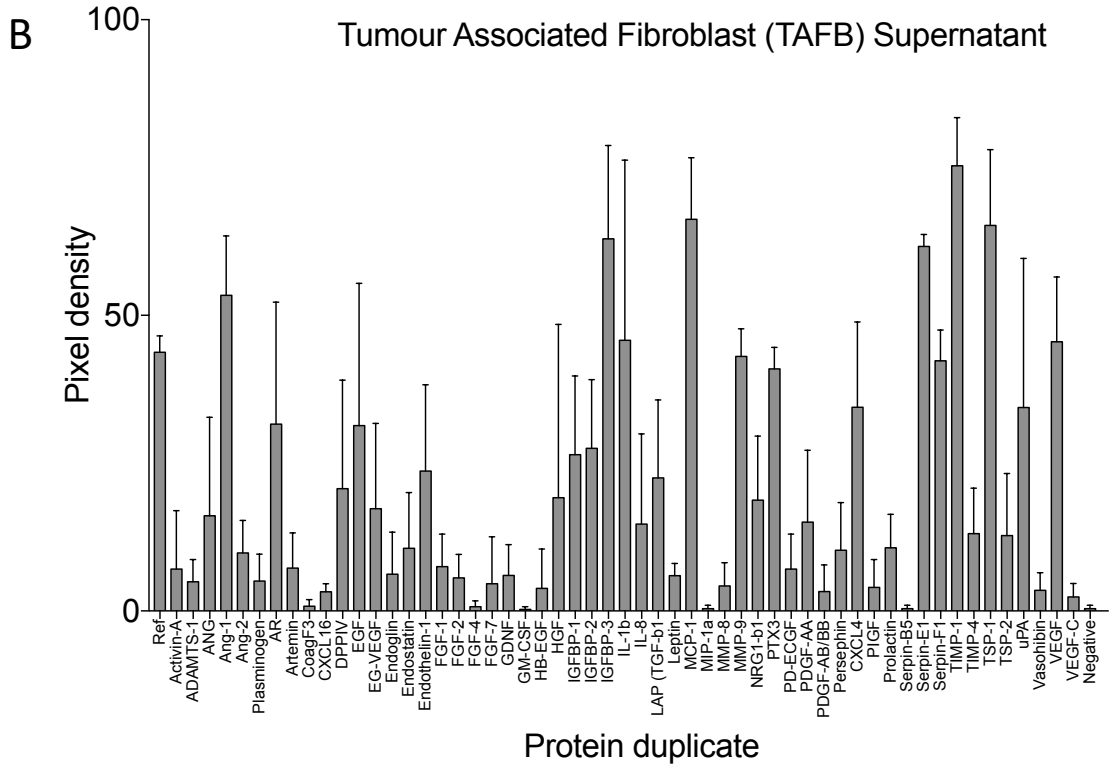
B
Tumour Associated Fibroblast (TAFB) Supernatant
Pixel density
100
50
0
Ref
Activin-A
ADAMTS-1
ANG
Ang-1
Ang-2
Plasminogen
AR
Artemin
CoagF3
CXCL16
DPPIV
EGF
EG-VEGF
Endoglin
Endostatin
Endothelin-1
FGF-1
FGF-2
FGF-4
FGF-7
GDNF
GM-CSF
HB-EGF
HGF
IGFBP-1
IGFBP-2
IGFBP-3
IL-1b
IL-8
LAP (TGF-b1
Leptin
MCP-1
MIP-1a
MMP-8
MMP-9
NRG1-b1
PTX3
PD-ECGF
PDGF-AA
PDGF-AB/BB
Persephin
CXCL4
PlGF
Prolactin
Serpin-B5
Serpin-E1
Serpin-F1
TIMP-1
TIMP-4
TSP-1
TSP-2
uPA
Vasohibin
VEGF
VEGF-C
Negative
Protein duplicate

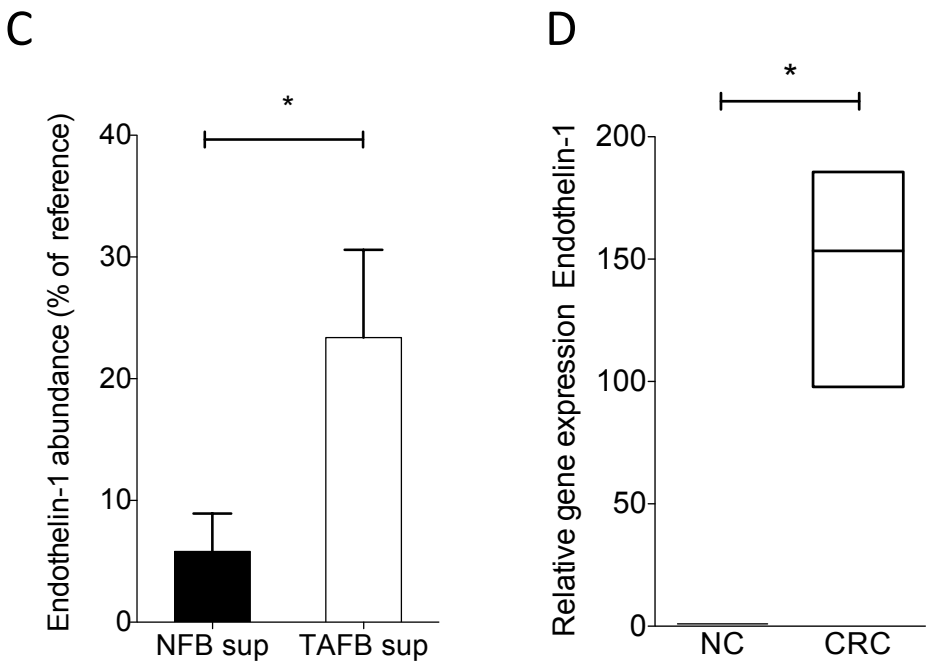

Figure 5.11: Endothelin-1 expression is elevated in supernatants from tumour associated fibroblasts compared to matched control tissue.

Graphs represent quantification of soluble proteins from the culture supernatant produced by primary fibroblasts isolated from human colorectal cancer and matched uninvolved colorectal tissue. Protein abundance was detected using a Proteome Profiler (Human angiogenesis Array Panel A, R&D, UK) as per manufacturers guidelines. The supernatants were incubated with a pre-mixed biotinylated detection antibody cocktail mix and a nitrocellulose membrane (pre-spotted with capture antibodies). Streptavidin-HRP and chemiluminescent reagents were used to the detect bound cytokine/detection antibody complexes. Quantification of the abundance of cytokine produced was performed by measuring the mean pixel density from 2 spots with Image J software. A and B illustrate a representative angiogenesis protein profiles from primary *in vitro* colorectal derived NFB and TAFB supernatants respectively. Graph C illustrates the pixel density of Endothelin-1 produced from independent Angiogenesis array panel experiments for 3 different NFB and TAFB supernatants presented as abundance relative to the mean positive control of the mean pixel density for the respective samples. For QPCR, *in vitro* endothelial cell homogenates underwent mRNA extraction (Qiagen Rneasy minikit, UK) and cDNA synthesis (Iscript, Biorad, uk). Real time qPCR was undertaken using an original concentration of 45ng/µl of mRNA for all samples using Taqman gene probes and primer (Invitrogen). CT values were calculated using Stratagene Mx3000P and analysis was performed using ΔΔCT method using GAPDH and Beta Actin as housekeeping genes and obtaining the TEC value as sample of interest against matched NEC. Statistical analysis was performed using paired Student's t-test.

5.2.7 Endothelin receptor B (ETb) is preferentially expressed by vascular endothelium from CRC *ex vivo* and primary human colorectal TEC *in vitro* and is up-regulated by TAFB supernatant on TEC but not NEC.

Elevated levels of Endothelin-1 in our tumour supernatants led us to investigate whether Endothelial receptor B was expressed on tumour vascular endothelium. Initially immunohistochemistry was performed to visualize ETb expression in both NC and CRC tissue sections. In NC, endothelial cells showed membrane and cytoplasmic ETb expression throughout the mucosal and submucosal layers. In CRC, both membranous and cytoplasmic ETb expression was observed on endothelial cells throughout the tumour and was also found at the invasive margin and central tumour areas. Semi-quantitative analysis of the IHC staining revealed that microvascular endothelial expression of ETb was observed across all vessels in CRC, with a maximum mean score of 3/3 whereas expression was lower in NC (2.3). However, the intensity of staining was similar between NC and CRC (Figure 5.12).

ETb expression in NEC and TEC was measured by ELISA. Indirect ELISA showed that, in one representative sample, increased ET_B expression was identified in *in vitro* TEC compared to NEC. The absorbance value for NEC was quantified as 0.05 compared to a value of 0.94 found by a matching TEC sample (Figure 5.12 D). This data was supported by QPCR data from 3 patient samples, where mean gene expression of EDNRB, the gene encoding for the protein ET_B, was significantly higher compared to the gene expression of NEC (mean gene expression for TEC26.8 ± S.D. 7.65, p=0.03, Figure 5.12 E).

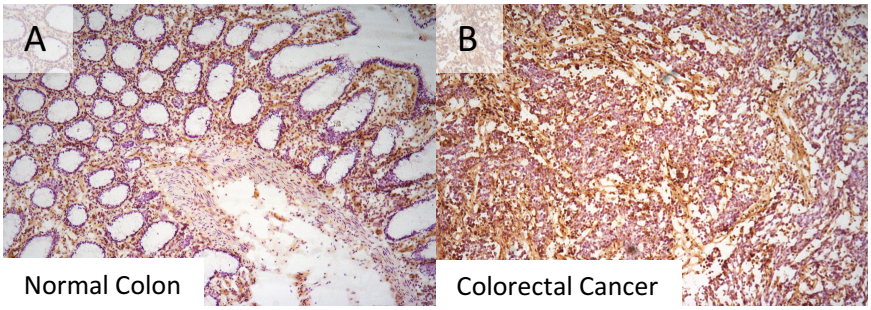

C

Endothelin receptor B (ETb)	NC (n=3)	CRC (n=3)
Proportion of vessels stained (range of score)	2.3 (2-3)	3
Intensity of staining (range of score)	2.3 (2-3)	2.6 (2-3)

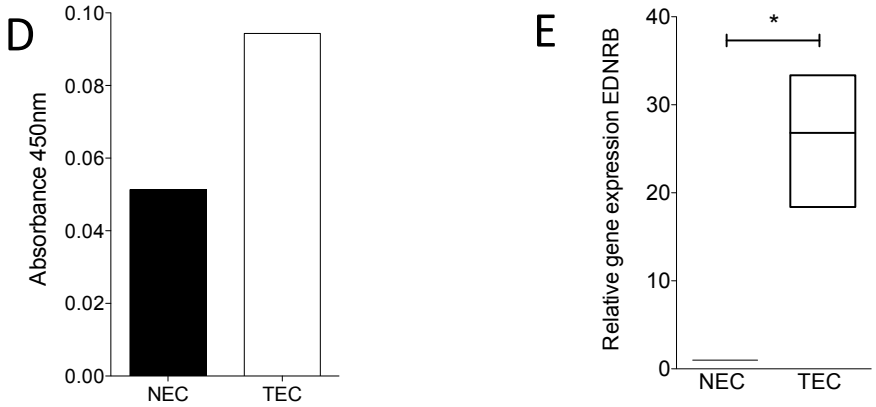

Figure 5.12: Endothelin receptor B expression in NC and CRC tissue and cultured NEC and TEC.
The expression of Endothelin receptor B was assessed in both whole tissue and endothelial cells derived from human CRC and matched NC. Immunohistochemical staining was performed on frozen sections of CRC and matched NC using mouse anti human-ETb antibody and DAB substrate. Sections were imaged with Zeiss Axiovert microscope and images were captured with Axiovision software. *In vitro* endothelial cell homogenates underwent mRNA extraction (Qiagen Rneasy minikit, UK) and cDNA synthesis (Iscript, Biorad, uk). Real time qPCR was undertaken using an original concentration of 45ng /µl of mRNA for all samples using Taqman gene probes and primer (Invitrogen). CT values were calculated using Stratagene Mx3000P and analysis was performed using ΔΔCT method using GAPDH and Beta Actin as housekeeping genes and obtaining the TEC value as sample of interest against matched NEC. A and B represent sections of NC and Dukes B CRC stained with human ETb antibody at x10 magnification. The ETb immunohistochemistry staining was scored on proportion of cells positively stained and the intensity of staining observed. Table C shows the mean scores and range of scores given for 3 sections of CRC and their matched NC. *In vitro* NEC and TEC expression of ETb was assessed using indirect ELISA. D shows the differences in Endothelin receptor B concentrations represented by absorbance at 450nm. Panel E shows QPCR data from NEC and TEC indicating the relative gene expression of ETb in NC compared to CRC. Statistical analysis was performed using the Student's t-test.

The baseline expression in NEC reduced slightly but not significantly following treatment with 3 different TAFB supernatants (Figure 5.13. In contrast ETb expression in untreated TEC increased significantly after conditioning with TAFB supernatants (0.09 to 0.12 ± 0.01 (p=0.0435), Figure 5.13).

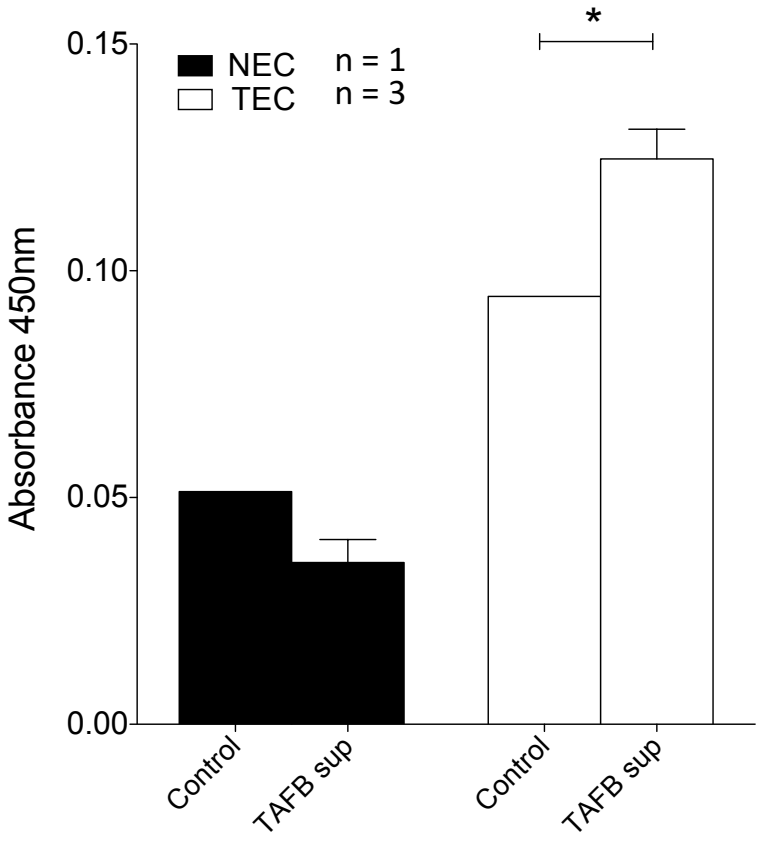

Figure 5.13: Endothelial receptor B (ETb) expression on colorectal derived NEC and TEC after conditioning with TAFB supernatant.
NEC and TEC were used in indirect ELISA experiments to compare the expression of ETb before and after stimulation with culture supernatant from TAFB. *In vitro* NEC and TEC were cultured at passage 4 in flat bottom 96 well plates until confluent. Where indicated, cells were conditioned with standardized concentration of TAFB supernatant for 24 hours. Expression was determined using indicated primary antibodies and HRP-conjugated secondary antibody with TMB substrate. Absorbance was read at 450nm and background values for isotype matched controls were subtracted from test data. Graphical data is presented as mean and SEM. Above is a graphical representation of this data. Statistical analysis was performed using Student's t-test.

5.2.8 Inhibiting the ET1/ETb axis in colorectal derived TEC up-regulates cell surface ICAM-1 expression and promotes CD8+ T-cell adhesion under static and flow conditions.

ICAM-1 expression by colorectal NEC and TEC before and after incubation with BR-788, a synthetic antagonist of Endothelin receptor B (ETb) was assessed using flow cytometry. The mean percentage expression of ICAM-1 by control NEC rose slightly but non-significantly after incubation with ETb antagonist (31.1± 12.4% to 45.2±7.7%, Figure 5.14). A similar trend was observed for median channel fluorescence values in NEC. In contrast the mean percentage of ICAM-1 expression by control TEC was 26.6±10.9% and this increased to 56.6±6.1% (p=0.041) after treatment with ETb antagonist (Figure 5.14). Similarly, MCV of control TEC ICAM-1 expression also increased from 19.2±16.1 to 73.2±7.1 after incubation with ETb antagonist (p=0.037).

I assessed the impact of inhibiting the ETb/ET1 axis on adhesion of to CD8+ T lymphocytes to tumour endothelium under static conditions. In 3 independent experiments, the mean number of adhered CD8+ T lymphocytes to untreated TEC was 164.7±18.8 cells per field view and after treatment with ETb antagonist this significantly increased to 226±26.2 (p=0.008, Figure 5.15). Flow based adhesion showed that 132.3±31.1 adherent cells per mm^2 /10^6 cells perfused bound to untreated TEC in 3 independent experiments. After treatment with ETb antagonist the mean increased significantly to 331.5±48(p=0.0063), and this could be abrogated with ICAM-1 blockade where adhesion reduced to a mean of 188.9±12.3 cells per mm^2 /10^6 (p=0.043). No significant difference in the percentage number of rolling CD8+ T cells was observed between the control and the treatment groups.

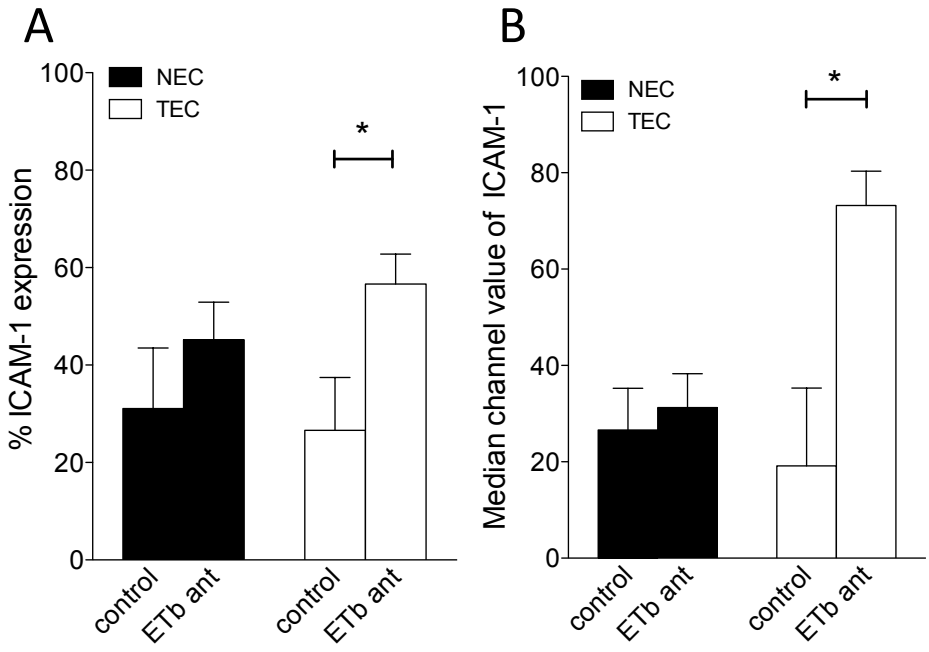

Figure 5.14: ICAM-1 expression by NEC and TEC after inhibition of Endothelial Receptor B (ETb) using synthetic antagonist BR-788.

Cell surface expression of ICAM-1 was quantified using single colour flow cytometry on primary human colorectal derived NEC and TEC incubated with 200ng/ml of the selective receptor B antagonist of Endothelin BR-788 (Enzo life science, U.K.). A illustrates the percentage ICAM-1 expression by NEC and TEC treated with ETb antagonist compared to NEC control. B illustrates median channel value of ICAM-1 expression by NEC and TEC treated with ETb antagonist compared to NEC control. Statistical analysis was performed using ANOVA and $p<0.05$was considered significant.

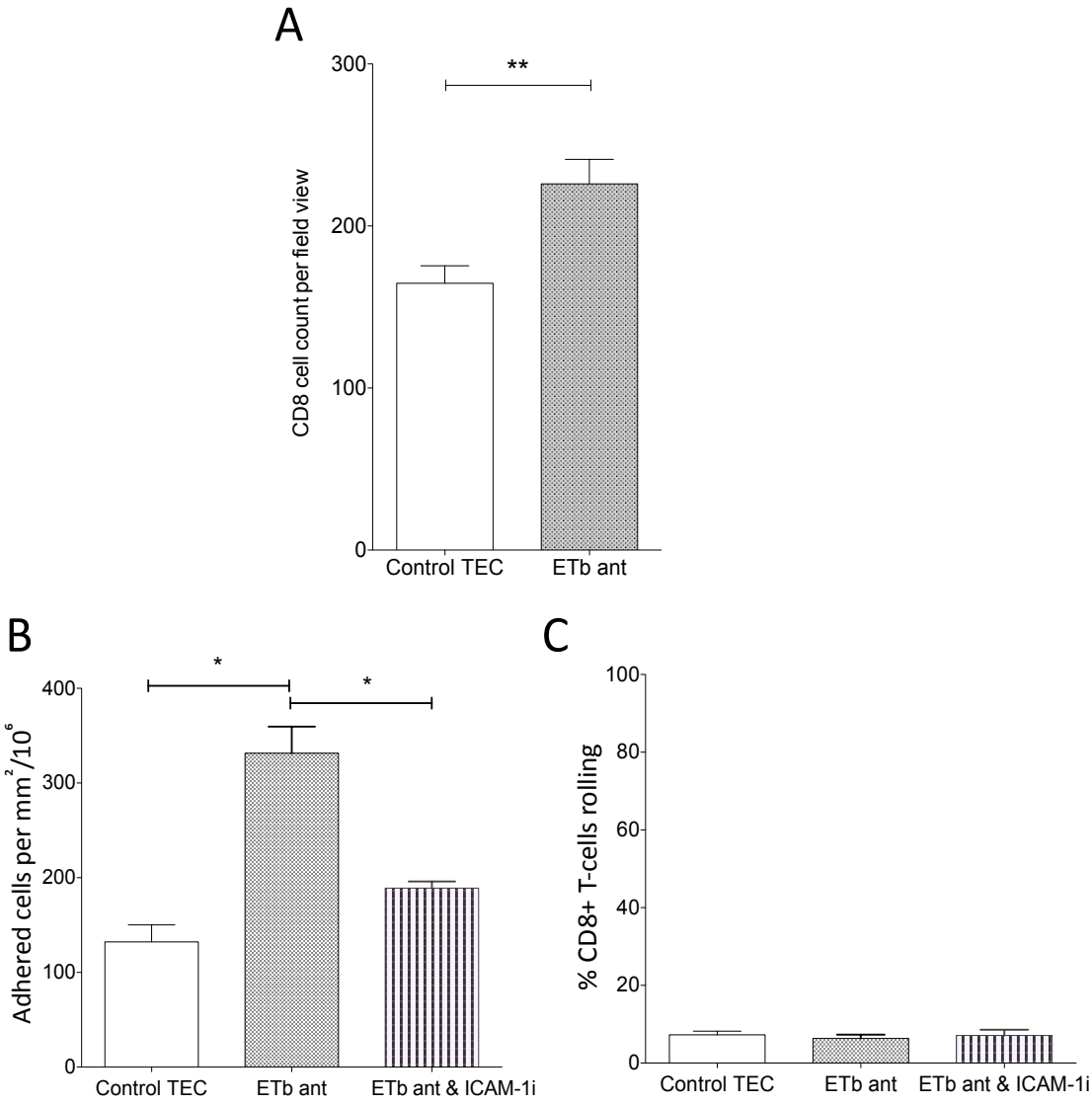

Figure 5.15: CD8+ T-cell adhesion to NEC and TEC after EDNRB inhibition under static and flow conditions.

The affect of inhibiting endothelial ETb on primary human colorectal TEC and their adhesive properties to CD8+ T lymphocytes was assessed by static and flow-based adhesion assays. For static experiments, cultures *of* colorectal TEC were pre-treated with 200ng/ml of the selective receptor B antagonist of Endothelin BR-788 (Enzo life science, U.K.) for 1 hour and then incubated with isolated CD8+T lymphocytes isolated from HFE blood, for 30 minutes. The number of adhered T cells were counted in both treated and non-treated (control) groups. Graph A illustrates data from 3 independent experiments. Flow assays were performed using primary colorectal derived NEC and TEC cultured in Ibidi chambers until confluent. EC were pre-treated with 200ng/ml of the selective receptor B antagonist of Endothelin BR-788 (Enzo life science, U.K.) for 1 hour prior to undergoing flow based adhesion assay with isolated CD8+ T-cells from HFE blood. Images were taken with a phase contrast microscope at x20 magnification. Images were captured using DVD recorder and assessed off-line. Graph B represents mean and SEM adhesion of cells/$mm^2/10^6$ cells perfused. Graph C represents the % of the adherent CD8+ T-cells that were observed rolling at low velocity over the EC surface. Data are derived from multiple replicate fields of view in 3 independent experiments. Statistical analysis was performed using ANOVA where $p<0.05$ was considered significant.

Results summary:

- Higher expression of αSMA by TAFB is found in tumours that comprise of fewer TILs.
- Normal and tumour fibroblast supernatant does not significantly change the phenotype of NEC.
- Tumour fibroblasts supernatant may suppress ICAM-1, but not MAdCAM-1 or VCAM-1 expression in TEC.
- Generally, adhesion of CD8+ T lymphocytes was augmented in NEC but reduced in TEC by normal and tumour fibroblasts.
- The chemokine, Il-6, is produced by tumour fibroblasts and is more abundant in tumour stroma.
- Despite no observed modulation in adhesion molecule expression, IL-6 promotes increased TEC adhesion to CD8+ T cell lymphocytes.
- The protein, Endothelin-1 is expressed more abundantly by tumour fibroblasts and its receptor, Endothelin receptor B, is expressed by tumour endothelium.
- Inhibiting the ET1/ETb axis augments ICAM-1 expression by TEC and increases TEC adhesion to CD8+T lymphocytes.

5.3 Discussion

The aim of this chapter was to explore how the cells within tumour stroma might influence adhesion of CD8+ T-lymphocytes to tumour endothelium. Previously I have shown that although higher numbers of CD8+ T-cells are found in CRC than NC, there are 2 clear subgroups of CRC specimens where some tumours contain high numbers of active stromal CD8+ T-cells or TIL, and some contain very few TIL. These tumours with few, inactive CD8+ T lymphocytes are often termed "non-immunogenic" in the literature (190, 236, 237) and are able to employ immune escape mechanisms. Thus in this chapter, I began by considering whether activated αSMA+ fibroblasts, otherwise known as tumour associated fibroblasts (TAFB), influence the CD8+ TIL density in a tumour by regulating recruitment by tumour endothelium.

5.3.1 αSMA expression by TAFB corresponds with fewer TIL in CRC.

By using immunohistochemistry, I could assess the percentage of αSMA expression and CD8+ T cell abundance in several different CRC samples. Mean αSMA expression varied from 5% to 30% in different samples and this variation was independent of standard histopathological staging but showed a significant inverse correlation with CD8+ TIL abundance. Data produced by Galon *et al* (2) illustrated that TIL abundance is independent of, and also a more accurate prognostic indicator of patient survival than standard histopathological staging of CRC. The correlation between αSMA expressing TAFB and CD8+ TIL abundance suggests that there may be causative link between TAFB and CD8+T cells within the tumour stroma. It is important to understand that the presence of CD8+ T cells does not imply the presence of activated CTLs as Granzyme-B production was not assessed. It is possible that cytokines such as IL-1 and IL-6 produced by tumour fibroblasts directly, or indirectly via myeloid derived suppressor cells

(MDSC), T-regs, or TH17 T helper cells, suppress activation of CD8+ T lymphocytes (238). Nevertheless, tumour fibroblasts could also contribute to fewer tumour infiltrating CD8+ T lymphocytes by triggering accelerated programmed cell death, death via FAS ligands, or even reducing recruitment by the tumour endothelium via regulating adhesion molecule expression. My data shows that TAFB supernatant did not affect adhesion molecule expression by NEC, but did suppress ICAM-1 in TEC. There was no observed change in MAdCAM-1 or VCAM-1 expression. This response has been supported by other studies using ECs derived from renal cell carcinoma or HUVEC which show a reduction in ICAM-1 surface expression when stimulated by TNF- α (239), basic fibroblast growth factor (βFGF) (95) or VEGF (215), all growth factors known to be produced by TAFB (229, 240, 241). Considering this data, we were surprised to observe no significant reduction of CD8+ T lymphocyte adhesion by TEC conditioned with tumour supernatant. However, significantly reduced adhesion was observed between TEC to NEC after TAFB supernatant conditioning, suggesting that regulation of CD8+ T lymphocyte adhesion may be tumour endothelial cell specific i.e. via binding of receptors specifically expressed or up-regulated by tumour endothelium. Data shown in Chapter 3 of this thesis indicate that receptors for adhesion molecule suppressing factors (for example, VEGFR-2) are expressed at lower levels in NEC, which may explain why TAFB can suppress ICAM-1 expression in TEC but not NEC.

When examining the effects of tumour fibroblast supernatant on matched TEC on an individual patient level both suppression and increased adhesion was observed. This data highlights that a larger cohort of patients and sub-group analysis based on the number of tumour infiltrating lymphocytes would be helpful to investigate tumour fibroblast and TEC effect on CD8+ T lymphocyte adhesion. It is conceivable, in-keeping with the concept supporting stratification of CRC into immunogenic and non-immunogenic tumour groups, that in patients with few TIL, the TAFB suppress the TEC adhesion and vice versa.

Stratification of patients based on the tumour mis-match repair (MMR) status, and thus abundance of TILs, has been performed in phase II human trials investigating the effects of anti-PD-1 blockade on intra-tumoural T cells. The authors observed improved immune-related response rate and progression free survival in patients with MMR deficient tumours compared to MMR proficient tumours (242). The modality of this immunologic relies on a high number of tumour infiltrating lymphocytes and therefore highlights the importance of targeting the tumour endothelium to increase recruitment of CD8+ T lymphocytes.
In light of this, I further investigated the composition of TAFB supernatants.

5.3.2 IL-6 is produced differentially by fibroblasts from tumour and normal colon and how this may affect the tumour microenvironment.

Data does exist to suggest that TAFB contribute to the tumour immune escape by producing the chemokine CCL12 to suppress anti-tumour responses (243). Suppressive or regulatory cell types such as M2 tumour associated macrophages, neutrophils, myeloid derived suppressor cells and T-regs are the predominant cell types found where TAFB are abundant (244). A pre-clinical study performed in murine breast cancer models shows that by eliminating the TAFB or "carcinoma associated fibroblasts" (CAF) from the tumour stroma using a vaccine targeting fibroblast activation protein, there was a shift in polarity of immune-environment from Th2 to Th1 resulting in significantly more intra-tumoural CD8+ T lymphocytes (245). Eliminating the tumour fibroblasts was linked with lower concentrations of intra-tumoural IL-4 and IL-6 and higher concentrations of IL2 and IL-7.

My data suggests that TAFB are a more abundant source of Il-6 than NFB. IL-6 has been reported to be critical in tumour progression in CRC, produced predominantly by cancer associated fibroblasts, promoting tumour angiogenesis and maintaining crosstalk

between tumour cells and fibroblasts (246). Despite no significant changes to the membranous adhesion molecule phenotype, ICAM-1 expression tended to increase with IL-6 treatment. Furthermore, a significant increase was observed in CD8+ T-cell adhesion under static and flow conditions to IL-6 stimulated TEC but not NEC. The reduced lymphocyte adhesion observed after blocking Il-6 receptors in TAFB supernatant conditioned TEC, implies IL-6 up-regulates adhesion molecule expression in TEC preferentially. Il-6 has been described to increase membrane ICAM-1, VCAM-1 and E-selectin on HUVEC facilitating increased CD4+ lymphocyte binding under static conditions (247). In addition, in inflammatory conditions such as rheumatoid arthritis, soluble factors produced by synovial fibroblasts, such as IL-6, increase lymphocyte recruitment by HUVEC (233).

The tumour specific ability of IL-6 to augment CTL adhesion to tumour endothelium and leave NEC unaffected provides an attractive potential to target IL-6 as a therapeutic target. Tumour specific qualities of IL-6 have been previously reported in murine models (248), increasing CD8+ T lymphocyte trafficking by up-regulating the expression of IL-6 subunit receptor, gp130, by tumour vessels using thermal therapy. However, elevated levels of soluble IL-6 in the serum of patients with CRC is linked to a poor prognosis (249) and elevated IL-6 mRNA expression in CRC tissue corresponds with a higher risk of CRC recurrence (250). IL-6 has been shown to promote invasion of tumour cells in CRC (251) which in turn initiates a positive feedback loop of IL-6 production by immune populations. Other tumour-promoting effects of IL-6 may include tumour associated macrophage differentiation towards the M2 polarity by inhibiting caspase-8 cleavage (252), recruitment of suppressive T-regs into the tumour stroma and contributing towards metastatic progression. This changes the focus of IL-6 and complicates its use as a

therapeutic target. It is interesting to consider whether high levels of IL-6 are produced by all TAFB, which would contradict the hypothesis that TAFB suppress CD8+ T lymphocyte adhesion as our data suggests otherwise and is supported by current data (248, 253, 254). It may be possible that relatively low levels of IL-6 are produced by TAFB from CRC that are more active at evading the hosts immune system and this could be addressed by stratification of samples by TIL subtypes and correlation with stromal IL-6 concentration.

5.3.3 Endothelin-1 (ET1) preferentially produced by tumour fibroblasts bind with endothelin receptor B (ET_B), inhibits ICAM-1 expression and reduces lymphocyte adhesion by TEC.

Endothelin-1 (ET1) is a potent peptide ligand of the endothelin system which consists of 4 ligands (endothelin 1-4), two receptors (endothelin receptor A and B), and endothelin converting enzymes. ET-1 is produced by stromal cells, notably endothelial cells where is can bind with endothelial membrane bound ET_A and $_B$. Downstream signaling causes potent vasoconstrictor affects and so therapeutics targeting this mechanism have, to date, been aimed towards anti-hypertensives (255, 256).

Endothelin-1 (ET1) expression in tumour stroma and ET_A and ET_B expression has been demonstrated in skin, small cell lung, breast, colorectal and oral cancers (257, 258, 259, 260). High levels of ET1 and receptors ET_A and ET_B, based on semi-quantitative analysis of IHC, correlate with a poor prognosis and shorter patient survival (261, 262, 263). My data reveals an increase in Endothelin-1 gene expression by whole CRC tissue and significantly elevated levels of ET1 in soluble protein form in the supernatant from TAFB compared to NFB supernatant. Although increased levels of ET1 are described in stroma and whole tumour tissue, there is no published evidence to date that stromal fibroblasts in tumours produce ET1.

Interestingly, in ovarian cancer models the gene for selective receptor ET_B is preferentially expressed by tumour endothelium of ovarian tumours that bear low numbers of TIL compared to ovarian tumours with high numbers of TIL. By inhibiting tumour endothelial expressed ET_B receptor, Buckanovich *et al.,* were able to augment EC membrane bound ICAM-1 and subsequently increase CD8+ T lymphocyte adhesion on HUVEC cell lines and recruitment into murine models (97). Few studies investigate the ET1 up-regulation in CRC stroma, however, there is evidence by immunohistochemical methods and whole patient tissue homogenates that support increased ET1 in CRC stroma (263). My data reveals that Endothelin-1 is present in whole CRC tissue and in the supernatant from TAFB at significantly higher levels than from NC and NFB supernatant respectively. Additionally, my data suggests higher expression of Endothelin receptor B (ET_B), one of the G-protein coupled receptors for ET1, by TEC compared to NEC. Furthermore, simulating the tumour microenvironment by conditioning TEC with TAFB supernatant, significantly increased ET_B expression by TEC was observed. Inhibition of the ET1/ ET_B axis has shown increased ICAM-1 expression via reducing nitrous oxide synthesis in HUVEC and murine ovarian cancer models, but is not yet described in primary cell lines or CRC. To see if this happened in primary colorectal tumour endothelial cells, I used an ET_B specific antagonist, BQ-788 to block the ET1/ ET_B axis. I found that in primary CRC TEC, but not NEC, membrane expression of ICAM-1 increases. In keeping with the phenotypic change, I was able to increase CD8+ T-lymphocyte adhesion in TEC under static and flow conditions.

BQ-788 has been used in several cardiovascular human trials safely (264)(265) which supports potential use as a therapeutic target in CRC patients. Recently, a proof of concept study was published using BQ-788 as an intra-lesional therapy for malignant melanoma (266). They reported no adverse effects in patients who received BQ-788. Furthermore, although their study was small, using immunohistochemistry after treatment, the authors found more blood vessels and lymphocytes, in BQ-788 treated tumors. Although studies to date have investigated ET-1 and its receptors in tumours including CRC, the focus has been on ET_A owing to the downstream events of binding, that contribute to tumour growth. Blockade of ET-1 showed some inhibition of cancer cell and CAF/TAFB proliferation in CRC (259) via the mitogen activated protein kinases (MAPK) pathway or via β-catenin (267). In addition, one study shows relative down regulation of ET_B despite up regulation of ET-1 and ET_A within 9 CRC specimen (268) and others suggest that ET_B and ET_A would have an augmented anti-tumour effect (269). In the literature to date, there is only one study that analyses the expression of ET-1, ET_A and ET_B in sub divided tumours based in the number of tumour infiltrating lymphocytes (97). Although tumour regression was seen in murine ovarian cancer models, patient survival data is not available. In CRC specifically, my data suggests that in some CRCs, blockade of endothelial cell ET_B can increase adhesion to CD8+CTLs.

This chapter presents novel data supporting the role of stromal fibroblasts in regulating the tumour endothelium to evade the host anti-tumour immune response. My data suggests that in CRC the numbers of TAFB are inversely related to TIL CD8+ T-lymphocytes and that the supernatant derived from CRC TAFB can have a suppressive effect on the adhesion profile of primary human CRC TEC by producing soluble factors such as Endothelin-1. Furthermore, this suppressive affect may be overcome by inhibition of endothelial ET_B resulting in augmented CD8+ T-cell adhesion using a novel *in vitro*

primary human CRC TEC model under static and shear forces. My data supports the importance of further study into commercially available ET_B receptor inhibitor BQ-788 to therapeutically improve adhesion and recruitment of CD8+ T-lymphocytes in tumours that evade an immune response.

CHAPTER 6

General discussion

6.1 Summary of key findings

To investigate the tumour vasculature in colorectal cancer, it was essential that I develop a reliable *in-vitro* tumour endothelium culture model derived from human colorectal cancer tissue. Furthermore, it was essential that the *in vitro* model was based upon human primary cells for several reasons. Firstly, there is good evidence that rodent tumour models do not fully recreate the histological patterns of human disease or responses to treatment (270, 271). There is also well documented evidence that murine immune cell function, and some factors governing recruitment and angiogenesis (272, 273) are different to those of human species.

Furthermore, by using samples derived from human primary tumours I have been able to study samples from patients with tumours that evade an immune response and those that don't. Thus, my data may be more representative of typical patient cohorts than studies using cell lines. More importantly, the tumour microenvironment helps regulates endothelial cell phenotype and such interactions may be tumour specific. Therefore, by using matched tumour fibroblasts to condition the primary endothelium I have developed a model system that is more representative of the situation *in vivo* and this could not be achieved using cell lines.

By modifying existing in-house protocols for non-tumour endothelial cell isolation, and learning from a published protocol for human tumour endothelial cell isolation (136) and one which reported some success with human primary tumour

endothelial cell culture (60), I have produced a reproducible protocol for the long-term culture of human colorectal tumour endothelial cells.

I have confirmed the vascular endothelial phenotype of my primary cells. The data presented in Chapter 3 confirms this by revealing basal CD31, vWF and VE-Cadherin positivity and up-regulation of VCAM-1 and ICAM-1 in response to TNFα and IL-1β which is consistent with available published data (60). Our gene and protein expression analyses confirmed that my cells express characteristic profiles of adhesion molecules and inflammatory markers but importantly confirmed that subgroups of genes involved in angiogenesis (e.g. VEGFR-1, eNOS) and inflammation (E-Selectin, VCAM-1, IL-6) were expressed to a higher level on the tumour-derived endothelium.

We also report expression of the tumour specific endothelial marker, TEM-8, which is preferentially expressed by colorectal TEC compared to NEC, in agreement with other studies (44, 4). I also present novel data showing maintained expression of TEM-8 throughout long-term culture of cancer endothelial cells. This is in contrast with expression of CD13 which has raised interest because of reports of increased expression in angiogenic tissue such as tumours (274, 275). Interestingly I found little tumour specificity of CD13 expression in TEC derived from CRC using antibody WM15 but inhibition of CD13 WM15 epitope slowed migration or proliferation of metastatic endothelial cells.

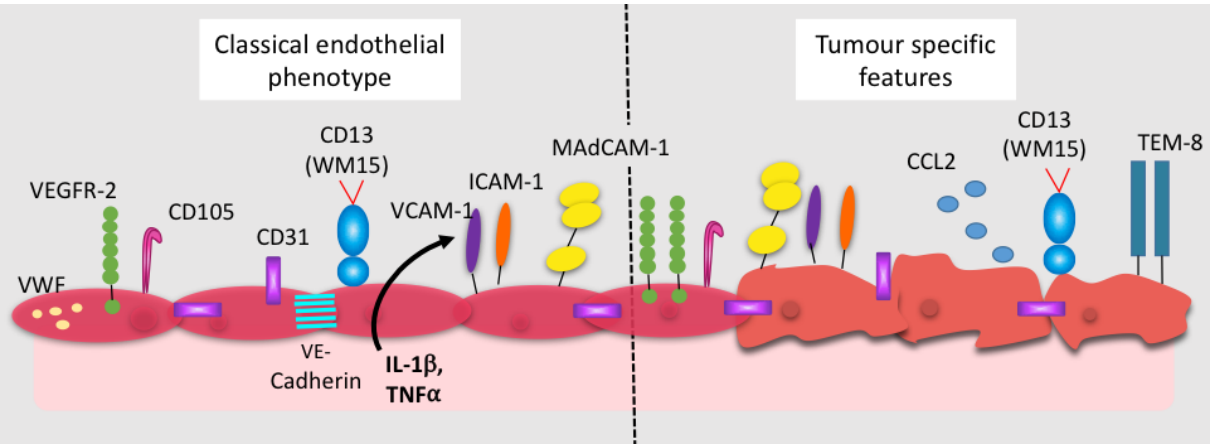

Figure 6.1: The endothelial phenotype of NEC and TEC derived from CRC.
This schematic represents the phenotype that was identified as a result of the investigation in this thesis. On the left of the diagram, the classic phenotype of EC isolated from NC, is displayed. EC express basal CD31 VWF, CD105, VE-Cadherin, low levels of VEGFR-2, MAdCAM-1 and CD13 (WM15). ICAM-1 and VCAM-1 were upregulated with IL-1β and TNFα. The tumour specific phenotypic characteristics include basal CD31, CD105, VEGFR-2, CD13 (WM15), MAdCAM-1 and ICAM-1 and VCAM-1 were upregulated with IL-1β and TNFα. TEM-8 was expressed by TEC through long term culture. CCL2 is preferentially produced by TEC compared to NEC. Image is authors own.

In chapter 4, I presented data describing variation in tumour infiltrating CD8+ T-lymphocyte numbers between colorectal cancers specimens. This is strongly supported by current literature linking high numbers of CD8+T-cell in tumours to improved patient prognosis, data which is key to the reasoning behind current therapies that target anti CD8 checkpoint blockade mechanisms. I was able to link CD8+ T-cell numbers with percentage CD31 expression which suggests tumours with high levels of CD8+ T-cells may also have an increased vessel density. Although adhesion molecule expression did not differ between *in vitro* TEC and NEC we did find that *in vivo* CRC vessels show less intense ICAM-1 expression and fewer vessels in CRC express MAdCAM-1. Despite this CD8+ T cell were still more adherent to tumour endothelium in CRC and *in vitro* TEC and inhibition of the key adhesion molecules investigated, resulted in reduced CD8+ T cell adhesion to NC and CRC. We found that

the chemokine CCL2 was produced in higher concentrations by TEC than NEC which may act as a chemoattractant. Certainly, Inhibition of CCL2 and pertussis toxin-sensitive receptors in addition to ICAM-1, VCAM-1, MAdCAM-1 receptors resulted in reduced CD8+ T cell adhesion to NEC and TEC.

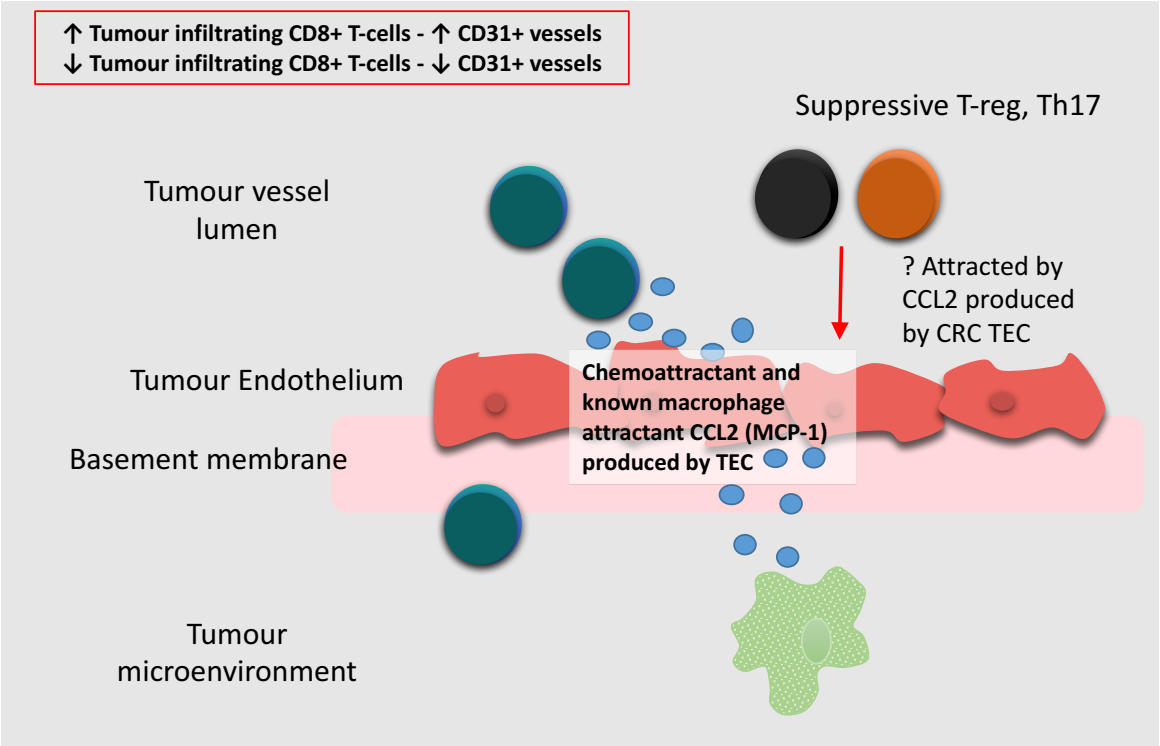

Figure 6.2: TEC preferentially produce chemoattractant CCL2 compared to NEC but may be stratified per tumour infiltrating CD8+ T-lymphocytes.
This schematic illustrates TEC producing CCL2, a known monocyte chemoattractant protein (also known as MCP-1), which aids CD8+ T-lymphocyte attraction and adhesion to TEC. These may not be CD8+ T-cell specific and it is possible that suppressive T-cell populations and macrophages are also attracted to the tumour microenvironment by CCL2. Image is authors own.

In chapter 5 the tumour microenvironment was explored for effects on the recruitment abilities of TEC. Specifically more αSMA tumour associated fibroblasts were identified in tumours containing fewer tumour infiltrating CD8+ T-cells. Interestingly, the supernatant from neither NFB nor TAFB did not significantly alter the phenotype of NEC which suggests the difference in NEC/TEC phenotype is, to some extent independent of protein signalling in the tumour microenvironment. However, TAFB supernatant was found to suppress ICAM-1 in some cases can also reduce CD8+ T-cell adhesion to TEC compared to TEC alone. This led to analyzing the differing constituents of normal and tumour fibroblast supernatant. IL-6 and Endothelin-1 were expressed in greater concentrations by TAFB. IL-6 actually increased CD8+ T-cell adhesion. The pro-tumour effects via STAT3 of IL-6 are well described (276, 277) however data also support increased lymphocyte trafficking in the presence of IL-6 (277, 248).

Recombinant Endothelin-1 suppressed ICAM-1 expression and CD8+ T-cell adhesion under static and flow conditions. Furthermore, inhibition of Endothelin Receptor B, which was up-regulated on TEC, and blocking the ET-1/ETb axis, ICAM-1 expression was recovered and CD8+ T-cell adhesion under static and flow conditions was augmented. Suggested mechanisms of Endothelin-1 contributing to TIL density are outlined in Figure 6.3. There is no similar data in the literature, however, in murine and ovarian cancer cell lines, Endothelin-1 suppressed tumour endothelial ICAM-1 expression in tumours with low numbers of TIL (97).

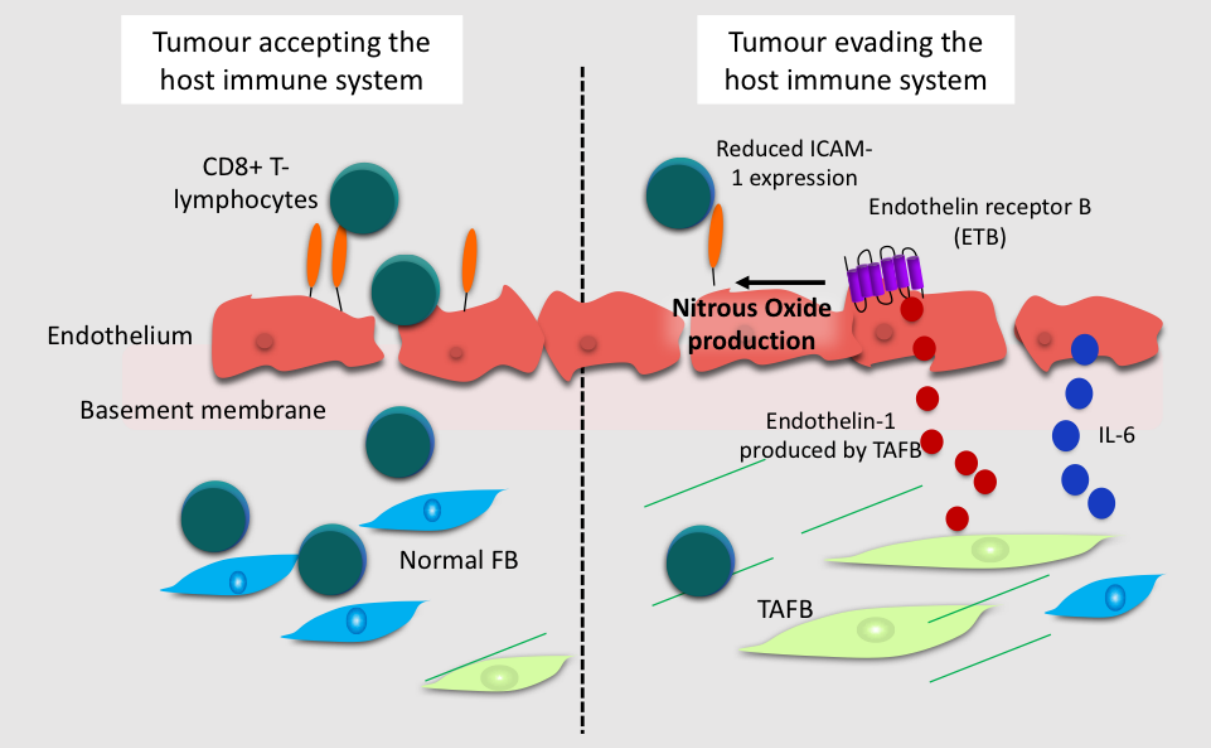

Figure 6.3: Suggested mechanisms by which tumour associated fibroblasts regulate tumour endothelial adhesion of CD8+ T-lymphocytes.

The schematic represents tumours with low numbers of TAFB (on the left) in which there are higher numbers of tumour infiltrating CD8+ T-lymphocytes as the adhesion profile of the tumour endothelium has not been regulated and ICAM-1 expression is not suppressed. Overproduction of Endothelin-1 by TAFB, which are found within CRC tumours that actively evade the hosts anti tumour immune response (represented by the right hand side) binds to Endothelin Receptor B reducing tumour endothelial ICAM-1 expression via nitrous oxide synthase. Image is authors own.

6.2 Significance of my findings

Developing a reliable *in vitro* TEC model has provided an opportunity to investigate recruitment, angiogenic, migratory and proliferative behaviours of tumour endothelium. In this thesis, TEM-8 has facilitated validation of the tumour specific phenotype of TEC *in vitro* model. To date, TEM-8 has been used as a target for anti-tumour vaccines based on tumour specificity in HCC cell lines in murine models and shown success. The efficacy of TEM-8 targeted vaccines in colorectal mouse models or human cancer trials has not yet been explored. My data illustrates that TEM-8 is specific in human colorectal cancer and supports further investigation of TEM-8 targeted vaccines in human colorectal cancer and the use of TEM-8 as a tumour marker to aid cancer detection by positron emission tomography (PET) scanning (278).

Other biomarkers explored in this thesis include CD13 which has raised interest because of increased expression in angiogenic tissue. My data show that there was little tumour specificity of CD13 (WM15) expression in TEC derived from CRC and CD13 expression was also identified in NEC. This may be explained by glycosylation differences that exist resulting in at least 5 CD13 sub-populations (279). It is possible that the WM15 monoclonal antibody used in our studies did recognize other sub-types of the molecule and more tumour specific motifs exist (280). The CD13 ligand, NGR, tagged with nanogold particles, to deliver anti-tumour cytokine tumour necrosis factor (TNF) is currently being investigated (281). CD13 has many functions in angiogenesis, cell motility, cell adhesion, and promoting tumour invasion, owing to signalling and enzymatic mechanism (282).

My data suggests that chemical inhibition of CD13 (WM15) using Bestatin slowed CRLMEC migration or proliferation of colorectal metastatic endothelial cells which is supported by *in vitro* studies using fibrosarcoma cell lines (283). Mechanisms by which CD13 can contribute to increased cell motility, which is key for tumour invasion (284) include increased bradykinin activated filopodia formation and protease enzymatic activity (285). These data are further supported by trial data in which CD13 inhibition by Bestatin improved patient survival with squamous cell carcinoma, but not adenocarcinoma of the lung (286, 54) *In vitro* primary colorectal TEC and metastatic EC are useful tools to understand these complex cellular functions in the context of colorectal cancer further, in particular how the tumour microenvironment regulates intra and extracellular expression of CD13 and how CD13 may contribute to lymphocyte adhesion.

Chapter 4 identified CCL2/MCP-1 as preferentially produced by colorectal TEC displaying chemotactic and T-lymphocyte adhesion properties to TEC. Solid tumours such as hepatocellular carcinoma and breast cancer produce CCL2 (224, 287) and the role of CCL2 in tumour progression has been explored. The anti-tumour effects of CCL2 include stimulation of monocytes (288), increasing CD8+ T-lymphocyte recruitment to tumours (289) and improved tumour antigen presentation (290). However, CCL2 also promotes tumour growth by enhancing angiogenesis and promoting M2 TAMs (291), and facilitating tumour cell invasion and extravasation (292). CCL2 is, in particular, implicated in progression of lung metastases (293, 294). Carlumab, an *in vitro* CCL2 specific monoclonal antibody, has undergone a phase II trial in metastatic prostate cancer but with no observed anti-tumour activity (295). Furthermore, one study suggests that actual cessation of CCL2 inhibition in breast cancer could lead to a spurt in metastases formation via IL-6 and VEGFR-2 driven

tumour angiogenesis (297) and another study of CCL2-/- mice suggests that CCL2 inhibition may be efficacious in regression of established tumours but complete inhibition of CCL2/CCR2 may suppress the hosts immune response to metastases development (225).

Data presented in chapter 5 illustrates preferential IL-6 production by TAFB. Despite the overall effects of TAFB conditioning of TEC in suppressing ICAM-1 expression, IL-6 within the tumour microenvironment enhances CD8+ T-lymphocyte adhesion to tumour endothelium. These conflicting findings suggest that the microenvironment comprises a balance of anti and pro-inflammatory mediators. Our data highlights the pro-inflammatory, and potentially beneficial, anti-cancer functions of IL-6 which is also supported in the literature (298, 253, 299, 248). In clinical trials in the 1990's IL-6 was trialed as a therapeutic for renal cell carcinoma with no reported toxicity but with no anti-tumour effects (300). Subsequent trials have focused on inhibiting IL-6 using monoclonal antibodies in multiple myeloma patients again with no conclusive anti-tumour effects (301). Siltuximab, an anti-IL-6 monoclonal antibody, has undergone a phase I trial in ovarian cancer patients showing IL-6 inhibition, reduced angiogenesis and macrophage infiltration (302). Complete inhibition may reduce angiogenesis and macrophage infiltration but it may also compromise the host's anti-tumour immune response.

αSMA expressing TAFB found in the stroma of CRC are potentially able to regulate the immune profile of tumours and employ immune escape by producing soluble Endothelin-1. Data in chapter 5 shows TAFB from CRC produce more Endothelin-1 and is described in a study using ovarian cancer patients and cell lines (97). Additionally, ET_B, an Endothelin-1 receptor is preferentially expressed by TEC and up-regulated by conditioning TEC with CRC TAFB supernatant. The relevance of this

lies in the downstream effects of ET1-ET_B axis in which binding of ET1 to ET_B causes nitric oxide synthase production resulting in nitric oxide (303) and consequently down regulates endothelial cell ICAM-1 expression (304, 305). By inhibiting this complex, as shown in static and flow assays, adhesion of CD8+ T lymphocytes to tumour endothelium was amplified. Based on my data and supporting evidence in other cancer types, inhibition of ET1/ETb binding using a specific monoclonal antibody is an attractive potential anti-cancer therapy in CRC.

6.3 Limitation of this work

The value of primary cell cultures is well described. However, there are practical limitations. Reliably reproducible long-term cultures require months of work and a relatively low yield of successful cultures from several samples. Maintenance of EC cultures requires input 7 days a week and as such is labour intensive. Using cell lines could mitigate time lost for protocol development and reduce the work load however the resultant data may fall short of accurate *in vivo* representation. The time taken to establish our in vitro model is comparable to murine models and compare favourably in terms of financial expenses, which results only from cell culture medium and consumables. The resultant cell yields were often sufficient to obtain both pre and post-culture phenotyping and analysis of gene expression from the same sample. In the original experimental design, however, pre and post-culture phenotyping and gene expression data in addition to functional adhesional data by EC from the same sample was preferred. Theoretically, this would allow linear comparison of cell adhesion molecule profile and functional adhesion properties for each sample. Unfortunately, this was not possible with the resultant cell yields.

Within endothelial cultures, a typical cobblestone appearance of clusters was always identified. However, subjectively, after analyzing the cell morphology over the course of the thesis, I noticed pleomorphism in nuclear size and shape. In addition, overall cell shape could vary within endothelial cells isolated from the same specimen at the same time and maintained in the same conditions. The significance of this feature is unknown. Pleomorphism is a morphological characteristic frequently seen in primary and metastatic malignant cells and reactive inflammatory cells but not usually resting benign cells. The changes may perhaps represent reactive changes or represent structural, phenotypic and genotypic changes occurring in the tumour endothelium.

The most accessible technique for investigating functional adhesion of CD8 T cells to either NEC or TEC, was by static adhesion assay. This provided some insight into the endothelial-lymphocyte interactions. The disorganised and often static flow of blood described in tumours (3) suggests that actually, although purported as a crude measurement of adhesional function, may represent intra tumoural blood flow more accurately. Conversely, static adhesion studies are unlikely to accurately reflect the blood flow in normal colon. This highlights the importance of identifying the most representative flow rates that can replicate the physiological flows to use when comparing normal and tumour endothelium. There are no data currently surrounding this. Our adhesion assays used blood from patients with haemachromatosis and not matched patient blood or even unmatched blood from other patients with colorectal cancer. HFE blood is unlikely to be enriched in CD8+ T-lymphocytes.

6.4 Further work

Addressing existing limitations of the studies

To address the issue of significant inter-specimen heterogeneity, inevitable with primary samples, I aim to continue TEC phenotyping to provide larger cohort numbers. By utilizing dual immunofluorescence, positive staining with adhesion markers, angiogenic factors or tumour specific markers can be compared directly to CD31 staining. Collating all the endothelial cell phenotype data with abundance of CD8+ CTL in the tumour stroma, conventional histological staging and crucially 5-year survival data would be interesting in light of data that significantly links tumours with high numbers of tumour infiltrating CD8+CTLs (2, 102).

Investigation the monocyte recruitment abilities of CD13 (WM15) could reveal anti-tumour effects as could further exploration of the anti-migratory and anti-proliferative effects of CD13 (WM15) Other CD13 epitopes for enhanced tumour specificity could be further investigated for targeting vaccines or directing PET scan imaging.

Future assays developed from TEC model

I would aim to utilize the TEC *in vitro* model to explore the recruitment of specific subsets of immune cells to identify if $ET1/ET_B$ axis blockade would facilitate increased adhesion of CD4+ memory cells and pro-tumour TAMs, TH17 cells, T-Regs with the aim to identify a CD8+ T lymphocyte specific mechanism that could be preferentially exploited.

Given the data produced by supernatant conditioning of the TEC *in vitro* model by fibroblast supernatant, co-culturing TEC with matched cultured primary fibroblasts and tumour cells using fenestrated inserts, or development of an *in vitro* CRC 3D

tumour model is possible. Co-culturing of primary cells from the tumour stroma and matched primary cancer cells could provide additional insight into how the tumour microenvironment governs the its immune profile.

Furthermore, to answer the question "does increasing the recruitment of CD8+ T lymphocytes into the stroma across tumour endothelium increase the density of CD8+ T-cells and therefore improve patient outcomes?" which would require investigation of the fate of CD8+Tcells after transmigration through TEC in the presence of TAFB compared to NFB using the TEC model.

Future work towards therapeutic aim

The two key areas highlighted by this thesis for potential therapeutic aim include; the use of TEM-8 as a tumour specific anti-tumour vaccine in colorectal cancer; and the use of ET1/ET_B axis blockade with the aim to increase numbers of tumour infiltrating CD8+ T-cells. Human primary 3D tumour models may provide useful to investigate the delivery of TEM-8 labelled anti-tumour vaccines as opposed to using murine models.

To further investigate the therapeutic potential of ET1/ET_B inhibition requires investigation of whether up-regulating ICAM-1 expression indiscriminately by the endothelium of colorectal tumours causes an increased risk of inflammatory disorders such as colitis. These questions could be addressed by using murine models and early phase 1 and II trials. Before trialing ET1/ET_B blockade, consideration should be made as to whether more benefit would be achieved by selecting patients based upon the number of TILs, whereby patients whose tumours are found to have "low" numbers of TILs are specifically recruited. Should ET_B inhibition prove successful, there would also be implications of how the biopsy diagnosis was made and if based on conventional

TNM staging histology would require additional CD8+ IHC and additional histopathology review.

6.5 Conclusion

This thesis has demonstrated successful development of a validated *in vitro* TEC model for CRC and has revealed novel data of a tumour specific phenotype by expressing TEM-8. CD13 (WM15) was found to not be specific to CRC TEC, although more tumour specific subtypes are reported to exist (282). CCL2 produced by CRC TEC and IL-6 preferentially expressed by CRC tumour fibroblasts are both a CD8+ T-lymphocyte towards TEC, however, both of these cytokines have pro and anti-tumour effects that complicate complete inhibition in clinical anti-cancer studies (225, 299). Endothelin-1 is also preferentially produced by CRC TAFB and the receptor ET_B is upregulated on tumour endothelium. Inhibition of $ET1/ET_B$ binding augmented TEC ICAM-1 expression and facilitated increased recruitment of CD8+ T-lymphocytes into the tumour stroma. $ET1/ET_B$ inhibition has shown promise in *in vitro* ovarian cancer studies (97) and commands further investigation with the aim of developing an anti-cancer therapy in CRC.

REFERENCES

1. Office for National Statistics. Cancer incidence and Mortality in the United Kingdom 2008-2010. http://www.ons.gov.uk/ons/dcp171778_289890.pdf

2. Galon J, Costes A, Sanchez-Cabo F, Kirilovsky A, Mlecnik B, Lagorce-Pagès C, et al. Type, Density, and Location of Immune Cells Within Human Colorectal Tumors Predict Clinical Outcome. Science. 2006 Sep 29;313(5795):1960–4.

3. Dudley AC. Tumor endothelial cells. Cold Spring Harb Perspect Med. 2012 Mar;2(3):a006536.

4. Rmali KA, Puntis MCA, Jiang WG. Tumour-associated angiogenesis in human colorectal cancer. Colorectal Dis. 2007 Jan 1;9(1):3–14.

5. Hurwitz H, Fehrenbacher L, Novotny W, Cartwright T, Hainsworth J, Heim W, et al. Bevacizumab plus Irinotecan, Fluorouracil, and Leucovorin for Metastatic Colorectal Cancer. N Engl J Med. 2004 Jun 3;350(23):2335–42.

6. Ferrara N, Hillan KJ, Novotny W. Bevacizumab (Avastin), a humanized anti-VEGF monoclonal antibody for cancer therapy. Biochem Biophys Res Commun. 2005 Jul 29;333(2):328–35.

7. Polakis P. The adenomatous polyposis coli (APC) tumor suppressor. Biochim Biophys Acta BBA - Rev Cancer. 1997 Jun 7;1332(3):F127–47.

8. Leslie A, Carey FA, Pratt NR, Steele RJC. The colorectal adenoma-carcinoma sequence. Br J Surg. 2002 Jul;89(7):845–60.

9. Burmer GC, Loeb LA. Mutations in the KRAS2 oncogene during progressive stages of human colon carcinoma. Proc Natl Acad Sci U S A. 1989 Apr;86(7):2403–7.

10. Robinson MJ, Cobb MH. Mitogen-activated protein kinase pathways. Curr Opin Cell Biol. 1997 Apr;9(2):180–6.

11. Patai ÁV, Molnár B, Tulassay Z, Sipos F. Serrated pathway: Alternative route to colorectal cancer. World J Gastroenterol WJG. 2013 Feb 7;19(5):607–15.

12. Bettington M, Walker N, Clouston A, Brown I, Leggett B, Whitehall V. The serrated pathway to colorectal carcinoma: current concepts and challenges. Histopathology. 2013 Feb 1;62(3):367–86.

13. Fleming M, Ravula S, Tatishchev SF, Wang HL. Colorectal carcinoma: Pathologic aspects. J Gastrointest Oncol. 2012 Sep;3(3):153–73.

14. Stephenson TJ, Cross SS, Chetty R. Standards and datasets for reporting cancers, 2012. http://www.rcpath.org/NR/rdonlyres/047C7409-1755-4529-8720-E5F3940801A0/0/G098_Thyroid_Dataset_Feb14.pdf

15. National Institute for Health and Care Excellence. The diagnosis and management of colorectal cancer, December 2014. https://www.nice.org.uk/guidance/cg131/resources/guidance-colorectal-cancer-pdf

16. Benson AB, Bekaii-Saab T, Chan E, Chen Y-J, Choti MA, Cooper HS, et al. Metastatic Colon Cancer, Version 3.2013 Featured Updates to the NCCN Guidelines. J Natl Compr Canc Netw. 2013 Feb 1;11(2):141–52.

17. Aird WC. Phenotypic Heterogeneity of the Endothelium: I. Structure, Function, and Mechanisms. Circ Res. 2007 Feb 2;100(2):158–73.

18. Carson-Walter EB, Watkins DN, Nanda A, Vogelstein B, Kinzler KW, St Croix B. Cell surface tumor endothelial markers are conserved in mice and humans. Cancer Res. 2001 Sep 15;61(18):6649–55.

19. Couty J-P, Rampon C, Leveque M, Laran-Chich M-P, Bourdoulous S, Greenwood J, et al. PECAM-1 engagement counteracts ICAM-1-induced signaling in brain vascular endothelial cells. J Neurochem. 2007 Oct;103(2):793–801.

20. Lalor PF, Lai WK, Curbishley SM, Shetty S, Adams DH. Human hepatic sinusoidal endothelial cells can be distinguished by expression of phenotypic markers related to their specialised functions in vivo. World J Gastroenterol WJG. 2006 Sep 14;12(34):5429–39.

21. Konerding MA, Fait E, Gaumann A. 3D microvascular architecture of pre-cancerous lesions and invasive carcinomas of the colon. Br J Cancer. 2001 May 18;84(10):1354–62.

22. Skinner SA, Frydman GM, O'Brien PE. Microvascular structure of benign and malignant tumors of the colon in humans. Dig Dis Sci. 1995 Feb;40(2):373–84.

23. Seguin J, Doan B-T, Latorre Ossa H, Lauriane, Gennisson J-L, et al. Evaluation of Nonradiative Clinical Imaging Techniques for the Longitudinal Assessment of Tumour Growth in Murine CT26 Colon Carcinoma, Evaluation of Nonradiative Clinical Imaging Techniques for the Longitudinal Assessment of Tumour Growth in Murine CT26 Colon Carcinoma. Int J Mol Imaging Int J Mol Imaging. 2013 Jul 2;2013, 2013:e983534.

24. Chaplin DJ, Olive PL, Durand RE. Intermittent Blood Flow in a Murine Tumor: Radiobiological Effects. Cancer Res. 1987 Jan 15;47(2):597–601.

25. Moulder JE, Rockwell S. Hypoxic fractions of solid tumors: experimental techniques, methods of analysis, and a survey of existing data. Int J Radiat Oncol Biol Phys. 1984 May;10(5):695–712.

26. Nordsmark M, Bentzen SM, Overgaard J. Measurement of human tumour oxygenation status by a polarographic needle electrode. An analysis of inter- and intratumour heterogeneity, Acta Oncol. 1994;33(4):383-9.

27. Folkman J. Angiogenesis in cancer, vascular, rheumatoid and other disease. Nat Med. 1995 Jan;1(1):27–31.

28. Gerhardt H, Golding M, Fruttiger M, Ruhrberg C, Lundkvist A, Abramsson A, et al. VEGF guides angiogenic sprouting utilizing endothelial tip cell filopodia. J Cell Biol. 2003 Jun 23;161(6):1163–77.

29. Hellström M, Gerhardt H, Kalén M, Li X, Eriksson U, Wolburg H, et al. Lack of Pericytes Leads to Endothelial Hyperplasia and Abnormal Vascular Morphogenesis. J Cell Biol. 2001 Apr 30;153(3):543–54.

30. Nagy JA, Chang S-H, Dvorak AM, Dvorak HF. Why are tumour blood vessels abnormal and why is it important to know? Br J Cancer. 2009 Mar 24;100(6):865–9.

31. Dudley AC. Tumor Endothelial Cells. Cold Spring Harb Perspect Med. 2012 Mar Cold Spring Harb Perspect Med. 2012 Mar;2(3):a006536.

32. Teicher BA. A systems approach to cancer therapy. (Antioncogenics + standard cytotoxics-->mechanism(s) of interaction). Cancer Metastasis Rev. 1996 Jun;15(2):247–72.

33. Jain RK. Normalizing tumor vasculature with anti-angiogenic therapy: A new paradigm for combination therapy. Nat Med. 2001 Sep;7(9):987–9.

34. Nissen NN, Polverini PJ, Koch AE, Volin MV, Gamelli RL, DiPietro LA. Vascular endothelial growth factor mediates angiogenic activity during the proliferative phase of wound healing. Am J Pathol. 1998 Jun;152(6):1445–52.

35. Elice F[1], Rodeghiero F. Side effects of anti-angiogenic drugs. Thromb Res. 2012 Apr;129 Suppl 1:S50-3.

36. Tonnesen MG, Feng X, Clark RAF. Angiogenesis in Wound Healing. J Investig Dermatol Symp Proc. 2000 Dec;5(1):40–6.

37. Gordon CR, Rojavin Y, Patel M, Zins JE, Grana G, Kann B, et al. A review on bevacizumab and surgical wound healing: an important warning to all surgeons. Ann Plast Surg. 2009 Jun;62(6):707–9.

38. Deshaies I, Malka D, Soria J-C, Massard C, Bahleda R, Elias D. Antiangiogenic agents and late anastomotic complications. J Surg Oncol. 2010 Feb 1;101(2):180–3.

39. Maharaj ASR, D'Amore PA. Roles for VEGF in the adult. Microvasc Res. 2007 Nov;74(2–3):100–13.

40. Jain RK, Duda DG, Clark JW, Loeffler JS. Lessons from phase III clinical trials on anti-VEGF therapy for cancer. Nat Clin Pract Oncol. 2006;3(1):24–40.

41. Hida K, Hida Y, Amin DN, Flint AF, Panigrahy D, Morton CC, et al. Tumor-Associated Endothelial Cells with Cytogenetic Abnormalities. Cancer Res. 2004 Nov 15;64(22):8249–55.

42. St Croix B, Rago C, Velculescu V, Traverso G, Romans KE, Montgomery E, et al. Genes expressed in human tumor endothelium. Science. 2000 Aug 18;289(5482):1197–202.

43. Cullen M, Seaman S, Chaudhary A, Yang MY, Hilton MB, Logsdon D, et al. Host-Derived Tumor Endothelial Marker 8 (TEM8) Promotes the Growth of Melanoma. Cancer Res. 2009 Aug 1;69(15):6021–6.

44. Rmali KA, Watkins G, Harrison G, Parr C, Puntis MCA, Jiang WG. Tumour endothelial marker 8 (TEM-8) in human colon cancer and its association with tumour progression. Eur J Surg Oncol J Eur Soc Surg Oncol Br Assoc Surg Oncol. 2004 Nov;30(9):948–53.

45. Ruan Z, Yang Z, Wang Y, Wang H, Chen Y, Shang X, et al. DNA vaccine against tumor endothelial marker 8 inhibits tumor angiogenesis and growth. J Immunother Hagerstown Md 1997. 2009 Jun;32(5):486–91.

46. Mina-Osorio P. The moonlighting enzyme CD13: old and new functions to target. Trends Mol Med. 2008 Aug;14(8):361–71.

47. Kramer W, Girbig F, Corsiero D, Pfenninger A, Frick W, Jähne G, et al. Aminopeptidase N (CD13) Is a Molecular Target of the Cholesterol Absorption Inhibitor Ezetimibe in the Enterocyte Brush Border Membrane. J Biol Chem. 2005 Jan 14;280(2):1306–20.

48. Fukasawa K, Fujii H, Saitoh Y, Koizumi K, Aozuka Y, Sekine K, et al. Aminopeptidase N (APN/CD13) is selectively expressed in vascular endothelial cells and plays multiple roles in angiogenesis. Cancer Lett. 2006 Nov 8;243(1):135–43.

49. Tani K, Ogushi F, Huang L, Kawano T, Tada H, Hariguchi N, et al. CD13/aminopeptidase N, a Novel Chemoattractant for T Lymphocytes in Pulmonary Sarcoidosis. Am J Respir Crit Care Med. 2000 May 1;161(5):1636–42.

50. Curnis F, Arrigoni G, Sacchi A, Fischetti L, Arap W, Pasqualini R, et al. Differential binding of drugs containing the NGR motif to CD13 isoforms in tumor vessels, epithelia, and myeloid cells. Cancer Res. 2002 Feb 1;62(3):867–74.

51. Di Matteo P, Arrigoni GL, Alberici L, Corti A, Gallo-Stampino C, Traversari C, et al. Enhanced expression of CD13 in vessels of inflammatory and neoplastic tissues. J Histochem Cytochem Off J Histochem Soc. 2011 Jan;59(1):47–59.

52. Ito S, Miyahara R, Takahashi R, Nagai S, Takenaka K, Wada H, et al. Stromal aminopeptidase N expression: correlation with angiogenesis in non-small-cell lung cancer. Gen Thorac Cardiovasc Surg. 2009 Nov 12;57(11):591–8.

53. Liu C, Yu W, Chen Z, Zhang J, Zhang N. Enhanced gene transfection efficiency in CD13-positive vascular endothelial cells with targeted poly(lactic acid)–poly(ethylene glycol) nanoparticles through caveolae-mediated endocytosis. J Controlled Release. 2011 Apr 30;151(2):162–75.

54. Ichinose Y, Genka K, Koike T, Kato H, Watanabe Y, Mori T, et al. Randomized Double-Blind Placebo-Controlled Trial of Bestatin in Patients With Resected Stage I Squamous-Cell Lung Carcinoma. J Natl Cancer Inst. 2003 Apr 16;95(8):605–10.

55. Huminiecki L, Gorn M, Suchting S, Poulsom R, Bicknell R. Magic roundabout is a new member of the roundabout receptor family that is endothelial specific and expressed at sites of active angiogenesis. Genomics. 2002 Apr;79(4):547–52.

56. Seth P, Lin Y, Hanai J, Shivalingappa V, Duyao MP, Sukhatme VP. Magic roundabout, a tumor endothelial marker: expression and signaling. Biochem Biophys Res Commun. 2005 Jul 1;332(2):533–41.

57. Park KW, Morrison CM, Sorensen LK, Jones CA, Rao Y, Chien C-B, et al. Robo4 is a vascular-specific receptor that inhibits endothelial migration. Dev Biol. 2003 Sep 1;261(1):251–67.

58. Mura M, Swain RK, Zhuang X, Vorschmitt H, Reynolds G, Durant S, et al. Identification and angiogenic role of the novel tumor endothelial marker CLEC14A. Oncogene. 2012 Jan 19;31(3):293–305.

59. P J Noy PL. Blocking CLEC14A-MMRN2 binding inhibits sprouting angiogenesis and tumour growth. Oncogene. 2015;

60. Schellerer VS, Croner RS, Weinländer K, Hohenberger W, Stürzl M, Naschberger E. Endothelial cells of human colorectal cancer and healthy colon reveal phenotypic differences in culture. Lab Invest. 2007 Sep 17;87(11):1159–70.

61. Lalor PF, Curbishley SM, Adams DH. Identifying Homing Interactions in T-Cell Traffic in Human Disease. T-Cell Trafficking, Methods in Molecular Biology Volume 616, 2010, pp 231-252

62. Ley K, Laudanna C, Cybulsky MI, Nourshargh S. Getting to the site of inflammation: the leukocyte adhesion cascade updated. Nat Rev Immunol. 2007 Sep;7(9):678–89.

63. Zou X, Patil VRS, Dagia NM, Smith LA, Wargo MJ, Interliggi KA, et al. PSGL-1 derived from human neutrophils is a high-efficiency ligand for endothelium-expressed E-selectin under flow. Am J Physiol - Cell Physiol. 2005 Aug 1;289(2):C415–24.

64. Ley K. The role of selectins in inflammation and disease. Trends Mol Med. 2003 Jun;9(6):263-8.

65. Rodgers SD, Camphausen RT, Hammer DA. Sialyl LewisX-Mediated, PSGL-1-Independent RollingAdhesion on P-selectin. Biophys J. 2000 Aug;79(2):694–706.

66. Hynes RO. Integrins: Versatility, modulation, and signaling in cell adhesion. Cell. 1992 Apr 3;69(1):11–25.

67. The integrin VLA-4 supports tethering and rolling in flow on VCAM-1. J Cell Biol. 1995 Mar 2;128(6):1243–53.

68. Stanley P, Hogg N. The I Domain of Integrin LFA-1 Interacts with ICAM-1 Domain 1 at Residue Glu-34 but Not Gln-73. J Biol Chem. 1998 Feb 6;273(6):3358–62.

69. Lefort CT, Ley K. Neutrophil arrest by LFA-1 activation. Chemoattractants. 2012;3:157.

70. Zlotnik A, Yoshie O. Chemokines: A New Classification System and Their Role in Immunity. Immunity. 2000 Feb 1;12(2):121–7.

71. Weber KSC, Klickstein LB, Weber C. Specific Activation of Leukocyte β2 Integrins Lymphocyte Function–associated Antigen-1 and Mac-1 by Chemokines Mediated by Distinct Pathways via the α Subunit Cytoplasmic Domains. Mol Biol Cell. 1999 Apr;10(4):861–73.

72. Piali L, Fichtel A, Terpe HJ, Imhof BA, Gisler RH. Endothelial vascular cell adhesion molecule 1 expression is suppressed by melanoma and carcinoma. J Exp Med. 1995 Feb 1;181(2):811-6.

73. Lloyd AR, Oppenheim JJ, Kelvin DJ, Taub DD. Chemokines regulate T cell adherence to recombinant adhesion molecules and extracellular matrix proteins. J Immunol. 1996 Feb 1;156(3):932–8.

74. Campbell JJ, Hedrick J, Zlotnik A, Siani MA, Thompson DA, Butcher EC. Chemokines and the Arrest of Lymphocytes Rolling Under Flow Conditions. Science. 1998 Jan 16;279(5349):381–4.

75. Peled A, Kollet O, Ponomaryov T, Petit I, Franitza S, Grabovsky V, et al. The chemokine SDF-1 activates the integrins LFA-1, VLA-4, and VLA-5 on immature human CD34+ cells: role in transendothelial/stromal migration and engraftment of NOD/SCID mice. Blood. 2000 Jun 1;95(11):3289–96.

76. Campbell JJ, Haraldsen G, Pan J, Rottman J, Qin S, Ponath P, et al. The chemokine receptor CCR4 in vascular recognition by cutaneous but not intestinal memory T cells. Nature. 1999 Aug 19;400(6746):776–80.

77. Kinashi T. Intracellular signalling controlling integrin activation in lymphocytes. Nat Rev Immunol. 2005 Jul;5(7):546–59.

78. Springer TA. Traffic Signals on Endothelium for Lymphocyte Recirculation and Leukocyte Emigration. Annu Rev Physiol. 1995;57(1):827–72.

79. Calderwood DA, Ginsberg MH. Talin forges the links between integrins and actin. Nat Cell Biol. 2003 Aug;5(8):694–7.

80. Ziegler WH[1], Gingras AR, Critchley DR, Emsley J. Integrin connections to the cytoskeleton through talin and vinculin. Biochem Soc Trans. 2008 Apr;36 (Pt 2):235-9.

81. Humphries JD, Wang P, Streuli C, Geiger B, Humphries MJ, Ballestrem C. Vinculin controls focal adhesion formation by direct interactions with talin and actin. J Cell Biol. 2007 Dec 3;179(5):1043–57.

82. Lub M, van Kooyk Y, van Vliet SJ, Figdor CG. Dual role of the actin cytoskeleton in regulating cell adhesion mediated by the integrin lymphocyte function-associated molecule-1. Mol Biol Cell. 1997 Feb;8(2):341–51.

83. Ley K, Zarbock A. Immunity. 2006 Aug;25(2):185-7. Hold on to your endothelium: postarrest steps of the leukocyte adhesion cascade.

84. Muller WA. Mechanisms of Leukocyte Transendothelial Migration. Annu Rev Pathol. 2011;6:323–44.

85. Martìn-Padura I, Lostaglio S, Schneemann M, Williams L, Romano M, Fruscella P, et al. Junctional adhesion molecule, a novel member of the immunoglobulin superfamily that distributes at intercellular junctions and modulates monocyte transmigration. J Cell Biol. 1998 Jul 13;142(1):117–27.

86. Del Maschio A, De Luigi A, Martin-Padura I, Brockhaus M, Bartfai T, Fruscella P, et al. Leukocyte recruitment in the cerebrospinal fluid of mice with experimental meningitis is inhibited by an antibody to junctional adhesion molecule (JAM). J Exp Med. 1999 Nov 1;190(9):1351–6.

87. PECAM-1 is required for transendothelial migration of leukocytes. J Exp Med. 1993 Aug 1;178(2):449–60.

88. Lampugnani MG, Resnati M, Raiteri M, Pigott R, Pisacane A, Houen G, et al. A novel endothelial-specific membrane protein is a marker of cell-cell contacts. J Cell Biol. 1992 Sep;118(6):1511–22.

89. Buul JD van, Kanters E, Hordijk PL. Endothelial Signaling by Ig-Like Cell Adhesion Molecules. Arterioscler Thromb Vasc Biol. 2007 Sep 1;27(9):1870–6.

90. Granger DN, Kubes P. The microcirculation and inflammation: modulation of leukocyte-endothelial cell adhesion. J Leukoc Biol. 1994 May 1;55(5):662–75.

91. Kunkel EJ, Campbell JJ, Haraldsen G, Pan J, Boisvert J, Roberts AI, et al. Lymphocyte Cc Chemokine Receptor 9 and Epithelial Thymus-Expressed Chemokine (Teck) Expression Distinguish the Small Intestinal Immune Compartment. J Exp Med. 2000 Sep 5;192(5):761–8.

92. Zabel BA, Agace WW, Campbell JJ, Heath HM, Parent D, Roberts AI, et al. Human G protein-coupled receptor GPR-9-6/CC chemokine receptor 9 is selectively expressed on intestinal homing T lymphocytes, mucosal lymphocytes, and thymocytes and is required for thymus-expressed chemokine-mediated chemotaxis. J Exp Med. 1999 Nov 1;190(9):1241–56.

93. Pachynski RK, Wu SW, Gunn MD, Erle DJ. Secondary lymphoid-tissue chemokine (SLC) stimulates integrin alpha 4 beta 7-mediated adhesion of lymphocytes to mucosal addressin cell adhesion molecule-1 (MAdCAM-1) under flow. J Immunol Baltim Md 1950. 1998 Jul 15;161(2):952–6.

94. Briskin M, Winsor-Hines D, Shyjan A, Cochran N, Bloom S, Wilson J, et al. Human mucosal addressin cell adhesion molecule-1 is preferentially expressed in intestinal tract and associated lymphoid tissue. Am J Pathol. 1997 Jul;151(1):97–110.

95. Griffioen AW, Damen CA, Martinotti S, Blijham GH, Groenewegen G. Endothelial Intercellular Adhesion Molecule-1 Expression Is Suppressed in Human Malignancies: The Role of Angiogenic Factors. Cancer Res. 1996 Mar 1;56(5):1111–7.

96. Piali L, Fichtel A, Terpe HJ, Imhof BA, Gisler RH. Endothelial vascular cell adhesion molecule 1 expression is suppressed by melanoma and carcinoma. J Exp Med. 1995 Feb 1;181(2):811–6.

97. Buckanovich RJ, Facciabene A, Kim S, Benencia F, Sasaroli D, Balint K, et al. Endothelin B receptor mediates the endothelial barrier to T cell homing to tumors and disables immune therapy. Nat Med. 2008 Jan;14(1):28–36.

98. Matsumura S, Wang B, Kawashima N, Braunstein S, Badura M, Cameron TO, et al. Radiation-induced CXCL16 release by breast cancer cells attracts effector T cells. J Immunol Baltim Md 1950. 2008 Sep 1;181(5):3099–107.

99. Rosenberg SA, Spiess P, Lafreniere R. A new approach to the adoptive immunotherapy of cancer with tumor-infiltrating lymphocytes. Science. 1986 Sep 19;233(4770):1318–21.

100. Cutler CW, Jotwani R, Pulendran B. Dendritic Cells: Immune Saviors or Achilles' Heel? Infect Immun. 2001 Aug;69(8):4703–8.

101. König R. Interactions between MHC molecules and co-receptors of the TCR. Curr Opin Immunol. 2002 Feb 1;14(1):75–83.

102. Galon J, Fridman W-H, Pagès F. The adaptive immunologic microenvironment in colorectal cancer: a novel perspective. Cancer Res. 2007 Mar 1;67(5):1883–6.

103. Diederichsen ACP, Hjelmborg JV, Christensen PB, Zeuthen J, Fenger C. Prognostic value of the CD4(+)/CD8(+) ratio of tumour infiltrating lymphocytes in colorectal cancer and HLA-DR expression on tumour cells. Cancer Immunol Immunother. 2003 Jul;52(7):423–8.

104. Hodi FS, O'Day SJ, McDermott DF, Weber RW, Sosman JA, Haanen JB, et al. Improved Survival with Ipilimumab in Patients with Metastatic Melanoma. N Engl J Med. 2010 Aug 19;363(8):711–23.

105. Topalian SL, Hodi FS, Brahmer JR, Gettinger SN, Smith DC, McDermott DF, et al. Safety, Activity, and Immune Correlates of Anti–PD-1 Antibody in Cancer. N Engl J Med. 2012 Jun 28;366(26):2443–54.

106. Zhou L, Chong MMW, Littman DR. Plasticity of CD4+ T cell lineage differentiation. Immunity. 2009 May;30(5):646–55.

107. Kimura A, Kishimoto T. IL-6: regulator of Treg/Th17 balance. Eur J Immunol. 2010 Jul;40(7):1830–5.

108. Tartour E, Pere H, Maillere B, Terme M, Merillon N, Taieb J, et al. Angiogenesis and immunity: a bidirectional link potentially relevant for the monitoring of antiangiogenic therapy and the development of novel therapeutic combination with immunotherapy. Cancer Metastasis Rev. 2011 Jan 20;30(1):83–95.

109. Yamagiwa S, Gray JD, Hashimoto S, Horwitz DA. A role for TGF-beta in the generation and expansion of CD4+CD25+ regulatory T cells from human peripheral blood. J Immunol Baltim Md 1950. 2001 Jun 15;166(12):7282–9.

110. Shevach EM. CD4+CD25+ suppressor T cells: more questions than answers. Nat Rev Immunol. 2002 Jun;2(6):389–400.

111. Sakaguchi S. Naturally arising Foxp3-expressing CD25+CD4+ regulatory T cells in immunological tolerance to self and non-self. Nat Immunol. 2005 Apr;6(4):345–52.

112. Zou W. Regulatory T cells, tumour immunity and immunotherapy. Nat Rev Immunol. 2006 Apr;6(4):295–307.

113. Curiel TJ, Coukos G, Zou L, Alvarez X, Cheng P, Mottram P, et al. Specific recruitment of regulatory T cells in ovarian carcinoma fosters immune privilege and predicts reduced survival. Nat Med. 2004 Sep;10(9):942–9.

114. McCoy MJ, Hemmings C, Miller TJ, Austin SJ, Bulsara MK, Zeps N, et al. Low stromal Foxp3(+) regulatory T-cell density is associated with complete response to neoadjuvant chemoradiotherapy in rectal cancer. Br J Cancer. 2015 Dec 22;113(12):1677–86.

115. Davies LC, Jenkins SJ, Allen JE, Taylor PR. Tissue-resident macrophages. Nat Immunol. 2013 Oct;14(10):986–95.

116. Murdoch C, Giannoudis A, Lewis CE. Mechanisms regulating the recruitment of macrophages into hypoxic areas of tumors and other ischemic tissues. Blood. 2004 Oct 15;104(8):2224–34.

117. Allavena P, Sica A, Solinas G, Porta C, Mantovani A. The inflammatory micro-environment in tumor progression: the role of tumor-associated macrophages. Crit Rev Oncol Hematol. 2008 Apr;66(1):1–9.

118. Mantovani A, Sozzani S, Locati M, Allavena P, Sica A. Macrophage polarization: tumor-associated macrophages as a paradigm for polarized M2 mononuclear phagocytes. Trends Immunol. 2002 Nov;23(11):549–55.

119. Martinez FO, Sica A, Mantovani A, Locati M. Macrophage activation and polarization. Front Biosci J Virtual Libr. 2008;13:453–61.

120. Martinez FO, Helming L, Gordon S. Alternative activation of macrophages: an immunologic functional perspective. Annu Rev Immunol. 2009;27:451–83.

121. Hao N-B, Lü M-H, Fan Y-H, Cao Y-L, Zhang Z-R, Yang S-M. Macrophages in tumor microenvironments and the progression of tumors. Clin Dev Immunol. 2012;2012:948098.

122. Kalluri R, Zeisberg M. Fibroblasts in cancer. Nat Rev Cancer. 2006 May;6(5):392–401.

123. Kalluri R, Zeisberg M. Fibroblasts in cancer. Nat Rev Cancer. 2006 May;6(5):392–401.

124. Liao D, Luo Y, Markowitz D, Xiang R, Reisfeld RA. Cancer Associated Fibroblasts Promote Tumor Growth and Metastasis by Modulating the Tumor Immune Microenvironment in a 4T1 Murine Breast Cancer Model. PLoS ONE. 2009 Nov 23;4(11):e7965.

125. Jain RK, Koenig GC, Dellian M, Fukumura D, Munn LL, Melder RJ. Leukocyte-endothelial adhesion and angiogenesis in tumors. Cancer Metastasis Rev. 1996 Jun;15(2):195–204.

126. Rubie C, Kempf K, Hans J, Su T, Tilton B, Georg T, et al. Housekeeping gene variability in normal and cancerous colorectal, pancreatic, esophageal, gastric and hepatic tissues. Mol Cell Probes. 2005 Apr;19(2):101–9.

127. Pfaffl MW. A new mathematical model for relative quantification in real-time RT–PCR. Nucleic Acids Res. 2001;29(9):e45–e45.

128. Warren RS, Yuan H, Matli MR, Gillett NA, Ferrara N. Regulation by vascular endothelial growth factor of human colon cancer tumorigenesis in a mouse model of experimental liver metastasis. J Clin Invest. 1995 Apr;95(4):1789–97.

129. Asano M, Yukita A, Matsumoto T, Kondo S, Suzuki H. Inhibition of Tumor Growth and Metastasis by an Immunoneutralizing Monoclonal Antibody to Human Vascular Endothelial Growth Factor/Vascular Permeability Factor121. Cancer Res. 1995 Nov 15;55(22):5296–301.

130. Wood JM, Bold G, Buchdunger E, Cozens R, Ferrari S, Frei J, et al. PTK787/ZK 222584, a novel and potent inhibitor of vascular endothelial growth factor receptor tyrosine kinases, impairs vascular endothelial growth factor-induced responses and tumor growth after oral administration. Cancer Res. 2000 Apr 15;60(8):2178–89.

131. Haraldsen G, Kvale D, Lien B, Farstad IN, Brandtzaeg P. Cytokine-regulated expression of E-selectin, intercellular adhesion molecule-1 (ICAM-1), and vascular cell adhesion molecule-1 (VCAM-1) in human microvascular endothelial cells. J Immunol Baltim Md 1950. 1996 Apr 1;156(7):2558–65.

132. Swerlick RA, Lee KH, Li LJ, Sepp NT, Caughman SW, Lawley TJ. Regulation of vascular cell adhesion molecule 1 on human dermal microvascular endothelial cells. J Immunol. 1992 Jul 15;149(2):698–705.

133. Naschberger E, Schellerer VS, Rau TT, Croner RS, Stürzl M. Isolation of Endothelial Cells from Human Tumors. Methods Mol Biol. 2011;731:209-18

134. Jayasinghe C, Simiantonaki N, Michel-Schmidt R, Kirkpatrick CJ. Comparative study of human colonic tumor-derived endothelial cells (HCTEC) and normal colonic microvascular endothelial cells (HCMEC): Hypoxia-induced sVEGFR-1 and sVEGFR-2 levels. Oncol Rep. 2009 Apr;21(4):933–9.

135. Haraldsen G, Rugtveit J, Kvale D, Scholz T, Muller WA, Hovig T, et al. Isolation and longterm culture of human intestinal microvascular endothelial cells. Gut. 1995 Aug 1;37(2):225–34.

136. van Beijnum JR, Rousch M, Castermans K, van der Linden E, Griffioen AW. Isolation of endothelial cells from fresh tissues. Nat Protoc. 2008 Jun;3(6):1085–91.

137. Jackson CJ, Garbett PK, Nissen B, Schrieber L. Binding of human endothelium to Ulex europaeus I-coated Dynabeads: application to the isolation of microvascular endothelium. J Cell Sci. 1990 Jun 1;96(2):257–62.

138. Woodfin A, Voisin M-B, Nourshargh S. PECAM-1: A Multi-Functional Molecule in Inflammation and Vascular Biology. Arterioscler Thromb Vasc Biol. 2007 Dec 1;27(12):2514–23.

139. Buckley CD, Doyonnas R, Newton JP, Blystone SD, Brown EJ, Watt SM, et al. Identification of alpha v beta 3 as a heterotypic ligand for CD31/PECAM-1. J Cell Sci. 1996 Feb 1;109(2):437–45.

140. Pusztaszeri MP, Seelentag W, Bosman FT. Immunohistochemical Expression of Endothelial Markers CD31, CD34, von Willebrand Factor, and Fli-1 in Normal Human Tissues. J Histochem Cytochem. 2006 Apr 1;54(4):385–95.

141. DeLisser HM, Newman PJ, Albelda SM. Molecular and functional aspects of PECAM-1/CD31. Immunol Today. 1994 Oct;15(10):490–5.

142. Manes TD, Pober JS. Identification of endothelial cell junctional proteins and lymphocyte receptors involved in transendothelial migration of human effector memory CD4+ T cells. J Immunol Baltim Md 1950. 2011 Feb 1;186(3):1763–8.

143. Murakami S, Morioka T, Nakagawa Y, Suzuki Y, Arakawa M, Oite T. Expression of adhesion molecules by cultured human glomerular endothelial cells in response to cytokines: comparison to human umbilical vein and dermal microvascular endothelial cells. Microvasc Res. 2001 Nov;62(3):383–91.

144. Romer LH, McLean NV, Yan HC, Daise M, Sun J, DeLisser HM. IFN-gamma and TNF-alpha induce redistribution of PECAM-1 (CD31) on human endothelial cells. J Immunol Baltim Md 1950. 1995 Jun 15;154(12):6582–92.

145. Diederichsen AC, Zeuthen J, Christensen PB, Kristensen T. Characterisation of tumour infiltrating lymphocytes and correlations with immunological surface molecules in colorectal cancer. Eur J Cancer Oxf Engl 1990. 1999 May;35(5):721–6.

146. Van Damme N, Baeten D, De Vos M, Demetter P, Elewaut D, Mielants H, et al. Chemical agents and enzymes used for the extraction of gut lymphocytes influence flow cytometric detection of T cell surface markers. J Immunol Methods. 2000 Mar 6;236(1–2):27–35.

147. Grange C, Létourneau J, Forget M-A, Godin-Ethier J, Martin J, Liberman M, et al. Phenotypic characterization and functional analysis of human tumor immune infiltration after mechanical and enzymatic disaggregation. J Immunol Methods. 2011 Sep 30;372(1–2):119–26.

148. Scott PA, Bicknell R. The isolation and culture of microvascular endothelium. J Cell Sci. 1993;105:269–269.

149. Voyta JC, Via DP, Butterfield CE, Zetter BR. Identification and isolation of endothelial cells based on their increased uptake of acetylated-low density lipoprotein. J Cell Biol. 1984 Dec 1;99(6):2034–40.

150. Schellerer VS, Mueller-Bergh L, Merkel S, Zimmermann R, Weiss D, Schlabrakowski A, et al. The clinical value of von Willebrand factor in colorectal carcinomas. Am J Transl Res. 2011;3(5):445–53.

151. Sadler JE. Biochemistry and Genetics of Von Willebrand Factor. Annu Rev Biochem. 1998;67(1):395–424.

152. Zanetta L, Marcus SG, Vasile J, Dobryansky M, Cohen H, Eng K, et al. Expression of von Willebrand factor, an endothelial cell marker, is up-regulated by angiogenesis factors: A potential method for objective assessment of tumor angiogenesis. Int J Cancer. 2000 Jan 15;85(2):281–8.

153. Page C, Rose M, Yacoub M, Pigott R. Antigenic heterogeneity of vascular endothelium. Am J Pathol. 1992 Sep;141(3):673–83.

154. Saad RS, Liu YL, Nathan G, Celebrezze J, Medich D, Silverman JF. Endoglin (CD105) and vascular endothelial growth factor as prognostic markers in colorectal cancer. Mod Pathol Off J U S Can Acad Pathol Inc. 2004 Feb;17(2):197–203.

155. Wong SH, Hamel L, Chevalier S, Philip A. Endoglin expression on human microvascular endothelial cells. Eur J Biochem. 2000 Sep 1;267(17):5550–60.

156. Burrows FJ, Derbyshire EJ, Tazzari PL, Amlot P, Gazdar AF, King SW, et al. Up-regulation of endoglin on vascular endothelial cells in human solid tumors: implications for diagnosis and therapy. Clin Cancer Res Off J Am Assoc Cancer Res. 1995 Dec;1(12):1623–34.

157. Ríus C, Smith JD, Almendro N, Langa C, Botella LM, Marchuk DA, et al. Cloning of the Promoter Region of Human Endoglin, the Target Gene for Hereditary Hemorrhagic Telangiectasia Type 1. Blood. 1998 Dec 15;92(12):4677–90.

158. Li C, Issa R, Kumar P, Hampson IN, Lopez-Novoa JM, Bernabeu C, et al. CD105 prevents apoptosis in hypoxic endothelial cells. J Cell Sci. 2003 Jul 1;116(Pt 13):2677–85.

159. Balza E, Castellani P, Zijlstra A, Neri D, Zardi L, Siri A. Lack of specificity of endoglin expression for tumor blood vessels. Int J Cancer J Int Cancer. 2001 Nov;94(4):579–85.

160. Corada M, Mariotti M, Thurston G, Smith K, Kunkel R, Brockhaus M, et al. Vascular endothelial–cadherin is an important determinant of microvascular integrity in vivo. Proc Natl Acad Sci. 1999 Aug 17;96(17):9815–20.

161. Corada M, Liao F, Lindgren M, Lampugnani MG, Breviario F, Frank R, et al. Monoclonal antibodies directed to different regions of vascular endothelial cadherin extracellular domain affect adhesion and clustering of the protein and modulate endothelial permeability. Blood. 2001 Mar 15;97(6):1679–84.

162. Aberle H, Schwartz H, Kemler R. Cadherin-catenin complex: Protein interactions and their implications for cadherin function. J Cell Biochem. 1996 Jun 16;61(4):514–23.

163. Leckband D, Sivasankar S. Mechanism of homophilic cadherin adhesion. Curr Opin Cell Biol. 2000 Oct 1;12(5):587–92.

164. Moll T, Dejana E, Vestweber D. In Vitro Degradation of Endothelial Catenins by a Neutrophil Protease. J Cell Biol. 1998 Jan 26;140(2):403–7.

165. Esser S, Lampugnani MG, Corada M, Dejana E, Risau W. Vascular endothelial growth factor induces VE-cadherin tyrosine phosphorylation in endothelial cells. J Cell Sci. 1998 Jul 1;111(13):1853–65.

166. Gutwein LG, Al-Quran SZ, Fernando S, Fletcher BS, Copeland EM, Grobmyer SR. Tumor endothelial marker 8 expression in triple-negative breast cancer. Anticancer Res. 2011 Oct;31(10):3417–22.

167. Besschetnova TY, Ichimura T, Katebi N, St. Croix B, Bonventre JV, Olsen BR. Regulatory mechanisms of anthrax toxin receptor 1-dependent vascular and connective tissue homeostasis. Matrix Biol. 2015 Mar;42:56–73.

168. Beauregard KE, Collier RJ, Swanson JA. Proteolytic activation of receptor-bound anthrax protective antigen on macrophages promotes its internalization. Cell Microbiol. 2000 Jun 1;2(3):251–8.

169. Mogridge J, Cunningham K, Lacy DB, Mourez M, Collier RJ. The lethal and edema factors of anthrax toxin bind only to oligomeric forms of the protective antigen. Proc Natl Acad Sci U S A. 2002 May 14;99(10):7045–8.

170. Matteo PD, Arrigoni GL, Alberici L, Corti A, Gallo-Stampino C, Traversari C, et al. Enhanced Expression of CD13 in Vessels of Inflammatory and Neoplastic Tissues. J Histochem Cytochem. 2011 Jan;59(1):47–59.

171. Mishima Y, Terui Y, Sugimura N, Matsumoto-Mishima Y, Rokudai A, Kuniyoshi R, et al. Continuous treatment of bestatin induces anti-angiogenic property in endothelial cells. Cancer Sci. 2007;98(3):364–372.

172. Ju S, Qiu H, Zhou X, Zhu B, Lv X, Huang X, et al. CD13 + CD4 +CD25 hi regulatory T cells exhibit higher suppressive function and increase with tumor stage in non-small cell lung cancer patients. Cell Cycle. 2009 Aug 15;8(16):2578–85.

173. Zhang B, Wang Z, Wu L, Zhang M, Li W, Ding J, et al. Circulating and tumor-infiltrating myeloid-derived suppressor cells in patients with colorectal carcinoma. PloS One. 2013;8(2):e57114.

174. Burnet M. Cancer—A Biological Approach. Br Med J. 1957 Apr 13;1(5023):841–7.

175. Ikehara S, Pahwa RN, Fernandes G, Hansen CT, Good RA. Functional T cells in athymic nude mice. Proc Natl Acad Sci U S A. 1984 Feb;81(3):886–8.

176. Prehn RT, Main JM. Immunity to methylcholanthrene-induced sarcomas. J Natl Cancer Inst. 1957 Jun;18(6):769–78.

177. Boon T, Cerottini JC, Van den Eynde B, van der Bruggen P, Van Pel A. Tumor antigens recognized by T lymphocytes. Annu Rev Immunol. 1994;12:337–65.

178. Sykulev Y, Joo M, Vturina I, Tsomides TJ, Eisen HN. Evidence that a Single Peptide–MHC Complex on a Target Cell Can Elicit a Cytolytic T Cell Response. Immunity. 1996 Jun 1;4(6):565–71.

179. Dean DM, Pross HF, Kennedy JC. Spontaneous human lymphocyte-mediated cytotoxicity against tumor target cells--III. Stimulatory and inhibitory effects of ionizing radiation. Int J Radiat Oncol Biol Phys. 1978 Aug;4(7–8):633–41.

180. Thomas L. On immunosurveillance in human cancer. Yale J Biol Med. 1982;55(3–4):329–33.

181. Haskill S, Becker S, Fowler W, Walton L. Mononuclear-cell infiltration in ovarian cancer. I. Inflammatory-cell infiltrates from tumour and ascites material. Br J Cancer. 1982 May;45(5):728–36.

182. Zhang L, Conejo-Garcia JR, Katsaros D, Gimotty PA, Massobrio M, Regnani G, et al. Intratumoral T Cells, Recurrence, and Survival in Epithelial Ovarian Cancer. N Engl J Med. 2003 Jan 16;348(3):203–13.

183. Smyth MJ, Trapani JA. Granzymes: exogenous porteinases that induce target cell apoptosis. Immunol Today. 1995 Apr;16(4):202–6.

184. Ashkenazi A, Dixit VM. Apoptosis control by death and decoy receptors. Curr Opin Cell Biol. 1999 Apr 1;11(2):255–60.

185. Ashkenazi A, Dixit VM. Death Receptors: Signaling and Modulation. Science. 1998 Aug 28;281(5381):1305–8.

186. Dunn GP, Old LJ, Schreiber RD. The three Es of cancer immunoediting. Annu Rev Immunol. 2004;22:329–60.

187. Dunn GP, Bruce AT, Ikeda H, Old LJ, Schreiber RD. Cancer immunoediting: from immunosurveillance to tumor escape. Nat Immunol. 2002 Nov;3(11):991–8.

188. Callahan MK, Wolchok JD. At the Bedside: CTLA-4- and PD-1-blocking antibodies in cancer immunotherapy. J Leukoc Biol. 2013 Jul;94(1):41–53.

189. Chambers CA, Kuhns MS, Egen JG, Allison JP. Ctla-4-mediated inhibition in regulation of t cell responses: Mechanisms and Manipulation in Tumor Immunotherapy. Annu Rev Immunol. 2001;19(1):565–94.

190. Gajewski TF, Schreiber H, Fu Y-X. Innate and adaptive immune cells in the tumor microenvironment. Nat Immunol. 2013 Oct;14(10):1014–22.

191. Cushing SD, Berliner JA, Valente AJ, Territo MC, Navab M, Parhami F, et al. Minimally modified low density lipoprotein induces monocyte chemotactic protein

1 in human endothelial cells and smooth muscle cells. Proc Natl Acad Sci U S A. 1990 Jul;87(13):5134–8.

192. Gunn MD, Nelken NA, Liao X, Williams LT. Monocyte chemoattractant protein-1 is sufficient for the chemotaxis of monocytes and lymphocytes in transgenic mice but requires an additional stimulus for inflammatory activation. J Immunol Baltim Md 1950. 1997 Jan 1;158(1):376–83.

193. Nelson H, Ramsey PS, Donohue JH, Wold LE. Cell Adhesion Molecule Expression within the Microvasculature of Human Colorectal Malignancies. Clin Immunol Immunopathol. 1994 Jul;72(1):129–36.

194. Kelly CP, O'Keane JC, Orellana J, Schroy PC, Yang S, LaMont JT, et al. Human colon cancer cells express ICAM-1 in vivo and support LFA-1-dependent lymphocyte adhesion in vitro. Am J Physiol - Gastrointest Liver Physiol. 1992 Dec 1;263(6):G864–70.

195. Schellerer V. Tumor-associated fibroblasts isolated from colorectal cancer tissues exhibit increased ICAM-1 expression and affinity for monocytes. Oncol Rep [Internet]. 2013 Nov 20 [cited 2016 Jun 3]; Available from: http://www.spandidos-publications.com/10.3892/or.2013.2860

196. Howard K, Lo KK, Ao L, Gamboni F, Edil BH, Schulick R, et al. Intercellular adhesion molecule-1 mediates murine colon adenocarcinoma invasion. J Surg Res. 2014 Mar;187(1):19–23.

197. Alexiou D, Karayiannakis AJ, Syrigos KN, Zbar A, Kremmyda A, Bramis I, et al. Serum levels of E-selectin, ICAM-1 and VCAM-1 in colorectal cancer patients: correlations with clinicopathological features, patient survival and tumour surgery. Eur J Cancer. 2001 Dec;37(18):2392–7.

198. Maurer CA, Friess H, Kretschmann B, Wildi S, Müller C, Graber H, et al. Over-expression of ICAM-1, VCAM-1 and ELAM-1 might influence tumor progression in colorectal cancer. Int J Cancer. 1998 Feb 20;79(1):76–81.

199. Griffioen AW, Damen CA, Martinotti S, Blijham GH, Groenewegen G. Endothelial Intercellular Adhesion Molecule-1 Expression Is Suppressed in Human Malignancies: The Role of Angiogenic Factors. Cancer Res. 1996 Mar 1;56(5):1111–7.

200. Kuzu I, Bicknell R, Fletcher CDM, Gatter KC. Expression of adhesion molecules on the endothelium of normal tissue vessels and vascular tumors. Lab Invest. 1993;69(3):322–8.

201. Bufill JA. Colorectal Cancer: Evidence for Distinct Genetic Categories Based on Proximal or Distal Tumor Location. Ann Intern Med. 1990 Nov 15;113(10):779–88.

202. Delattre O, Law DJ, Remvikos Y, Sastre X, Feinberg AP, Olschwang S, et al. Multiple genetic alterations in distal and proximal colorectal cancer. The Lancet. 1989 Aug 12;334(8659):353–6.

203. Lindblom A. Different mechanisms in the tumorigenesis of proximal and distal colon cancers. Curr Opin Oncol. 2001 Jan;13(1):63–9.

204. Iacopetta B. Are there two sides to colorectal cancer? Int J Cancer. 2002 Oct 10;101(5):403–8.

205. Phillips SM, Banerjea A, Feakins R, Li SR, Bustin SA, Dorudi S. Tumour-infiltrating lymphocytes in colorectal cancer with microsatellite instability are activated and cytotoxic. Br J Surg. 2004 Apr 1;91(4):469–75.

206. Sica A, Allavena P, Mantovani A. Cancer related inflammation: the macrophage connection. Cancer Lett. 2008 Aug 28;267(2):204–15.

207. Barbera-Guillem E, Nyhus JK, Wolford CC, Friece CR, Sampsel JW. Vascular Endothelial Growth Factor Secretion by Tumor-infiltrating Macrophages Essentially Supports Tumor Angiogenesis, and IgG Immune Complexes Potentiate the Process. Cancer Res. 2002 Dec 1;62(23):7042–9.

208. De Palma M, Venneri MA, Galli R, Sergi Sergi L, Politi LS, Sampaolesi M, et al. Tie2 identifies a hematopoietic lineage of proangiogenic monocytes required for tumor vessel formation and a mesenchymal population of pericyte progenitors. Cancer Cell. 2005 Sep;8(3):211–26.

209. Maltby S, Khazaie K, McNagny KM. Mast cells in tumor growth: angiogenesis, tissue remodelling and immune-modulation. Biochim Biophys Acta. 2009 Aug;1796(1):19–26.

210. Ma L, Cheung KCP, Kishore M, Nourshargh S, Mauro C, Marelli-Berg FM. CD31 Exhibits Multiple Roles in Regulating T Lymphocyte Trafficking In Vivo. J Immunol Author Choice. 2012 Oct 15;189(8):4104–11.

211. Suzuki Y, Ohtani H, Mizoi T, Takeha S, Shiiba K 'ichi, Matsuno S, et al. Cell Adhesion Molecule Expression by Vascular Endothelial Cells as an Immune/Inflammatory Reaction in Human Colon Carcinoma. Jpn J Cancer Res. 1995 Jun 1;86(6):585–93.

212. Madhavan M, Srinivas P, Abraham E, Ahmed I, Vijayalekshmi NR, Balaram P. Down regulation of endothelial adhesion molecules in node positive breast cancer: possible failure of host defence mechanism. Pathol Oncol Res POR. 2002;8(2):125–8.

213. Tsujisaki M, Imai K, Hirata H, Hanzawa Y, Masuya J, Nakano T, et al. Detection of circulating intercellular adhesion molecule-1 antigen in malignant diseases. Clin Exp Immunol. 1991 Jul 1;85(1):3–8.

214. Tromp SC, Egbrink MGA oude, Dings RPM, Velzen S van, Slaaf DW, Hillen HFP, et al. Tumor angiogenesis factors reduce leukocyte adhesion in vivo. Int Immunol. 2000 May 1;12(5):671–6.

215. Dirkx AEM, Egbrink MGA oude, Kuijpers MJE, Niet ST van der, Heijnen VVT, Steege JCAB, et al. Tumor Angiogenesis Modulates Leukocyte-Vessel Wall

Interactions in Vivo by Reducing Endothelial Adhesion Molecule Expression. Cancer Res. 2003 May 1;63(9):2322–9.

216. Svensson H, Olofsson V, Lundin S, Yakkala C, Björck S, Börjesson L, et al. Accumulation of CCR4+ CTLA-4hi FOXP3+CD25hi Regulatory T Cells in Colon Adenocarcinomas Correlate to Reduced Activation of Conventional T Cells. PLoS ONE [Internet]. 2012 Feb 1 [cited 2013 Jan 28];7(2). Available from: http://www.ncbi.nlm.nih.gov/pmc/articles/PMC3271060/

217. Yu P, Lee Y, Liu W, Chin RK, Wang J, Wang Y, et al. Priming of naive T cells inside tumors leads to eradication of established tumors. Nat Immunol. 2004 Feb;5(2):141–9.

218. Koch M, Beckhove P, op den Winkel J, Autenrieth D, Wagner P, Nummer D, et al. Tumor Infiltrating T Lymphocytes in Colorectal Cancer. Ann Surg. 2006 Dec;244(6):986–93.

219. Shetty S, Weston CJ, Oo YH, Westerlund N, Stamataki Z, Youster J, Hubscher SG, Salmi M, Jalkanen S, Lalor PF, Adams DH. Common lymphatic endothelial and vascular endothelial receptor-1 mediates the transmigration of regulatory T cells across human hepatic sinusoidal endothelium. J Immunol. 2011 Apr 1;186(7):4147-55.

220. Florczyk U, Czauderna S, Stachurska A, Tertil M, Nowak W, Kozakowska M, et al. Opposite effects of HIF-1α and HIF-2α on the regulation of IL-8 expression in endothelial cells. Free Radic Biol Med. 2011 Nov 15;51(10):1882–92.

221. Liu L-B, Xie F, Chang K-K, Li M-Q, Meng Y-H, Wang X-H, et al. Hypoxia promotes the proliferation of cervical carcinoma cells through stimulating the secretion of IL-8. Int J Clin Exp Pathol. 2014 Jan 15;7(2):575–83.

222. Borghese C, Cattaruzza L, Pivetta E, Normanno N, De Luca A, Mazzucato M, et al. Gefitinib inhibits the cross-talk between mesenchymal stem cells and prostate cancer cells leading to tumor cell proliferation and inhibition of docetaxel activity. J Cell Biochem. 2013 May 1;114(5):1135–44.

223. Yao M, Yu E, Staggs V, Fan F, Cheng N. Elevated expression of chemokine C-C ligand 2 in stroma is associated with recurrent basal-like breast cancers. Mod Pathol. 2016 Apr 29.

224. Li X, Yao W, Yuan Y, Chen P, Li B, Li J, Chu R, Song H, Xie D, Jiang X, Wang H. Targeting of tumour-infiltrating macrophages via CCL2/CCR2 signalling as a therapeutic strategy against hepatocellular carcinoma Gut. Oct 9 2015, 310-514.

225. Li M, Knight DA, A Snyder L, Smyth MJ, Stewart TJ. A role for CCL2 in both tumor progression and immunosurveillance. Oncoimmunology , Jul 1 2013;2(7).

226. Qian B-Z, Li J, Zhang H, Kitamura T, Zhang J, Campion LR, et al. CCL2 recruits inflammatory monocytes to facilitate breast-tumour metastasis. Nature. 2011 Jul 14;475(7355):222–5.

227. Sandhu SK, Papadopoulos K, Fong PC, Patnaik A, Messiou C, Olmos D, Wang G, Tromp BJ, Puchalski TA, Balkwill F, Berns B, Seetharam S, de Bono JS, Tolcher AW. A first-in-human, first-in-class, phase I study of carlumab (CNTO 888), a human monoclonal antibody against CC-chemokine ligand 2 in patients with solid tumors Cancer Chemother Pharmacol. 2013 Apr;71(4):1041-50.

228. Powell DW, Mifflin RC, Valentich JD, Crowe SE, Saada JI, West AB. Myofibroblasts. I. Paracrine cells important in health and disease. Am J Physiol. 1999 Jul;277(1 Pt 1):C1-9.

229. Kalluri R, Zeisberg M. Fibroblasts in cancer. Nat Rev Cancer. 2006 May;6(5):392–401.

230. Thiery JP. Epithelial–mesenchymal transitions in tumour progression. Nat Rev Cancer. 2002 Jun;2(6):442–54.

231. Nakashima J, Tachibana M, Horiguchi Y, Oya M, Ohigashi T, Asakura H, et al. Serum Interleukin 6 as a Prognostic Factor in Patients with Prostate Cancer. Clin Cancer Res. 2000 Jul 1;6(7):2702–6.

232. Chung Y-C, Chang Y-F. Serum interleukin-6 levels reflect the disease status of colorectal cancer. J Surg Oncol. 2003 Aug 1;83(4):222–6.

233. McGettrick HM, Smith E, Filer A, Kissane S, Salmon M, Buckley CD, et al. Fibroblasts from different sites may promote or inhibit recruitment of flowing lymphocytes by endothelial cells. Eur J Immunol. 2009 Jan;39(1):113–25.

234. Buckley CD, Rainger GE, Nash GB, Raza K. Endothelial cells, fibroblasts and vasculitis. Rheumatol Oxf Engl. 2005 Jul;44(7):860–3.

235. McGettrick HM, Butler LM, Buckley CD, Rainger GE, Nash GB. Tissue stroma as a regulator of leukocyte recruitment in inflammation. J Leukoc Biol. 2012 Mar;91(3):385–400.

236. Blankenstein T, Coulie PG, Gilboa E, Jaffee EM. The determinants of tumour immunogenicity. Nat Rev Cancer. 2012 Mar 1;12(4):307–13.

237. Willimsky G, Czéh M, Loddenkemper C, Gellermann J, Schmidt K, Wust P, et al. Immunogenicity of premalignant lesions is the primary cause of general cytotoxic T lymphocyte unresponsiveness. J Exp Med. 2008 Jul 7;205(7):1687–700.

238. Cheng L[1], Wang J, Li X, Xing Q, Du P, Su L, Wang S. Interleukin-6 induces Gr-1+CD11b+ myeloid cells to suppress CD8+ T cell-mediated liver injury in mice. PLoS One. 2011 Mar 4;6(3):e17631.

239. Griffioen AW, Damen CA, Blijham GH, Groenewegen G. Tumor angiogenesis is accompanied by a decreased inflammatory response of tumor-associated endothelium. Blood. 1996 Jul 15;88(2):667–73.

240. Chaffer CL, Weinberg RA. A Perspective on Cancer Cell Metastasis. Science. 2011 Mar 25;331(6024):1559–64.

241. Fukumura D, Xavier R, Sugiura T, Chen Y, Park EC, Lu N, et al. Tumor induction of VEGF promoter activity in stromal cells. Cell. 1998 Sep 18;94(6):715–25.

242. Le DT, Uram JN, Wang H, Bartlett BR, Kemberling H, Eyring AD, Skora AD, Luber BS, Azad NS, Laheru D, Biedrzycki B, Donehower RC, Zaheer A, Fisher GA, Crocenzi TS, Lee JJ, Duffy SM, Goldberg RM, de la Chapelle A, Koshiji M, Bhaijee F, Huebner T, Hruban RH, Wood LD, Cuka N, Pardoll DM, Papadopoulos N, Kinzler KW, Zhou S, Cornish TC, Taube JM, Anders RA, Eshleman JR, Vogelstein B, Diaz LA Jr. PD-1 Blockade in Tumors with Mismatch-Repair Deficiency. N Engl J Med. 2015 Jun 25;372(26):2509-20

243. Raman D, Baugher PJ, Thu YM, Richmond A. Role of chemokines in tumor growth. Cancer Lett. 2007 Oct 28;256(2):137–65.

244. Harper J, Sainson RCA. Regulation of the anti-tumour immune response by cancer-associated fibroblasts. Semin Cancer Biol. 2014 Apr;25:69–77.

245. Liao D, Luo Y, Markowitz D, Xiang R, Reisfeld RA. Cancer Associated Fibroblasts Promote Tumor Growth and Metastasis by Modulating the Tumor Immune Microenvironment in a 4T1 Murine Breast Cancer Model. PLoS ONE. 2009 Nov 23;4(11):e7965.

246. Nagasaki T, Hara M, Nakanishi H, Takahashi H, Sato M, Takeyama H. Interleukin-6 released by colon cancer-associated fibroblasts is critical for tumour angiogenesis: anti-interleukin-6 receptor antibody suppressed angiogenesis and inhibited tumour–stroma interaction. Br J Cancer. 2014 Jan 21;110(2):469–78.

247. Watson C, Whittaker S, Smith N, Vora AJ, Dumonde DC, Brown KA. IL-6 acts on endothelial cells to preferentially increase their adherence for lymphocytes. Clin Exp Immunol. 1996 Jul;105(1):112–9.

248. Fisher DT, Chen Q, Skitzki JJ, Muhitch JB, Zhou L, Appenheimer MM, et al. IL-6 trans-signaling licenses mouse and human tumor microvascular gateways for trafficking of cytotoxic T cells. J Clin Invest. 2011 Oct 3;121(10):3846–59.

249. Chen Z-Y, Raghav K, Lieu CH, Jiang Z-Q, Eng C, Vauthey J-N, et al. Cytokine profile and prognostic significance of high neutrophil-lymphocyte ratio in colorectal cancer. Br J Cancer. 2015 Mar 17;112(6):1088–97.

250. Olsen J, Kirkeby LT, Olsen J, Eiholm S, Jess P, Gögenur I, et al. High interleukin-6 mRNA expression is a predictor of relapse in colon cancer. Anticancer Res. 2015 Apr;35(4):2235–40.

251. Patel SAA, Gooderham NJ. IL6 mediates immune and colorectal cancer cell crosstalk via miR-21 and miR-29b. Mol Cancer Res MCR. 2015 Jul 16;

252. Roca H, Varsos ZS, Sud S, Craig MJ, Ying C, Pienta KJ. CCL2 and Interleukin-6 Promote Survival of Human CD11b+ Peripheral Blood Mononuclear Cells and Induce M2-type Macrophage Polarization. J Biol Chem. 2009 Dec 4;284(49):34342–54.

253. Rose-John S. IL-6 Trans-Signaling via the Soluble IL-6 Receptor: Importance for the Pro-Inflammatory Activities of IL-6. Int J Biol Sci. 2012 Oct 24;8(9):1237–47.

254. Romano M, Sironi M, Toniatti C, Polentarutti N, Fruscella P, Ghezzi P, et al. Role of IL-6 and its soluble receptor in induction of chemokines and leukocyte recruitment. Immunity. 1997 Mar;6(3):315–25.

255. Lüscher TF, Barton M. Endothelins and Endothelin Receptor Antagonists Therapeutic Considerations for a Novel Class of Cardiovascular Drugs. Circulation. 2000 Nov 7;102(19):2434–40.

256. Tripathi D, Therapondos G, Ferguson JW, Newby DE, Webb DJ, Hayes PC. Endothelin-1 contributes to maintenance of systemic but not portal haemodynamics in patients with early cirrhosis: a randomised controlled trial. Gut. 2006 Sep;55(9):1290–5.

257. Ahmed SI, Thompson J, Coulson JM, Woll PJ. Studies on the expression of endothelin, its receptor subtypes, and converting enzymes in lung cancer and in human bronchial epithelium. Am J Respir Cell Mol Biol. 2000 Apr;22(4):422–31.

258. Tamkus D, Sikorskii A, Gallo KA, Wiese DA, Leece C, Madhukar BV, et al. Endothelin-1 enriched tumor phenotype predicts breast cancer recurrence. ISRN Oncol. 2013;2013:385398.

259. Haque S-U, Dashwood MR, Heetun M, Shiwen X, Farooqui N, Ramesh B, et al. Efficacy of the Specific Endothelin A Receptor Antagonist Zibotentan (ZD4054) in Colorectal Cancer: A Preclinical Study. Mol Cancer Ther. 2013 Aug;12(8):1556–67.

260. Ishimoto S, Wada K, Tanaka N, Yamanishi T, Ishihama K, Aikawa T, et al. Role of endothelin receptor signalling in squamous cell carcinoma. Int J Oncol. 2011 Nov 10;40(4):1011–9.

261. Wülfing P, Diallo R, Kersting C, Wülfing C, Poremba C, Rody A, et al. Expression of Endothelin-1, Endothelin-A, and Endothelin-B Receptor in Human Breast Cancer and Correlation with Long-Term Follow-Up. Clin Cancer Res. 2003 Sep 15;9(11):4125–31.

262. Asham E, Shankar A, Loizidou M, Fredericks S, Miller K, Boulos PB, et al. Increased endothelin-1 in colorectal cancer and reduction of tumour growth by ET A receptor antagonism. Br J Cancer. 2001 Nov;85(11):1759–63.

263. Haque S, Dashwood M, Welch H, Ogunbiyi O, Loizidou M. Characterising colorectal cancer binding sites for Endothelin-1 and antagonistic action by the Endothelin A receptor antagonist Zibotentan (ZD4054). Eur J Surg Oncol EJSO. 2011 Nov;37(11):1011.

264. Cardillo C, Kilcoyne CM, Waclawiw M, Cannon RO, Panza JA. Role of endothelin in the increased vascular tone of patients with essential hypertension. Hypertension. 1999 Feb;33(2):753–8.

265. Strachan FE, Spratt JC, Wilkinson IB, Johnston NR, Gray GA, Webb DJ. Systemic blockade of the endothelin-B receptor increases peripheral vascular resistance in healthy men. Hypertension. 1999 Jan;33(1 Pt 2):581–5.

266. Wouters J, Hunger RE, Garrod T, Dubuis B, Hunziker T, Oord JJ van den, et al. First-in-Human Proof-of-Concept Study: Intralesional Administration of BQ788, an Endothelin Receptor B Antagonist, to Melanoma Skin Metastases. The Oncologist. 2015 Oct;20(10):1121.

267. Wang R, Dashwood RH. Endothelins and their Receptors in Cancer: Identification of Therapeutic Targets. Pharmacol Res Off J Ital Pharmacol Soc. 2011 Jun;63(6):519–24.

268. Hoosein MM, Dashwood MR, Dawas K, Ali HMMDA, Grant K, Savage F, et al. Altered endothelin receptor subtypes in colorectal cancer. Eur J Gastroenterol Hepatol. 2007 Sep;19(9):775–82.

269. Coffman L, Mooney C, Lim J, Bai S, Silva I, Gong Y, et al. Endothelin receptor-A is required for the recruitment of antitumor T cells and modulates chemotherapy induction of cancer stem cells. Cancer Biol Ther. 2013 Feb;14(2):184–92.

270. Nietzer S, Baur F, Sieber S, Hansmann J, Schwarz T, Stoffer C, et al. Mimicking Metastases Including Tumor Stroma: A New Technique to Generate a Three-Dimensional Colorectal Cancer Model Based on a Biological Decellularized Intestinal Scaffold. Tissue Eng Part C Methods. 2016 Jun 3;

271. Frese KK, Tuveson DA. Maximizing mouse cancer models. Nat Rev Cancer. 2007 Sep;7(9):654–8.

272. Bader BL, Rayburn H, Crowley D, Hynes RO. Extensive vasculogenesis, angiogenesis, and organogenesis precede lethality in mice lacking all alpha v integrins. Cell. 1998 Nov 13;95(4):507–19.

273. Mestas J, Hughes CCW. Of Mice and Not Men: Differences between Mouse and Human Immunology. J Immunol. 2004 Mar 1;172(5):2731–8.

274. Schmitt C, Voegelin M, Marin A, Schmitt M, Schegg F, Hénon P, et al. Selective aminopeptidase-N (CD13) inhibitors with relevance to cancer chemotherapy. Bioorg Med Chem. 2013 Apr 1;21(7):2135–44.

275. Ichimura E, Yamada M, Nishikawa K, Abe F, Nakajima T. Immunohistochemical expression of aminopeptidase N (CD13) in human lung squamous cell carcinomas, with special reference to Bestatin adjuvant therapy. Pathol Int. 2006;56(6):296–300.

276. Hirano T[1], Ishihara K, Hibi M. Roles of STAT3 in mediating the cell growth, differentiation and survival signals relayed through the IL-6 family of cytokine receptors. Oncogene. 2000 May 15;19(21):2548-56.

277. Coussens LM, Werb Z. Inflammation and cancer. Nature. 2002 Dec 19;420(6917):860–7.

278. Quan Q, Yang M, Gao H, Zhu L, Lin X, Guo N, et al. Imaging tumor endothelial marker 8 using an 18F-labeled peptide. Eur J Nucl Med Mol Imaging. 2011 Oct;38(10):1806–15.

279. O'Connell PJ, Gerkis V, d'Apice AJ. Variable O-glycosylation of CD13 (aminopeptidase N). J Biol Chem. 1991 Mar 5;266(7):4593–7.

280. Curnis F, Arrigoni G, Sacchi A, Fischetti L, Arap W, Pasqualini R, et al. Differential Binding of Drugs Containing the NGR Motif to CD13 Isoforms in Tumor Vessels, Epithelia, and Myeloid Cells. Cancer Res. 2002 Feb 1;62(3):867–74.

281. Curnis F, Fiocchi M, Sacchi A, Gori A, Gasparri A, Corti A. NGR-tagged nano-gold: A new CD13-selective carrier for cytokine delivery to tumors. Nano Res. 2016 Mar 4;9(5):1393–408.

282. Mina-Osorio P. The moonlighting enzyme CD13: old and new functions to target. Trends Mol Med. 2008 Aug;14(8):361–71.

283. Hashida H, Takabayashi A, Kanai M, Adachi M, Kondo K, Kohno N, et al. Aminopeptidase N is involved in cell motility and angiogenesis: its clinical significance in human colon cancer. Gastroenterology. 2002 Feb;122(2):376–86.

284. Arjonen A, Kaukonen R, Ivaska J. Filopodia and adhesion in cancer cell motility. Cell Adhes Migr. 2011 Oct;5(5):421–30.

285. Petrovic N, Schacke W, Gahagan JR, O'Conor CA, Winnicka B, Conway RE, et al. CD13/APN regulates endothelial invasion and filopodia formation. Blood. 2007 Jul 1;110(1):142–50.

286. Takada M, Fukuoka M, Negoro S, Kusunoki Y, Matsui K, Masuda N, et al. Combination therapy with bestatin in inoperable lung cancer. A randomized trial. Acta Oncol Stockh Swed. 1990;29(6):821–5.

287. Svensson S, Abrahamsson A, Rodriguez GV, Olsson A-K, Jensen L, Cao Y, et al. CCL2 and CCL5 Are Novel Therapeutic Targets for Estrogen-Dependent Breast Cancer. Am Assoc Cancer Res. 2015 Aug 15;21(16):3794–805.

288. Rollins BJ, Sunday ME. Suppression of tumor formation in vivo by expression of the JE gene in malignant cells. Mol Cell Biol. 1991 Jun 1;11(6):3125–31.

289. Harlin H, Meng Y, Peterson AC, Zha Y, Tretiakova M, Slingluff C, et al. Chemokine Expression in Melanoma Metastases Associated with CD8+ T-Cell Recruitment. Cancer Res. 2009 Apr 1;69(7):3077–85.

290. Manome Y, Wen PY, Hershowitz A, Tanaka T, Rollins BJ, Kufe DW, et al. Monocyte chemoattractant protein-1 (MCP-1) gene transduction: an effective tumor vaccine strategy for non-intracranial tumors. Cancer Immunol Immunother CII. 1995 Oct;41(4):227–35.

291. Arendt LM, McCready J, Keller PJ, Baker DD, Naber SP, Seewaldt V, et al. Obesity promotes breast cancer by CCL2-mediated macrophage recruitment and angiogenesis. Cancer Res. 2013 Oct 1;73(19):6080-93

292. Wolf MJ, Hoos A, Bauer J, Boettcher S, Knust M, Weber A, et al. Endothelial CCR2 Signaling Induced by Colon Carcinoma Cells Enables Extravasation via the JAK2-Stat5 and p38MAPK Pathway. Cancer Cell. 2012 Jul 10;22(1):91–105.

293. Kitamura T, Qian B-Z, Soong D, Cassetta L, Noy R, Sugano G, et al. CCL2-induced chemokine cascade promotes breast cancer metastasis by enhancing retention of metastasis-associated macrophages. J Exp Med. 2015 Jun 29;212(7):1043–59.

294. Qian B-Z, Li J, Zhang H, Kitamura T, Zhang J, Campion LR, et al. CCL2 recruits inflammatory monocytes to facilitate breast tumor metastasis. Nature. 2011 Jun 8;475(7355):222–5.

295. Pienta KJ, Machiels J-P, Schrijvers D, Alekseev B, Shkolnik M, Crabb SJ, et al. Phase 2 study of carlumab (CNTO 888), a human monoclonal antibody against CC-chemokine ligand 2 (CCL2), in metastatic castration-resistant prostate cancer. Invest New Drugs. 2012 Aug 21;31(3):760–8.

296. Bonapace L, Coissieux M-M, Wyckoff J, Mertz KD, Varga Z, Junt T, et al. Cessation of CCL2 inhibition accelerates breast cancer metastasis by promoting angiogenesis. Nature. 2014 Nov 6;515(7525):130–3.

297. Scheller J, Chalaris A, Schmidt-Arras D, Rose-John S. The pro- and anti-inflammatory properties of the cytokine interleukin-6. Biochim Biophys Acta BBA - Mol Cell Res. 2011 May;1813(5):878–88.

298. Fisher DT, Appenheimer MM, Evans SS. The Two Faces of IL-6 in the Tumor Microenvironment. Semin Immunol. 2014 Feb;26(1):38–47.

299. Tate J, Olencki T, Finke J, Kottke-Marchant K, Rybicki LA, Bukowski RM. Phase I trial of simultaneously administered GM-CSF and IL-6 in patients with renal-cell carcinoma: Clinical and laboratory effects. Ann Oncol. 2001 May 1;12(5):655–9.

300. Bataille R, Barlogie B, Lu ZY, Rossi JF, Lavabre-Bertrand T, Beck T, et al. Biologic effects of anti-interleukin-6 murine monoclonal antibody in advanced multiple myeloma. Blood. 1995 Jul 15;86(2):685–91.

301. Coward J, Kulbe H, Chakravarty P, Leader D, Vassileva V, Leinster DA, et al. Interleukin-6 as a therapeutic target in human ovarian cancer. Clin Cancer Res Off J Am Assoc Cancer Res. 2011 Sep 15;17(18):6083–96.

302. Hirata Y, Emori T, Eguchi S, Kanno K, Imai T, Ohta K, et al. Endothelin receptor subtype B mediates synthesis of nitric oxide by cultured bovine endothelial cells. J Clin Invest. 1993 Apr;91(4):1367–73.

303. Biffl WL, Moore EE, Moore FA, Barnett C. Nitric oxide reduces endothelial expression of intercellular adhesion molecule (ICAM)-1. J Surg Res. 1996 Jun;63(1):328–32.

304. Vallance P, Hingorani A. Endothelial nitric oxide in humans in health and disease. Int J Exp Pathol. 1999 Dec;80(6):291–303.